# Sample Conditioning for Multi-Sensor Systems

# Probenaufbereitung für Multisensorsysteme

## DISSERTATION

der Fakultät für Chemie und Pharmazie
der Eberhard-Karls-Universität Tübingen

zur Erlangung des Grades eines Doktors
der Naturwissenschaften

2001

vorgelegt von

STEFAN STRATHMANN

Tag der mündlichen Prüfung:     2. Februar 2001


Dekan:                          Prof. Dr. H. Probst

1. Berichterstatter:            Prof. Dr. C. Ziegler

2. Berichterstatter:            Prof. Dr. J.R. Stetter

# Content

# Abbreviations

| | |
|---|---|
| A/D | analogue/digital |
| AGS | amperometric gas sensor |
| amu | atomic mass unit |
| b.p. | boiling point |
| bl | blank |
| C | capacitor |
| CE | counter electrode |
| DSC | differential scanning calorimetry |
| EC | electrochemical sensor or cell |
| EN | electronic nose |
| GC | gas chromatography |
| HC | hydrocarbon |
| HS | headspace |
| HSA | headspace analysis |
| hss | headspace sampler |
| i.d. | inner diameter |
| JP | jumper, connector |
| KNN | K nearest neighbor |
| LOD | limit of detection |
| MI | membrane inlet |
| MOX | metal oxide |
| MS | mass spectrometry |
| MSD | mass selective detector |
| o.d. | outer diameter |
| O.D. | optical density |
| PARC | pattern recognition |
| PC | principal component |
| PCA | principal component analysis |
| PCR | principal component regression |
| PDMS | polymethyldisiloxane |

| | |
|---|---|
| PEG | polyethyleneglycol |
| PLOT | porous layer open tubular (column) |
| ppm | parts per million |
| PRESS | predicted error sum of squares |
| PT | purge and trap |
| PTFE | polytetrafluorethylene |
| Q | transistor |
| QMB | quartz micro balance |
| R | resistance |
| r.h. | relative humidity |
| RE | reference electrode |
| ref | reference |
| SAW | surface acoustic wave |
| SE | solvent extraction |
| SFE | super critical fluid extraction |
| SPE | solid phase extraction |
| SPME | solid phase micro extraction |
| std | standard |
| SVD | singular value decomposition |
| SVOC | semi volatile organic compound |
| TD | thermal desorption |
| TG | thermal gravimetry |
| U | linear component or port |
| VOC | volatile organic compound |
| WE | working electrode |

# Symbols

| | | | |
|---|---|---|---|
| A | area | n | peak capacity (of a column) |
| A,B,C | compounds or constants | p | pressure |
| $b_{1/2}$ | width at half maximum | $p_x$ | partial pressure of x |
| C | concentration | $R_S$ | chromatographic resolution |
| $\mathbb{C}$ | matrix of concentrations | $\mathbb{R}$ | regression coefficients matrix |
| C* | bulk concentration | s | index of substance, compound |
| $C_s$ | concentration of species s | S,s | index of sorbent |
| D | diffusion coefficient | $\mathbb{S}$ | matrix of sensor responses |
| F | Faraday constant | t | time |
| g | index of gas phase | $t_M$ | dead time |
| H | theoretical plate height | $t_R$ | retention time |
| I | current | $t_R'$ | net retention time |
| $I_L$ | limiting current | T | temperature |
| i,j | sample, compound index | u | linear velocity |
| J | flow rate | u | score |
| K | partition coefficient | U | voltage, potential |
| K | number of constituents | U | operation amplifier |
| k' | capacity factor | $\mathbb{U},\mathbb{V}$ | orthogonal matrices |
| l | length | $V_B$ | breakthrough volume |
| l,m | orders of reaction | $V_{BS}$ | specific breakthrough volume |
| M,m | index of mobile phase | $V_F$ | total elution volume |
| M | number of samples | $V_R$ | retention volume |
| m | mass | $V_R'$ | net retention volume |
| $m_A$ | adsorbent mass | $V_S$ | safe sample volume |
| $m_{max}$ | adsorption capacity | W | peak width |
| N | number of particles | x | direction of diffusion |
| N | number of theoretical plates | x | preprocessed feature, variable |
| N | number of sensors | x' | feature |
| n | number of electrons | $\mathbb{X}$ | data matrix |
| n | index for sensor | $\mathbb{X}^{\mathbf{T}}$ | transposed data matrix |

| | |
|---|---|
| **S** | matrix of singular values |
| $\alpha$ | transfer coefficient |
| $\alpha$ | selectivity factor |
| $\beta$ | phase ratio |
| $\delta$ | diffusion layer thickness |
| $\eta$ | overvoltage |
| $\sigma$ | singular value |
| $\sigma$ | peak variance |
| $\bar{v}$ | average velocity |

# 1. INTRODUCTION AND MOTIVATION

## 1.1. Motivation

The goal of this work was the improvement in identification of target constituents in varying or interfering matrices with chemical sensors and the correlation of sensor signals with volatile compounds and instrumental chemical analysis. The characterization of trace concentrations of analytes against a background of substances in concentrations which may be a magnitude higher requires improvements in the specificity, selectivity, and sensitivity of the detection method. Therefore, different methods of optimizing the sensor array instrument towards the detection of certain analytes in complex matrices were investigated for several application examples.

## 1.2. Introduction

The electronic nose, short e-nose or EN, is a new type of analytical instrument consisting of an array of chemical sensors, a suitable sampling system, and pattern classifier algorithm. The earliest reported e-nose instrument was based on a heterogeneous array of combustible and electrochemical sensors [1]. The e-nose approach to analysis is particularly effective for comparing or classifying complex mixtures, such as aromas and flavors, which defy more conventional methods of characterization or chemical analysis. The qualitative discrimination power of the e-nose often has an uncanny resemblance to the subjective discrimination of odors by the human nose [2,3].

The electronic nose has previously been defined as "...an instrument, which comprises an array of chemical sensors with partial specificity and an appropriate pattern-recognition system, capable of recognizing simple or complex odors" [4,5]. Additionally, the sample uptake and various more or less selective sensing principles e.g. biosensors can be included in the definition of the overall system. A single chemical gas sensor will respond to many different gases. Although this is an interference when the intention is to measure a single compound alone, an array of different types of gas sensors will produce a set of responses whose relative magnitudes form a unique pattern for each sample [6,7,8]. A simple histogram of such a set of responses is usually readily

distinguished from an analogous histogram made with the same array and a different analyte. The accuracy of classification can be improved by using branching algorithms which pre-process the data and limit the number of possible choices available to the pattern classifier [9].

Most often the electronic nose (EN) is used for qualitative analysis but can be used for quantitative analysis [10] also. But even qualitative analyses with the EN, especially for mixtures, do not typically specify the exact chemical compound responsible for chemical sensor signals.

A definition of the EN in terms of its structure and function, rather than application, would be: "the EN is an instrument comprised of a sampling system, gas/vapor sensor array, and pattern classifier for the purpose of qualitative or quantitative analysis" [11]. The chemical analysis information is encoded in the relative responses of the array's chemical sensors. Chemical sensors are miniaturized devices which convert a chemical state, e.g. concentration of particles, molecules or any compound to be detected in gas, liquid or solid phase, into an electrical signal [12,13]. A chemical sensor comprises a sensitive material or layer as recognition site interfaced to a transducer converting chemical into physical information. An electronic nose can be visualized as shown in Figure 1 with the analysis steps and functional components resembling the biological process of odor recognition, which similarly consists of a relatively small number of different chemical receptors combined with a pattern recognizer, the brain [3,14].
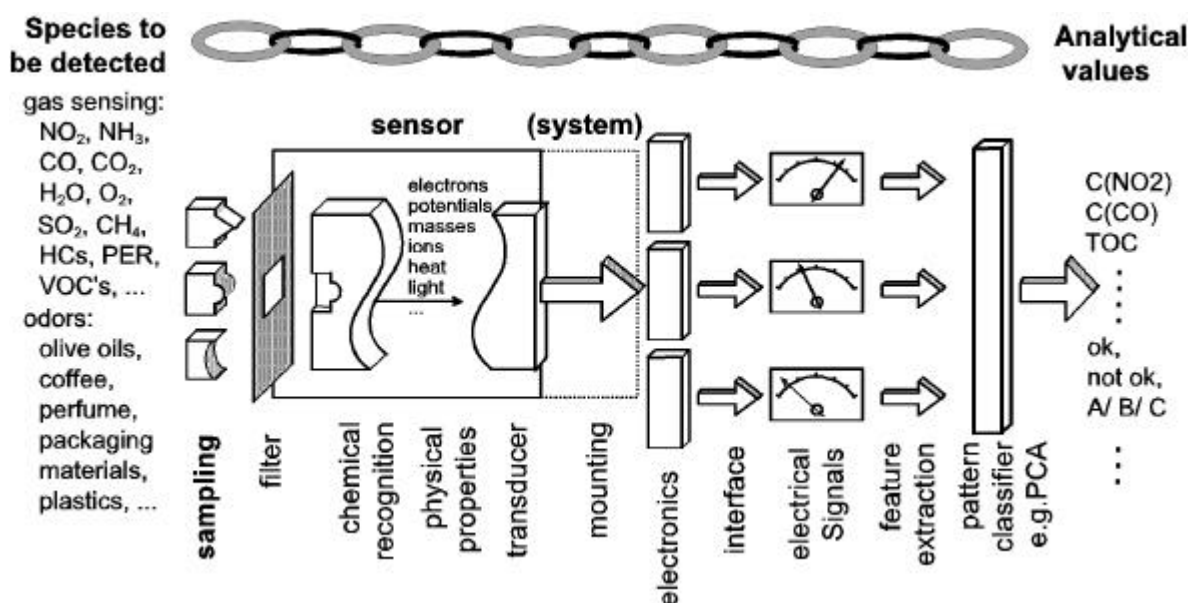


*Figure 1: Schematic of an analysis with an electronic nose [15].*

Depending on the investigated substance or mixture, sample uptake is followed by sample conditioning and an optional filter as first step. The second step is the actual measurement with chemical sensors resulting in signals, which have to be evaluated as third step by extracting specific features and submitting them to a pattern classifier or pattern recognition method before the analysis result is finally visualized. The system can be seen as a chain, in which the weakest link determines the level of analytical performance.

This work focuses on two key basic elements of e-nose analysis, which had to be improved for a variety of applications: Chemical sensors and sampling.

An electronic nose that uses chemical sensors of several classes, i.e. sensors whose chemical principles are different, gives data that are more effective for comparing samples than an instrument where simply the number of sensors of a single class [15,16,17] is increased. Moreover, while different sensors of the same type in an array are required to give the array widespread applicability, sensors that not contribute information will always contribute noise. Thus, there is an optimum array size for any given set of analytes in qualitative detection applications [18]. Redundant sensors can lead to improvements in sensitivity [19]. Sensors with chemically independent responses, or orthogonal sensors, which are more likely to be sensors of different classes, are valuable and make the array more versatile and able to distinguish more analyte differences. Thus, the first approach within this work to improve both the selectivity and sensitivity of the e-nose towards specific analytes, was to interface a complementary array of gas sensors with a unique characteristic, which is deriving from the transducer type implemented, to the existing set-up of an e-nose.

The second approach towards improving the versatility and analytical performance addressed the very first step of any analysis, the sample uptake. Development of the sampling system and of the sample pretreatment are fundamental ways to increase the utility and performance of instrumental analyses, and sensor arrays are no exception. While sampling for classic analytical instruments evolved to a variety of sophisticated methods to gain optimal instrument performance, the potential in sampling for e-noses has not yet thoroughly been investigated. By simply taking over established sampling techniques for classic analytical instruments, the special requirements and potentialities of e-noses have often been neglected.

Evaluating and adapting sample uptake techniques for sensor arrays in this work showed that substantial improvements in overall performance were achievable, often even by simplifying existing sampling set-ups. For instance, focusing

analytes prior to injection into the analytical instrument, which is necessary for operation coupled to chromatographic separation techniques, is not only unnecessary for operation with chemical sensors, but it is even contrary to the goal of extracting a maximum of information from a single measurement.

The structure of this work follows the approach taken. A survey of existing sampling methods is presented in section 2. Then a short overview of the theoretical background to the techniques chosen for implementation is given in chapter 3. The experimental set-up with tests and modifications is described in chapter 4, and finally the results achieved in several applications are presented in chapter 5.

# 2. SURVEY OF SAMPLE UPTAKE AND CONDITIONING METHODS

To analyze an investigated substance with an e-nose, the sample has to be brought into the sensor chamber. For the process sampling, i.e. of taking up the sample, of conditioning it, and of transferring it to the analytical various methods exist. In the following sections sampling methods in analytical chemistry, especially in conjunction with e-noses and suited for chemical sensor measurements, are briefly described.

## 2.1.   Analyte sampling without preconcentration

The simplest possible method of introducing a sample to the e-nose is drawing in gaseous compounds by activating a pump, mostly designed to be located behind the sensor array in the gas flow path. This method of non automated sampling exhibits poor repeatability, no sample conditioning, and is common in hand held devices where precise sampling is traded in for weight and space.

### 2.1.1.  Static headspace sampling

Static headspace analysis (HSA) is a method for analyzing a gas in contact with a liquid or solid sample. Thus, information concerning the nature and composition of the sample is drawn. Static headspace sampling can be automated with programmable sample conditioning parameters. Without further steps like preconcentration, sample extraction or chemical treatment it is a highly reproducible method of sample introduction to an analytical instrument making a high sample throughput possible. By taking an aliquot of the gas phase, the volatile components in an essentially nonvolatile matrix can be investigated without interference. In a closed or static system the gas or vapor phase will be in equilibrium with the condensed phase. Analytes are distributed between the condensed phase matrix and the vapor phase. Conditions are adjusted so that the analyte distribution favors the vapor phase. HSA is an extraction technique for semi volatile and volatile compounds. When the system is in equilibrium, the composition of the vapor phase is in quantity and quality representative of the composition of the original sample. An aliquot is taken from the gas phase and transferred to analysis. All non volatile compounds will not be analyzed. The matrix, which is often interfering, is eliminated thus enabling high sensitivities [20, 21]. HSA consists of two steps. In the first step, the sample is placed in a

vial. The closed vial is thermostatted and, if necessary, shaken for a defined time until equilibrium between phases is reached. After a pressurization and venting step an aliquot of the vial's gas phase (headspace) is introduced into the carrier gas stream and is transferred to analysis. The second step is performed either by a balanced-pressure system or over a pressure/loop system [20]. In the balanced-pressure system the sample is injected over a specified time by carrier gas first pressurizing the vial from which the sample is then transferred at pressure equaling that of the analytical instrument inlet. In the pressure/loop system the vial is also first pressurized, however, in the next step the vial is opened toward a sample loop and equilibrated against ambient pressure. Then, the loop is flushed by carrier gas transferring the sample. With the concentrations of the analyte i in the gas phase $C_{i(g)}$ and liquid/solid sample phase $C_{i(s)}$, the partition coefficient K is given by

$$K = \frac{C_{i(s)}}{C_{i(g)}} \tag{1}$$

The area of the signal peak $A_i$ for component i is proportional to the concentration in the gas phase $C_{i(g)}$ and proportional to the original concentration in the sample [21].

Figure 2 shows a schematic of the signal deriving from sample concentration and a schematic drawing of a headspace sampler as used in this work [22].
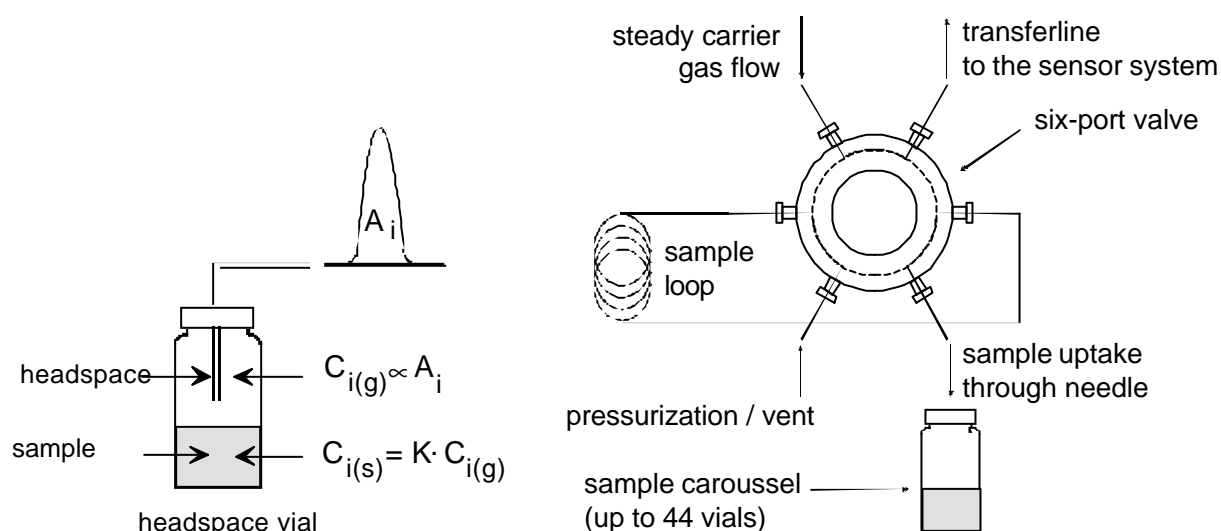


*Figure 2: Operation principle of static headspace analysis and schematic set-up of a pressure/loop headspace sampler with the centrally heated six-port valve, which introduces an aliquot of the headspace into the carrier gas flow.*

With a six-port valve controlling the transfer, the carrier gas flows continuously resulting in only a very small pressure peak. The sample volume is defined by the loop geometry.

Partition coefficients can be altered by changes in the sample matrix. With water as matrix the addition of an electrolyte will lead to a higher signal for the volatile non aqueous components (salting out effect) [23].

For routine analysis with electronic noses static headspace analysis is the most common sampling method. A precise, automated and highly reproducible sampling technique is crucial for analytical performance. The sample uptake requires the control of different parameters with temperature, pressure, volume and time being the most critical ones. The performance of the HSA is limited by the partition coefficient, the vial volume determining the maximum sample amount, and the matrix. The extraction procedure determines the measurable sample characteristics and is application specific.

The operational parameters of which temperature, equilibration times, and matrix are the most important, are optimized prior to an application.

## 2.2.  Sampling with preconcentration

In order to improve sensitivity and to take advantage of large sample volumes, methods of preconcentrating analytes prior to investigation can be used. Methods mostly focussing on the analysis of volatile organic compounds (VOCs) are described briefly in the following chapters.

### 2.2.1. Overview

Especially for trace analysis, but also for every other application, preconcentration methods are common practice in analytical chemistry. Application examples can be found in trace analysis, water analysis, aromatic compounds analysis [24,25], in environmental analysis, air quality control (VOCs, halogenated organic substances) [26, 27, 28, 29, 30], for soil samples [25, 31], in odor analysis [32], and in natural products investigation [33].

For preconcentration of volatile organic compounds various methods are described in literature [29]. An overview of preconcentration methods is given in Table 1. Advantages and disadvantages are listed according to operation in conjunction with a chemical sensor system [21, 34]. Also included in the list are extraction techniques as far as they are applicable in conjunction with chemical sensors.

| preconcentration method | advantage | disadvantage |
|---|---|---|
| **from the gas phase** | | |
| Thermodesorption (TD) | high capacity, mobile | only thermally stable analytes |
| | preferential sampling | preferential sampling |
| | sampling and pump can be operated separated from the analytical device | calibration needed for quantitative analysis |
| | automatic sampling | |
| Cryogenic trap | simple set-up | water condensation, costly and voluminous |
| **from solids or liquids** | | |
| Purge and trap (PT), (dynamic headspace) | high sensitivity | long sampling time |
| direct thermodesorption (TD) | complete extraction | only thermally stable solids |
| Solvent extraction (SE) | high recovery / capacity | solvent removal necessary prior to sensor measurement |
| Solid phase extraction (SPE) | high recovery / capacity | solvent removal necessary prior to sensor measurement |
| Solid Phase Micro Extraction (SPME) | mobile sampling | low capacity, low sample volume |

*Table 1: Preconcentration methods.*

Especially in combination with chemical sensors for measurements in the gas phase, thermodesorption methods on solid materials are suited best. Cryogenic preconcentration from humid air often leads to water condensation and therefore to the collection of large quantities of water, which presents a major problem in the subsequent analysis. For measurements with sensors sensitive to a background of water, the humidity has to be removed first. Often, sample preconcentration is combined with sample preconditioning, especially when selectivity enhancement is an objective. Methods combining both principles are also discussed in chapter 2.3.

For adsorption and thermal desorption on solids a distinction is made between the methods depending on the analyte phase: For the sampling from solid or liquid substances preconcentration is achieved by purge and trap (PT). For the preconcentration from the gas phase and following thermal desorption from the

sorption material to the analytical instrument, the general term thermodesorption (TD) is used. Depending on the target analyte different absorbents are used (Table 3). Methods and materials used with chemical sensor arrays will be further discussed in the following.

### 2.2.2. Dynamic headspace sampling

Dynamic headspace sampling or Purge and Trap (PT) is a method for extracting volatile material from an often liquid matrix and for collecting and concentrating the analytes in an adsorption trap. The analytes are then flushed by thermal desorption into the analytical instrument. The purge and trap method consists of three steps: Purging, desorption and a so called bake phase.

A high purity purge gas, helium or nitrogen, extracts analytes from the matrix, which is most often kept in U-shaped glass tubing with a fritt to the carrier gas side. The complete set-up is heated. The extracted volatiles are trapped and concentrated in a tube filled with anadsorption resin. Figure 3 schematically shows the gas flow in the purge phase. The carrier gas continuously flushes the sensor system.



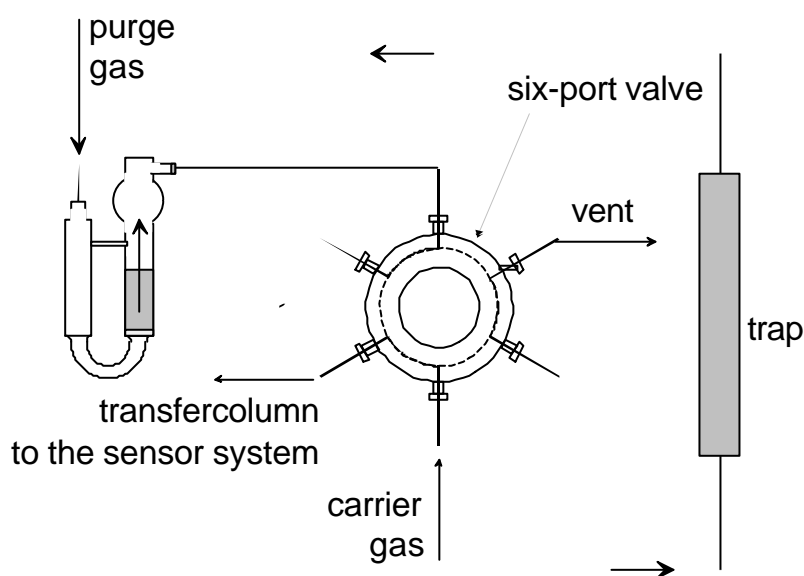*Figure 3: Schematic gas flow in the purge phase for a dynamic headspace (PT) sampler.*

The amount of extracted analyte depends on the purge volume, i.e. the volume of carrier gas the sample is purged with. The purge efficiency, i.e. the amount of analyte purged with a certain amount of gas, depends on purge volume, sample temperature, analyte vapor pressure, and sample matrix. The purge efficiency

determines the recovery rate. The trap efficiency rises with decreasing trap temperature. Water can be removed with a dry purge step.

For the desorption phase the six-port valve is turned so that the carrier gas passes through the now heated trap via the valve into the sensor system. The flow direction through the trap hereby is reversed (back flush method). This desorption mode will deliver focussed analyte peaks for operation with a gas chromatograph (GC). Time and trap temperature determine the chromatography during the desorption phase. For fast desorption often a preheat step without gas flow and temperatures lower than the desorption temperature of the target analyte precedes the actual desorption.

The desorption efficiency depends on the temperature and on the gas flow and desorption time, the product of which is the desorption volume.

The bake phase completes the sampling cycle. Here the trap is heated above the desorption temperature for some time to elute any compounds interfering with the next analysis.

The non-equilibrium PT method can achieve a higher extraction from samples than static headspace sampling, especially for analytes with high partition coefficient, and profits of larger sample quantities. Disadvantages are difficulties in automation, higher cycle times and the possibility of carry-overs or contamination.

Table 2 shows a comparison of headspace (HS) and Purge and Trap (PT) limit of detection (LOD) values measured with GC/MS and the electronic nose MOSES II [35, 36] for aldehydes in an inert matrix of deodorized corn oil.

| | limits of detection [ppm] | | | |
|---|---|---|---|---|
| Analyte | HS - GC | PT - GC | HS - e-nose | PT - e-nose |
| Hexanal | 0.1 | 0.01 | 1 | 0.01 |
| Heptanal | 0.1 | 0.01 | 1 | 0.1 |
| Octanal | 0.1 | 0.01 | 10 | 1 |
| Nonanal | 0.1 | 0.1 | 100 | 1 |

*Table 2: Comparison of measured limits of detection in ppm. Orders of magnitude are displayed.*

## 2.2.3. Thermal desorption

Thermal desorption or thermodesorption is the trapping of air contaminants or gaseous samples and subsequent desorption or the direct desorption of volatiles from solid samples, mostly used with an additional cryo-trap [37,38]. Thermal desorption allows the preconcentration from large gas volumes, which is important for trace analysis of air contaminants. It is the most generally applicable analysis approach for VOCs in air, very often together with GC or GC-MS, for which most thermodesorption set-ups were developed [37,39,40], but also with other analytical techniques [41].

Trap materials are similar to those used in PT as is the principle set-up with back flush desorption over a heated transfer capillary.

Sample uptake can be active with a pump constantly drawing in e.g. air in a personal air sampler, can be passive over diffusion, or, solid samples can directly be filled in desorption tubes and be thermally desorbed [41]. For quantitative evaluations the thermodesorption tubes need to be calibrated.

The desorption usually is done in a two step process with a second (cryo-) trap focussing the analytes and is automated in commercial instruments [21, 42, 43].

Thermodesorption set-ups have been realized, apart from using separately temperature controlled tubes of mostly 3 to 4 mm. i.d. [37,39,44], also as capillary tubes enclosed in a separate heating set-up [26] or coated open tubular traps [45] optimized for GC requirements.

Thermodesorption tube trapping is usually operated in a way that volatiles are quantitatively enriched, i.e. operation parameters are selected in a way that no constituents elute from the trap during the adsorption phase; the sampling is stopped before breakthrough of target analytes occurs. A different approach is equilibrium sorptive enrichment for trace analysis of weakly retained compounds, where the target analytes are in equilibrium with the sorptive material [46,47]. This technique is reported to obtain enrichment factors of about one hundred but is limited to samples with a constant concentration over the sampling time and will not be further discussed in this work.

Thermal desorption in conjunction with chemical sensors has been reported by Grate et al. [48] for use in the conventional back flush set-up and later by Groves and Zellers [49,50] together with polymer coated surface acoustic wave sensors (SAW). Recent publications describe up to 10-fold increases in sensitivity using either packed [51] capillary traps or coated porous layer open tubular (PLOT) capillaries [52]. Apart from lowering the LOD for analytes, the role of the

11

preconcentrator is to focus the sample, to counteract sensor baseline drift, and to alleviate water influence, e.g. by inserting a dry purge step into the operation cycle [38,52].

An advantage of the thermodesorption technique apart from automation, high recovery rate and thus sensitivity achievable, is, that sampling and desorption can be conducted at separate times and locations. Disadvantages are a possibly higher cycle time, the danger of artifact formation on the trap, and the possibility of carry-overs or contaminations [38,40,45].

### 2.2.4. Solid phase micro extraction

Non or semi volatile components are usually extracted with solid phase extraction (SPE) employing silica gels, or liquid extraction with supercritical $CO_2$ (SFE). For fluids and solids these methods are time consuming and costly, require extensive sample conditioning, and result in problems for the e-nose set-up, such as a strong solvent peak by transformation into the gas phase after extraction. Solid Phase Micro Extraction (SPME) on fused silica fibers not needing solvents does not have most of the disadvantages listed above [53]. In SPME a polymer coated fiber mounted in a protective needle extracts within up to 30 minutes analytes from a septum covered vial containing the investigated sample. The adsorbed analytes are then thermally desorbed. Up to now, this method showed little advantage in preconcentration compared to methods using traps but showed problems in repeatability, which is crucial for sensor array measurements. However, successful coupling with MS and multivariate analysis have been reported [54] and first commercial attempts have been made to combine this relatively new method with e-noses [55].

### 2.2.5. Sorption materials

Materials used for thermodesorption and Purge and Trap preconcentration are summarized in Table 3. The sorption materials listed partly are also used in chromatography as stationary phases, e.g. polydimethylsiloxane (PDMS) and its derivatives, and, modified with functional groups, as coating for mass sensitive sensors, e.g. QMBs [22].

The materials commonly used for preconcentration are based on adsorption of the analyte to more or less selective active sites, e.g. porous polymers, carbon and silica materials. Also materials based on absorption into the matrix, e.g. rubbery polymers as PDMS, are reported for being used in thermodesorption

set-ups, especially for the accumulation of polar analytes [44,56]. Requirements for sorption materials in sample preconcentration are:

- thermal stability and inertness against the analyte

- fast desorption kinetics and high adsorption capacity

- low affinity to water

The optimal trapping material and the amount needed for quantitative trapping in an application can be selected by using the breakthrough volume ($V_B$) for a specific analyte and trap (see chapter 3.2.8). The specific breakthrough volume, which, within limits, is independent from the experimental set-up, is usually expressed in liters/gram. It is defined as the volume of carrier gas per gram of adsorbent resin which causes the analyte molecules to migrate from the front of the adsorbent bed to the back of the adsorbent bed.

Within limitations in operation parameters, the breakthrough volume can be calculated together with the number of theoretical plates using the retention volume and instrumentation parameters (see chapter 3.2.8).

The calculation of retention volume for absorbent material (PDMS), especially used for the enrichment of polar substances with low volatility and high molecular weight, is described in [56] and compared to adsorbents in [44].

Table 3 gives a review of common sorption materials. An overview is also given in [21,25,29,57]. Properties of different materials and their performance in applications are compared in literature [40,50,58,59]; an excellent overview, also about the procedure of determining the performance, is given in [60].

Theoretical models for the prediction of sorbent material performance are discussed in [56,60,61].

| Material | Brand Name | Properties | Application |
|---|---|---|---|
| Graphite carbon | Carbotrap, Carbopack | non-porous, hydrophobic, variable particle size, only dispersion (London) interaction | org. substances, air contaminants C4,5-C9-30 |
| Carbon molecular sieve | | specific surface area: 5-100 $m^2/g$ C-structure from pyrolysis hydrophobic, porous | specific adsorption dependent on pore shape and size |
| | Carboxen (Ambersorb) | specific surface area: 400-500 $m^2/g$ | small molecules without cryogenic cooling in high humidity, often last stage |
| | Carbosieve SIII | specific surface area: 820 $m^2/g$, defined pores 1.5-4 nm | small molecules in air, high breakthrough volume |
| Active charcoal | | specific surface area: 1100 $m^2/g$ less hydrophobic, thermally stable, polar functional groups | small molecules in air , high boiling points, high adsorption capacity |
| Porous polymers, synthetic resins | Tenax TA | polymeric diphenylene oxide, stable up to 350°C, spec. surface area: 19-35 $m^2/g$, pore vol. 2.4 $cm^3/g$, pore i.d. 720 nm, affinity to polar subst.($H_2O$, MeOH) low | volatile and semi-volatile substances, esp. non-polar HC,C5-12 in air |
| | Tenax GR | 30% graphite | higher retention volume, C3-12 in air |
| | Amberlite XAD 2 | specific surface area: 300 $m^2/g$, less polar than Tenax | ,C2-10 in air, vinylchloride, halogenated HC, HC |
| | Chromosorb | styro-divinylbenzene polymer specific surface area: 750 $m^2/g$, stable up to 250°C | small molecules in air |
| Rubbery polymers, GC phases | PDMS and its functionalized derivatives, SE 30 | polydimethylsiloxane (non polar), polyaminopropylmethylsiloxane (polar,basic), PCPMS (polar) | polar and semi-volatile substances , high molecular weight |
| Inorg. adsorbent, silica gel | Porasil | surface< 750 $m^2/g$ | polar analytes |
| Silica/glass pearls (filter in front of adsorption tube) | | surface< 5 $m^2/g$ | large molecules |
| Multi-bead adsorption tubes | | only back-flush | large and small molecules |

*Table 3: Common sorption materials.*

For selective preconcentration and trapping chromatographic adsorption material can be used in purge and trap. Adsorbents for specific classes of substances are commercially available and can be filled in adsorption tubes. Target analytes can be selectively trapped by choosing the suitable pore size, polarity, and particle size.

The most commonly used adsorption material in chemical gas analysis is the porous polymer Tenax™ [62] based on 2,6-diphenyl-p-phenylene oxide [58]. Due to its low affinity to water, Tenax is especially useful for the purging and trapping of volatiles from high moisture content samples including the analysis of volatile organic compounds in water. Detection of volatile organics in the ppb and ppt level is feasible. Tenax is most suited for the preconcentration of substances with boiling temperatures between 80 and 200°C [36]. The stability of Tenax at elevated temperatures, up to 350°C in inert atmosphere, is especially important for use together with metal oxide (MOX) chemical sensors, which require an oxygen containing sample gas stream. Investigations of Tenax filled adsorption tubes showed that apart from adsorption on the surface also absorption or volume effects characterize the behavior of the material [36]. Properties of Tenax are discussed in [56-60] and have been studied in [63].

## 2.3.  Sample preconditioning concepts

Much of the recent gas analysis sampling literature describes means of mitigating the effects of solvents to determine minor and trace components in process samples. There are several strategies in conventional analytical chemistry and increasingly also for e-nose investigations for preconditioning samples. For methods combined with headspace sampling an overview is given in [20]. The methods can be categorized roughly in five groups:

1. Alteration of the matrix, e.g. salting out [23,64,65]: As any change in the composition of the sample will substantially influence the composition of the gas phase sampled for the sensor measurements, careful control and monitoring of the effects are crucial to reproducibility. Furthermore, the monitoring is important for the evaluation of the validity of the extract and for ensuring it is not changing its characteristic of being representative. This also applies to the methods of sample treatment described in the following.

2. Controlled modulation of the gas phase constituents and their concentrations, e.g. pyrolysis or the use of catalysts in front of the sensors [66].

3. Elimination of interfering components from the gas phase prior to analysis, especially for the investigation of polar substances in a water containing matrix e.g. by desiccants, drying with adsorbents or removal of interfering components by passing the sample stream over solid sate reactants [67]. Also reported is the use of scrubbers [38,68], membranes or filters [69,70], and the removal of water by cryogenic trapping [71]. An overview and comparison of methods for the removal of humidity is given in [72].

4. Separation techniques based on chromatography, e.g. the coupling of e-noses with a GC column [73,74,75] and hyphenated techniques.

5. Selective enrichment of target analytes (see previous chapters).

A relatively new and interesting technique employed in mass spectrometry is the introduction of the sample extract into the analytical instrument by permeating the target analytes through a semi permeable membrane, the membrane inlet (MI) method [76,77], or the pervaporation through a membrane [78]. The extraction with membranes can displace a headspace sampler for certain applications, especially for non-polar semi volatile organic compounds (SVOC) contained in a water matrix, and can be used for preconcentration [79,80]. A mode of operation also employing separation by temperature programmed thermal desorption is reported [81].

Techniques with potential for substantially improving the performance of e-noses are described in more detail in the following chapters.

### 2.3.1. Catalytic oxidation or decomposition

Oxidation or decomposition with a catalytic filament makes compounds, which can not readily be evaporated or desorbed from a matrix, accessible to analysis. Through temperature dependent chemical reactions induced by the fast heating of samples also compounds more active for the analytical instrument can be generated, e.g. electrochemically active compounds for amperometric gas sensor detection.

Placing a heated filament in the sample line prior to the sensor arrays was one of the earliest modifications to be used [1,7]. If air is used as carrier gas, the filament performs catalytic oxidation and if the sample is in an inert gas or vacuum, the term pyrolyzer is more appropriate for the filament. The first use of the filament-chemical sensor combination used both a Rhodium and a Platinum filament in the sampling line to broaden the range of detectable analytes [7,82] of amperometric gas sensors and to provide an increased qualitative capability

to chemical sensor arrays [8]. Additional work on organic vapors [83] and specific chlorinated hydrocarbons [84] is published. The filament was also used with a photoinoziation detector to detect hydrazine and in a commercial instrument for chlorinated hydrocarbons [85,86]. Recently, the technique has been used for the selective detection of pollen grains [87]. In a more subtle or dual use, Scintrex, Inc. [Thorndale, Ontario, Canada] built an explosives detector from a coated Rh filament and an electrochemical sensor. Apparently the Rh metal has an exceptional affinity for compounds with the $-NO_2$ group contained in most explosives like trinitrotoluene (TNT). In this application, a high volume of air is passed over the filament at a low temperature to collect the TNT vapors. Then, a low flow sampling stream is switched to place the filament in line with the detector. A rapid pulse of power to the filament converts the sorbed TNT to $NO_x$ for subsequent sensitive detection by an electrochemical $NO_2$ sensor [88]. In this manner an LOD < 0.1 ppb can be achieved in a portable instrument. The Pt-filament has also been used to increase the sensitivity of the Pd-MOX sensor [89], and a variation of the reactor chamber using a spark reactor reportedly increases the analytical performance of a single MOX sensor [90]. Whether used as a pyrolyzer or catalytic oxidizer, the heated filament prior to sensing worked reproducible, reliable, fast, easy, and even operates on low power. Furthermore, it allows the sampling of solids and liquids as well as gases with a gas sensor. However, a single sensor and filament suffer from a lack of specificity since a sensor signal could mean a low level of $NO_2$ or a high level of a different pollutant to which the sensor has a lower response. Using the time-dependent sensor signals produced by a variable temperature filament provides additional specificity at the expense of time. Time-dependent use of the filament allowed the construction of a more sophisticated sensor system and provided an entire array of data from a single sensor.[91,92,93 and refs. therein]. However, no sensor system has yet demonstrated perfect selectivity in real analytical applications. So, complex mixtures containing trace analytes like TNT have to be separated on a GC prior to analysis by either sensor or e-nose [94], or the filament with a sensor array must be used to provide the added selectivity.

### 2.3.2. Membrane separators and dryers

Membrane separators have been used with analytical instruments to develop methods in mass spectrometry [95], for isomeric [96], and enantiomeric separation [97] applications. The membrane can function as a separator, purifier, and chemical enrichment system. Nafion® has been used primarily as a membrane dryer [98]. In general, Nafion dryers have been used in

instrumentation and are the subject of many patents having tube, flat membrane, or even heated configurations, but the Nafion dryer has never before been used with sensor array systems. Nafion is not merely a dryer if positioned prior to sensor analysis because it removes alcohols and other primarily polar gases too. So, it is really a separator and it fractionates the sample in a known and repeatable manner prior to. Other materials can be used to filter the analyte gas and remove intervening compounds e.g. charcoal for selective CO measurement, sodium sulfate for the removal of water or various reducing agents for the removal of reactive inorganic interfering compounds [99]. Theoretical and practical aspects of filters and membranes together with chemical sensors are discussed in [69] and references therein.

To conclude this section: The requirements to an ideal sample conditioning method would be to provide an increase in sensitivity and selectivity to the sensor array. The described methods of analyte concentration are not equally well suited for operation in conjunction with e-noses and only few offer the possibility of selectively enriching target substances.

Table 4 gives another brief overview of the enrichment techniques described. The methods are grouped according to the phase of the sample and the enrichment material (matrix).

| sample phase \ matrix phase | no matrix | liquid | solid |
|---|---|---|---|
| **gaseous** | cryogenic trapping | | TD |
| **liquid** | | SE | PT, SPE, SPME |
| **solid** | | SE | direct TD |

*Table 4: Overview of common preconcentration techniques.*

Of the sampling techniques offering a noticeable concentration effect, thermal desorption (TD) and Purge and trap (PT) appear to be most suited for the electronic nose. Apart from a high capacity for sample enrichment, both methods allow, to a certain degree and depending on the sorbent, selective sampling. At least the accumulation of water can be suppressed using a suitable sorbent material. Thermal desorption, within limits, further permits to make use of the chromatographic properties of the sorbent materials for the separation of mixture constituents (see section 3.2.8).

The limitations of both methods have been discussed in the previous sections.

## 2.4. Chromatography - hyphenated systems

Chromatography can be used as sample preconditioning or sample preparation prior to investigation with an analytical instrument. In this case two analytical techniques are coupled with the goal of obtaining a faster and more efficient analytical tool. In general, the combination of techniques includes the coupling of two separation processes, two spectroscopic methods, or a separation with a spectroscopic or other analytical method leading to a so-called hyphenated technique [100,101]. An example for the latter coupling is GC-MS with gas chromatography (GC) used for separation and mass spectrometry (MS) for identification. Combining techniques which are orthogonal, i.e. they provide different information, allows multidimensional analysis of the data with the hyphenated technique providing more information than the separate techniques. If the combination is done in two separate steps, the first step is called sample preparation, e.g. thermal desorption prior to GC-MS, while the second step terms the analyis.

Separation of compounds prior to analysis by adding chromatographic methods to the sampling or analytic system have been studied with a variety of set-ups using chromatographic columns [24-31,28,29,33,102], separation in the transfer line [103], or using a trap as chromatographic column with heat ramps [27]. The latter can be realized in a modified thermal desorption set-up. Also possible is an elimination of separated substance classes from the sample with filters, membranes or catalytic conversion dependent on the application. As up to date, though, the combination with sensor arrays as detector with unique requirements and characteristics has mostly been realized using gas chromatographic columns [104].

# 3. THEORY

The fundamentals of the experimental techniques employed in this work are discussed in the following chapters. After an introduction to the operation principle of the sensors added to the electronic nose, the fundamentals of chromatographic separation and data evaluation are briefly described.

## 3.1. Electrochemical gas sensors

Electrochemical gas sensors as used in this work are based on the measurement of current in an electrochemical cell between a sensing or working electrode (WE) and an auxiliary or counter electrode (CE) at certain potential and is therefore referred to as amperometric gas sensor (AGS) in the following.

Amperometric sensing, in which current is measured at constant potential, belongs to the field of electrochemical analysis where in general current versus potential curves are investigated [105]. Amperometric sensors [106,107] are distinguished from potentiometric sensors, in which the potential is measured as signal at near zero current flow, or conductometric sensors, in which change in impedance is measured.

### 3.1.1. Amperometric gas sensors (AGS)

Amperometric gas sensors are based on the electrochemical oxidation or reduction of the analyte gas at a catalytic electrode surface that is in contact with an electrolyte, and operate on the same principle as liquid electrolyte fuel cells [108, 109].

The sensor is designed in such a way that the magnitude of the current generated by the electrochemical reaction of the analyte is directly proportional to the analyte concentration in the sample gas stream. Often, the mass transfer through the membrane is the main factor controlling the limiting current output of the amperometric gas sensor. Some aspects of this will be discussed in the two following sections.

### 3.1.2. Sensor structure

Figure 4 shows in a schematic drawing the operating principle and basic construction of a three electrode amperometric gas sensor as used in the

MOSES module. The reaction for detecting carbon monoxide as an analyte gas is shown here as example.

The sensor signal or current I deriving from the electrochemical oxidation is proportional to the partial pressure of CO ($p_{CO}$) measured at constant potential U. For two electrode sensors, the Clark electrode for oxygen being the earliest design [110], there is a constant potential between sensing and auxiliary electrode. The auxiliary or counter electrode should therefore be polarized in order to maintain the constant potential during the measurement. This problem is solved with a three electrode set-up in which a potentiostat keeps the potential constant between working and reference electrode.

The three electrode configuration guarantees precise operation even with microelectrodes.



anode reaction:
$$CO + H_2O \longrightarrow CO_2 + 2H^+ + 2e^-$$

cathode reaction:
$$\tfrac{1}{2}O_2 + 2H^+ + 2e^- \longrightarrow H_2O$$
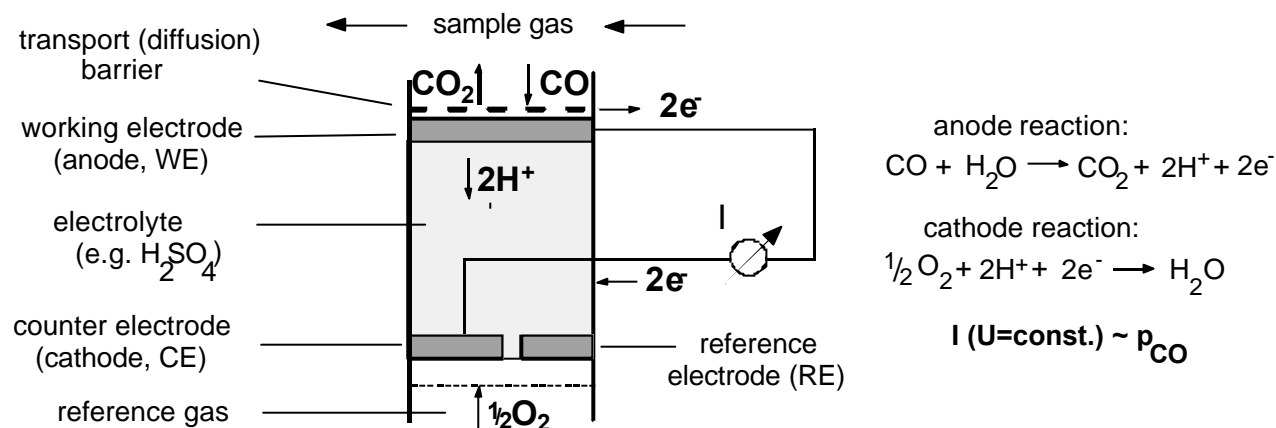
$$I\ (U=const.) \sim p_{CO}$$

*Figure 4: Schematic sensor structure of a three electrode amperometric gas sensor with CO as example for an analyte gas and the oxidation reaction to CO₂ as electrochemical reaction [111].*

The sensor consists of seven major parts:

An optional filter, a transport barrier, such as a membrane or capillary, an electrolyte, a sensing or working electrode (WE), a reference electrode (RE), a counter electrode (CE), and a potentiostat. Each part of the sensor influences the overall performance and analytical characteristic of the sensor.

The analyte gas may pass a filter prior to entering the sensor which removes unwanted substances or alters the analyte composition and thus improves selectivity and sensitivity to target analytes if needed.

The sensitivity of the sensor can be controlled by providing a mass transport barrier which limits the rate at which the analyte gas reaches the electrode

surface. The analyte gas diffuses through a mass transport barrier and then reacts on the catalytic electrode surface at the three phase boundary between the solid electrode, the liquid electrolyte, and the gaseous analyte. This transport barrier can be a membrane or a capillary. It prevents the leakage of the electrolyte allowing the analyte to diffuse to the working electrode. The transfer across the transport barrier is usually characterized by a Fick's type diffusion as expressed in equation. It is often designed to be the rate limiting process in sensor operation [107].

The electrolyte is often a concentrated aqueous solution of sulfuric acid or potassium hydroxide, which are most commonly used, depending on the sensor chemistry. The use of concentrated aqueous electrolyte minimizes problems caused by changes in humidity and by the evaporation of the aqueous electrolyte under conditions of low humidity apart from efficiently carrying the ionic current and solubilizing the analyte. Solid polymer electrolytes (SPE, e.g. Nafion) combined with the Teflon bonded gas diffusion electrode are a leak-free alternative design, applicable for certain target analytes [111,112,113]. Dissolution of the electrochemically active species in the electrolyte and liquid phase diffusion to the electrode interface follow and may also be rate limiting. Here, a diffusion limited process is usually described by Fick's and Faraday's law as expressed in equation (8) [107].

The adsorption on the electrode surface is followed by the electrochemical reaction and desorption of the products.

Typically, the working or sensing electrode consists of a layer of noble metal or other catalyst. Combined with carbon it is coated onto a hydrophobic membrane allowing gas diffusion and keeping the electrolyte in the cell.

The two remaining electrodes, the counter and reference electrodes, are located within the body of the device in the bulk of the solution.

The reference electrode, which is used to maintain the sensing electrode at a known electrochemical potential, is preferably not exposed and must be stable in the electrolyte.

The counter electrode completes the electrochemical cell by performing the half cell reaction, the nature of which is preferably in opposition to the sensing electrode reaction.

The measured current arises from the electrochemical oxidation or reduction of the target gas at the electrode surface. Some examples with the reactions at counter and working electrode are listed in Table 5.

| working electrode (anode) | counter electrode (cathode) | electro-catalyst | Ref. |
|---|---|---|---|
| $CO + H_2O \rightarrow CO_2 + 2H^+ + 2e^-$ | $1/2\ O_2 + 2H^+ + 2e^- \rightarrow H_2O$ | Pt | [114] |
| $SO_2 + H_2O \rightarrow SO_4^{2-} + 2H^+ + 2e^-$ | $1/2\ O_2 + 2H^+ + 2e^- \rightarrow H_2O$ | Au | [115] |
| $H_2S + 4H_2O \rightarrow H_2SO_4 + 8H^+ + 8e^-$ | $2\ O_2 + 8H^+ + 8e^- \rightarrow 4H_2O$ | Pt | [116] |
| $NO + 2H_2O \rightarrow HNO_3 + 3H^+ + 3e^-$ | $O_2 + 4H^+ + 4e^- \rightarrow 2H_2O$ | Au | [117] |
| $NO_2 + 2H^+ + 2e^- \rightarrow NO + H_2O$ | $H_2O \rightarrow 1/2\ O_2 + 2H^+ + 2e^-$ | Au | [118] |
| $Cl_2 + 2H^+ + 2e^- \rightarrow 2HCl$ | $H_2O \rightarrow 1/2\ O_2 + 2H^+ + 2e^-$ | Pt | [119] |

*Table 5: Reactions at working and counter electrode in amperometric sensors with common electro-catalyst and references for the reaction mechanism.*

The type of reaction, i.e. oxidation or reduction of the target analyte, determines the sign of the sensor signal. Also, the signal intensity can be estimated for sensors optimized for a specific reaction.

Finally, a potentiostat and associated electronics are part of the sensor operation. A potentiostat is used with the three electrode sensor to provide a fixed potential for the working electrode relative to the reference electrode in the electrolyte. Apart from applying a voltage bias to the working electrode the potentiostat is used to convert the sensor's current signal into a voltage signal for measurement. A simple circuit as shown in Figure 5 with two operation amplifiers U1 and U2 for converting current to voltage, maintaining the voltage at a selected potential (bias), and generating the current producing voltage at the counter electrode. It is completed in commercial sensor potentiostats by gain and offset (zero) adjustments, temperature compensation, and computer control.
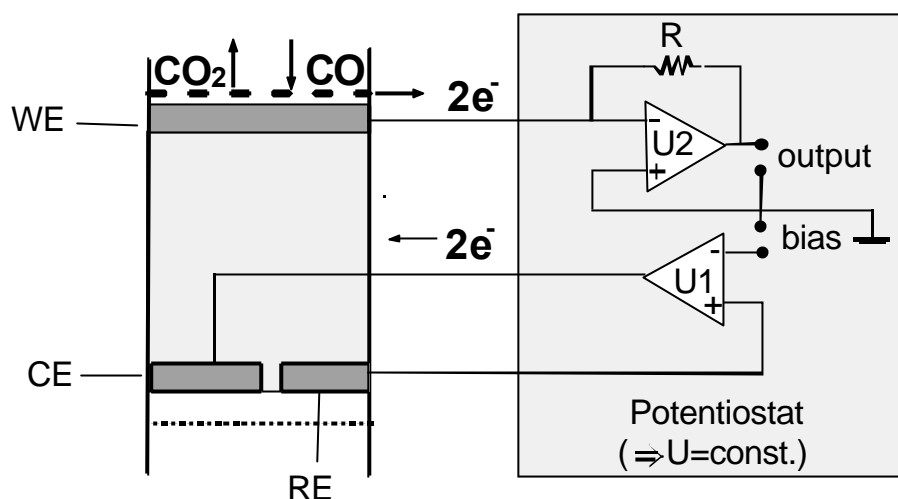
*Figure 5: Schematic circuit for an amperometric sensor potentiostat [107].*

The thermodynamic electrochemical potential at the working electrode, which can be obtained from the bias voltage setting between WE and RE, has a direct effect on the selectivity of the sensor.

Commercial electrochemical gas sensors are available for a wide range of toxic gases including $CO$, $H_2S$, $NO_x$, $O_2$, and $SO_2$. In each case the concentration of gas is determined by measurement of the current flowing in the sensor. Important for the analytical sensor characteristics and selectivity are the sample flow rate, the nature of the electro-catalyst (WE), the type of electrolyte, the porosity or permeability of the transport barrier, and the electrochemical potential of the working electrode.

Devices of this type have detection limits of the order of 0.1 ppm and response times of around 10s. In general, sensors of this type are quite selective, because of the mechanism they operate with.

The response characteristic of the sensor is determined by the rate limiting step in measurement. As stated before the sensor is preferably working in the "limiting current region" [106] in which the sensor signal is practically independent from the electrode potential.

### 3.1.3. Theory of the limiting current or steady state sensor response

The limiting current region is achieved by designing the rate limiting step occuring prior to electron transfer.

Provided that the working electrode is highly active for the oxidation or reduction of the analyte gas, the current is determined by the rate at which the

gas arrives at the electrode surface which, in turn, is limited by mass transport through the membrane or capillary. Thus, the output current is linearly related to the gas concentration.

The steady state models are based on Faraday's and Fick's law. Fick's law establishes the derivative of number of particles N over time t to be proportional to the concentration gradient of a species s over the direction of diffusion ($dC_s/dx$) with the diffusion coefficient D and the area A or cross section perpendicular to x is given by

$$\frac{dN(t)}{dt} = -D \cdot A \frac{dC_s(x)}{dx} \quad , \tag{2}$$

and Faraday's law, which relates the number of electrons to the current and is given by

$$\frac{dN(t)}{dt} = -\frac{I}{nF} \quad , \tag{3}$$

with the Faraday constant F, the number of electrons n, and the current I at x=0.

There several possibilities for the realization of the limited current $I_L$: If the current is limited by transport to the sensor from the outside world, or in other words the gas transport is limited by the transport barrier, the limiting current is given by

$$I_L = nFDA \frac{DC_s}{d} \tag{4}$$

Here $\Delta C_s$ is the gas concentration minus the concentration of the same compound in the sensor following the integration of equation 4 within the boundaries x=0 and x=$\delta$. Here, $\delta$ is the thickness of the membrane or the length of the capillary used as a mass transport barrier in the design of the sensor. Note that here D is the diffusion constant in the membrane or capillary and A the area of diffusion (cross section).

If the reaction within the sensor is fast compared to the mass transport, $\Delta C_s$ equals the gas concentration $C_s$ (equation 6).

Second, the rate of diffusion across the diffusion layer in the electrolyte to the electrode surface may be limiting the current. Then the current is given as

$$I = nFDA\frac{C_s^* - C_s(0)}{d} \qquad (5)$$

with the bulk concentration of gas in the electrolyte $C_s^*$ and the concentration at the electrode surface $C_s(0)$ for x=0, and the diffusion layer thickness $\delta$. There are two different diffusion coefficients, i.e. in the electrolyte and in the barrier. Here, D becomes the diffusion constant in the solution and A the area of the electrode surface. The concentration in the electrolyte is correlated to the gas concentration with the partition coefficient (see equation 1).

Provided that the working electrode is highly active for the oxidation or reduction of the analyte gas, the current is determined by the rate at which the gas arrives at the electrode surface which, in turn, is limited by mass transport through the transport barrier or is limited by diffusion across the diffusion layer in the solution. For the rate of charge transfer being very high the concentration at the electrode surface $C_s(0)$ will be zero:

$$I_L = nFDA\frac{C_s}{d} \qquad (6)$$

For mass transport controlled only by diffusion with

$$d = (2Dt)^{1/2} \quad , \qquad (7)$$

the limiting output current is linearly related to the gas concentration by the Cottrell equation:

$$I = \frac{nFAD^{1/2}C_s}{2^{1/2}t^{1/2}} \qquad (8)$$

For microelectrodes the '2' in the Cottrell equation for planar diffusion is replaced by '$\pi r$' for radial diffusion.

For a constant potential applied if no stagnant diffusion or depletion layer (Prandtl layer) is allowed to build up at the electrode surface, the limiting current $I_L$ can be expressed by

$$I_L = nFAm_sC_s \quad , \qquad (9)$$

with the mass transport coefficient $m_S$, which is regarded as constant at constant temperature. For sensing purposes, a constant potential in the region of the diffusion limiting current is applied to the working electrode [120]. Equation 9 gives the current vs. gas concentration relation for the operation of amperometric gas sensors for both cases of diffusion limited current. Thus, the limiting current is proportional to the gas concentration.

If the rates of diffusion are much faster than the rate of reaction, then the current is controlled by the electrode kinetics. The current can be expressed by

$$I = nFKAC_A^l C_B^m \cdot e^{\frac{\alpha F}{RT \eta}} ,$$
(10)

where K represents the standard rate constant, the superscripts *l* and *m* express the order of the reaction for the concentrations of reactants A and B, $\alpha$ the transfer coefficient, and $\eta$ the overvoltage of the reaction [106]. The $NO_2$ gas sensor with low surface area gold electrode is an example for this behavior [88].

Each of the above equations for the relation of output current to the gas concentration predicts a linear sensor response.

Theory and modeling are discussed in [106] and [120], but a complete model for many gas phase electro-catalytic systems does not yet exist. Sensor output and characteristics are optimized by design and calibrated on species of interest.

### 3.1.4. Application of amperometric gas sensors in e-noses

An overview of amperometric gas sensor applications is given in [106, 107] and therein. Amperometric gas sensors show a number of favorable characteristics for operation in arrays e.g. reliability, ruggedness, linear response, low drift, and high sensitivity mostly limited by the noise and background current. One of the first e-noses were amperometric sensors in an array in the 'Stetter nose' [1, 82, 121, 122]. An advantage for modular e-noses is that amperometric sensors do not show cross sensitivity to water over a large range of relative humidities in contrast to several other transducer types [123]. Disadvantages in e-noses are the size of the amperometric sensor and a high selectivity for a limited number of permanent gases [108].

## 3.2. Fundamentals of chromatographic separation

Physical separation procedures based on the principle of partitioning constituents of a sample by their distribution between two immiscible phases,

i.e. a mobile phase which alone is responsible for the mass transport and a stationary phase, are called chromatography. The molecules are separated on the basis of differences in the strengths of interaction with the stationary phase. A quantitative measure of these interactions is represented by the partition coefficient K.

It is estimated that approximately 60% of all analyses worldwide can be attributed to chromatography [100]. The two most important separation principles in the passage between mobile and stationary phase are distribution and adsorption. Distribution chromatography is based on the different solubility of analytes in two phases. Adsorption chromatography is based on the direct interaction of the analyte with the surface of the solid stationary phase, the adsorbent. An example is gas chromatography (GC). Adsorption and desorption phenomena as basis for adsorption chromatography are discussed in [124] and references therein. The following short reflections on the fundamentals of chromatography will focus on column chromatography.

### 3.2.1. Theory of theoretical plates

In the classic theory of chromatography the chromatographic column is understood as the logical transposition of identical discrete partition steps or theoretical plates H (i.e. height equivalent of a theoretical plate). A substance i will move from one separation stage or discrete equilibrated mobile phase volume to the next. In each of these smallest volume elements an equilibrium between phases is established, substance i will be partitioned between the mobile and the stationary phase. In the simplest case, the passage of analyte molecules between the mobile phase m and the stationary phase s is determined by a partition equilibrium with partition coefficient K (see also equation 1), with the concentrations $C_i$, particle numbers $N_i$, and volumes $V_s$ and $V_m$ for a compound i, K is given by

$$K = \frac{C_{i(s)}}{C_{i(m)}} = \frac{\dfrac{N_{i(s)}}{V_s}}{\dfrac{N_{i(m)}}{V_m}} , \qquad (11)$$

After a multitude of these steps two compounds i and j will be separated in the mobile phase eluted from the column as peaks at two discrete retention times $t_{Ri}$ and $t_{Rj}$. The differences in retention time are due to differences in the

interaction with the stationary phase. Thus, the continuous chromatographic process is seen as a sequence of many discrete steps of adsorption or dissolving in the stationary phase and desorption or elution in the mobile phase.
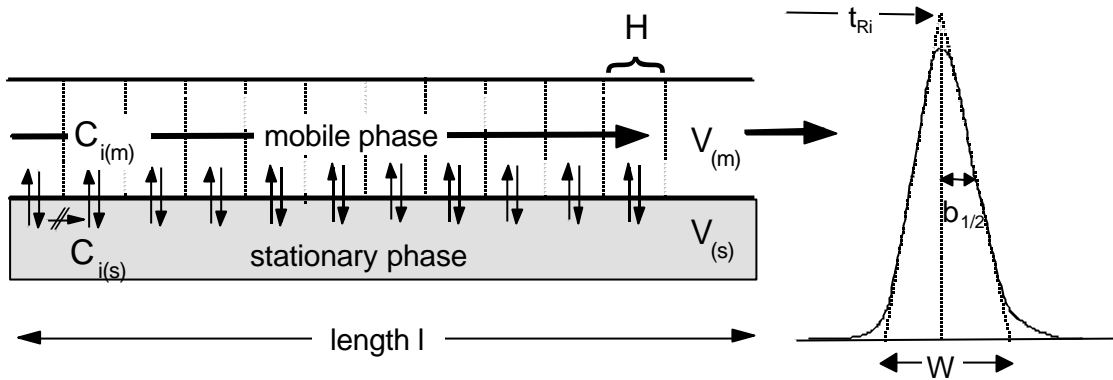


*Figure 6: Schematic drawing of a chromatographic column and an eluted peak.*

The number of theoretical plates N results from the height equivalent to the theoretical plate ‚or short plate height H, and the length of the column l as

$$N = \frac{l}{H} \ .$$

(12)

The number of the theoretical plates is calculated from the peak profile. Ideally, the detector signals for the compounds eluted with the mobile phase or peaks, have the form of a Gaussian distribution curve. After N equilibria in the migration distance part H the peak variance $\sigma_l^2$ (in $cm^2$) is given by:

$$\boldsymbol{s}_l^2 = H \cdot l \qquad \text{or} \qquad H = \frac{\boldsymbol{s}_l^2}{l}.$$

(13)

In other words the height equivalent to the theoretical plate H is defined as ratio of the peak broadening to the column length or retention time respectively. To obtain the relationship between the variance of the peak, and the plate height with the retention time $t_R$ at the peak maximum, the variance is transformed in time dimension $[s^2]$ resulting in

$$H = \frac{\boldsymbol{s}_t^2 l}{t_R^2}$$

(14)

For a Gaussian partition the base line peak width W, determined from the intersection of tangents to a Gaussian curve with the baseline, or width at half maximum $b_{1/2}$ for unsymmetrical peaks, is a function of the peak variance $\sigma_t$:

$$W = 4s_t^2 \ . \tag{15}$$

Therefore, the relationship between the baseline width of the peak W, the migration distance or length l, the retention time $t_R$, and the plate height H follows

$$H = \frac{W^2}{16} \frac{l}{t_R^2} \ . \tag{16}$$

The number of theoretical plates N calculated from the width at half maximum $b_{1/2}$ is given by

$$N = 8 \ln 2 \cdot \left( \frac{t_R}{b_{1/2}} \right)^2 . \tag{17}$$

The peak width becomes smaller with more theoretical plates, or, the lower the plate height is, the higher is the obtainable resolution and, therefore, the column efficiency. However, the plate theory merely represents an approximation of the process in the column, the repeated establishment of separate equilibria is often unrealistic. When plate theory and the number of plates is used for comparing columns, this should only be done for the same sample substance.

In practice, the chromatogram is used for directly determining the number of theoretical plates with the measured width at half peak maximum and the retention time.

### 3.2.2. Characteristic values of a chromatogram

A chromatogram is the recording of detector signals as function of elution time or elution volume in column chromatography. As described earlier, compounds traveling through the column have a specific migration rate determined by the retention in the stationary phase and thus by the partition coefficient K.

The partition coefficient giving the concentration ratio in the two phases cannot directly be deduced from the chromatogram. But with the concentration correlated to the time a compound is retained in the two phases over the length

of the separation column, K allows for conclusions about the chemical nature of the compound.

The chromatogram shows the detector signals for the compounds eluted with the mobile phase as Gaussian curves or peaks. These peaks carry quantitative and qualitative information. Figure 7 schematically shows the peaks for an inert unretained substance, an analyte i, and a further compound j, which may be a reference, in a chromatogram.
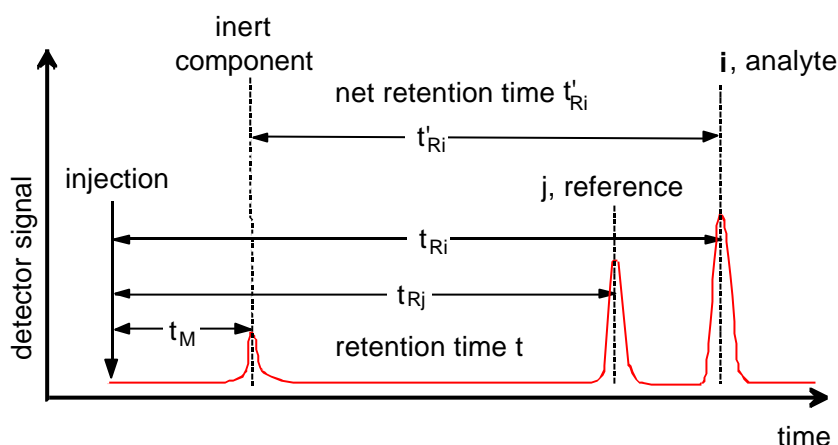


*Figure 7: The chromatogram and its characteristic values.*

Qualitative information can be obtained from the retention times: The retention time $t_{Ri}$ of a compound i is the time span from injection to the registration of the maximum of the peak for substance i. The retention time $t_R$ is constant for constant chromatographic operation parameters and therefore allows identification of a compound using a standard as reference. The small, first peak at retention time $t_M$ (dead time) arises from an inert compound not retained at all and corresponds exactly to the time required for molecules of the mobile phase to pass through the column. It is the so-called dwell time of all components in the mobile phase. Therefore, the linear velocity u for molecules of the mobile phase is proportional to the length of the column l and is given by

$$u = \frac{l}{t_M} \quad .$$

(18)

The average velocity for analyte migration $\overline{v}$ then is:

$$\overline{v} = \frac{l}{t_R},\tag{19}$$

with a retention time $t_R$. The difference between total retention time $t_R$ and dead time $t_M$ is the adjusted or net retention time $t_R'$. For a compound i $t_{Ri}'$ gives the time it is retained in the stationary phase referred to as residence time of compound i in the stationary phase.

With a constant flow J [ml/min] of the mobile phase, $t_R$ is directly proportional to the retention volume $V_R$, which in turn is the amount of mobile phase molecules passing the system until half of the compound amount is eluted:

$$V_R = t_R \cdot J \ .\tag{20}$$

In order to obtain a comparable parameter independent of flow and column length, the adjusted retention time is divided by the dead time yielding the capacity factor k', which is then given by

$$k' = \frac{t_R - t_M}{t_M} = \frac{t_R'}{t_M} = K \cdot \frac{V_s}{V_M} = \frac{K}{b} \ .\tag{21}$$

The capacity factor k' is directly correlated to the partition coefficient K. It is proportional to the volume of the stationary phase $V_S$ and reverse proportional to the volume of the mobile phase $V_M$. The volumes of the phases give the phase ratio $\beta = V_M / V_S$. Thus, the capacity factor correlates the migration rate with partition coefficient and retention time of a compound. The retention capacity of a column k' is small for capillary columns compared to packed columns because of the higher phase ratio $\beta$, making the use of longer columns with higher separation capacity possible whilst keeping the time for an analysis constant. A capacity factor of k' = 5 would mean that a substance elutes after five times the dead time (single plus fourfold dead time).

For two compounds i and j a measure for their relative retention and therefore for their separation is now given by the separation or selectivity factor $\alpha$ as:

$$a = \frac{k_i'}{k_j'} = \frac{t_{Ri}'}{t_{Rj}'} = \frac{K_i}{K_j} \ . \qquad (k_i' > k_j' \ ; \ \alpha \geq 1)\tag{22}$$

The separation factor gives the selectivity of a column for two compounds. A separation factor $\alpha = 1$ means that the two components will not be separated

(co-elution). The selectivity of a method is the ability for detecting a compound in a complex matrix without interference from other compounds present. The more selective the stationary phase of a column retains one of the compounds of a mixture, the bigger is the differences in retention times and, therefore, the magnitude of the separation factor.

The chromatogram also contains quantitative information. The area of the peaks are proportional to the amount of analyte compound in a sample. Thus, unknown quantities can be determined by correlation with peak areas from known concentrations [125, 126, 127].

### 3.2.3. Kinetic theory

As stated earlier, eluted peaks ideally have the form of a Gaussian curve. A simple explanation for a peak broadening is the differing path length for the analyzed compounds through the separation system (multipath effect) caused by diffusion processes (Eddy-diffusion). Figure 8 schematically indicates the peak broadening and distribution of three compounds A, B, and C in the flow direction x and in the direction z of a cross section perpendicular to x.
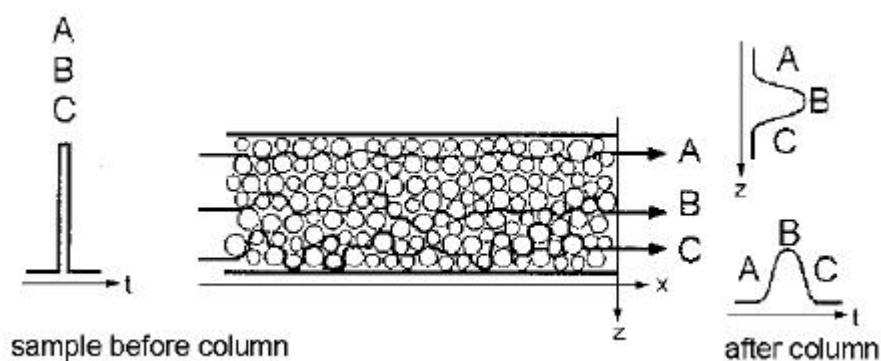


*Figure 8: Schematic Eddy-diffusion in packed columns (multipath effect, peak broadening) [21].*

Peak broadening results from a kinetic effect, which is deriving from the finite rate at which mass transfer processes occur during the analyte migration. The extent of this effect depends on the duration of possible passages between phases and thus is proportional to the flow rate of the mobile phase. On the other hand diffusion within the mobile phase, which also leads to peak broadening, is prevented by high flow rates. The flow rate, therefore, has to be optimized to obtain the maximum number of theoretical plates in the shortest analysis time possible.

The Van Deemter theory states that plate height and the number of theoretical plates depend on the flow or linear velocity for molecules of the mobile phase (see equations 17 and 22) [21]. The Van Deemter equation as an empirical model in the simplest form is given by:

$$H = A + \frac{B}{u} + C \cdot u \qquad , \qquad (23)$$

with the linear velocity for molecules of the mobile phase u and constants for Eddy diffusion (A), longitudinal diffusion (B), and mass transfer phenomena between phases (C), all for one specific system. A minimal plate height and a maximum plate number are realized if all constants are as small as possible. Figure 9 illustrates the Van Deemter curve as resulting function of the listed phenomena.
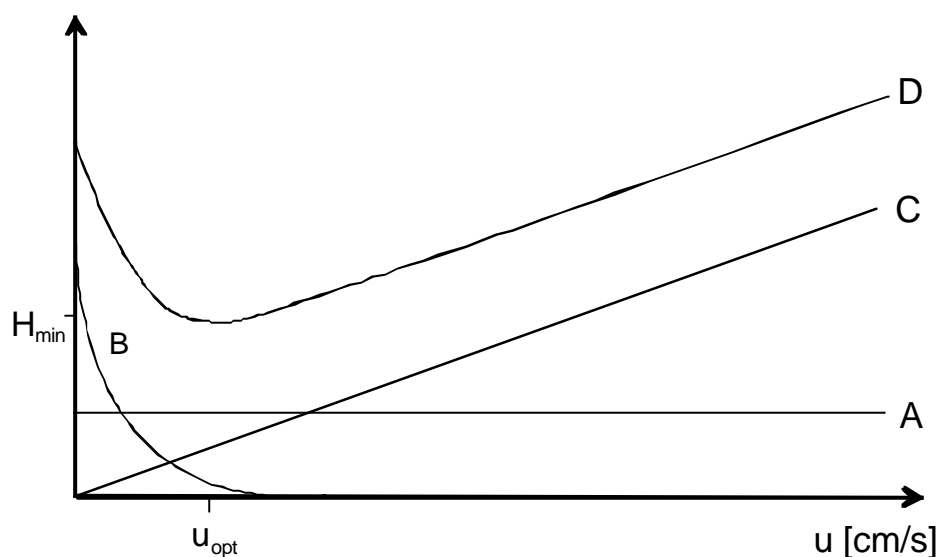


*Figure 9:   Van Deemter curve (D) showing the plate height H as function of the flow velocity u with contributions from influencing dynamic phenomena (A, B, and C)*

The Van Deemter curve (D) is determined empirically with its minimum indicating the optimal flow rate $u_{opt}$ and minimal peak broadening. Therefore, the minimum velocity of the mobile phase is given by:

$$u_{min} = \sqrt{\frac{B}{C}} \quad , \qquad (24)$$

as first derivative of equation 23. With C corresponding to the slope of the Van Deemter curve at high flow rates, equation 24 also allows the determining of C. The minimum plate height $H_{min}$ is then given by

$$H_{min} = A + 2\sqrt{B \cdot C} \, . \tag{25}$$

The optimal flow rate is not influenced by Eddy diffusion (linear A term) in open tabular or capillary column where there is no or little volume packed with the stationary phase. Here, A will be close to zero. A is independent of the mobile phase.

The longitudinal diffusion B is the only term independent from the particle size of the stationary phase. B is directly proportional to the diffusion coefficient of a substance in the mobile phase and, therefore, temperature dependent. B is important for gas chromatography and inversely proportional to the flow rate.

Term C describes the mass transfer to and from the stationary phase. For a solid stationary phase C depends on the rate of the adsorption and desorption processes.

In chromatography the goal is an efficient separation in short analysis time. In practical application the above described optimization of parameters is achieved by small particle size solid stationary phases or low liquid film thickness, a homogeneous and dense column packing, a small column diameter, and large diffusion coefficients in the stationary phase whilst keeping diffusion coefficients in the mobile phase low by operating at low temperatures.

### 3.2.4. Resolution and capacity

For evaluating the selectivity of two constituents in chromatography the selectivity factor $\alpha$ (see equation 22) describes the phase system used. In order to characterize the selectivity of the whole chromatographic system and taking into account the number of theoretical plates and therefore the efficiency of the system, the chromatographic resolution $R_s$ is used. For similar peak widths for two compounds $W_i \approx W_j \approx W$ the resolution corresponds to the ratio of their difference in retention times to the base peak width:

$$R_s = \frac{D t_R}{W} \, . \tag{26}$$

The peak width of a chromatogram thus determines the resolution. Insertion of equations 16 , 21, and 22 and, simplified for similar capacity factors $k_i' \approx k_j' \approx k'$, gives the resolution:

$$R_s = \frac{1}{4}(a-1)\frac{k'}{1+k'}\sqrt{N} \qquad (27)$$

$$\text{I} \qquad \text{II} \qquad \text{III}$$

Based on the dependencies of the resolution, separation can be optimized for the variables, which can be altered fairly independently from one another, indicated by the three terms I, II, and III in equation 27.

$R_s$ is directly proportional to the selectivity term (I). Optimization of the selectivity by lowering the temperature or the selection of a better suited stationary phase is the most effective way of improving separation performance. The retardation term (II) gives the dwell time of a component in the stationary phase and is also temperature dependent. The dispersion term (III) can be optimized through the column length, compromising on analysis time and plate height. In practice, for equally intensive symmetrical peaks a resolution of $R_s = 1$ or $4\sigma$ resolution means a 94% separation for Gaussian curves, a $6\sigma$ resolution ($R_s = 1,5$) means baseline separation and is considered to be optimal.

The peak capacity of a column is limited. The peak capacity reflects the maximum number of peaks which can be resolved. According to Giddings the peak capacity n can be calculated approximately to

$$n = 1 + \frac{\sqrt{N}}{4} ln \frac{V_R^n}{V_R^1} \text{ ,} \qquad (28)$$

with $V_R^1$ and $V_R^n$ signifying the retention volumes of the peaks eluted first and last, respectively. If the number of constituents exceeds the peak capacity, peaks will overlap.

### 3.2.5. Gas chromatography

In gas chromatography the compounds to be analyzed are vaporized and eluted with a carrier gas as mobile phase from the column. Interactions of the mobile phase with the analyte are of no significance, the carrier gas is inert. In order to take into account the influence of pressure and temperature, retention volume is often employed instead of retention time (see equation 19).

In previous equations, the retention time can be replaced with the ratio of retention volume to flow with the carrier gas flow J in ml/min. For the compensation of pressure variations of the volume a correction factor to the retention volume must be used in calculations.

### 3.2.6. Columns

The predominant separation principle in gas chromatography is the partition of substances between a liquid stationary phase and the gaseous mobile phase. In capillary gas chromatography, thin film or thin layer fused silica capillary columns allow for column lengths of up to 100m and thus theoretical plates of up to 100 000 can be realized. The stationary phase, which has to be thermally and chemically stable, selective and of low volatility to avoid bleeding, can be chosen from a variety of phases to match the analyte requirements [20, 100, 128]. These phases often contain functional groups determining their polarity.

In adsorption gas chromatography separation occurs by adsorption/desorption processes with a solid stationary phase. Advantages to partition chromatography are the wide temperature range, rapid equilibration steps, and a good base line stability. Disadvantages imply asymmetric peaks due to the small linear range of the adsorption isotherm, long retention times, heterogeneous surfaces of many adsorbents, and a limited number of adsorption media, which are difficult to standardize [100]. Common adsorption media for gas chromatography are polymers based on (functionalized) PDMS, which is also used as sensitive layers for chemical sensors [22], or polymerized polyethylene glycols (PEG), molecular sieves based on carbon or silicates, and silica gels. Sorbents applicable also for preconcentration are listed in chapter 2.2.5 (Table 3), properties and brand names are listed in supplier catalogues [129,130].

### 3.2.7. Practical chromatography

Apart from deviations from the classic theory behavior described in the previous models for chromatography, e.g. kinetic effects, and especially gas chromatographic separation is influenced by pressure, adsorption/desorption characteristics, the activity coefficients of the analytes, and various instrumental parameters described in detail in literature [100]. As a rule, the reproducibility of retention data is considerably less than that of data obtained with other spectroscopic techniques. Chromatography alone allows for analysis, e.g. with column parameter independent retention indices after Kovats [100]. However, often the coupling with a spectroscopic or highly selective system, e.g. mass

spectroscopy, ensures the analytical performance (see hyphenated systems in chapter 2.4).

One supposition, usually made for theoretical considerations about the chromatogram and especially the peak form, is, that the detector responds relatively fast to the eluted analyte. If chemical sensors or sensor arrays are used as detectors together with a chromatographic system, the response time, chamber volume, and selectivity of this system also have to be considered when evaluating a chromatogram.

### 3.2.8. Thermodesorption

Extensive research has been devoted to the behavior of VOCs on solid sorbents. Comparative studies give data on the chromatographic behavior of different sorbents used for preconcentration [40,50,59-61,131]. Theoretical models for sorption properties of trap materials are published for various operating parameters [60,132,133] and experimental results for the capacity of these trap materials are available [29,63,99,134]. However, within these publications different definition of terms and, depending on the mode of operation, different models for the prediction of trap attributes are used. For a characterization of sorbent properties in thermal desorption it is necessary to precisely define the operating conditions and thus the definition of terms describing trap performance [135].

3.2.8.1.    Breakthrough volume

For the characterization of adsorbent beds used in thermal desorption and for the selection of trapping material and its optimal amount for a given application the breakthrough volume $V_B$ is used. The breakthrough volume $V_B$ is the volume of air that can be drawn through the sampling tube without appreciable analyte loss in the effluent or breakthrough. Thus it characterizes the capacity of trap.

It is necessary to distinguish two principle modes of operation of traps and measurement procedures and consequently two definitions of the breakthrough volume, although often the term $V_B$ is used inchoately for any sampling on solid sorbent material.

In the simplest case a very small amount of a single analyte is trapped after a single injection and subsequently thermally desorbed, e.g. in the case of sample application with an headspace sampler. The second case is continuous vapor assault for a given enrichment time and/or high concentration gas mixtures, e.g.

in the case of sample accumulation in air contaminant analysis. The latter case will be discussed in the following chapter (3.2.8.2).

The breakthrough volume is defined as the volume of carrier gas that causes the analyte molecules to migrate from the front of the adsorbent bed to the back of the adsorbent bed. Figure 10 schematically shows a thermodesorption tube with adsorbent resin and the breakthrough volume $V_B$, the retention volume $V_R$, and the total elution volume $V_F$ for a small narrow plug of an analyte.
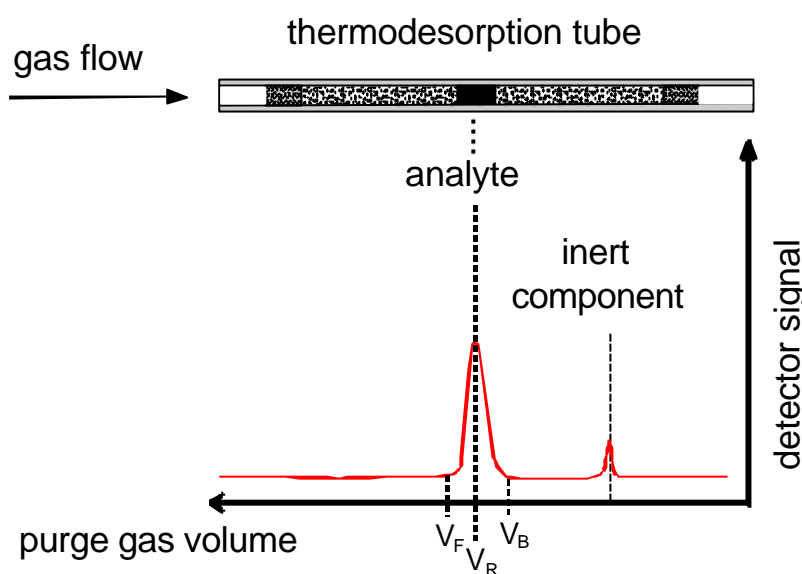


*Figure 10: Schematic diagram illustrating of the determination of the breakthrough volume.*

Note that the assumption that a small narrow plug of the analyte migrates through the adsorbent resin bed is valid only for direct injection or injection from an headspace sampler, but is not valid the case when collecting air samples or purging gas samples from liquid or solid samples, which is broadening the peak substantially.

A resin bed of a thermodesorption trap essentially is a chromatographic column in which an analyte is injected onto the front of the resin bed and then purged with carrier gas at a constant flow rate to be eluted; ideally detected as peak with a Gaussian partition which broadens as it migrates through the resin bed.

In this simplest case the breakthrough volume $V_B$ can then be calculated from the retention volume $V_B$ or form the retention time $t_R$, respectively, by multiplying the adjusted retention time, at peak maximum, with the flow rate in ml/min to determine the net retention volume $V_R'$ (equation 21) and then subtracting half of the effluent.

For compounds strongly retained in the sorbent bed retention property measurements are extrapolated to sampling temperature, which in general is room temperature, assuming a linear relationship which is not necessarily valid [29,135] (see also chapter 3.2.8.2).

With equations 12,17 and 20 to 28, $V_B$ can be determined indirectly [61,133]:

$$V_B = V'_R \cdot \left( 1 - \frac{2}{\sqrt{N}} \right),$$ (29)

with the number of theoretical plates N for each substance and for a specific trapping temperature. The vapor of a compound, which has been quantitatively adsorbed, is eluted when the gas volume flowing through the adsorbent tube is equal to its retention volume less the volume corresponding to the elution of half of the solute band.

For characterizing the properties of a sorbent independent from a given preconcentration set-up, the breakthrough volume $V_B$ is divided by the weight of the adsorbent resin packed in the tube $m_A$ in gram yielding the specific breakthrough volume $V_{BS}$:

$$V_{BS} = \frac{V_B}{m_A} \ .$$ (30)

Here, the specific breakthrough volume is defined as the calculated volume of carrier gas per gram of adsorbent resin which causes the analyte molecules to migrate from the front of the adsorbent bed to the back of the adsorbent bed and is usually expressed in liter per gram [25,60,136,135]. Depending on operating conditions the calculated value has to be corrected for temperature differences of sample gas and adsorbent, pressure drop over the trap or compressibility, and a geometric factor in practical application [60]. The specific breakthrough volume $V_{BS}$ is then given by:

$$V_{BS} = \frac{V_B}{m_A} \cdot \frac{T_S}{T_G} \cdot \frac{3 \left( p_i/p_0 \right)^2 - 1}{2 \left( p_i/p_0 \right)^3 - 1} \ .$$ (31)

Here are $T_S$ and $T_G$ the temperatures of the sorbent and the gas in Kelvin and $p_i$ and $p_0$ the pressure in Pascal in the front and in the back of the trap, respectively. The required conditions under which the correction terms can be neglected vary in literature [59-61,131-135] as much as the breakthrough volumes. Therefore, $V_B$ should also be determined empirically for a given experimental set-up (see section 5.4.2).

The chromatographic properties of a sorbent described by the breakthrough volume and the effects of parameters such as tube temperature, analyte boiling point (b.p.), and analyte vapor pressure have been determined for sorbents with specific breakthrough volumes calculated indirectly with equation 29. By correlating properties of chemicals to their specific breakthrough volumes for sorbents the prediction of sorption behavior of analytes is possible. It is reported that the specific breakthrough volume of Tenax is increasing linearly with the reciprocal value of trap temperature and with the boiling point of an analyte within a class of chemicals of similar polarity [60].

As stated previously the model is valid only for the assumption of small focussed concentrations of analyte migrating solitarily through the trap, which is not the case for operation in air collection. In more recent literature, therefore, the term 'safe sample volume' $V_S$ has been suggested to be used instead of breakthrough volume as distinction when vapors are continuously applied or are present in high concentrations [135].

### 3.2.8.2.   Safe sample volume

Safe sample volume calculations may be distorted by several parameters. The width of the peaks are a function of sample volume injected and injection time, i.e. $V_S$ is concentration dependent. Competition for the active sites of the adsorbent resin for continuously added analytes will cause a decrease in the breakthrough volume. The same effect can occur with sample overloading or excessive flow rate. The effect of humidity from samples is negligible unless water is condensing in the adsorption process.

$V_B$ is reported to be independent from analyte concentration but premature breakthrough was observed above 50 or 100 ppm of continuously sampled vapor [29,59,61], but also concentration dependency for analyte content exceeding 1 ppm has been published [136]. For continuous sampling of analytes in high concentrations Langmuir derived equations for the prediction of solid adsorbent safe sample volumes for a component *i* in a mixture can be used [136]. This relation is given by:

$$V_{iS} = \frac{m_{i\,max} \cdot K_i}{1 + \sum (C_j\,K_j)},$$

(32)

where $m_{max}$ is the adsorption capacity, K is the distribution coefficient between solid and gas phase, and $C_j$ are the concentrations of other constituents present.

The model assumes that the gas/solid interaction in thermal desorption tubes is governed by a Langmuir sorption process. Reported data show the usefulness of this approach in comparison to empirical data [132]: The logarithmic retention volume is linearly increasing with the boiling point and the enthalpy of desorption within a class of chemicals and decreasing with the vapor pressure and can thus be predicted by known thermodynamic data. Safe sample volumes are correlated to adsorption isotherms of compounds on a sorbent [135,136].

Measurements of breakthrough or safe sample volume data under continuous sample exposition with detection of a first detectable part of the effluent analyte, usually 5%, are referred to as direct measurements as distinction to the indirect method using retention times.

In this work thermal desorption was used in conjunction with an headspace sampler providing one or more single injections of analytes in small concentrations. Therefore, models for continuous sampling of high concentrations are not further discussed. Models and theory for the latter can be found in [50,132,136].

Nevertheless it is important for the practical use of thermal desorption to ensure that the model for the prediction of trap performance with its limitations matches empirical measurement data and therefore is applicable to a given set-up and application. Despite the possibility of describing breakthrough data theoretically, the variations in published data and comparisons of values derived using direct and indirect acquisition differ over one order of magnitude [132,135]. This shows, that empirical determination is indispensable (see chapter 5.4.2 and 5.4.3).

### 3.2.8.3.  Practical thermal desorption

Data tables on breakthrough volumes are published for different resins and analytes as a function of temperature [134]. These data are helpful for the practical use and choice of adsorbent resins and the selection of both adsorption and desorption parameters.

The known breakthrough volume determines the maximum carrier gas volume used in sampling and therefore, the maximum sampling time, whereas the minimal adsorption time, the gas volume, and also the trap loading weight and adsorbent type is determined by the detection limit of the analytical instrument.

To optimize thermodesorption sampling in practice, the safe sample volume $V_S$, and the complete sample elution volume $V_F$ are used to determine operation parameters and trap properties for adsorption and desorption, respectively. Both of these gas volumes can be predicted within the limitations of the models described above from the determined retention or breakthrough volume data.

With knowledge of the three volumes $V_S$, $V_R$, and $V_F$ a thermodesorption set-up can be used not only for quantitative preconcentration ($V_S$), but also for controlled chromatography ($V_R$) with separated samples completely eluted one at a time ($V_F$) in an idealized operation, or at least sufficiently separated for evaluation with a chemical sensor array (see section 5.4.3).

## 3.3. Introduction to multicomponent analysis

In order to acquire useful qualitative or quantitative information on samples investigated with an electronic nose, the sensor responses to the headspace content of each mixture have to be evaluated by statistical or mathematical techniques. This data analysis, the so called chemometrics, is described in several textbooks and publications [4,100,128,137,138,139]. This chapter gives only a brief overview of the techniques used in this work.

The different steps required to obtain an analytical information on M samples from the electrical signals generated from N sensors are described in the following. In Figure 1 in chapter 1, two of these steps, feature extraction and pattern recognition, are schematically shown as part of the overall analysis.

An array of N sensors will respond to M samples by generating multivariate data consisting of the responses of each sensor n to each sample i, forming a matrix of sensor responses $\mathbb{S}_{NxM}$.

The information content of the complete sensor signal curve is highly redundant. Therefore, it is not necessary to use the entire curve. One or more characteristic numeric values describing the sensor response are extracted, the so called features $x'_{ni}$.[140]. The descriptive values used for feature extraction depend on the sensor response characteristics. Examples are values obtained from the sensor in equilibrium or static signal properties, e.g. height, area, time dependent values, etc., or transient features like the response slope.

The feature space defined by the sensor array will have the dimension of N multiplied with the numbers of features extracted from each sensor [140]. An additional feature from a measurement can be seen as a more or less correlated additional sensor, depending on the feature.

For simplicity reasons in the following paragraphs it is assumed that only one feature is extracted from each signal. Then, the feature vectors $x'_{ni}$ form a matrix $\mathbb{X}'_{NxM}$ or a multidimensional feature space in which each measured sample is represented as a point.

### 3.3.1. Data preprocessing

Before entering a pattern recognition (PARC) engine, the data extracted from the sensor responses often have to be preprocessed. Techniques used for preprocessing include weighting and normalizing of the sensor responses [141].

Weighting or scaling multiplies each vector by a constant, thus manipulating its influence on the evaluation model. In a hybrid sensor system different types of transducers, e.g. MOX, QMB, and AGS, are generating signals measured in different scales. The signals can be standardized by dividing each vector by the standard deviation of that variable. This guarantees, that all sensors have the same impact on the analysis. Standardizing removes weighting that is artificially imposed by the scales of the variables. But it can also have adverse effects like enhancing the noise on sensors that produce little or no signal but are treated as being of equal importance in the following pattern recognition [4].

Normalization removes sample to sample absolute variability, putting it on the same scale by dividing each vector by the variable range, or in other words forcing the vector length to be one. Normalization also eliminates concentration information, which is only useful if, e.g. fluctuations in sample injection volume are to be disregarded. But normalization holds the assumption that the extracted features linearly correlate with signal intensity, which is not always the case [139]. It should be stressed, that the intensity of an odor signal often provides valuable information. Using normalization in the limiting case can lead to a scattering of vectors over the entire surface of the feature space only by displaying random noise [4].

Preprocessing can eliminate random or systematic sources of variation masking the variation of interest but it always changes the data set and, therefore, the information output of the system [142].

## 3.4. Pattern recognition

Pattern recognition (PARC) allows the identification and qualitative analysis of constituents of a complex mixture [22]. The following descriptions focus on the techniques employed within this work.

### 3.4.1. Principal component analysis (PCA)

PCA is used to depict data in a graphical representation which describes a majority of the variation in a data set. Therefore, the data set is plotted in a minimal new set of axes, which represents a maximum amount of variation. The co-ordinate axes of the newly defined space, the new feature space, are formed by linear combination of the original axes and need to be uncorrelated or orthogonal. One axis, or base vector, represents one virtual quality independent of all others and is called principle component (PC). The first axis is chosen in a way that it represents the direction along the largest variance, the second axis shows the second largest variance, and so on [143].

The reduction of the dimension required to visualize the data is a powerful tool for studying multi-dimensional data sets, for preliminary data exploration, and for the examination of data sets for clusters or outliers [139]. It is attempted to represent the data in two or three dimensions to visualize the similarities or dissimilarities in the investigated sample set. In most cases, it turns out that at least 80 percent of the information available can be displayed using only two dimensions [140,141].

If cross sensitivities exist between the sensors, their output values, i.e. the variables, are at least partially correlated. This means that the actual dimensionality of the data space is typically smaller than the maximum dimensionality defined by N times the number of extracted features. Principal component analysis (PCA) is an algorithm used to find the optimal representation of the given data set in a space of reduced dimensionality.

A scatter plot where the samples are represented by points distributed in the dimensions of the principal components is called 'scores plot'. The distance between points (Mahalanobis distance, see [139]) corresponds directly to their overall likeliness.

The plot of the features on the plane spanned by the PCs is called 'loadings plot' and shows the contribution of the features to the calculation of the PCs. By evaluating the loadings plot redundant features or sensors not contributing to the evaluation can be chosen for removal. Features displayed close to the origin

3. Theory

of the loadings plot have little influence; features close to each other or under the same angle (also mirrored in center) carry redundant information [138].

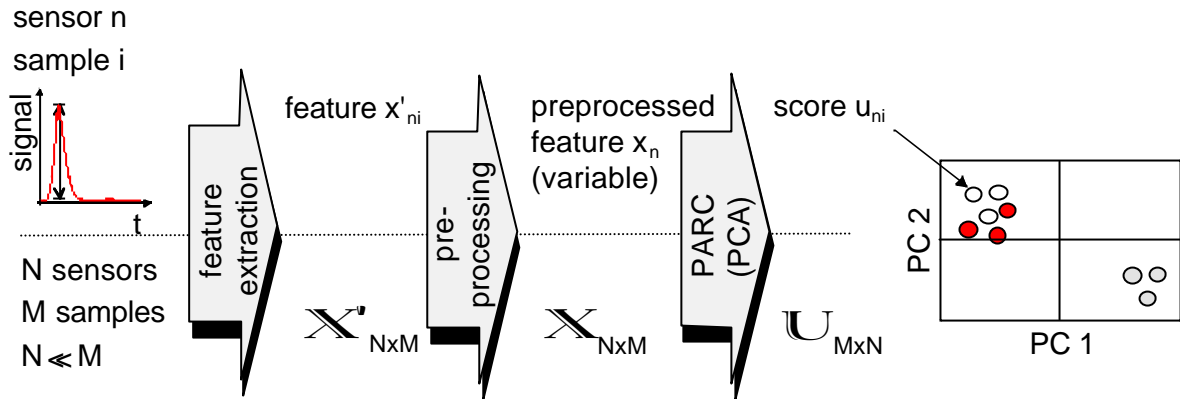Figure 11 gives a schematic overview of data analysis with PCA as used in this work.



*Figure 11: Schematic diagram of data analysis with PCA, description see text.*

### 3.4.2. Mathematical procedure

The underlying premise in PCA is that the raw data can be decomposed into eigenvectors and associated eigenvalues [141].

For a number of samples M greater than the number of sensors N the data matrix $\mathbb{X}$ derived from the data matrix $\mathbb{X}'$ after preprocessing can be decomposed through singular value decomposition (SVD):

$$\mathbb{X}_{M\times N} = \mathbb{U}_{M\times N} \acute{\mathbb{O}}_{N\times N} \mathbb{V}^{T}_{N\times N}$$

$$= (u_1, u_2, \ldots u_N) \begin{bmatrix} s_{11} & 0 & \cdots & 0 \\ 0 & s_{22} & \cdots & 0 \\ \vdots & \vdots & \ddots & \\ 0 & 0 & \ldots & s_{NN} \end{bmatrix} (v_1, v_2, \ldots v_N) , \qquad (33)$$

where $\mathbb{U}$ is a MxN orthogonal matrix, $\Sigma$ a NxN diagonal matrix of singular non negative values listed such as $\sigma_{11} > \sigma_{22} > \ldots > \sigma_{NN}$, and $\mathbb{V}$ a NxN orthogonal matrix. The singular values $\sigma_{NN}$ are the positive square roots of the eigenvalues of $\mathbb{X}$, the columns $u_1$ to $u_N$ denote eigenvectors of $\mathbb{X}\mathbb{X}^T$, the columns of $\mathbb{V}$ eigenvectors of $\mathbb{X}^T\mathbb{X}$ associated with eigenvalues $(\sigma_{11})^2 .. (\sigma_{NN})^2$. The eigenvectors forming $\mathbb{U}$ and $\mathbb{V}$

are termed principal components. PCA essentially removes collinearity from the data set and only makes sense with sensors which are correlated [4].

The amount of variance described by each eigenvector is determined by the magnitude of the associated eigenvalues. Since eigenvalues are sorted in descending order, the greatest amount of data variance will be described in the first PC. The PCs describing systematic variance in the data are termed primary components, the others secondary components. To the latter non systematic variation containing also noise are attributed.

Once the decomposition has been performed, the columns of $\mathbb{U}$, termed scores $u_{ni}$, can be used to project the data in scores plots. The score of an object is defined as its coordinate in this scores plot. The loading of a variable is defined as the product of its singular value with its corresponding principle component out of $\mathbb{V}$ and gives a measure for the evaluation of sensors. High loadings values indicate that the PC is aligned in a direction close to the original response of that sensor. Loadingplots can be used for determining which sensor contributes unique information and which sensors can be omitted [141]. Scores and loadings are interpreted in pairs and can be plotted against each other (so-called 'bi-plot').

PCA is a unsupervised orthogonal projection algorithm which means that no input from the operator is needed beyond the raw sensor data [140].

### 3.4.3. Principal component regression (PCR)

PCR is based on PCA but comprises a significant additional step and also needs additional input. After the determination of the PCs, a regression of the reference method on the scores is performed based on the correlation of quantities, e.g. concentrations $\mathbb{C}_{MxK}$ of the constituents K in the mixtures (samples) M and the measurement data $\mathbb{X}_{MxN}$ defined as:

$$\mathbb{C}_{M \times K} = \mathbb{X}_{M \times N} \mathbb{R}_{N \times K}, \tag{34}$$

where $\mathbb{R}_{MxK}$ is the matrix of regression coefficients. The calibration in $\mathbb{C}_{MxK}$ and $\mathbb{X}_{MxN}$ can be used to predict the regression coefficients [141]. By using a subset of the available PCs, only the systematic variance in the data is taken into account, which is introducing a small systematic error but which also improves the robustness of the prediction for generalization [22]. The subset of data used is obtained by cross validation, which means that the data set is split into two subsets, i.e. one for building the model and one for testing it (see also section 4.1.1.3 and [143]). With the resulting $\mathbb{R}_{MxK}$ matrix quantitative estimates for

unknown concentrations of species in mixtures, which are present in known amounts in reference data, can be obtained. Note, that the PCs are determined without regard to the predicted property.

PCR as linear technique will be most successful if sensor responses are linear. However, it will produce overly optimistic results if the prediction accuracy is based only on data used to generate the PCs and not independent data. PCR is a supervised technique as for the prediction the known concentrations of the reference sample are required as input.

### 3.4.4. Practical application

The described methods are linear methods based on, e.g. linear or close to linear sensor responses, M >> N, etc. They are valid only if these assumptions apply. The techniques are powerful tools for extracting information from sensor array measurements, filtering random variation from data, and evaluating the sensors themselves, but they can also lead to misleading interpretations.

Any multivariate analysis has to comprise some validation to assure that its results can be extrapolated to new data. This requires two independent procedures in the computation of each model component, i.e. the calibration and the validation with two independent data sets. After establishing a model test samples are applied to the calibrated model and the results compared to the known values. The sum of the prediction errors for each test sample (Predicted Error Sum of Squares, PRESS) is computed for the factor combinations building the model and optimized in an iterative process. This measure is valid only under the assumption that the new samples are similar to the ones used for calibration; otherwise the prediction error might be much higher [22,144].

The inherent dimensionality of the data set has to be determined. This is not always straight forward. In other words, not only that the number of sensors in the models has to be much smaller than the number of samples, a change in either number will also change the analysis output with sometimes undesired consequences. Examples are given in the following:

- If the number of samples building the model (the PCs) is changed the model displays the variance of the new data set. If all samples that differ strongly are removed, the PCA will build a model dominated by the variance in the remaining samples. In the extreme this means that the PCA can display a discrimination of two identical classes solely based on noise.

- The other extreme would be to add data from totally different mixtures to the model, thus feigning a likeliness of the investigated original samples.

- Elimination of sensors with low variance chosen by from the loadings plot can improve discrimination but also emphasize artificial discrimination.

- Outlier samples can have a large influence on the PCA model. Stray samples in scores plots have to be double checked.

In summary it has to be stressed that although PCA is an unsupervised method, the interpretation of results is not. PCA does not guarantee optimal discrimination of particular mixtures in an investigation, since PCA measures variance, not discrimination [145]. PCA does not consider class separability, since it does not take into account the class label of feature vectors.

For the preprocessing of data as well as for the interpretation of clustering or discrimination a priori information about the nature of the samples, the chemical and physical properties of the instrument, and the evaluation method are needed for obtaining results representing analytic properties of chemical mixtures correctly.

# 4. EXPERIMENTAL SECTION

The devices used in this work, their operation parameters and test results of experimental set-ups, are described in the following chapter.

## 4.1. MOSES

The electronic nose instrument used in this work was a MOSES II Electronic Nose built by Lennartz Electronic GmbH, Tübingen, Germany [146] and is described in detail by other authors [22, 147, 148, 149]. The MOSES II has an open architecture with interchangeable sensor modules and a sampling module which allows for several alternatives in sample introduction [150]. It is supplied with software for automatic operation as well as for pattern recognition. The MOSES II instrument used in this work was equipped with four modules, including an input module with sampling valves and pump, and sensor modules containing eight metal-oxide semiconductor (MOX) sensors and eight quartz microbalance (QMB) sensors. In addition, an electrochemical (EC) module containing four amperometric gas sensors (AGS) was included, for a total of 20 sensors of three different classes.

### 4.1.1. Data analysis

The MOSES II software uses a pattern recognizer based on principal components analysis (PCA) (see section 3.4 and [151]); results shown are mostly expressed as plots of the second principal component against the first.

#### 4.1.1.1. Feature extraction

Table 6 lists the features extracted from the sensor response for evaluation if not stated otherwise in the description of an investigation.

| transducer type | feature |
| --- | --- |
| QMB | Sig-Base |
| MOX | Sig-Base3 |
| AGS | Max - Min |

*Table 6: Features extracted with MOSES II.*

The features give a numerical value for the change in sensor signal during the exposition to the sample. The feature 'signal minus baseline' (Sig-Base) extracts the largest deviation from the baseline. 'Sig-Base3' uses an average over three adjacent data points for determining the baseline. The feature 'maximum minus minimum' (Max-Min) can be used instead if the baseline is stable over the measurement.

For time resolved signals the feature 'SigAt-BaseAt' was used where the baseline was subtracted from local maxima at certain retention times. This requires the definition of the retention time considered in the evaluation by the operator introducing a supervised step into the data analysis process. Also, time resolved feature extraction normally means that from the response of one sensor to one sample several features are extracted, which are not correlated or only correlated to the extent the analytes in the sample are correlated.

### 4.1.1.2. Data preprocessing

The measured data displayed in scores plots within this work were standardized. For samples where deviation from injected amount was intended to be suppressed and concentration information was negligible, a normalization was performed (see section 3.3.1), which is referred to in the description of the experiment.

### 4.1.1.3. Data visualization

The data of the gas sensor arrays were evaluated by PCA as a standard pattern recognition algorithm implemented in the MOSES software.

Measurement data are displayed in scores plots comprising PC1 and PC2 if not stated otherwise. Either a scale or the variance contained in a PC in percent of the total variation of the data set is displayed. All measurements included mixtures or substances in known concentrations used as reference or standard. The standard was chosen for each application to mimic a sample with respect to its sensor signals. Apart from providing a constant base with known properties for the building of the evaluation model, the standard was used for identifying changes in the instrument over the duration of an investigation.

An estimate of the prediction of concentrations with the e-nose was made using PCR, implemented in the ARGUS software package [152]. The estimate of the quality of the prediction was validated by cross-validation without using independent test samples. Within the cross-validation the same samples are used both for model estimating and testing. The method leaves out samples from the

calibration data set, then is calibrates the model on the remaining data points, and then predicts the values for the left-out samples and computes the prediction residuals. This procedure is repeated until every object has been left out once (leave-one-out method [137]); then all prediction residuals are combined to compute the PRESS. The cross-validation was automatically carried out with ARGUS. It has been stated in section 3.4.3, that the results obtained without independent test data might be optimistic. In this work however, PCRs were only used for comparison with each other, the comparison then is valid.

### 4.1.1.4. Classification

A classification of samples displayed in scores plots with confidence ellipsoids was performed by the MOSES II software for known sample classes. The deviation of the center of a class is used to emphasis it. The ellipsoids marking a class are drawn so that their principle axes correspond to three times the standard deviation of scores with respect to the corresponding PCs [140]. Note that in classification a pattern is a pair of variables, the feature corresponds to the observation whereas the class is a label put in by the operator.

### 4.1.2. Sample uptake

Sample handling was carried out with an automated headspace sampler (HSS 86.50, DANI Strumentazione Analitica spa, Monza, Italy, or HP 7694, Hewlett-Packard) connected to the input of the sensor modules of the MOSES II. The fully automated headspace sampler maintains a synthetic air carrier gas supply through the injection needle, sample loop, and transfer line to the e-nose throughout the measurement. Both headspace samplers are identical in operation principle. The operation parameters have been optimized for each application. Table 7 summarizes the measurement parameters used in the investigation for the different applications.

| investigation | | Bacteria | Cheese | TOPE* | Beer | Mayonnaise |
|---|---|---|---|---|---|---|
| measurements in chapter | | 5.2 | 5.3 | 5.4.3 | 5.5 | 5.6 |
| **headspace sampler operation parameter** | | | | | | |
| temperatures[°C] | oven | 60 | 60 | 60 | 50 | 50 |
| | sampling loop | 65 | 100 | 100 | 60 | 100 |
| | transfer line | 70 | 120 | 120 | 70 | 120 |
| time [min] | sample equilibration | 12 | 20 | 20 | 10 | 20 |
| | pressurization | 0.1 | 0.5 | 0.5 | 0.5 | 0.5 |
| | vent time | 0.1 | 0.3 | 0.3 | 0.3 | 0.3 |
| | vent equilibration | 0.05 | 0.05 | 0.05 | 0.05 | 0.05 |
| | injection | 1 | 1 | 1 | 2 | 1 |
| flow [ml/min] | auxiliary | 20 | 20 | 20 | 10 | 20 |

*Table 7: Headspace sampler operation parameters (*see section 4.5.2).*

The modular design of MOSES II allows flexibility in sampling and sensing and the sample could be exposed to any sensor array alone or in any order. The order used throughout this work was QMB, then MOX, then AGS.

Figure 35 in chapter 4.4.2 shows the set-up of the MOSES II e-nose together with the headspace sampler used connected by an additional set-up for sample conditioning.

## 4.2. The electrochemical sensor (EC) module

An electronic nose that uses chemical sensors of several unrelated types, or orthogonal sensors, gives data that are more effective in discriminating samples than simply increasing the number of sensors of a single class. The MOSES II electronic nose (Lennartz electronic GmbH) is constructed in modules to allow for the ready selection and interchange of sensor types and classes. To complement the existing MOX and QMB sensor arrays, an electrochemical gas sensor module (EC module) has been constructed using four commercially available amperometric gas sensors (TSI Inc. [153]). Figure 12 shows the interior of the module and a typical amperometric gas sensor.

16 mm
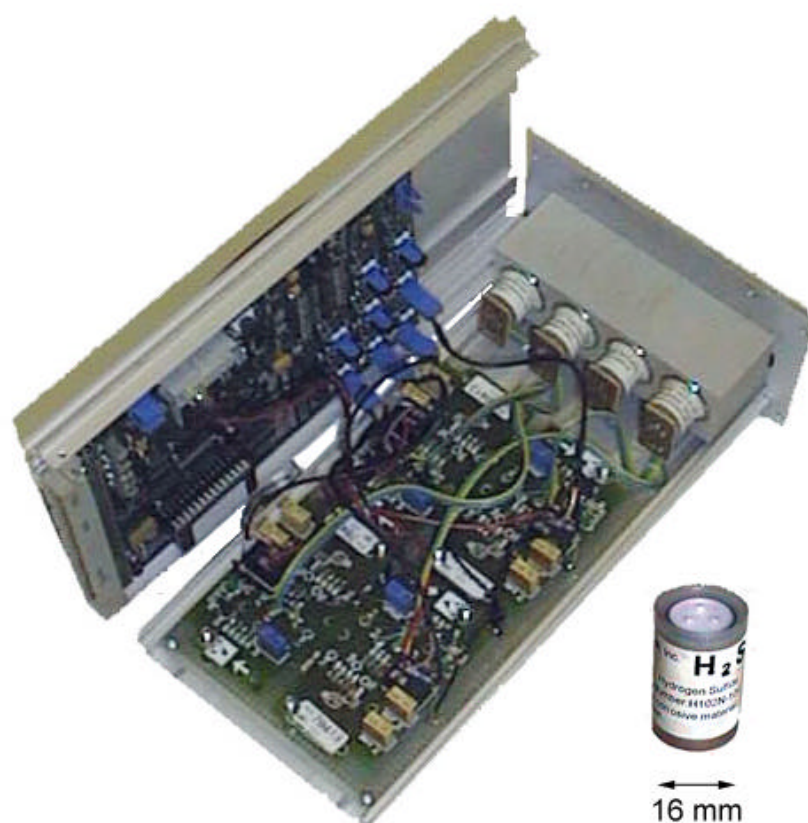
*Figure 12: Prototype of Electrochemical Sensor Module for the Lennartz electronic GmbH MOSES II Electronic Nose system. Displayed next to it is an enlarged electrochemical (amperometric) gas sensor (TSI, Inc. [153]).*

There are four types of AGS available, i.e. the CO sensor with and without a filter, an $H_2S$ sensor, an $NO_2$ sensor and an $SO_2$ sensor. The $H_2S$ and $SO_2$ sensors are essentially the same, but the $NO_2$ sensor has a lower surface area Au electrode. The $NO_2$ sensor is operated at a more cathodic potential than the others and will exhibit significantly different electro-catalytic properties, i.e. it reduces analytes like $O_3$, $Cl_2$, and $NO_2$, and offers selectivity to the electrochemical array. The Pt-catalyzed CO sensor possesses decidedly different catalytic activity than any of the Au catalyzed sensors, particularly with respect to responsiveness to many carbon-oxygen compounds.

Electrochemical sensors can have significant advantages over other sensor classes. They have a wide linear range, greater than four orders of magnitude of concentration, and are almost insensitive to changes in relative humidity. They also respond to quite different chemical properties than conductive polymer, mass-sensitive quartz microbalance (QMB), or metal oxide (MOX) sensors and thus provide complementary capability and increased chemical independence of

the array responses. Electrochemical sensors, however, do not respond to some common classes of compounds, such as saturated hydrocarbons (HC). HC can be measured by amperometric sensors by passing the sample stream over a heated noble metal catalyst generating partial combustion products, that are highly electrochemically active, with high reproducibility. However, for hydrocarbon analysis in conventional e-nose operation these sensors will only increase the noise of the array.

The electrochemical module is similar in size to the QMB module of the MOSES II instrument. The measurement chamber containing the four amperometric gas sensors is made from polypropylene. Excerpts from the sensor data sheets are listed in Table 8 and provide an estimate of sensor performance. Throughout this work, the AGS are labeled according to the sensor specification of the manufacturer, i.e. the analyte they are specified for: CO, $NO_2$, $SO_2$, and $H_2S$.

|  | Position in MOSES II | | | |
| --- | --- | --- | --- | --- |
|  | **1** | **2** | **3** | **4** |
| Sensor (model no.) TSI, Inc. | CO - MNS | $NO_2$ – MNL | $SO_2$ – MNS | $H_2S$ – MNS |
| Operating bias potential [mV] | +150 | - 100 | - 100 | + 300 |
| Sensitivity [µA/ppm] | 0.09 ± 0.04 | 0.17 ± 0.08 | 0.055 ± 0.025 | 0.5 ± 0.25 |
| Concentration range (linear) | 0 – 1000 ppm | 0 - 10 ppm | 0 - 100 ppm | 0 - 1000 ppm |
| Maximum concentration | >15,000 ppm | >50 ppm | 500 ppm | 2000 ppm |
| Response time ($t_{90}$, s) | < 30 | < 60 (at 3 ppm) | < 35 | < 60 |
| Resolution | 1 ppm | 10 ppb | 1 ppm | 0.5 ppm |
| Temperature range (°C) | -10° to +40° | -10° to +40° | -10° to +40° | -10° to +40° |
| Relative humidity range (%) | 15-90 | 15-90 | 15-90 | 15-90 |
| Precision/repeatability (%) | <1 | <2 | <2 | <2 |
| Catalyst | Pt | Au | Au | Au |

*Table 8: Electrochemical sensor data for commercial TSI sensors [154] [TSI Inc.].*

The bias potentials (potential of the working electrode relative to the reference electrode) were set according to manufacturer recommendation for optimized sensitivity, selectivity, and response time. Each sensor is operated with a modified Endress & Hauser GSTH standard 3 - electrode electrochemical sensor transmitter (see also chapter 4.2.1). The tubing used for the $NO_2$ and $SO_2$ test application was PFA, which showed no interference with sensor measurements

when tested for sorption. CO and organic components were applied using stainless steel tubing.

Sensors require time to stabilize and reach a steady state output. Once the sensors are in operation, a new measurement requires no further equilibration time since the sensors are stable for weeks and even years [155,156]. The response time of the sensors is less than 30 s to reach 90% of the maximum signal. For all of the sensors the range of humidity for continuous operation is 15% - 90% (see Table 8). Lower humidity results in a signal loss after several hours of operation on very dry gas most likely due to dryout. The electrochemical sensors incorporated in MOSES II are optimized for a single analyte like CO, $H_2S$, NO, $NO_2$, $SO_2$, $O_3$, or hydrazine. However, this type of sensor will respond to any analyte that is electro-active on that sensor just like the QMB sensor will respond to any absorbable gas on that coating. The nature of the electrode and electrolyte as well as the thermodynamic potential of the sensing electrode will control which types of chemicals react on the sensors (see chapter 3.1.2). The rate of diffusion, solubility in the electrolyte, and number of electrons produced per molecule (Fick's and Faraday's laws, see chapter 3.1.3) will control the observed sensitivity toward that analyte. In general, the active Pt catalyst will record a signal for any electro-oxidizable gas and vapor [CO, $SO_2$, $H_2S$, $NO_x$, EtOH]. The $NO_2$ sensor is operated with an Au electro-catalyst at more cathodic potentials in such a way, that only electro-reducible gases such as $NO_2$, $Cl_2$, and few others interact. The array, while not measuring a specific electrochemical property, has been carefully chosen to cover a wide range of electro-active substances. Those analytes will give signals that are electro-catalytically active on Pt or Au electro-catalysts at either anodic or cathodic potentials in sulfuric acid electrolyte.

Experimentally, the EC module can be installed in any slot of the MOSES II system. The module is recognized by the software in similar configuration as an additional MOX module. The sensor modules were installed to be operated together in the sequence QMB, MOX, and then EC. This configuration was chosen because the mass sensitive QMB sensors operate on adsorption/desorption without sample consumption, whereas the operation of MOX and AGS sensors imply a chemical reaction occurring at or in the sensor, respectively. The reaction is accompanied by sample consumption to a certain extent [157].

### 4.2.1. Sensor signals and potentiostat set-up

In total two EC modules have been built. The first prototype module had been built by G. Noetzel (now MoTech GmBH [152]). The second module containing identical components was subjected to minor modifications in wiring and potentiostat settings as result from measuring experiences with the first prototype module. The most significant difference was, that the power supply for the sensor electronics was connected to the negative voltage line. Thus, the sign of the output of sensor signals was changed with regard to virtual ground in the second module. Sensor signals generated with the second module are displayed so that for instance for the CO sensor oxidation of sample is shown with positive and reduction with negative sign. The absolute value for signals with both modules is the same, only the sign for the display was changed. Sensor responses are displayed in arbitrary units. Hereby a sensor signal of 1mA is displayed as 1310 arbitrary units, which for the CO sensor for example indicates a concentration of 10 ppm.

Figure 13 shows an enlargement of the potentiostats of the (second) EC module and wiring for the operation of the sensors. Each sensor is operated with a modified EH GSTH standard 3 - electrode electrochemical sensor transmitter (Endress + Hauser Meßtechnik GmbH + Co., Germany, [158]).
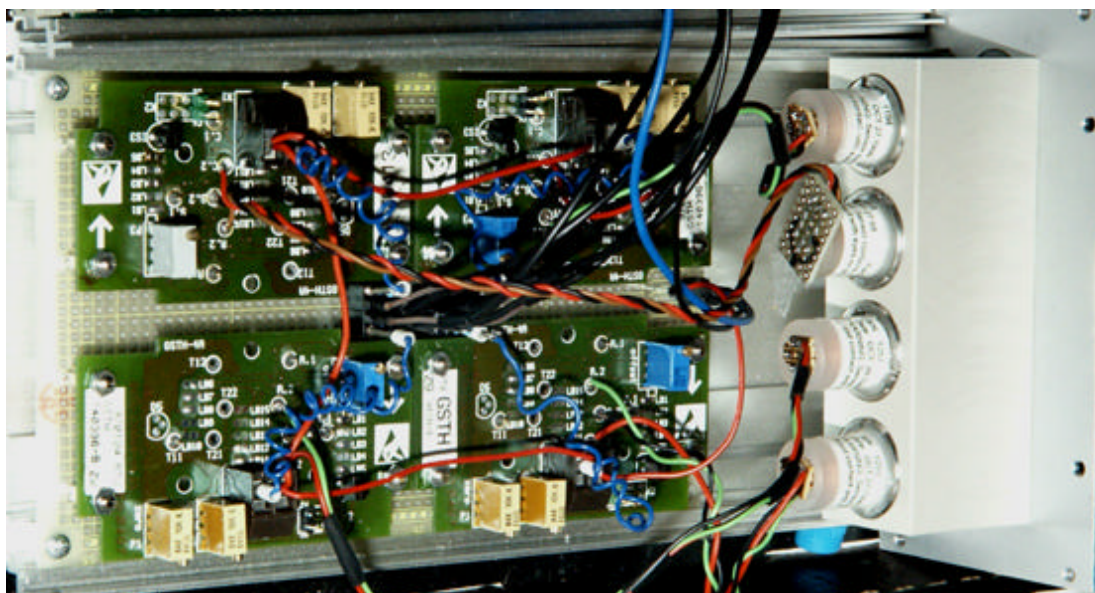


*Figure 13: Sensor potentiostats and wiring.*

The power supply for the potentiostats of the EC sensors can be seen as blue wires, black for ground, supplying a negative potential of 12V from the main board similar to the board used in the MOX module. The potentiostats can be

operated in a two wire mode with signal transmission and power supply over a current loop. The potentiostats are connected in the sequence of the sensors ($CO$-$NO_2$-$SO_2$-$H_2S$) to a common power. The sensor signals are relayed back to the main board A/D converters by the black wiring with the potentiostats connected between power supply and ground over a 100 Ohm resistance visible in the middle of the four potentiostats in the set-up. The output current lies between 4 and 20 mA. The sensor signal is read as the resistance by the main board A/D converters. The potentiostats provide the possibility of operating the sensors with different resistance settings. The bias is set in the offset variable resistance. The bias potentials (potential of the WE relative to the RE) were set according to manufacturer recommendations for each individual sensor (Table 8). The adjustable resistances for bias, span or amplification, and zero were adjusted when setting up the module with calibration gas mixtures to the correct setting and desired sensitivity for the target gases.

Figure 14 shows the circuit diagram of the slightly modified commercial potentiostats for the operation of the amperometric sensors. The connector or jumper JP1 of the potentiostat serves for the power supply and signal output. The here applied potential is rectified over bridge B1 and smoothed over reservoir capacitor C1. The signal is taken between voltages U+ and U-. The voltage is stabilized with the linear voltage regulator U1. The operational amplifier U9A generates a virtual ground for the succeeding current placing a symmetrical voltage feed over +UB and -UB at disposal. JP2 is the sensor connector with working- (WE), reference- (RE), and counter electrode (CE). The counter electrode is connected over the field effect transistor Q2 to ground potential when not operational in order to prevent polarization effects in the electrochemical cell. The operational amplifier U11A images the potential set with resistance R1 between reference and counter electrode. U9B and U10A generate an amplified voltage signal (OUT) from the cell current which is inverted over U10B (OUTINV). With U11B, U12A, U12B, and Q1 the voltage signal is again converted into a current signal for the current interface. With R29 and R30 offset and amplification of the potentiostat can be adjusted. With R24, R21, R27, R25, and the temperature dependent resistance TR1, a compensation for the temperature dependency of the sensor can be employed [159]. For the module the temperature compensation was not connected as the temperature can be constantly monitored over the input module. The values marked "var" were set according to manufacturer's data sheet recommendations [154,158].
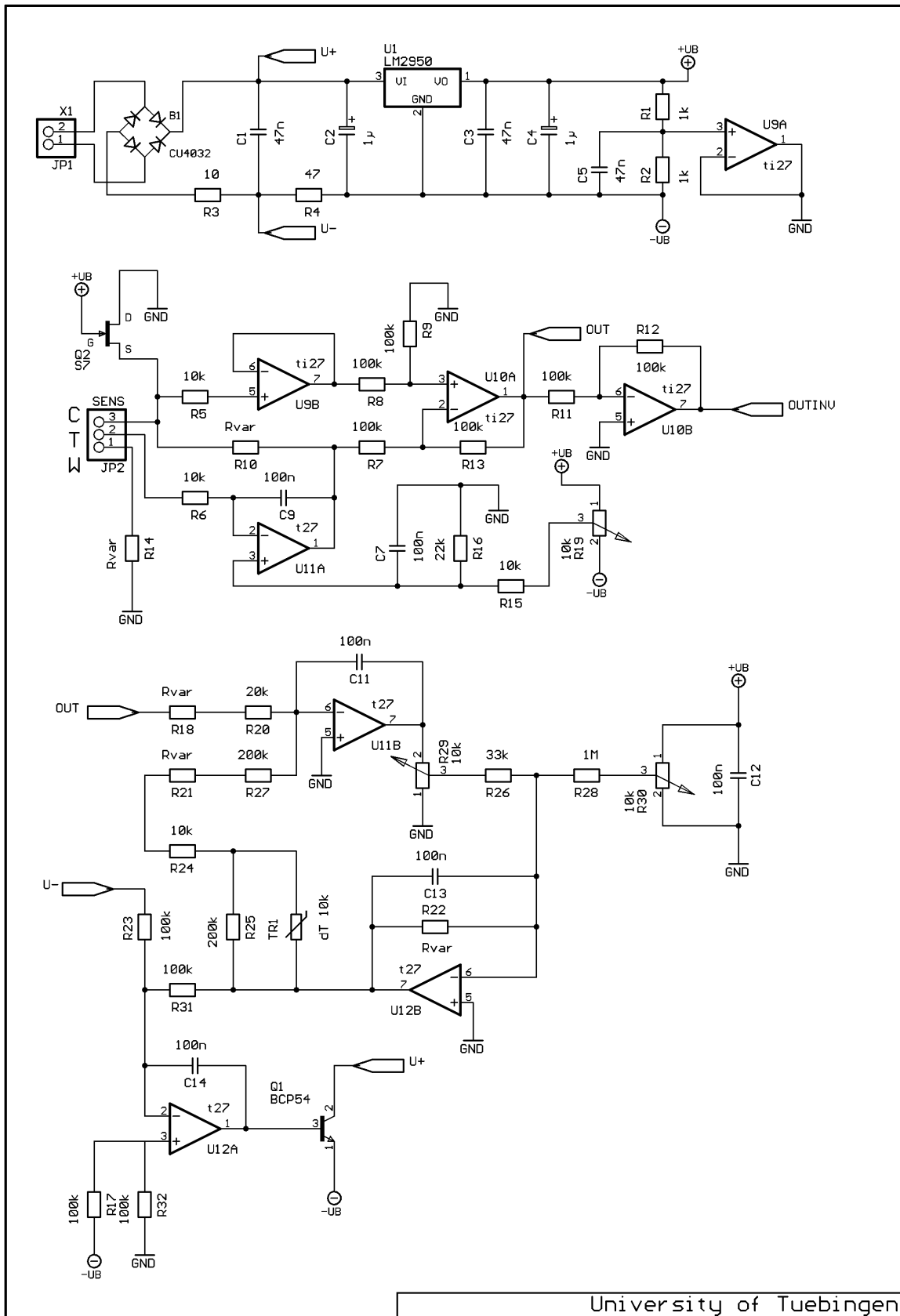
*Figure 14: Schematic wiring diagram of the sensor potentiostats [160].*

An exemplary diagram of the sensor signals of the EC module to CO and water exposure is shown in Figure 15. For comparison also the signals of the MOX module are displayed. The QMB display no signals for the target analyte CO. The humidity is monitored with the input module.
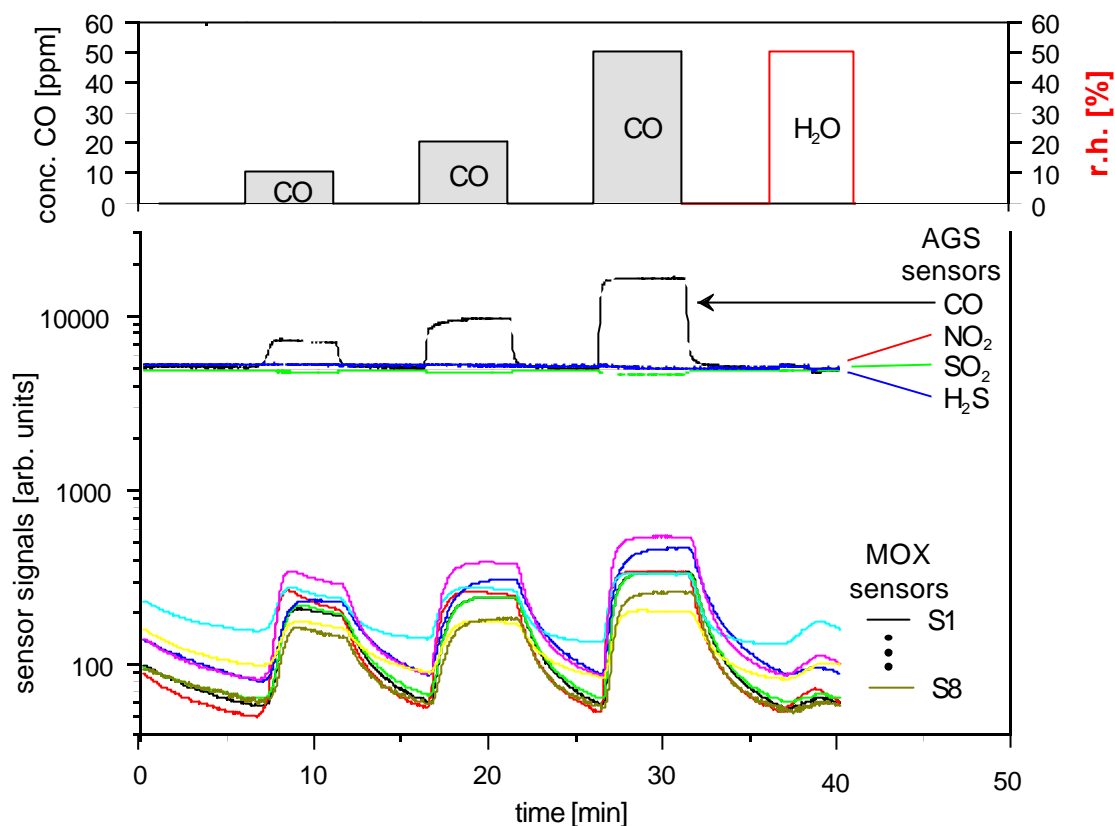


*Figure 15: Sensor signals to CO and water exposure.*

The sensor signals are displayed on a logarithmic scale to put emphasis on the difference in intensity. The EC sensor for CO reacts to the analyte exposition in a linear and highly sensitive way. The other EC sensors show little cross sensitivities. All MOX sensors react to CO exposition, however to a much smaller extend than the dedicated CO EC sensor. Also, the MOX sensors show a considerable influence on the change in relative humidity. The time shift between exposition to the gas and sensor reaction derives from the set-up of MOSES II connected to the gas mixing station where the gases were applied by 2m of 4mm ID tubing at a gas flow of 50 ml/min.

The electrochemical module has been extensively tested in the MOSES II instrument. Tested parameters are listed in the following chapters.

### 4.2.1.1. Sensor warm-up and response time

Electrochemical sensors need a warm-up time to reach equilibrium. This time was tested for the EC module. The CO and $H_2S$ sensors need to be powered for 1 h prior to the start of the measurement. The other two sensors reach equilibrium much faster and show no drift at the beginning of operation (see Figure 16). Once the sensors are in operation, a new measurement requires no further equilibration time for the sensors (see Figure 17). Although the response time of the sensors itself is less than 30s to reach 90% of the max. signal, the response time of the system is also determined by the geometry of the tubing and measurement chambers.

Figure 16 shows a typical measurement with the electrochemical sensor module. The sensors were exposed to 20,10, and 5 ppm CO at different humidities of 20, 50, and 80% r.h.. For 80 % r.h. 10 ppm CO was the maximum applicable concentration possible with the set-up of the gas mixing station used. Figure 17 shows a similar measurement for the exposure to $SO_2$ (50,20,10, and 5 ppm $SO_2$ at 50, 20 and 80 % r.h.). Here, all sensors show a high cross sensitivity to $SO_2$ compared to the signal of the specified $SO_2$ sensor ( see also Figure 20 and Figure 22 a).
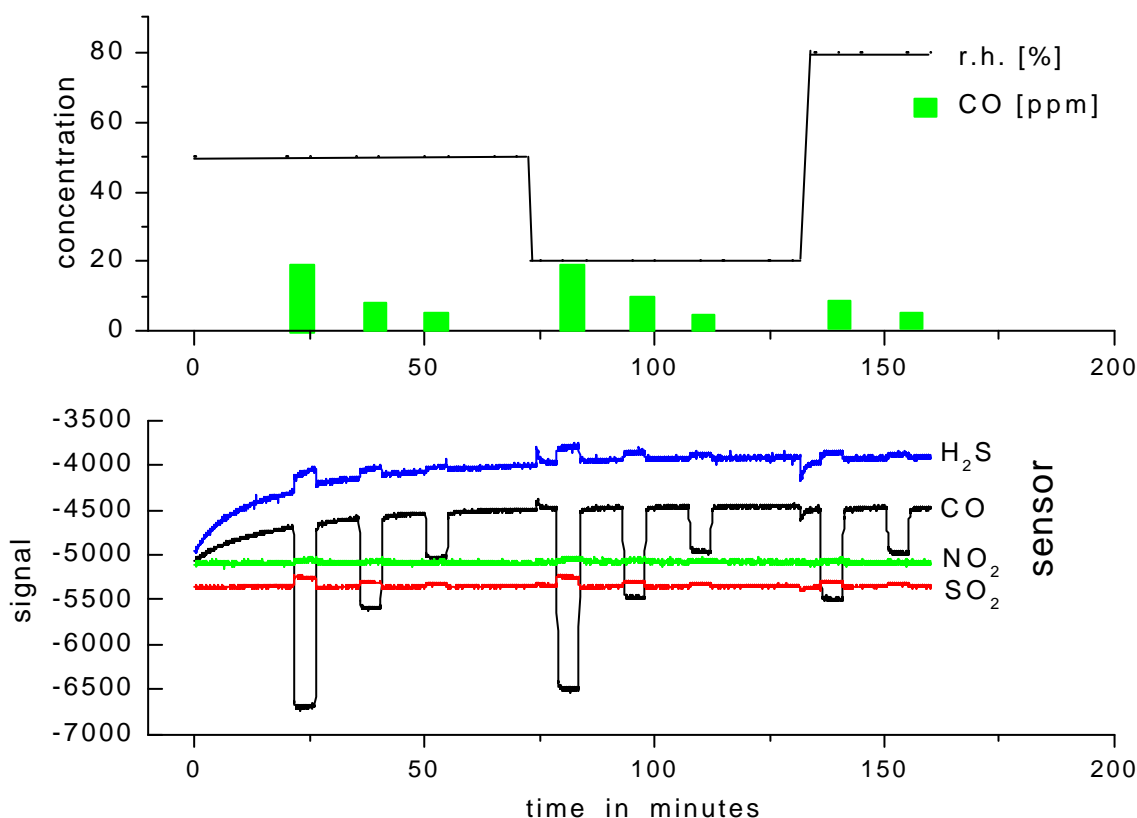


Figure 16: CO measurement at different humidities.
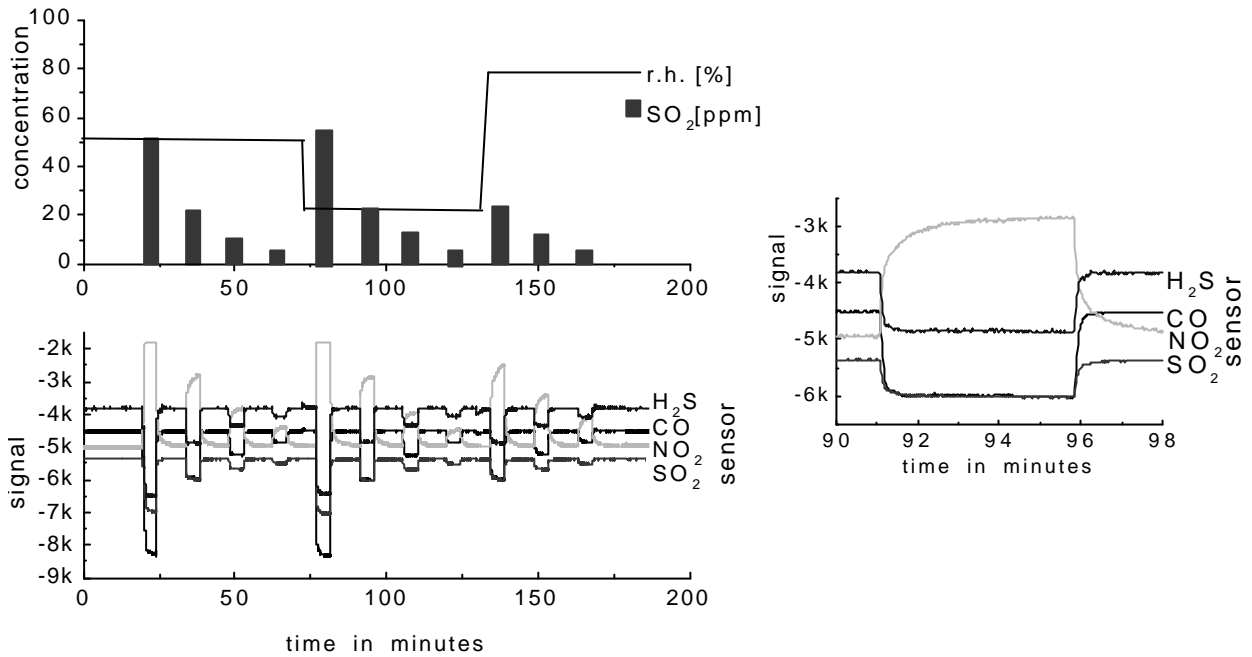
*Figure 17: SO₂ measurement at different humidities. Enlarged signals (right).*

The intensity of amperometric sensor signals is also dependent of operational parameters [107]. Figure 18 shows the signals for different concentrations of $NO_2$ and CO in synthetic air at 50% relative humidity at two different total flow rates of 100 ml/min and 50 ml/min, respectively.
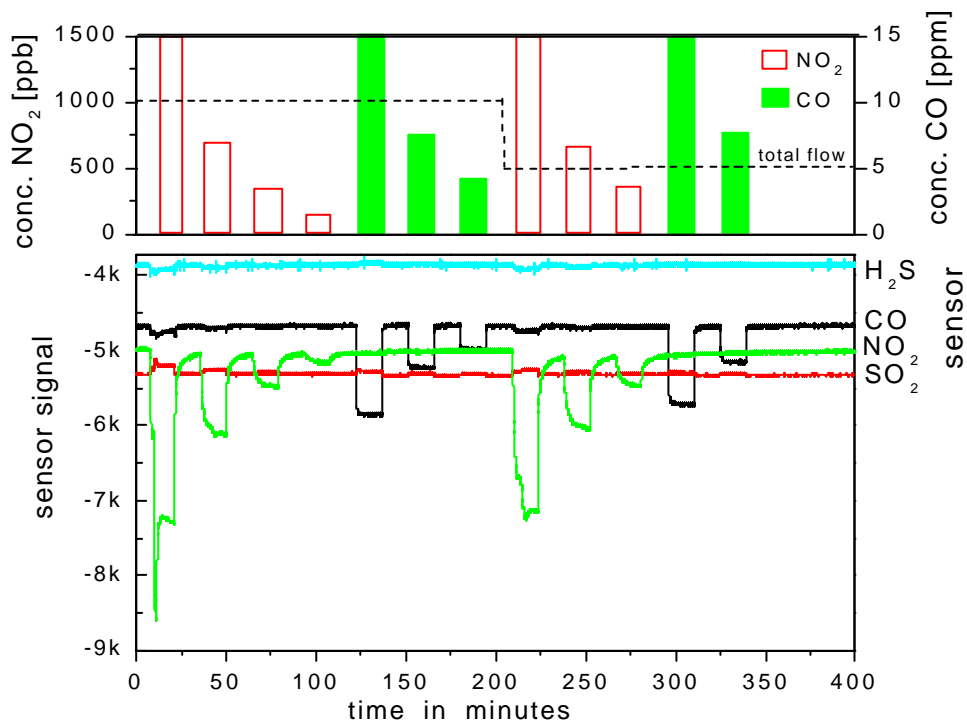


*Figure 18: Sensor signals for NO₂ and CO at 100 and 50 ml/min total flow rate.*

### 4.2.1.2. Humidity dependence

The sensors show almost no interference from changing relative humidity within the specified operation range. Figure 19 shows the signals of the CO sensor on CO exposition at different humidities.
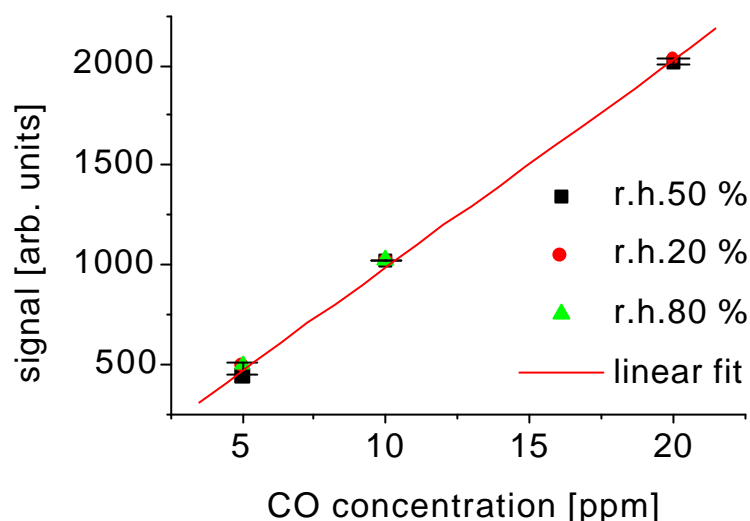


*Figure 19: Humidity influence for different concentrations of CO.*

The linear behavior and a high reproducibility insensitive to changes in relative humidity of the amperometric sensor responses is characteristic of the sensor principle and can be used in e-noses for referencing data with respect to humidity and for calibrating the instrument.

### 4.2.1.3. Selectivity of amperometric sensors for different analytes

The sensors of the EC module show cross sensitivities for gases they are not specified for. The sensors can be equipped with filters against certain interfering gases, but in general the sensors will respond to any analyte that is electro-active at the set bias potential, chosen electro-catalyst, etc. (see chapter 3.1). The operating bias can be adjusted to a range of less interference but then sensitivity to the target gas will not be at the optimal value. The sensor signals of the four sensors to the four specified target gases were compared. A separation is clearly possible because the operating potential of the sensors results in positive or negative signals (see Figure 17), even if the absolute values of the signals are similar.
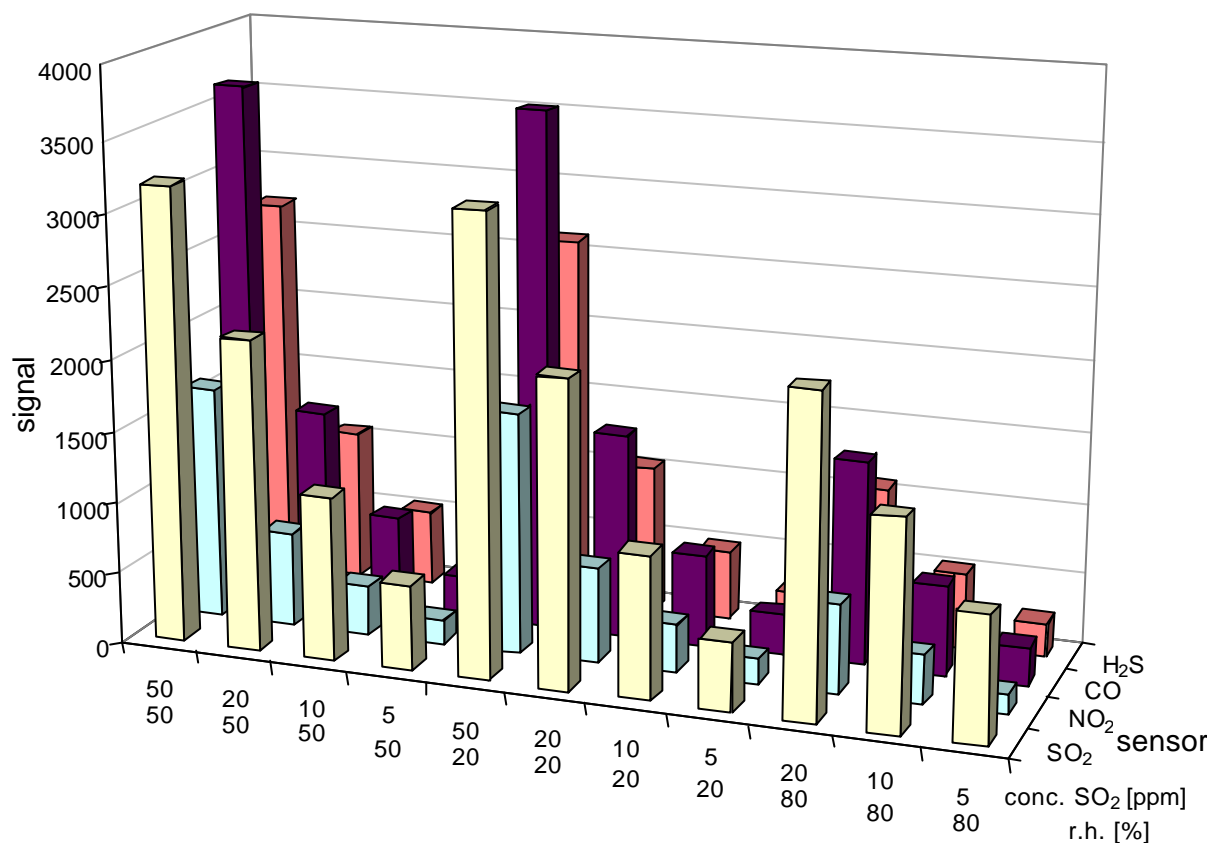
*Figure 20: Sensor signal to SO$_2$ exposure.*

All sensors show cross sensitivity for SO$_2$, and to a much smaller extent to CO and NO$_2$ (see Figure 16 and Figure 17). The electrochemical sensors also show cross sensitivities to various other interfering gases. Especially the H$_2$S sensor reacts strongly to most tested gases. For an example of interfering organic compounds, the sensors were also tested for ethanol methane and exposure at high concentrations. As an example, methane was chosen for hydrocarbons, to which MOX sensors show high cross sensitivities to [70].
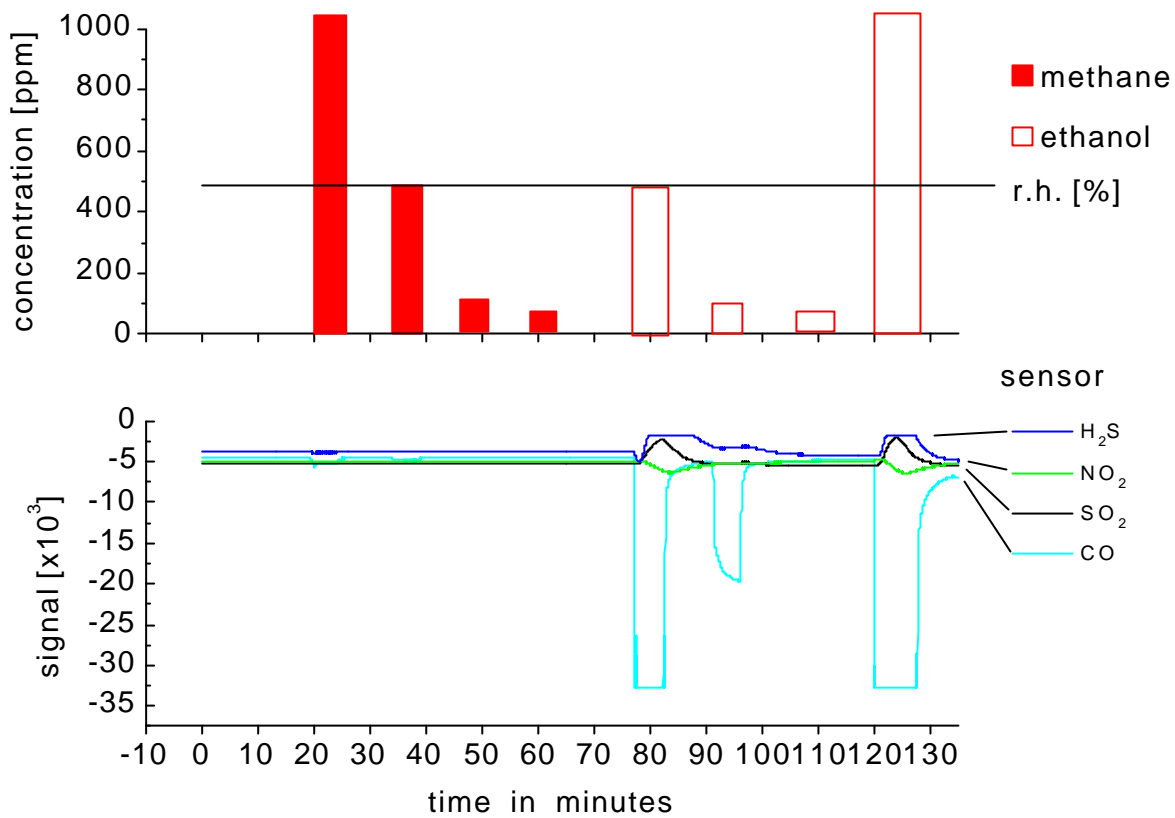
*Figure 21: Exposure to methane (1000, 500, 100, and 50 ppm) and Ethanol
(500, 100, 50, and 1000 ppm).*

Especially the CO sensor reacts strongly to Ethanol exposure. Methane does not interfere even at high concentrations.

Figure 22 a-c summarizes the cross sensitivities of the sensors for the exposure to CO, $NO_2$, and $SO_2$. The latter gives a strong signal especially with the $NO_2$ sensor and a signal from the $SO_2$ sensor which is not higher than that of the CO and $H_2S$ sensors.
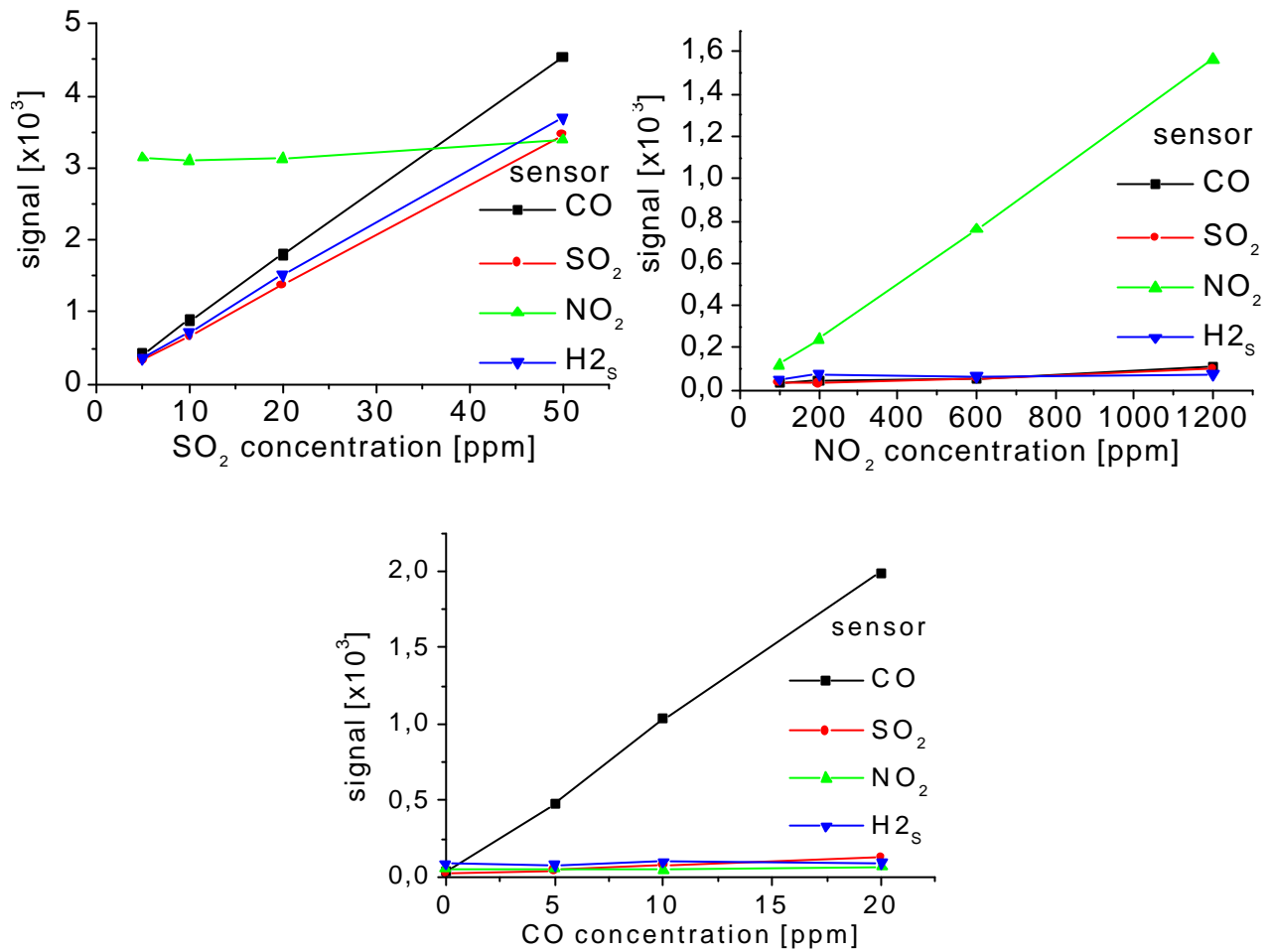
*Figure 22a-c: Cross sensitivities for SO₂, NO₂, and CO exposure.*

4.2.1.4.    Selectivity of the amperometric sensors for different analyte mixtures

The module was also tested for mixtures of analytes where a test gas was applied against a background of other test gases.

Tested were $NO_2$, CO, $SO_2$, and ethanol as interfering gases with all three modules. The electrochemical sensors give an improvement in the distinction of gases for which metal oxide sensors show cross interferences. Figure 23 and Figure 24 show this as an example for the exposure of the sensors to $NO_2$ against a background of CO in different concentrations. Figure 23 shows the sensor signals of the metal oxide sensor module and the amperometric sensor module to CO and $NO_2$. $NO_2$ was applied with 0.4, 0.8, and 1.6 ppm over a background of 4, 8, and 16 ppm CO. The relative humidity was kept constant at 50% over the measurement. The MOX sensors show sum signals for the two applied gases. For $NO_2$ and CO the sensor measured goes along with two different reaction mechanisms, reduction, and oxidation, respectively. This

implies the oxidation of CO oxygen consumption from the surface releasing electrons to the bulk and thus lowering sensor resistance. This is indicated as positive signals in the graphs shown below. Chemisorbed $NO_2$ traps electrons on the surface of the sensor and thus causes a decrease in free charge carrier concentration and, therefore, an increase in the sensor resistance. Signals for $NO_2$ are therefore displayed as negative values in the visualization. The sum signal of MOX sensors makes identification and especially quantification of the measured components of a mixture difficult. Having eight MOX sensors in an array is of little help in this case. Although the intensities of the signals for each sensor vary with the individual sensitive layer, the transduction principle or sensor type is the same and does not give a satisfactory quantitative information on gas concentrations for this particular measurement.
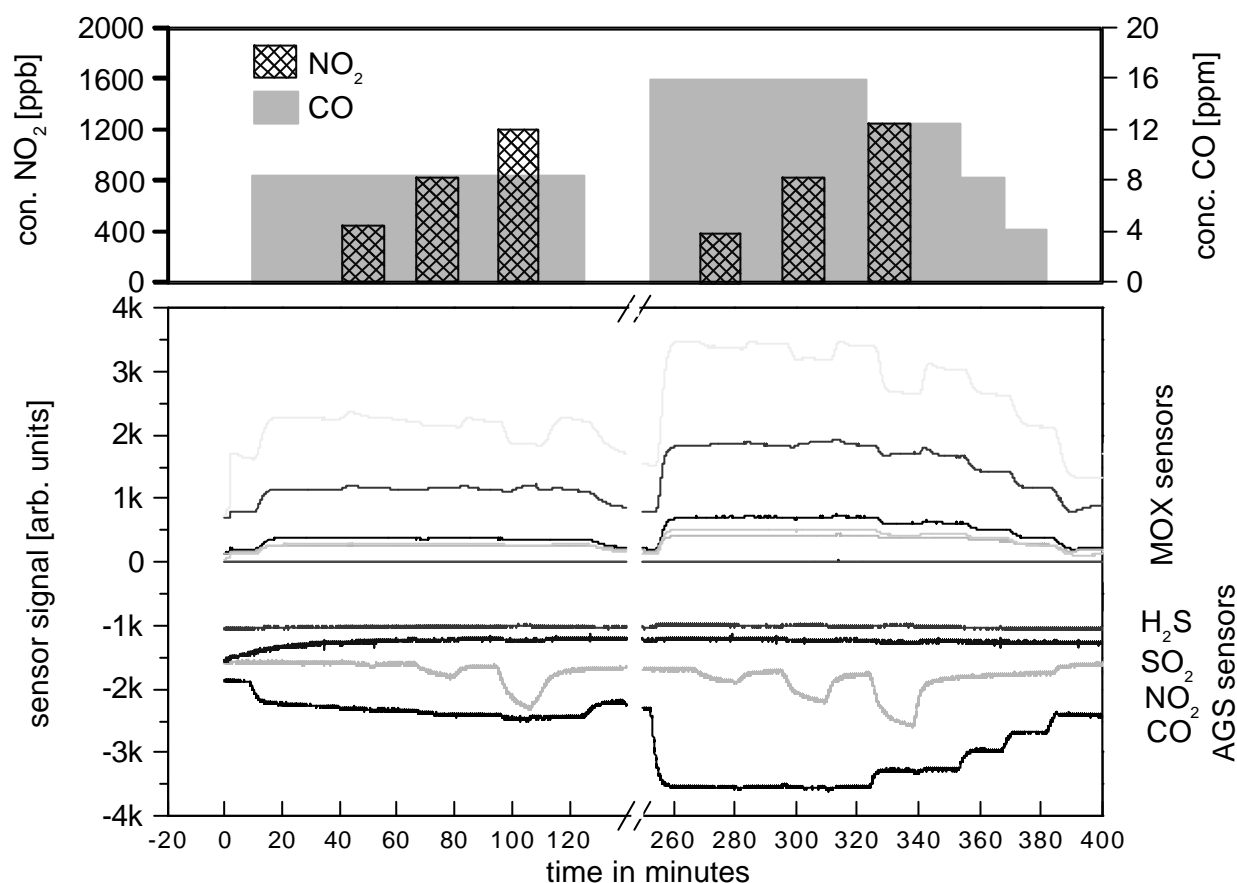


Figure 23: $SnO_2$ metal oxide and amperometric sensor signals for the exposure to $NO_2$ against a varying background of CO.

Figure 24 shows an enlargement of the same measurement. The amperometric sensor specified for the detection of $NO_2$ renders the different concentrations of $NO_2$ without interference, the CO sensor also only indicates the CO

concentration. The slow response of the $NO_2$ sensor in this measurement was due to the set-up of the gas mixing station rather than a sensor property. As $NO_2$ could not be applied using stainless steel tubing as the rest of the test gases, special PFA tubing had to be installed. The larger diameter and higher length of the PFA tubing resulted in a dilution of the test gas front reaching the sensors and a slow adjustment to the preset gas concentration.
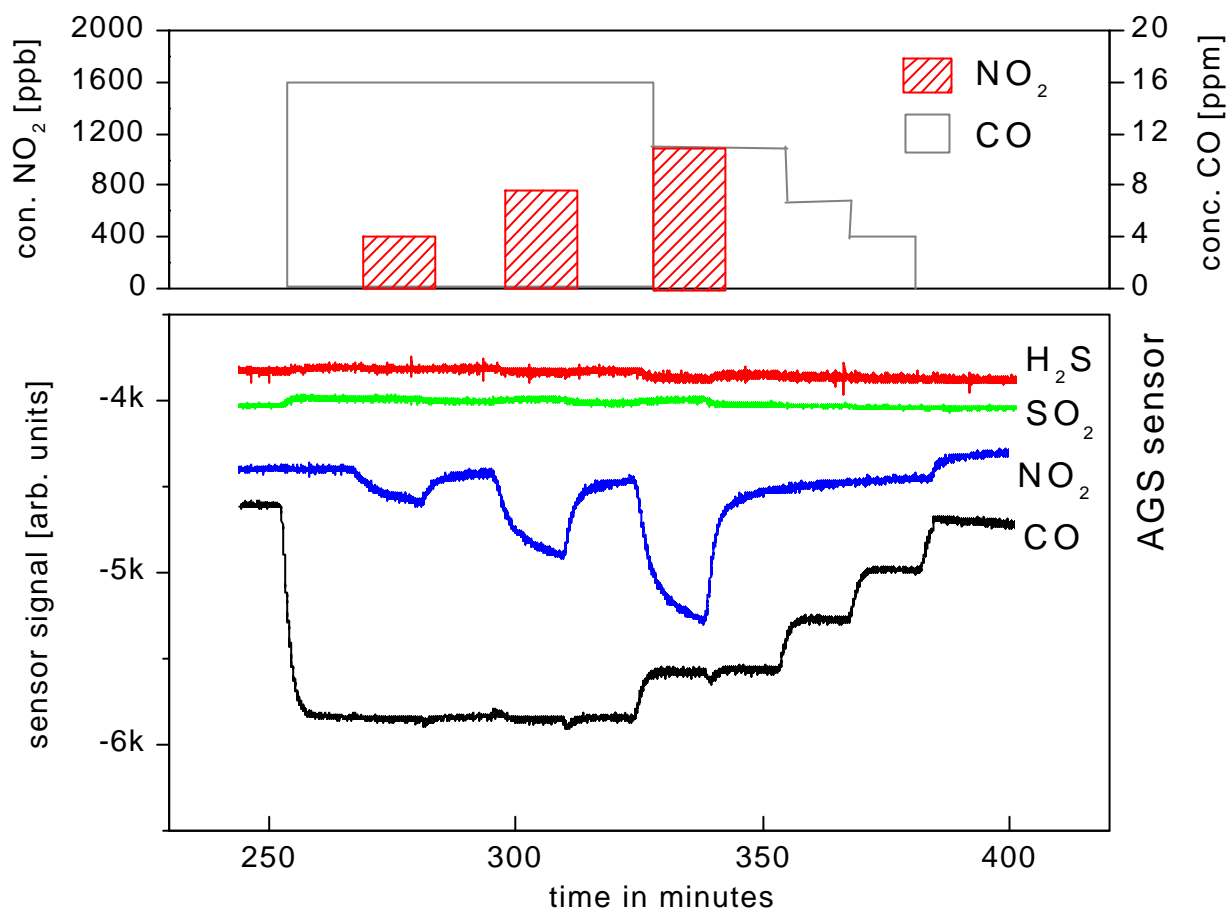


*Figure 24: Electrochemical sensor module responses to the simultaneous exposition to CO and $NO_2$.*

In summary the measurements characterizing mixtures of gases showed, that sensors from different classes achieved better results than using more sensors of the same type, especially in quantitative investigations. This applies at least to many permanent gases like CO, NO, $NO_2$, etc. although it may not necessarily be generally true for all gases, e.g. hydrocarbons for which AGS often does not contribute to detection.

For CO and $NO_2$ the metal oxide module alone, or together with the QMB module, which exhibits no signals for both gases, did not allow the distinction

between the two gases , whereas the electrochemical sensors show distinct signals for each of the two test substances.

### 4.2.1.5.  Sensitivity

Sensitivity measurements were carried out using a gas mixing station for the application of pure test gases diluted with synthetic air. A gas mixing station is a set-up for generating synthetic gas mixtures. Therefore, test gases from calibrated bottles of a compound in a certain concentration in synthetic air or vapors from thermostatted gas washing bottles are blended with a carrier gas flux of synthetic air. The flow rates of all components, synthetic air, and humidified synthetic air are adjusted by a specific software controlling valves and mass flow controllers. Every test gas application is followed by a purge phase allowing precise exposition times, stepwise concentration variation, and pulsed application of gases at different flow rates simulating dynamic measurements. The gas mixing station used in this work is specified in more detail in [22,70].

The gas mixing station allows the controlled application of gases in predetermined concentrations and also the exposure of sensors to complex mixtures of the test gases with given concentrations of each component within the limits achievable determined by the concentration in the test gas bottle or the vapor pressure of the test gas.

With the set-up of the gas mixing station used in this work, the sensitivity or resolution values of the sensors could only be extrapolated. The gas mixing station did not allow the application of test gases in concentrations as low as the limits of detection of the tested sensors with sufficient precision. In the set-up of the amperometric gas sensor module in MOSES, the concentration range of the sensors is limited by the sensitivity of the sensor and the maximum signal to be accepted by the MOSES software. For the lower limit of the concentration range the tripled value of the base signal noise was set as minimum concentration, the maximum concentration is dependent on the modus of operation of the sensor, e.g. operation potential and signal amplification (see also Table 8). The extrapolated concentration range for the CO sensor was 0.1 to 300 ppm CO and the tested range for the $NO_2$ sensor was 0.2 to 10 ppm. Due to the setting of the operation potential the range of the sensor $SO_2$ is limited from 1 to 28 ppm, here optimized for low concentrations. This range can be adjusted to values up to 100 ppm. For the $H_2S$ the full concentration range was not tested. The lower limit of detection though is 1 ppm.

## 4.3.  Sample preconditioning methods

Development of the sampling system and sample pretreatment are fundamental ways to increase the utility and performance of instrumental analyses, and sensor arrays are no exception. Virtually, every chemical classification or analysis technique requires a sampling system for obtaining reproducibly a truly representative sample. Appropriate and reliable sample transport and conditioning are key elements for obtaining good analytical results.

A majority of analytical problems can be attributed to problems in the sampling system, and consequently, a lot of effort has concentrated on improving the technology and design of the sampling system (see chapter 2.3). However, most of these sampling techniques have been designed for use in conventional analytical chemistry.

For investigations based on e-noses with their unique requirements to the sample uptake, sample conditioning methods need to be modified to optimize the analytical performance of the entire system. The adaptation to chemical sensors and further development of sample conditioning has been the goal of the following work on experimental set-ups for e-nose sampling.

The purpose of a sample system is more than presenting an appropriate and representative sample to an analyzer. Essentially, it amounts to making the sample compatible with the employed investigation technique , representative of the material being sampled, and adapted for the application at hand.

Many samples investigated with e-noses are liquid or solid; often a successful analysis depends on finding means of mitigating the effects of matrix and solvents to determine minor and trace components in samples prior to the measurement [72-81,123].

The requirements for the set-up are determined by the application and range from making the target analytes detectable with the chemical sensor type (see chapter 4.3.1) to enhancing the response to polar constituents contained in a matrix of water (see chapter 4.4.2 and 5.5).

Sample preconditioning techniques from conventional analytical chemistry, mostly initially developed for gas chromatography, have been adapted in this work to the requirements and analytical capabilities of chemical sensor arrays leading to new methods solely oriented to the enhancement of e-nose performance.

In this work, modified sampling systems, with a heated filament or with a membrane separator/dryer in the sample stream prior to the sensor arrays, have been set-up, evaluated, and optimized for specific applications. Thermal desorption trap units have been designed and optimized. The optimization of preconcentration set-ups for use with the e-nose resulted in a design and mode of operation merging the thermal desorption technique with advantages of chromatographic separation.

## 4.3.1. Catalyst

The catalytic filament (Bacharach, Inc., Pittsburgh, PA) was mounted in a metal tee fitting and heated with a controlled 1.7 volt supply, which caused the filament to glow visibly. The fitting could be inserted into the sample line between the headspace sampler and the MOSES II e-nose, or between any two sensor array modules of the MOSES II system which affords much flexibility. A second fitting was built that used a small, conical platinum wire coil to hold a tiny glass cup (2 mm i.d. x 4 mm) to hold the sample, which in this case was quartz sand impregnated with trinitrotoluene. This fitting was mounted ahead of the catalytic filament. Figure 25 shows the catalytic filament and sample holder.

A second set of experiments was performed using only a single filament (the second filament in Figure 25) in front of the sensor arrays. In these experiments, 10 µl of ethanol containing dissolved target analyte, here TNT, was placed on the Pt-filament and allowed to air-dry. The filament was then heated to desorb/react the material (TNT, DNT, EDTA) that was deposited on the filament and the sensor signals were recorded. The sensor signals were subtracted from those obtained in pure air since small signals were observed for the filament even in clean air. This is probably due to a small amount of $NO/NO_2$ that can form at high temperatures from the air. Details of the filament catalyst experiments and measurement results have been presented elsewhere [88].
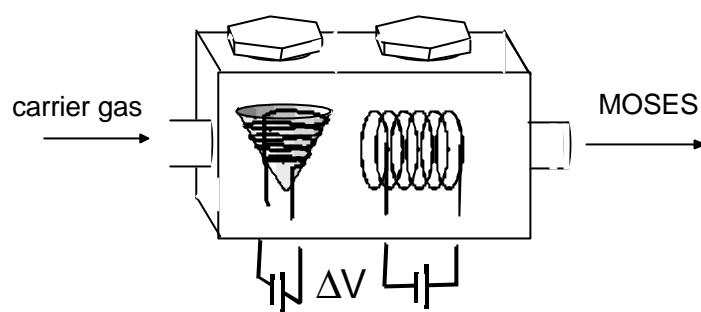
*Figure 25: Filament chamber and holder for the catalytic Pt filaments for sample volatilization and vapor reaction. During later experiments, the sample was volatilized and reacted from a single filament.*

The filament was used to enable the detection of electrochemically inactive analytes after passing the filament.

### 4.3.2. Nafion dryer

Often, chemical sensing of compounds against a background of water is a problem with MOX and QMB sensors, which display sensitivity to water. For removing this interfering background from the sample stream a Nafion gas dryer was used.

A simple gas dryer of Nafion tubing embedded in a desiccant has been built and tested. Besides reducing the relative humidity of samples, it also selectively removes some compounds from the sample stream.
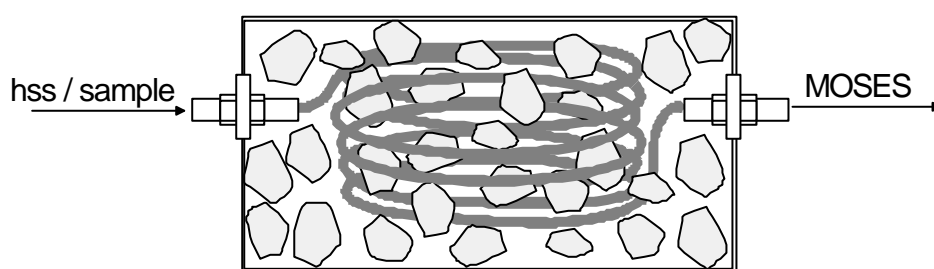


*Figure 26: Schematic drawing of Nafion dryer.*

The Nafion gas dryer was built from 32 cm of 1.5 mm o.d. Nafion tubing (Perma Pure, Inc., Toms River, NJ, U.SA). The coil of tubing was embedded in calcium chloride. Using the humidity sensor in the Input Module of MOSES II, it was determined that a sample r.h. of 80% could be reduced to 6% at 25 ml/min. Depending on the operation conditions over 99% of water vapor and alcohol are removed. Figure 27 shows the set-up as used with MOSES II.

*Figure 27: Nafion dryer connected to MOSES II.*

Nafion is a fluoropolymer with ion exchange capacity and will remove not only water but also other compounds from the sample stream and, therefore, passing the sample through the Nafion significantly alters the sample chemical properties. The Nafion tube shows a high permeability for water, which is adsorbed with a hygro-scopic dryer material outside the sampling system, in this case $CaSO_4$, but also removes volatile alcohols and some other polar solvents. Nafion belongs to the class of solid polymer electrolytes and has hydrophobic ($-CF_2-CF_2-$) and hydrophilic ($-SO_3H$) regions in its polymeric structure. When the sample exits the Nafion dryer, it has been depleted of water, methanol, ethanol, acetone and similar compounds, yet contains virtually all of the permanent gases such as $CH_4$, CO, $CO_2$, as well as many non-polar hydrocarbons like cyclohexane, benzene, and toluene. The dryerite insures that the r.h. is 0% on the outside of the Nafion, and so the driving force for water removal is the gradient across the tube and constant. Similarly, other adsorbents could be used to improve the efficiency of removal for alcohols or other compounds that are soluble in and transported through the Nafion. Therefore, the Nafion separator is capable of enriching or depleting the stream in any number of analytes to which it is permeable.

### 4.3.3. Sodium sulfate dryer

A second dryer using 3g of dehydrated $NaSO_4$ in 6mm Teflon tubing has also been tested. Figure 28 displays a schematic drawing of the dryer.
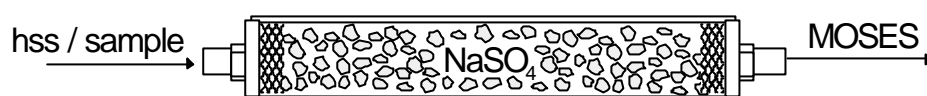
*Figure 28:Schematic drawing of NaSO$_4$ dryer.*

Other than the Nafion dryer, here the gas passes over the drying agent directly. This has two main consequence: The gas passes a higher surface area and the chromatographic effect of the filter is enhanced and second the water will be removed directly without the effect of Nafion absorbing polar organic compounds like ethanol.

## 4.4. Preconcentrator units

Preconcentration test units with different trap dimensions following the principal set-up shown in Figure 29 have been realized and tested. The goal was a minimized thermodesorption system for possible integration into MOSES as an additional module. Commercial preconcentration systems [36,161] are either specialized for the application with gas chromatographs or are too big for the integration in MOSES. The combination with a headspace sampler requires adapted dimensions of the trap.

The principle set-up of a thermodesorption unit is shown in Figure 29. Several set-ups have been designed and tested.
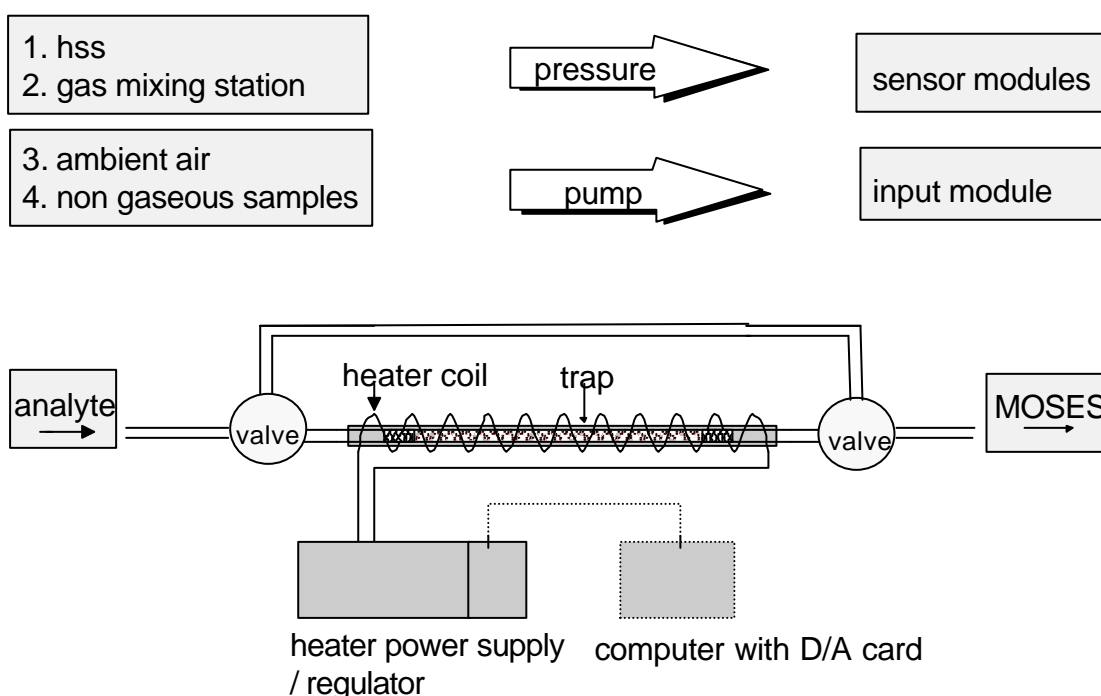


*Figure 29: Thermodesorption set-up.*

The schematic drawing of the trap set-up was a model for the set-ups built for tests with MOSES and mass spectrometry.

### 4.4.1.  Set-up of manually operated test traps

Several manually operated thermal desorption set-ups were built for optimizing the dimensions and operation parameters.

The adsorption tube material was stainless steel integrated in a copper tube for fast and heat transfer and even heat distribution. The outer tube was completely surrounded by a heater wire coil integrated in a thermally stable inert material for isolation. The length and outer diameter (o.d.) were varied in several set-ups form 3 to 6 mm o.d. and 100 to 200 mm length, respectively. The trap thus contained 80 to 160 mg of sorbent material (Tenax 60/80 mesh).

The set-up with two valves and a by-pass allowed several modes of operation for the use of the system. When using the pump of the input module of MOSES, ambient air, odors, or the headspace of non-gaseous samples could be trapped. If the system was attached to a gas mixing station or headspace sampler, pressure was the driving force for the analyte through the trap directly to the sensor modules. The optimized set-up allowed for an automated sample uptake under controlled and reproducible conditions. The power supply of the heater was sufficient for reaching 200°C for desorption inside the tubing in 2 min at 20 V power uptake using an 80 cm NiCr heater wire. However, the design with a heater coil did prevented easy exchange of the trap itself. Tests with a programmable oven capable of heating the trap to 200°C within one minute where conducted but power supply and dimensions of the oven proved incompatible with the goal of a system integrated in the MOSES II set-up. For minimizing analyte loss the system was optimized for low volume, which meant short and small transfer lines and minimal trap volume.

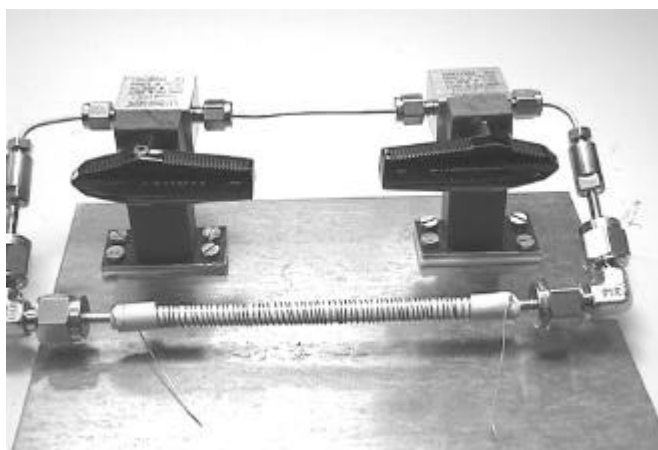Figure 30 shows the set-up with insulation of the heater coil.

*Figure 30: Set-up of manual trap (3mm o.d.).*

The trap was tested with MOSES and proved to allow quantitative adsorption and desorption for relatively high analyte concentrations. For a characterization of lower concentrations a more sensitive mass spectrometer was used (HIDEN dynamic sampling mass spectrometer, DSMS). The trap was exposed to various concentration of organic vapors generated in a gas mixing station. The analyte gases were applied in pulses in order to observe the breakthrough time and maximum quantity of analyte the trap material adsorbs.

Figure 31 shows the signal for the repeated exposure to iso-octanol (100 ppm). After 13 exposures for 10 min each with 200 ml/min the trap did not show a breakthrough of the alcohol. The analyte was then desorbed at 200°C.

The graph indicates that the adsorption or preconcentration of iso-octanol is not complete during exposure. Therefore, the trap geometry had to be changed. There were still peaks recognizable for the exposures to the analyte. The intensity of these peaks was even slightly decreasing with each repetition of exposure indicating that the trap was not being saturated. As solution to this problem it was again and successfully tested, to increase the length to diameter ratio in order to allow slower adsorption kinetics. The peak shape for the desorption showed that the process of desorption was also slower than the heating of the trap. The desorption section beginning at 290 min in Figure 31 shows a repeatable sharp peak followed by the broad peak of the desorbed iso-octanol. The mass spectrum was recorded at 57 mass units, characteristic for iso-octanol. To ensure that the first peak was an artifact or caused by another substance a second measurement focussing on a different mass was necessary. There was no decomposition of the trap material.
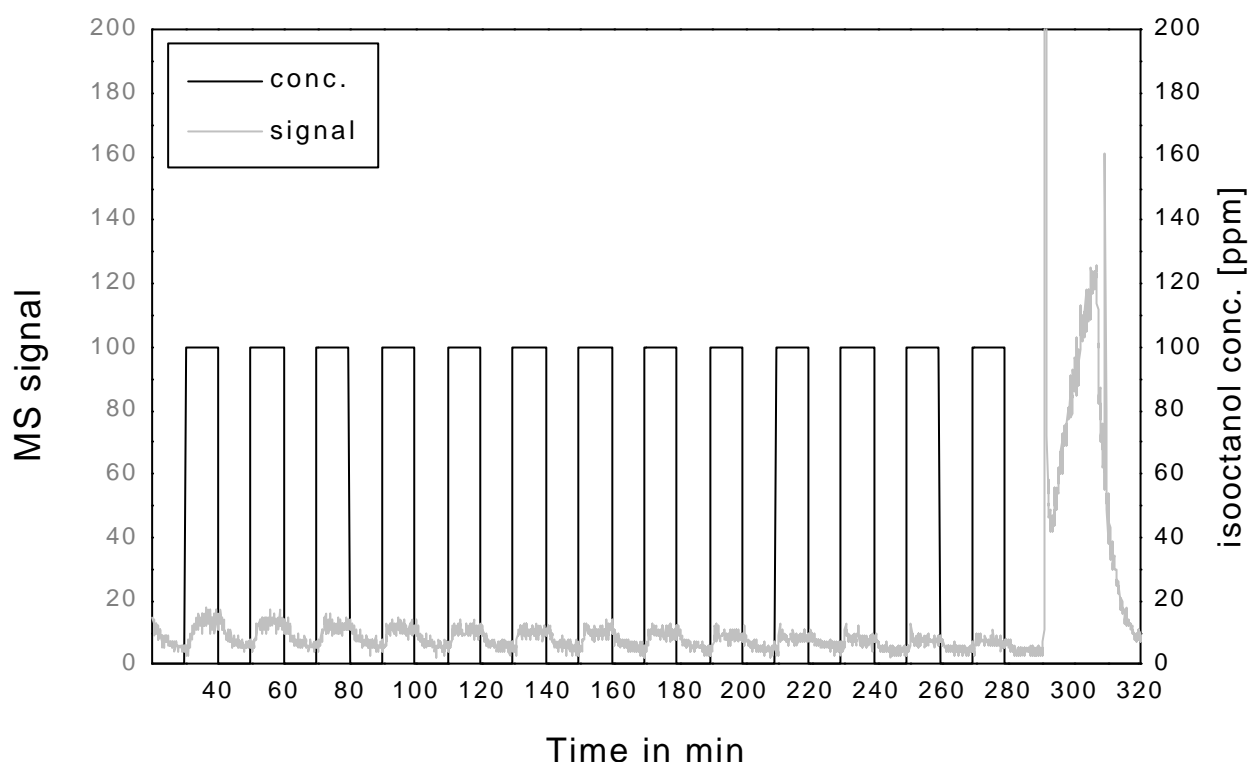
*Figure 31: Pulsed exposure of T2 trap to iso-octanol and desorption at 200°C.*

In order tominimize analyte loss the system was optimized for low volume and measurements together with a headspace sampler. Since DANI headspace sampler gives the opportunity of multiple extraction, either from one vial or from more than one sample, one possibility for the automation of the preconcentration set-up is the combination of headspace sampling with thermal desorption.

In order to test the capacity of minimized thermodesorption units and the influence of geometry, a second set of units was realized using a gold tubing with 1/16" o.d., also according to the set-up schematic in Figure 29. The transfer lines in the unit were 1/16" o.d. stainless steel using GC connectors for reduced dead volume. The overall set-up dimensions were 120 mm in length and 30 mm in height. The miniaturized system allows to concentrate all elements of the thermal desorption unit within the space provided in a standard MOSES module, that is the trap, the valves, the heater, and the thermal element for the heater control (Figure 29).

For improved heat transfer the trap itself was a gold capillary of 1 mm i.d.. It was coated with an insulation layer and a thin platinum wire as heater. Thereby the energy consumption and heating time could be reduced; the power requirement

to less than 12V, which is the voltage provided by the MOSES power supply. A thermal element for controlling desorption temperature was integrated under a second layer of insulation. The heat transfer was vastly improved by using gold as trap material and the trap could be used for small concentrations applied with the automated headspace sampler. However, the decrease of the inner diameter resulted in a high back pressure for flow rates sufficient for chemical sensors measurements (20 ml/min).

Testing also proved the insufficient capacity of the 16" trap for the required concentration range : A decrease of the inner diameter of the tube to half of its value leads to a sharp increase of the linear velocity of analyte in the trap and therefore to a decrease in trap efficiency (see also section 3.2.3).

The thermodesorption units tests with MOSES and MS indicated that the set-up required improvement in several details such as:

- Heating:

The heating response time within 2 minutes to 200°C was too slow for a good signal characteristic with the MS but sufficient for MOSES II. For operation as a conventional thermodesorption unit, and for preconcentration only, a heating time of 10°C / s would be preferable. This would be comparable to the time commercial purge and trap units allow, but required an external high output power supply. As flash heating was not required in the operation with MOSES II, the trap was optimized for low power consumption. Therefore a thinner stainless steel tube material or glass as trap material, providing similar heat transfer, was used in further experiments. The heater in the two tested set-ups though still required a separate power supply of up to 20 V for heating the trap sufficiently fast. Heating with a coil wound around the trap with an insulation layer made the change of the trap arduous.

- Heater insulation:

The heater insulation was made from folded ceramic paper. A coating of alumina ceramic proved not to be mechanically stable.

- Sorption material packing:

The sorption material required careful packing. Otherwise a pressure loss over the trap resulted from clogged sorption material when heated. This then altered the signals of the test gases and desorption kinetics were altered unfavorably. The 6 mm o.d. traps proved to be the easiest in handling and filling with different resins.

In summary, the tested thermal desorption units worked in principle, but several parameters had to be changed for use with MOSES.

This led to a different design of heater and trap setting with a more flexible temperature control described in the following chapter.

### 4.4.2. Differential thermal desorption

An automated thermal desorption set-up has been assembled and extensively tested for use with the e-nose. The design of the trap and the interfacing of the set-up to the e-nose based on the basic principle of thermal desorption shown in Figure 29. It was further modified to also yield additional benefits in operation described below. The computer control of the trap temperature over the entire cycle time of the measurement allows selective desorption of parts of a sample mixture at predetermined temperatures or differential thermal desorption.

Figure 32 schematically shows the set-up and interfacing of the modified thermal desorption unit to MOSES II and a commercial headspace sampler for sample uptake.
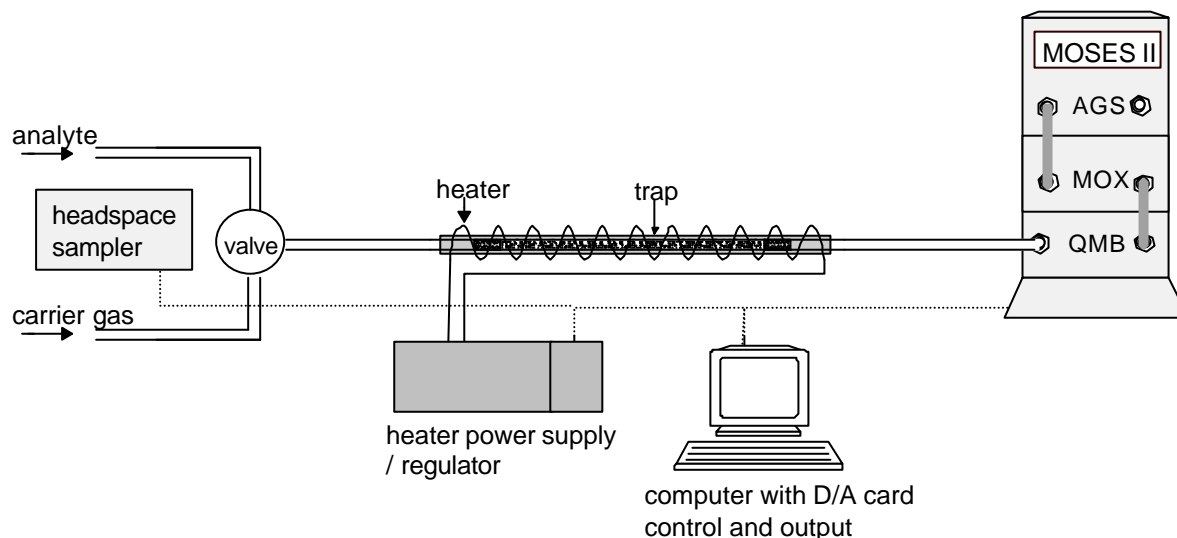
Figure 32: Schematic set-up of the differential thermal desorption sample uptake and the e-nose.

The MOSES II system was connected to the headspace sampler (HP 7694) via the sample conditioning set-up consisting of a Tenax thermal desorption tube situated in the adjustable heater assembly which was capable of reaching 230 °C within 2:30 min. The gas flow direction for loading the trap and desorption is the same unlike most set-ups of thermal desorbers in e.g. GC/GC-MS.

The heater of the differential thermal desorption set-up comprises two heater elements enclosing the thermal desorption tube and ensuring even temperature distribution along the trap. The heaters are clipped to the tube allowing an easy change of the tube with the adsorption resin and therefore an adjustment to a given application. For the 1/4" outer diameter and 3" length tubes different commercial and experimental traps have been evaluated. 230 mg of adsorbent resin, as used in commercially available traps, e.g. as used for the Perkin Elmer ATD 400 automated thermal desorber [162], proved to be sufficient for the tested applications thus enabling trap characterization and comparison with commercial thermal desorbers. The trap performance and heating characteristic provided to be independent from the used tubing material with a highly reproducibble temperature distribution for a given heater setting. Figure 33 (a) shows the temperature of trap material during a heating cycle for stainless steel and glass as trap materials. The temperature measured in the adsorbent resin indicates a small delay compared to the temperature measured at the tubing outer surface but the overall curve is the same as shown in Figure 33 b:
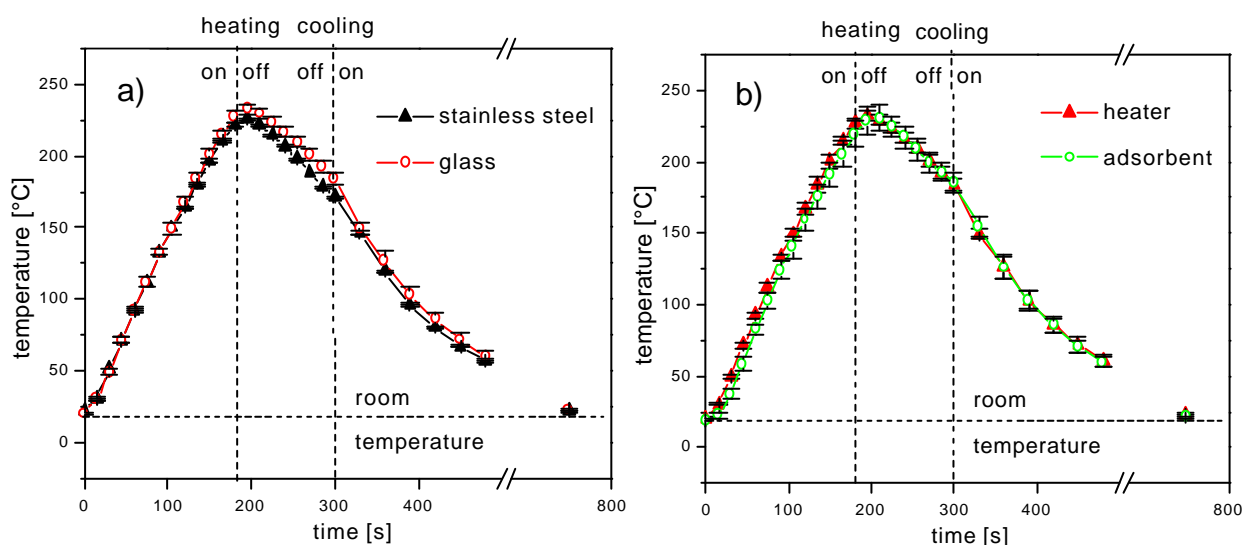


*Figure 33 (a,b): Trap temperature for a heating cycle for two trap materials (a) and temperature s measured in and outside of the trap (b). .*

By cooling the trap after the heating ramp, cycle times of less than 15 minutes can be achieved even for slow heating.

The heater is programmed by a C-Control BASIC programmable computer type M (1997 Conrad Electronic GmbH, Hirschau, Germany) based on a Motorola MC68HC05B6 micro controller with 16 digital and eight A/D ports. The control unit is integrated with the trap set-up and programmed via the computer

operating MOSES II. A measurement and a thermal desorption cycle can be started by the start signal of the headspace sampler to the e-nose or manually. Prior to the start of the measurement the thermal desorption cycle is programmed to determine the heating rate or slope of the temperature by heating pulse length modulation and cooling of the trap. The heating pulse modulation has been calibrated to the trap temperature for the measurements so that for any time during the thermal desorption cycle the temperature is determined with a precision of +/- 1 °C. The trap temperature can also directly be monitored during the measurement. The programmable heating allows to identify target key analytes from a sample for chromatographic separation within the thermal desorption process. Thus, the trap can be used as chromatographic column in addition to the conventional utilization as preconcentrator. Isothermal ramp sections at a selected temperature proved to be a controllable and suited way of separating compounds. The temperature is selected according to tabled values for breakthrough volumes of analytes on the adsorption resin or is empirically determined for unknown constituents (see also section 5.4.3). This novel mode of operation adds a range of parameters to the sample uptake possibilities and also multiplies the information content obtainable with a single e-nose measurement. Figure 34 shows the disassembled trap set-up with the control unit.
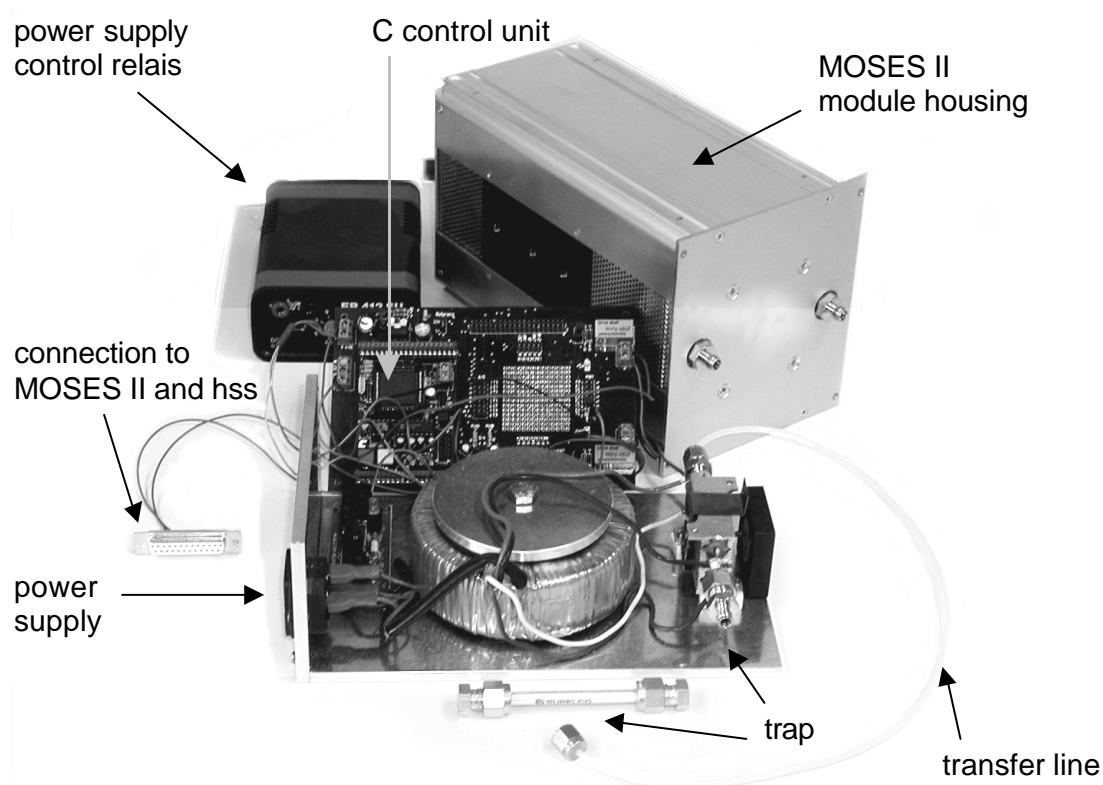


*Figure 34: Set-up of the differential thermodesorption unit.*

Originally the thermodesorption unit was designed to match the dimensions of a MOSES II module similar to the one housing the MOX sensors with the programmable control unit included. The external power supply for the solid state control relais exhibited will be replaced by an integrated unit. The complete unit set-up in an external housing provides an easy access to the thermodesorption tube enclosed by the two molded heaters for changing traps. For test measurements a stand alone prototype has been built (Figure 35).
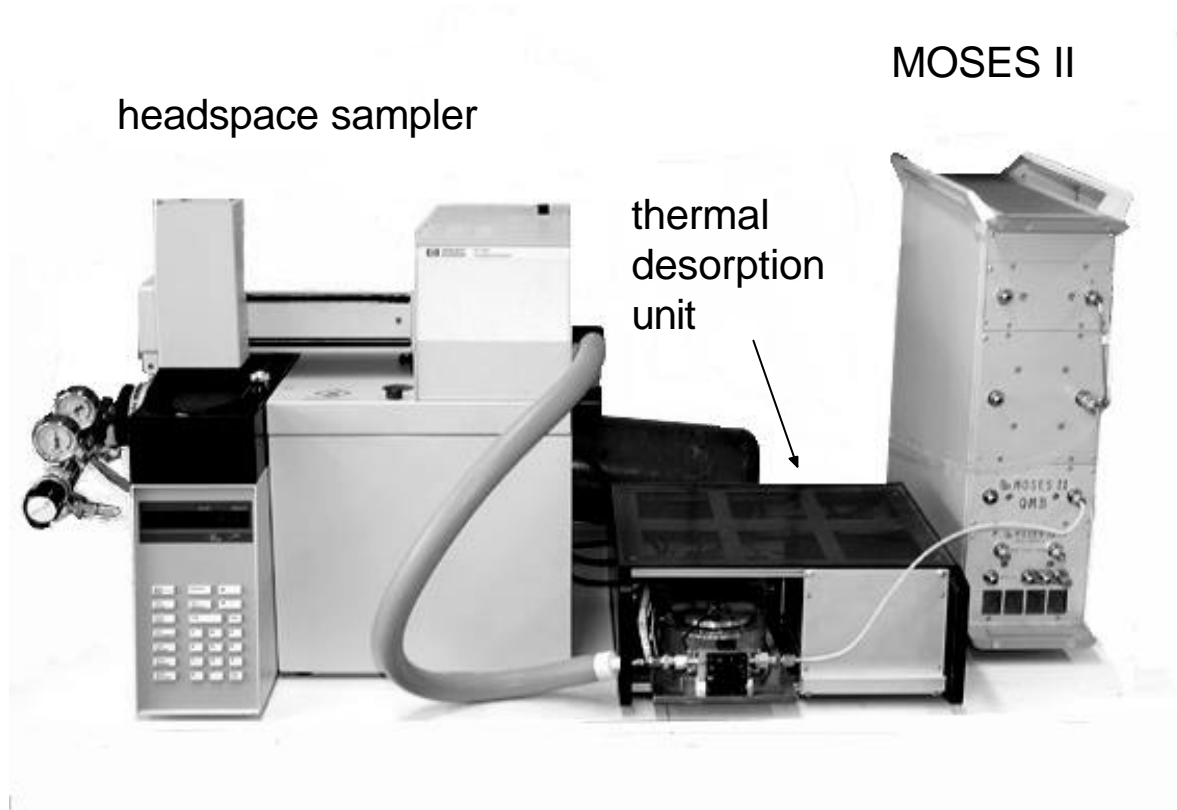


*Figure 35: Set-up of headspace sampler with carrier gas bottle,. differential thermodesorption unit, and the MOSES II e-nose.*

## 4.5. Sample preparation

In e-nose applications often the gas phase being in thermodynamic equilibrium with a liquid or solid sample is analyzed. However, the constituents of the actual sample and not of the extract are of interest. Therefore, constituent concentrations are generally referring to the sample phase.

Samples investigated and measured using a static headspace sampler in this work were weighed and filled into standard 20 ml glass vials and sealed by a cap containing a gas tight septum (PTFE-lined butyl rubber diaphragm). The quantity

investigated was optimized for each application. Concentrations are given in ppm and refer to the mass ratio in the liquid phase if not stated otherwise.

### 4.5.1. Bacteria samples

All experiments were designed to use the headspace sampler and sealed sample vial system originally designed for use with gas chromatography and GC/MS. An Erlenmeyer flask containing BHI medium was temperature controlled and shaken and then inoculated with culture. The culture was grown for one hour to establish log phase growth. At time zero in the experiment, 5 ml aliquots of the dilute culture were transferred into standard 20 ml headspace vials and sealed with PTFE-lined butyl rubber diaphragms. The cultures were allowed to grow in the vials at 37ºC for varying time periods before being killed by 10 minutes treatment in boiling water. Each time point consisted of five replicates, one of which was used for measuring the optical density of the culture. The remaining four replicates were measured by the MOSES II system. The sealed headspace vial approach effectively retained the volatiles produced by the growing cultures, and gave improved sensitivity and reproducibility over working with open, aerated cultures and the e-nose. Controls confirmed that the vials contained sufficient oxygen to maintain normal growth for at least 5 hours.

The organisms used in these studies were wild type Escherichia coli ATCC 15490 and 15992, and Enterobacter aerogenes ATCC 13048. Optical density measurements were made at each time period and converted to bacterial cell concentrations using the factor 109 cells/ml per O.D. unit at 600 nm, using a Spectronic 20 spectrophotometer (Beckman Instruments, Walnut Creek, CA).

Bacteria strains used in this work were provided courtesy of. M.L. Tortorello, national Center for Food Safety and Technology / U.S. Food and Drug Administration , Argo, Il, USA. Samples were prepared together with C. McEntegard, Illinois Institurte of Technology, Chicago, IL, USA.

### 4.5.2. TOPE

In order to evaluate the performance of experimental set-ups and the electronic nose, a model mixture of chemicals in an inert, non-volatile matrix of polyethyleneglycol 400 (PEG, Merck-Schuchhardt, Germany) was used. For this purpose a mixture of toluene, n-octane, 1-propanol and ethyl acetate (TOPE) in PEG was prepared. The TOPE test mixture, which has been used throughout this work, consists of known quantities of pure chemicals weighed into a known mass of the matrix PEG. Two concentrations, either 2000 ppm of each

constituent or 2000 ppm of analytes in total, contained in 10 g of PEG were applied in the studies. The chemicals where selected to represent different classes of chemicals with comparable volatility and are routinely used as test substance for sensor array performance [22,124].

## 4.6. Gas chromatography - mass spectrometry

GC-MS-headspace-analyses were carried out using a Hewlett-Packard gas chromatograph (HP 6890) coupled with a Hewlett-Packard mass selective detector (HP 5973 MSD) and a Hewlett-Packard headspace sampler (HP 7694). The fused silica capillary column was 0.32 mm i.d. coated with an intermediate polarity polysiloxane phase (HP 19091R-316, HP-VOC, Hewlett-Packard). The column length was 60m. The stationary phase film thickness was 1.8 µm. 6.0 purity quality Helium (Messer-Griessheim, Germany) was used as carrier gas.

The GC-MS operation parameters are listed below for the different applications (Table 9).

| Instrument | Operation parameter | Cheese | Beer | Mayonnaise |
|---|---|---|---|---|
| **GC** | Injection inlet temp. | 200 °C splitless | 200 °C split 1:150 | 250 °C splitless |
| | Oven: | 50 °C for 6 min, ramp 10°C/min, 230° for 10 min | 70 °C for 6 min, ramp 5°C/min, 230° for 4 min | 40 °C for 6 min, ramp 15°C/min, 230° for 10 min |
| | GC-MS interface temp. | 270°C | 270°C | 270°C |
| | He flow | 1,5 ml/min | 1,0 ml/min | 1,5 ml/min |
| **MSD** | Ion source temp. | 230°C | 230°C | 230°C |
| | Quadrupole temp. | 150°C | 150°C | 150°C |
| | Acquisition mode | 5 min solvent delay, Scan mode (33-250 amu) | 5 min solvent delay, Scan mode (10-250 amu) | 5 min solvent delay, Scan mode (33-250 amu) |
| | Threshold | 150 | 150 | 150 |

*Table 9: GC-MS operation parameters.*

Sampling with the Hewlett-Packard headspace sampler was performed with identical operation parameters as used for the e-nose investigations for each application.

GC/MS peak identification was performed by the Hewlett-Packard MSD Productivity ChemStation Software Rev. B.00.01. The software allows qualitative and quantitative predictions by taking retention time and peak area into account. In order to identify the peaks, pure compounds were chromatographed and the NIST (National Institute of Standards & Technology, Gaithersburg, USA) mass spectrum library served as reference data bank. Quantitative results however require a calibration with standards for a prediction of concentrations in ppm, which was not carried out. Peak areas are given in percentage of total peak area and therefore give only a semi-quantitative information. Since headspace concentrations were only considered comparatively, the absolute amount of a substance was not crucial.

Due to the relatively high film thickness (1.8 μm) of the chromatographic column (HP-VOC), a certain "column bleed" at higher oven temperatures was unavoidable. Thus, at longer retention times, the chromatograms showed a background, which could be subtracted (by an implemented function of the software) to result in mass spectra with only few peaks derived from the column film. Contamination from the septa of the headspace vials could not be subtracted and appear in the chromatograms as cyclotrisiloxane peaks.

## 4.7. Characterization of sorption materials with thermal analysis

The interaction of sorption materials with analytes was investigated with thermal analysis. Thermal analysis is a generic term for methods where physical or chemical properties of a substance are recorded as function of temperature and time while the temperature of the sample, in a specified atmosphere, is programmed [163]. Phenomena such as ad- and desorption can thus be monitored by recording changes in energy (DSC) and mass of a sample (TG).

Differential scanning calorimetry (DSC) is the measurement of a temperature difference of a sample to a reference versus ambient temperature and time, thus allowing the quantitative investigation of phenomena involving heat transfer, i.e. endothermal or exothermal processes. Thermal gravimetry (TG) very precisely measures the variation in sample mass when it undergoes temperature scanning in a controlled atmosphere.

Theory and application of thermal analysis are described in [163,164]. The measurement set-up and further investigation results are described in [70]. The measurements were conducted on a TG-DSC 92-12 thermal analyzer (Setaram, France)

For examination of the sorption material the samples were weighed and heated prior to measurements under nitrogen atmosphere for removal of possible humidity and contamination which could cover adsorption sites. The selection of the adsorbents was based on a review of the literature and the requirements of operation in conjunction with the e-nose, e.g. high temperature stability and low affinity to water.

Tenax, zeolite, and active charcoal as commonly used as sorption material (see Table 3) were investigated. The 100 µl-crucibles used in the TG/DSC device held about 10 mg of sample. The different investigated analytes were applied as vapor from the organic compound derived from a bubbler as mixture with dry air. The gases were applied in a gas flow of 50 ml/min added to the nitrogen flow constantly purging the instrument. The adsorption and desorption of the applied gases could be carried out reversible and reproducible in the described conditions. Figure 36 shows a TG/DSC measurement cycle with the exposition of Tenax adsorption resin to two different analytes and following desorption of the analytes. The sample temperature, the mass change in percentage of sorption material mass Δm, and the heat flow are plotted versus time. The integration over the heat flow gives the heat of enthalpic transitions.
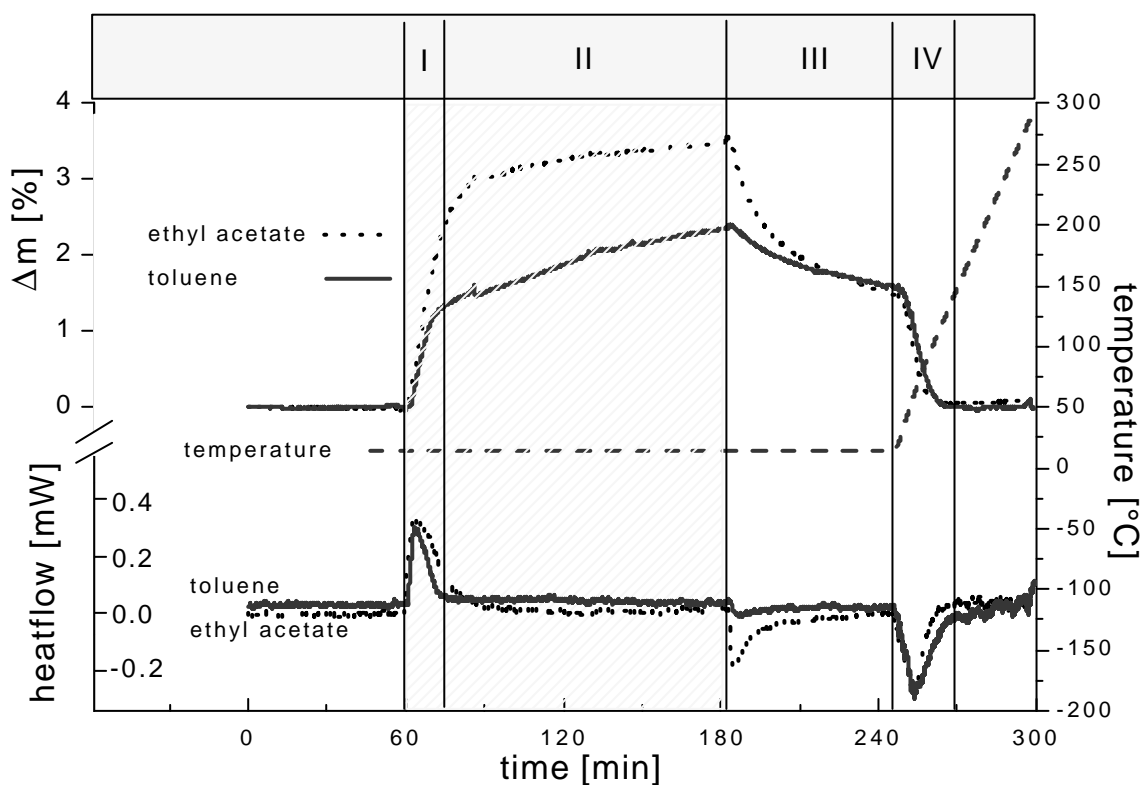


*Figure 36: Test results of the investigation of Tenax with TG-DSC.*

The interaction of trap material and analyte can be described in four phases. Since the goal of the measurement was to obtain information on the capacity of the sorption material, the resin was exposed for two hours to high concentrations of analyte in phase I and II. This is indicated hatched between 60 and 180 minutes of the measurement time in Figure 36. The time of analyte exposition can roughly be divided in two phases which can be best distinguished by looking at the heat flow. During the short phase one, analyte adsorption on the resin goes along with a sharp increase in measured resin weight and the peak in the heat flow measurement curve. The adsorption heat can be determined as integrated area under the heat flow curve, here for the exothermic adsorption as positive value.

The slower weight gain of phase two, Which is as a gradual process not detectable as heat flow, indicates condensation rather than adsorption as utilized in thermal desorption. The condensed or capillary absorbed analyte is released when the resin is purged with purge gas at the same flow rate of 50 ml/min as used for analyte application in phase III with the expected exponential desorption characteristic. Phase II and III can be interpreted, by taking a different point of view, as process of physisorption, reversible isothermal at room temperature. This is comparable to a sensitive layer with slow response time or slow on- and off-rate. The analyte adsorbed in phase I is eluted when heating the trap in phase IV, resembling the thermal desorption. The heat flow indicates the endothermal desorption going along with the again exponential weight loss of the resin. To determine the trap capacity for different analytes the weight change of the resin in phase IV is the maximum amount of analyte which the trap can reproducibly hold in thermodesorption operation. Any excess analyte will not be quantitatively and therefore reproducibly trapped. For ethyl acetate Figure 36 indicates that the analyte first adsorbed is not a safe measure for determining the point when the trap is overloaded.

The measurements showed fast adsorption and desorption, within 5 minutes for all compounds tested, for an amount of analyte determined to be lower than the adsorbent resin capacity. The kinetics of adsorption and desorption monitored in the TG/DSC measurements are considerably slower than those of a thermodesorption trap with analyte and purge gas stream passing through the trap due to the measurement set-up, which only allows for gas passing over the resin. Therefore, trap geometry optimization and the monitoring of sorption kinetics were performed on different traps rather than TG/DSC.

However, the obtained results are in compliance with findings reported in literature where trap characteristics are correlated to thermodynamic sorbent properties. However, these data show that the kinetic equilibrium of the breakthrough volume of a trap with a specific adsorbent is affected by geometric factors, whereas the saturation equilibrium represented by the adsorption isotherm is not affected. Thus, it is confirmed that the weight gain in sample enrichment corresponds to the adsorption isotherms of an analyte and can be determined gravimetrically [135].

The capacity of the sorption material proved to be most critical for Tenax with a maximum load of 1.8% of the resin mass compared to active charcoal which adsorbs up to 30% of its own mass of certain analytes. Also, adsorption capacity is reported to be concentration dependent for some compounds [50].

The safe region for trapping has to be determined for each analyte and resin separately. For the low analyte concentrations associated with most e-nose applications and for practical use of the trap as preconcentrator trap capacities or in then safe sample and breakthrough volumes are more conveniently calculated from retention time of the adsorbent tubes, but only if it is ensured that the linearity of the accumulation on the trap or the comparison of tabled breakthrough volume data [165] are applicable and valid within the operation conditions used (see section 3.2.8)

Tenax proved to have, in agreement with data from literature [165], the least affinity to water of the tested sorption materials. This property, together with the favorable sorption kinetics and stability at high temperatures, makes Tenax a well suited trapping agent for uilization in preconcentrators used for measurements with chemical sensors.

# 5. RESULTS AND DISCUSSION

Samples from different fields of applications where investigated employing and further optimizing the sampling techniques and set-up modifications to the e-nose developed in this work.

## 5.1. Optimized sample preconditioning without preconcentration

Many sample conditioning methods described in chapter 2.3 focus on means of mitigating the effects of water to determine minor and trace components necessary for the distinction of the sample class or quality.

The elimination of a sensor response to water covering information on the liquid or solid sample while preserving the response to target analytes was the main objective of the design of the sample conditioning set-up described in chapter 4.3.2. used for the following investigations. In combination with the amperometric sensors the system proved to be sensitive enough to make a preconcentration of sample constituents unnecessary. By optimizing a simple but effective method of separation via a membrane an additional step in sample handling involving thermal treatment would have been a superfluous complication.

All measurements were conducted with the MOSES II equipped with three sensor modules: The QMB module containing 8 sensors (Q1-8), the MOX module with 8 sensors (S1-8), and the EC module containing 4 sensors (S1-4).

## 5.2. Investigation of Coliform Bacteria

Recently, the electronic nose has been used to detect the volatiles emitted by growing bacteria. By using concentrated samples, the e-nose has consistently been able to discriminate among arbitrarily different types of bacteria, at least at the genus level [166, 167, 168]. These studies have generally been done with dense cultures, centrifuged cells, or colonies of bacteria grown on an agar surface. There has recently been a report of an e-nose being used to detect a pulmonary infection [169]. Since conventional bacterial taxonomy is based largely on differing nutritional requirements or metabolic products, it is not surprising that the volatiles in the headspace of a bacterial culture are determined by the metabolism of the specific strains of organisms.

In this work, it is attempted to assess the sensitivity of a modular electronic nose [147] for the detection and discrimination of microorganisms.

Sensor arrays, which are used for characterizing complex vapors and aromas, were tested for detection of bacterial contamination or infections to establish whether minimal standards of selectivity and sensitivity can be met by the sensors, associated instrumentation, and method used. In conventional microbiology, bacterial species are distinguished from one another in part using their metabolic properties. Some waste products of metabolism tend to be small, volatile molecules. Therefore, headspace air above a bacterial culture therefore was investigated aiming at the discrimination of bacterial species as well as quantification of the growth rate.

Tests were made on five growth media (Brain-Heart Infusion, Nutrient Broth, Tryptone Yeast Broth, Tryptone Soy Broth, and Luria-Bertani, all from Difco, Inc.) to measure the growth rate of *E. coli*, as well as the ability to detect growing bacteria with the e-nose sensors. The Brain-Heart Infusion (BHI) promoted the fastest growth rate, and also gave the lowest backgrounds on the sensor array. In the PCA plots throughout this work, the zero-time controls, which consisted of BHI medium inoculated with bacteria and immediately killed, always overlapped the plain water blanks. This implies that few volatiles were produced by the uninoculated medium. Therefore, BHI was used for all following experiments.

All measurements on bacteria have been performed at the Illinois Institurte of Technology, Chicago, IL, USA.

Figure 37 shows an example of the principal components plot obtained from the responses of the MOSES 8+8+4 = 20-sensor array to samples taken at different periods during bacterial growth.
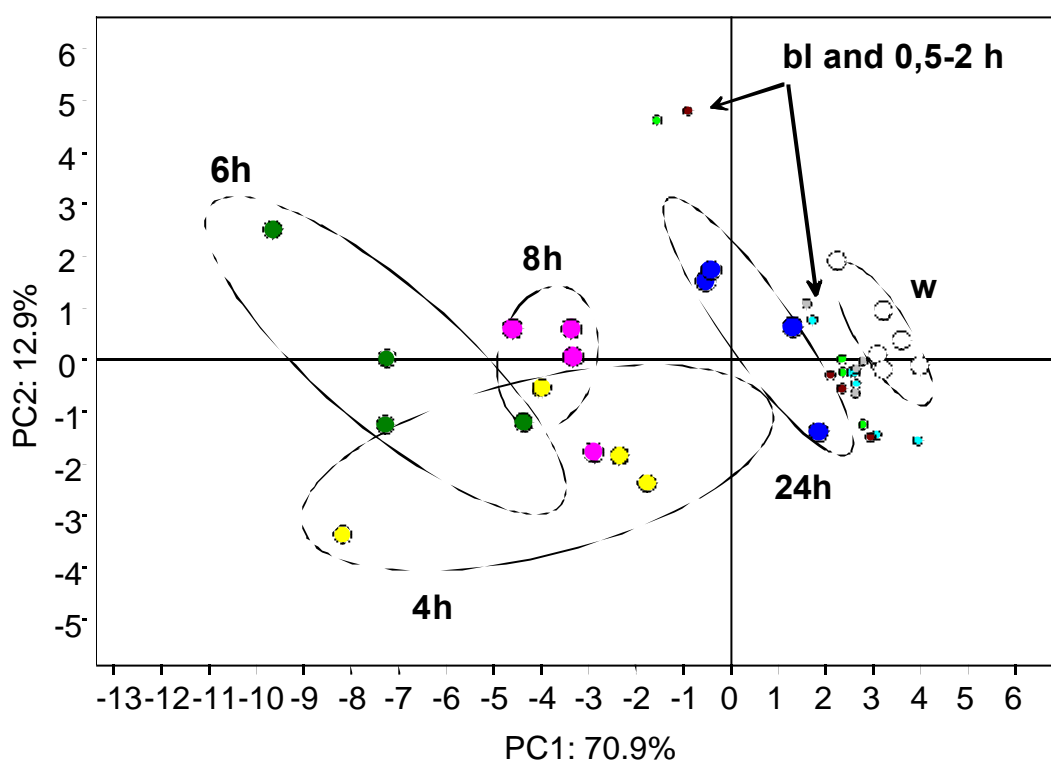
*Figure 37: PCA of a culture of* E. coli *ATCC 15490. The class numbers represent the number of hours that the cells were grown in the headspace vials before destruction by brief heating in boiling water. Other classes: "w" = distilled water blanks; "bl" = blanks made by heating inoculated vials at zero time.*

Each ellipse represents a different sample class and is indicating the 0.95 confidence limit for samples of a given class labeled by the number of hours of growth. The original medium is indistinguishable from water and from the early cultures (0.5, 1 and 2 hours); all these points are grouped under "blanks". Only after 4 hours do the sensor responses become statistically distinguishable from the original medium using this method. Thus, headspace analysis can in principle be used to detect growth of E. coli in the BHI growth medium.

Examination of individual sensor responses revealed that the largest contribution to the response of the QMB and MOX sensors was due to water vapor. The amperometric sensors gave little or no response to changes in the relative humidity of the sample vapor. However, for the majority of the sensors in the array, the useful data were found by computing the difference between two large sensor responses. This would inevitably have decreased the signal/noise ratio of the data. Because of the known interference of water vapor on the responses of the quartz microbalance and metal oxide semiconductor sensors,

the experiment was repeated using a Nafion membrane gas dryer developed specifically for these experiments and inserted between the autosampler and the sensor arrays [170]. Figure 38 shows that the ellipses separate differently with the water and small hydrophilic compounds removed.
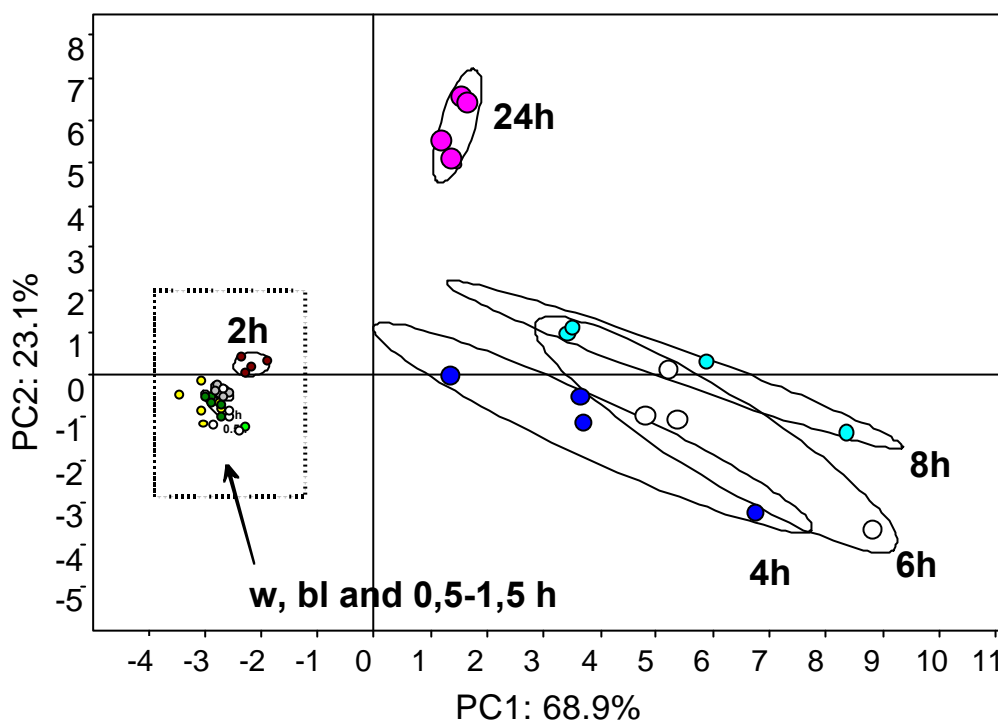


*Figure 38: Plot of the second principal component against the first for a culture of* E. coli *ATCC 15490. The flow from the headspace sampler was passed through a 1.5 mm x 4 m Nafion tube removing water vapor and small hydrophilic molecules. Blanks and early samples (up to 2 h) are clustered in the tight zone marked "w". The dashed box around this part of the plot is expanded in Figure 39.*

The cultures grown for 2 hours now separate from the blank and earlier samples. Figure 39 is a magnification of the cluster of ellipses on the left side of Figure 38, displaying more clearly the separation of the 2-hour points from the blank and earlier samples.
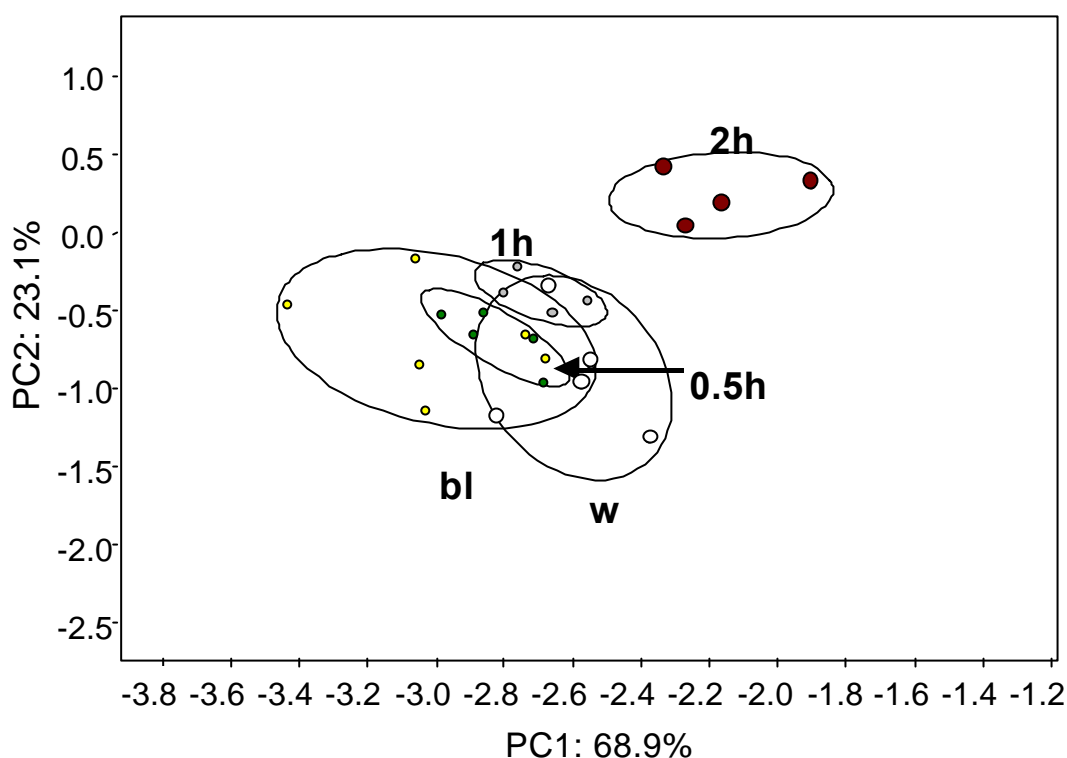
*Figure 39: An expansion of the dashed portion of Figure 38, showing the clear separation of the samples incubated for two hours (2 h) from the water (w), blanks (bl), 0.5 h, and 1 h classes. The number of organisms reach 5 x $10^8$/mL approximately 2 hours into the experiment.*

Detailed analysis of the data from individual sensors shows that the Nafion dryer causes a dramatic change in the sensor responses, reflecting a change in the chemical composition of the sample.

The $H_2S$ electrochemical sensor that typically responds to oxidizable compounds gives oxidizing signals with the untreated (high humidity) samples, and a reducing signal of nearly equal magnitude when the water and some other polar compounds are removed by the Nafion treatment (Figure 40). Note that this measurement has been performed using the prototype EC-module, the signals of which are inverted in the visualization (see section 4.2.1).

This may be attributed to the removal of electro-active compounds by Nafion treatment, leaving unspecified, but apparently electro-reducible compounds. The net current measured by the electrochemical sensors in the sensor array is the algebraic sum of anodic and cathodic currents at the working electrode [107] and results from exposure to the mixture of oxidizable and reducible compounds. The relative concentration of these species has changed upon passage through the Nafion tube.
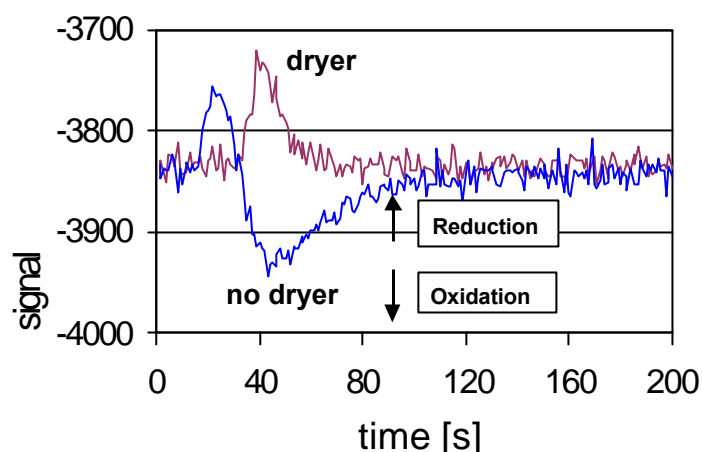
*Figure 40: Response of the H₂S electrochemical sensor to a bacterial sample incubated for 4 hours, with and without the Nafion gas dryer. The dryer appears to remove the oxidizable portion of the sample.*

The following experiments were conducted using the Nafion dryer.

An experiment similar to the one shown in Figure 37 was repeated later by C. McEntegart during the same investigation using identical measurement parameters, comparing cultures of *E. coli* and *Enterobacter aerogenes* grown in parallel in two sets of headspace vials [170]. Samples were taken at specific time intervals, as before, and measured with the Nafion gas dryer in the flow circuit. The results are shown in Figure 41, with the trajectories of the error ellipses of the two bacterial types marked with arrows.
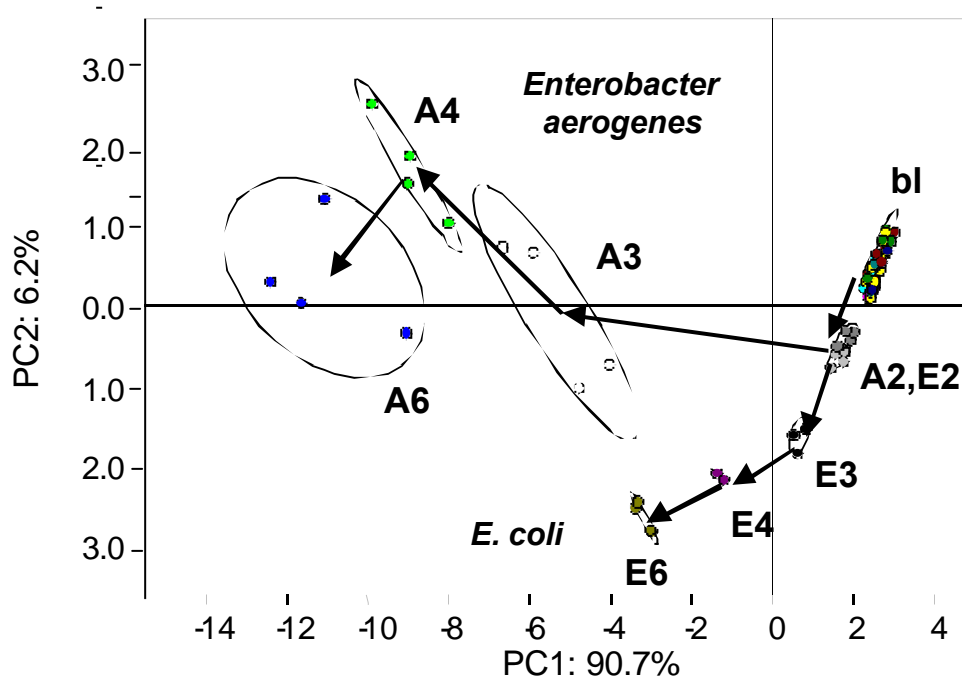


*Figure 41: Discrimination of* Enterobacter aerogenes (A) *and* Escherichia coli (E).

Beginning at 2 hours, the two cultures follow clearly distinguished trajectories. The numbers 2, 3, 4, and 6 represent hours of incubation. The two bacteria grew at almost the same rate [170].

The behavior of the two species is clearly divergent, reflecting distinct metabolic differences resulting in different headspace vapor composition and, therefore, different sensor response patterns.

Also compared were the headspace vapors produced by two strains of the same species using two strains of *E. coli*, ATCC 15490 and 15922. The results are shown in Figure 42.
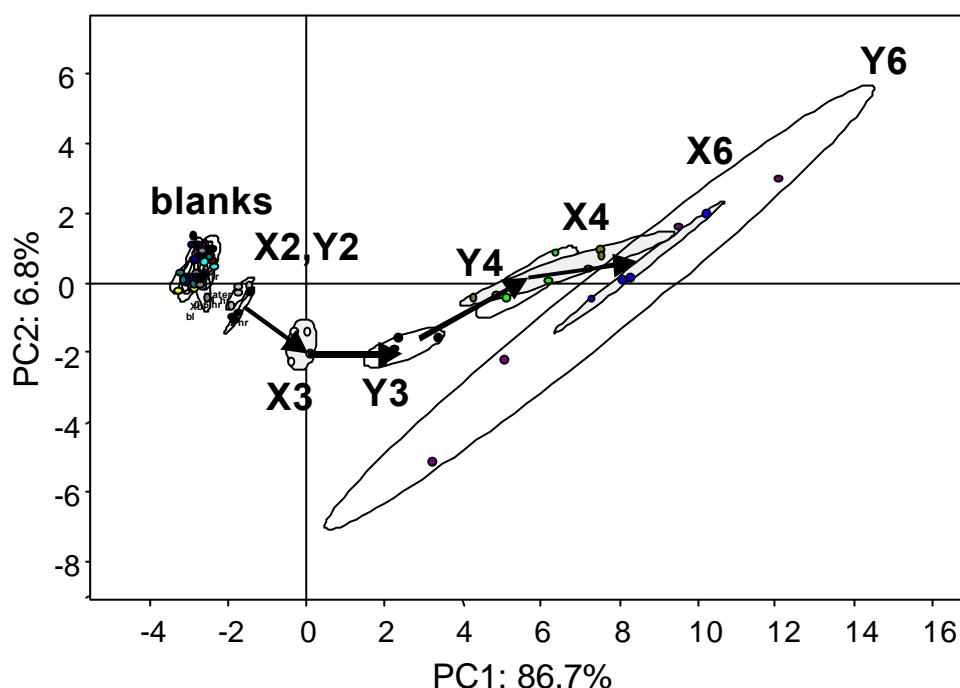


*Figure 42: Two strains of E. coli ( ATC 15490 and 15922) are not discriminated by the e-nose. Although each strain describes a trajectory in PCA-space, these trajectories overlap [170].*

In this case, the principal components plot shows the two cultures following the same general trajectory. The 2-, 4-, and 6-hour samples overlap with one another, and follow a common path through the 2-dimensional PCA space. Although the 3-hour samples do not overlap with one another, it is nevertheless clear that they lay on the common trajectory indicating compositional similarities.

Metabolic products of aqueous bacterial growth could be sensitively detected. The experiments indicate that it is possible to identify bacteria growth based

entirely on the volatile materials that are produced during growth and accumulate in the headspace.

Here, sensitivity was increased by collecting and retaining volatile compounds generated during growth in a sealed container. Clearly, the choice of sensors, their sensitivities to the types of volatiles produced, the selection of growth media, and the vigor of the organism, play a role in determining how early detection can occur.

Using the Nafion membrane to remove water vapor, plus some low-molecular-weight hydrophilic compounds, further improves sensitivity of the analysis for bacteria by suppressing the background that is common to all samples.

As a result, bacteria could be detected at an optical density representing about 5 x $10^8$ organisms/ml, or about 1000 times less than the densities found in mature cultures using a heterogeneous sensor array, even one with water-sensitive sensors.

Since e-nose results are strongly dependent on the choice of the array and the sampling conditions, it is important to carefully describe apparatus and specific method when comparing results from the e-nose.

## 5.3.   Investigation of cheese

The application of electronic noses in the investigation of foodstuff has been widely reported and well received [4]. Here, not only the contamination with microorganisms, but a variety of effects determining the olfactory properties of the products were investigated. Examples include quality assessment, the effects of ageing, the detection of off-odors caused by packaging, and the discrimination of different brands or mixtures to name a few. Chemical sensor systems here are used to discriminate between complex odors. Often the investigation encounters the problem of interfering mixture constituents and/or matrix effects. High and varying humidity content is a problem for the investigation of most foodstuff.

In this work, it is attempted to assess the applicability of a modular electronic nose for the discrimination of cheese brands and to establish the modifications to the sample uptake necessary for a successful investigation.

For distinguishing cheese brands with chemical sensor arrays, the constituents of the samples were investigated. The goal of the investigation was the discrimination of brands not solely based on the content of water. For the e-

nose, the analytical task was the discrimination of complex mixtures based on target analytes within a matrix the sensors also respond to. Table 11 in section 5.3.2 summarizes the investigated cheese brands.

### 5.3.1. GC-MS investigation

Cheese was investigated with GC-MS in order to identify the target analytes for the classification of different cheese brands.

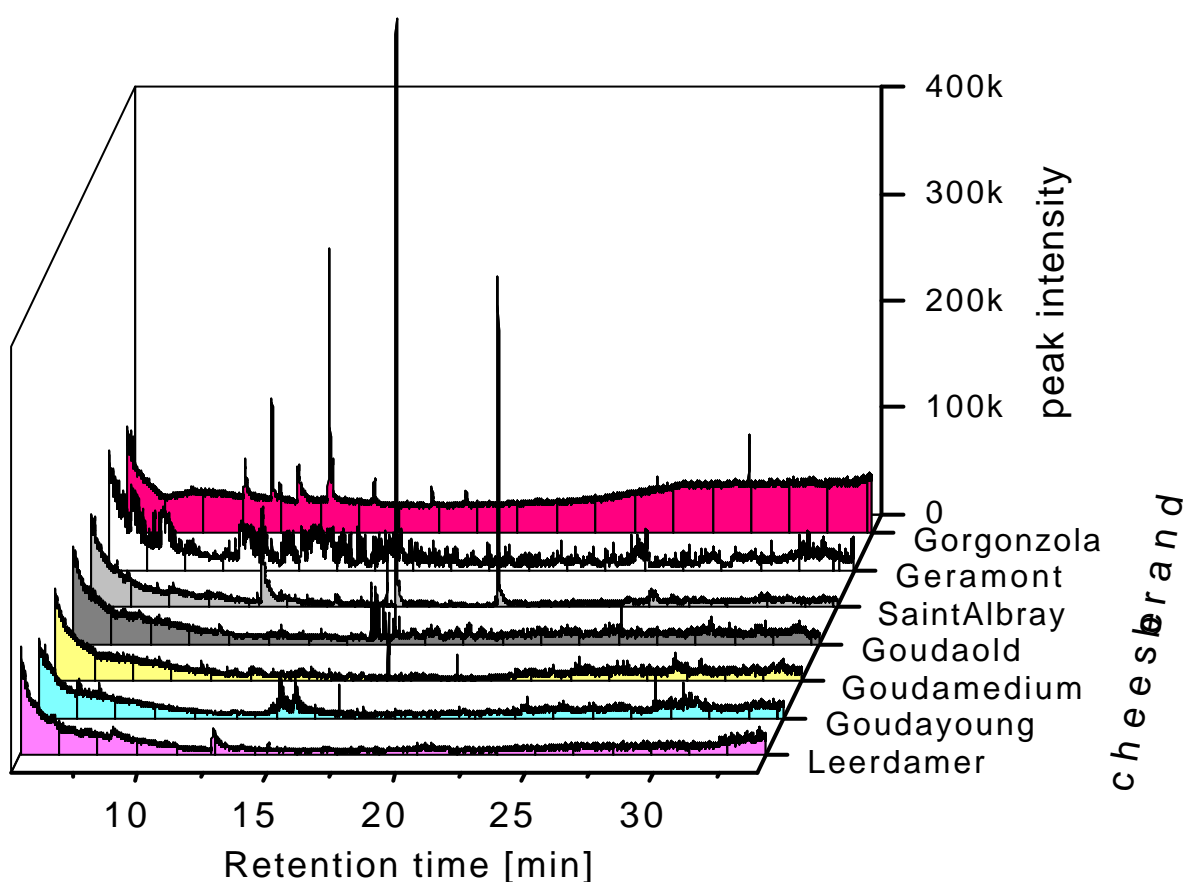Figure 43 shows the chromatograms for the different cheese brands without a dryer inserted and for a relatively low extraction temperature of 50°C.



*Figure 43: Chromatograms for the different cheese brands.*

The chromatograms of the cheeses indicate that the three ages of gouda cheese and Leerdamer are difficult to distinguish whereas the three other cheeses give distinguished signals. The peaks for the four cheese brands Gouda old, Gouda medium, Gouda young, and Leerdamer, which where not clearly identifiable with the GC-MS database, show the similarity of the chromatograms. The slope of the curve obtained from 5 to 10s retention time is largely due to water, also seen as background over the chromatogram for Gorgonzola cheese.

The characteristic peaks of the same chromatograms for the first three cheeses are enlarged in Figure 44 and labeled accordingly. These peaks can be utilized for the classification of samples. The identified compounds are displayed in the sample color as the chromatogram and, if present in more than one brand, with the area percentages of each chromatogram.
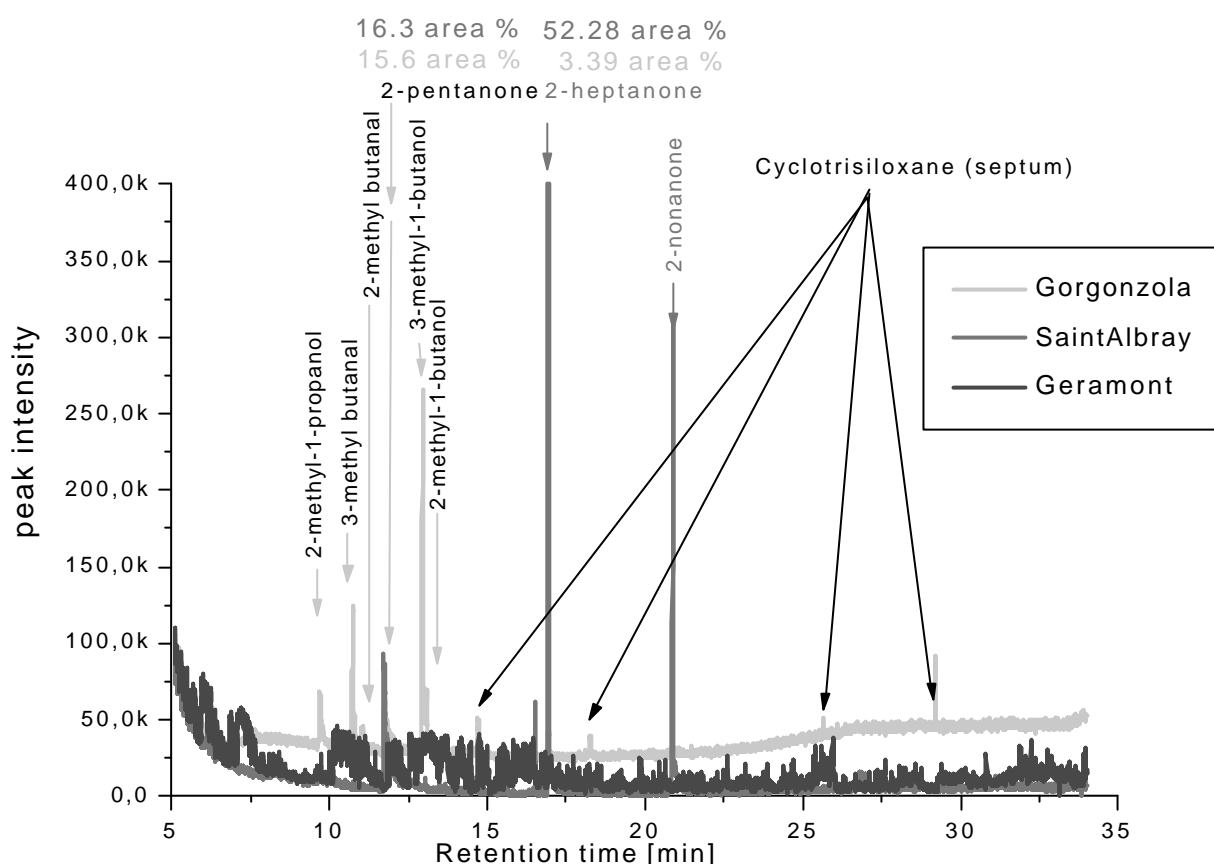


*Figure 44: The characteristic peaks of the first three cheeses.*

The characteristic peaks for cheeses are mainly 3-and 2-methyl butanol or butanal as well as the 5,7, and 9 C ketones in varying concentrations. The polar compounds are likely to be removed by dryers. As an example, Figure 64 in section 5.5.1 shows the removal of butanol derivatives by the same Nafion dryer in a different application.

The parameters of the MS scan can be set to optimize the sensitivity to higher molecular weight compounds by neglecting masses below 33 mass units and thus removing the background of e.g. water, nitrogen, oxygen, nitrous oxide, and carbon monoxide. Also the headspace sampler settings could be optimized to enhance the signal intensity of the characteristic peaks for separation.

### 5.3.2. MOSES investigation

Table 10 displays the measurement settings for the two methods of operation which were tested. The equilibration temperature was higher for the MOSES investigation than for the GC-MS measurements. A preliminary investigation had shown, that higher analyte concentrations in the headspace were required.

| # | hss temperature settings | | | dryer |
|---|---|---|---|---|
| | Oven [°C] | Loop [°C] | Tr.line [°C] | |
| 1 | 60 | 70 | 80 | - |
| 3 | 60 | 70 | 80 | $NaSO_4$ |

*Table 10: Measurement settings.*

Seven different brands of cheese have been investigated. Reference sample vials are marked bl (blank). 10 ml vials were filled with 1g of sample substance.

| # | abbreviation | cheese |
|---|---|---|
| 1 | GA | Gouda old |
| 2 | GM | Gouda medium |
| 3 | GJ | Gouda young |
| 4 | G | Geramont Camembert |
| 5 | L | Leerdamer |
| 6 | GO | Gorgonzola |
| 7 | S | Saint Albray |

*Table 11: Investigated samples and abbreviations.*

All figures of the measurements are shown standardized and normalized with redundant sensor information not displayed and eliminated prior to evaluation. Normalization was used to eliminate small variations in sample surface introduced by filling the vials with cheese cuts of different proportions to the specified weight.

Table 12 shows the sensors and features used in the evaluations of the cheese measurements. The evaluation of features by means of evaluating loadings plots has been described in section 3.4.2.

| # | feature | MOSES module | sensor |
|---|---------|--------------|--------|
| 1 | Max - Min | Quartz-module | Q2,Q5 |
| 2 | Max - Min | EC-module | S1,S4 |
| 3 | Max - Min | MOX-module | S2,S5 |
| 4 | Sig-Base3 | MOX-module | S1 |
| 5 | P3* | Quartz-module | Q5 |

*Table 12: Sensors displayed in the evaluation graphs. *P3 is a time dependent feature: Sensor response at 5/4 the time of the peak maximum.*

The Figures 45 - 46 indicate that with and without the dryer the cheese samples cannot be clearly distinguished. However, the distinction of the different ages of Gouda cheese is performed better with the dryer. As the insertion of the $NaSO_4$ dryer resulted in peak tailing (see peak broadening in section 3.2.3), a feature evaluating this effect has been entered into the pattern recognition: 'P3'. The 'P3' feature denotes the sensor response decay after the peak maximum, or, more precisely, it records the signal intensity at five quarters of the time the sensors show their highest response at. Evaluating the sensor decay does not influence the pattern recognition of the measurement without a dryer.

Both methods show the difficulty in distinguishing between the different ages of Gouda and Leerdamer, whereas the separation of the three soft cheese brands (S, GO and G) with a higher water content can be achieved with both methods. The distinction of the total class of soft cheeses with a high water content from the total of the other cheeses is, as expected, better without dryer. Using the water content as information here adds variance to the classification. The distinction within the two classes of hard cheeses and soft cheese brands is improved by the dryer.

The scores for the Leerdamer cheese still overlap with other cheese brands and the discrimination is not completely successful. Apparently the dryers remove too much of the characteristic compounds in the headspace of the samples together with water. This interpretation was supported within a different investigation (see section 5.5.1) where butanol derivatives did not pass the same Nafion dryer.
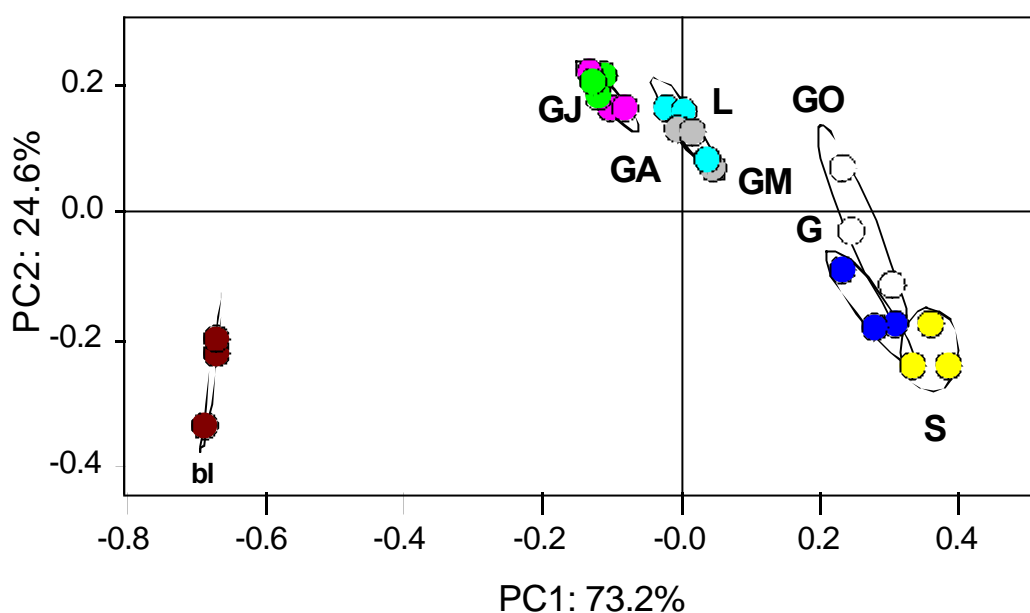
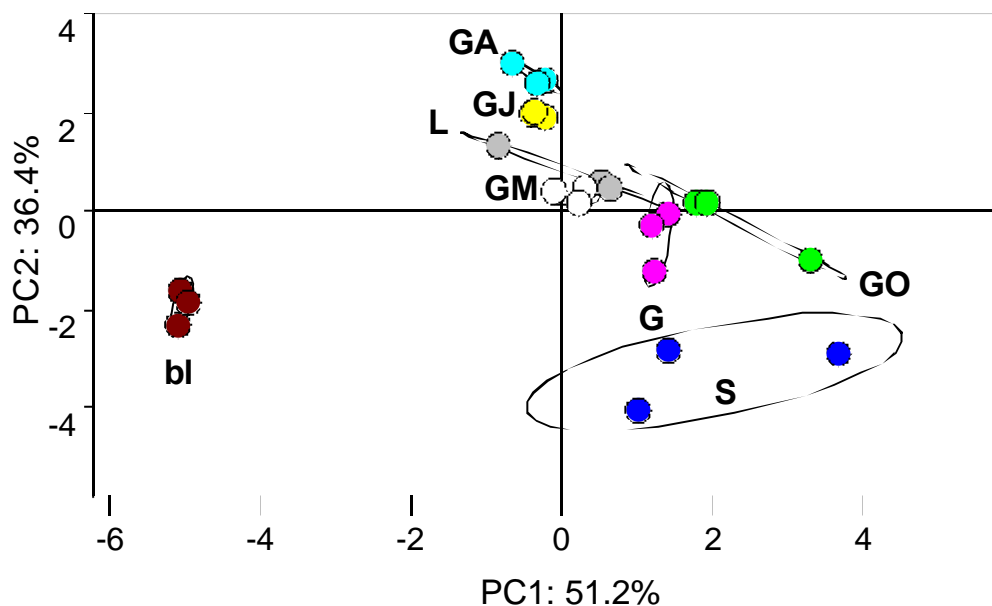*Figure 45: PCA of sensor signals for different cheese brands without dryer.*



*Figure 46: PCA of sensor signals for different cheese brands with NaSO$_4$ dryer.*

The measurements proved that the insertion of a dryer for removing constituents of the headspace prior to the investigation provides valuable additional information for the classification of samples. Also, the evaluation showed, that the selection of sensors with different transduction principles improved the result of the measurement whereas using all sensors or more sensors of the same class with only a variation in the properties of the sensitive layer give redundant information which decreases the performance of the PCA evaluation.

## 5.4. Preconcentration and chromatographic separation

For specific applications where target analytes are only present in trace concentrations, investigations with electronic noses require enrichment steps in addition to sample conditioning as static headspace sampling not always provides a sufficient amount of analyte. Possibilities for removal of interfering compounds, information gained by chromatographic separation of samples, and the preconcentration of analytes by thermal desorption have been evaluated and compared. The properties and operation parameters of a set-up combining the benefits of both techniques have been investigated and optimized for use in conjunction with a chemical sensor array and applied to test mixtures and samples which require sophisticated sample uptake procedures.

### 5.4.1. Separation with chromatographic columns

By the separation of mixture constituents prior to analysis in MOSES II several benefits to the analytical capability were expected, especially in the suppression of effects of interfering constituents. Unlike in the conventional use of sensor arrays, now single substances contained in chemically more complicated mixtures can separately be detected disregarding sensor responses not characteristic for an application task. The quantitative and qualitative evaluation of responses to target constituents allows classification of samples in groups not necessarily dominated by components in high concentrations. An alternative understanding of the set-up is that chemical sensors are used as detectors in an hyphenated system interfaced to the chromatographic separation.

Using one [75,171] or several SAW [73,74] sensors as detectors for chromatographic systems has been reported giving hope for successful use of a system coupling chromatographic separation with a multi sensor system.

To evaluate sensor responses at selected retention times, the feature extraction software used was modified to allow time resolution. Test measurements have been conducted with a thermostatted chromatographic column (Chrompack CP Sil-88) situated in-line between headspace autosampler and the e-nose.

The set-up performance was evaluated using a model mixture of chemicals in an inert matrix of poly-ethylene-glycol (PEG). Figure 47 shows the QMB sensor signals for a mixture of Toluene, n-Octane, 1-Propanol, and Ethyl acetate (TOPE) in PEG. These compounds represent different classes of chemicals with comparable volatility and are used throughout this work. The analyte concentration was 2000 ppm each, referring the mass ratio in the liquid phase.

The CP-Sil 88 column used for separation is of high polarity, the solid phase is cyanopropylsiloxane, and exhibited the best separation among several other columns tested [124]. The measurements were performed at 50°C column temperature and 5ml/min carrier gas flow.
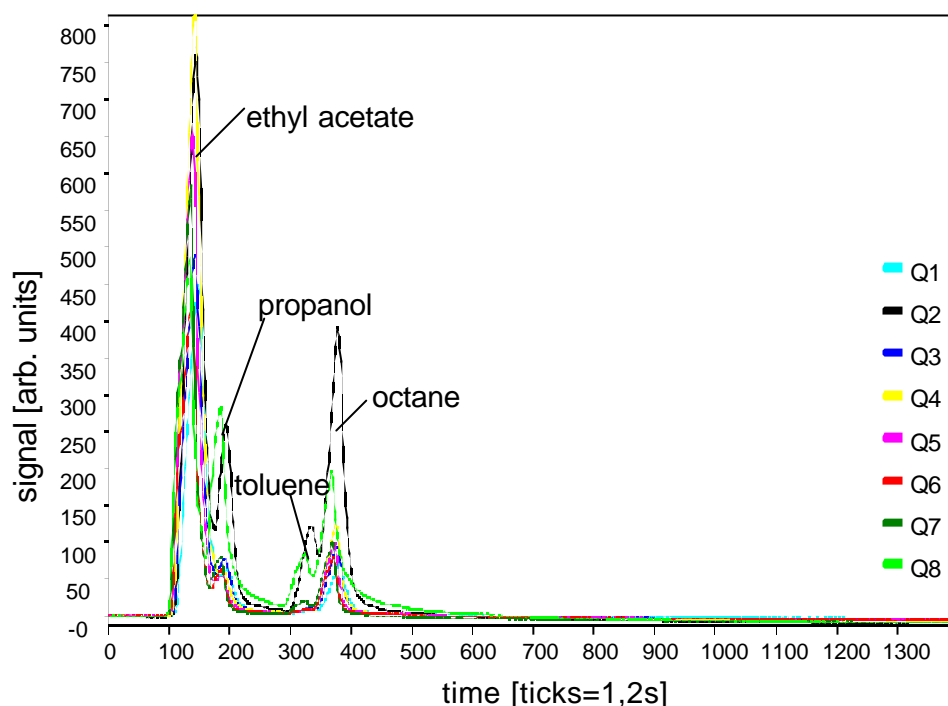


*Figure 47: QMB sensor signals of a TOPE mixture after separation by a fused silica chromatographic column (CP-Sil 88) [124].*

Figure 47 shows that the intensity of sensor responses to the four constituents of the TOPE mixture is not equal. This is because the QMB sensors show different sensitivities for each of the compounds, but also because the concentration of the substances in the gas phase is unequal.

The concentrations of constituents in the gas phase diverges from that of the liquid phase substantially, depending on the partitioning during the extraction procedure in the headspace sampler (see section 2.1.1). The extracted headspace of the TOPE mixture has been investigated by GC-MS. Here, the ratio of constituents of the vapor phase was determined by evaluating the integrated peaks of the chromatogram for TOPE. The concentration of constituents in the gas phase depends on the matrix and the overall composition of a mixture.

| Compound | 1-propanol | ethyl acetate | toluene | octane |
|----------|-----------|---------------|---------|--------|
| peak area | 1.6 % | 13.4 % | 27.3 % | 57.4 % |

*Table 13: TOPE mixture analyte concentration in the headspace.*

Form the chromatogram of TOPE several characteristic values could be determined using equations 17-22 in section 3.2: The net retention time and volume $T_R'$ and $V_R'$, respectively, the separation factor $\alpha$, and the number of theoretical plates N. The selectivity factor for a compound relates to the compound eluted just prior to this compound.

| Compound | $t_R'$ [s] | $V_R'$ [ml] | N | **a** |
|----------|-----------|-------------|---|-------|
| Ethyl acetate | 74 | 6.2 | 82 | |
| 1-Propanol | 134 | 11.2 | 365 | 1.81 |
| Toluene | 302 | 25.2 | 663 | 2.25 |
| Octane | 354 | 29.5 | 663 | 1.17 |

*Table 14: Characteristic values of the chromatogram of TOPE (Figure 47).*

Figure 47 already shows that the signals for toluene and octane, and to a lesser extent of ethyl acetate and 1-propanol are not well separated. This is verified by the resolution $R_S$ of 0.75 and 0.82 for the two pairs, the value calculated with equation 26 in section 3.2. Performing the measurements at a lower column temperature could improve the quality of separation but would also extend the time for a single measurement of 15 min at 50°C and therefore the cycle time substantially. A resolution of less then one means that the peaks are not well enough separated for integration (1.5 is considered to be optimal). However, for the evaluation with MOSES, which in the feature extraction used here extracts the signal at the local maximum (compound $t_R$), it is sufficient to obtain quantitative information on a specific mixture constituent. Time resolved feature extraction of sensor responses allows the identification of compounds and the selection of sensor responses to sample constituents relevant for the classification problem of an application. Compounds in relatively small concentrations or concentration differences thus are also recorded for evaluation. Further investigations and results for a chromatographic column coupled to MOSES II can be found in [124].

Despite the success in operating a chemical sensor array in conjunction with a chromatographic column there are practical and principal disadvantages using this technique, especially for capillary columns:

1. The set-up for precisely controlling the temperature of the column is sumptuary, spacious, and inconvenient. For the measurement discussed above the column was placed in the liquid filled through of a cryostat (Julabo HD 34). The precise, and close to room temperature arduous, temperature control is necessary to obtain reproducible retention times, which is important for the feature extraction with the e-nose if several samples are to be compared.

2. Most commercially available fused silica capillaries are specified for operation with inert carrier gas whereas the semiconductor $SnO_2$ based sensors used in the MOX module require an oxygen containing atmosphere.

3. Fused silica capillaries of 0.32 mm i.d. require a high pressure from the headspace sampler to maintain an acceptable flow rate. The maximum flow rate achievable was 5ml/min whereas MOSES II is normally operated at a flow rate of 20ml/min. Lower flow rates, especially if the peak height is extracted as signal, result in significantly lower detection limits of the system.

To overcome these difficulties a set-up using a thermodesorption tube for chromatographic separation as well as for a means of sample enrichment was employed.

### 5.4.2. Differential thermodesorption

Trapping and preconcentrating with Tenax adsorption tubes is a technique well established in classical analytical chemistry. The advantages of the chromatographic properties of the method in conjunction with e-noses with no need to focus an analyte peak after desorption, are obvious.

For measurements with the electronic nose this method of improving the sensitivity of the analytical instrument was investigated, modified, and adapted to the special requirements of this instrument.

### 5.4.2.1. Chromatographic properties

To a first approximation, a thermodesorption tube packed with a solid adsorbent for trapping small quantities of headspace can be considered as a chromatographic column. The chromatographic properties of a thermodesorption tube have been investigated for the set-up described in section 4.4.2. operated isothermally at different temperatures.

The thermodesorption glass tube of 4 mm i.d. by 9 cm length contained 230 mg of adsorbent material, Tenax 60/80 mesh.

| Compound | $V_R'$ [l] | | | | N | | | a | |
|---|---|---|---|---|---|---|---|---|---|
| flow rate [ml/min] | 10 | 20 | 20 | 60 | 10 | 20 | 20 | 20 | 100 |
| temperature [°C] | 100 | 100 | | | 100 | 100 | 60 | | |
| 1-Propanol | 0.9 | 0.8 | 5.8 | | 58 | 41 | 116 | | |
| Ethyl acetate | 1.5 | 1.5 | 16.9 | | 44 | 34 | 120 | 1.76 | |
| Octane | 3.3* | 3.5 | 39.8 | | 81 | 38 | * | 2.29 | |
| Toluene | * | 5.5* | * | | * | 47 | * | 1.88 | |

*Table 15: Characteristic chromatographic properties of a Tenax filled thermodesorption tube for TOPE (* high uncertainty because of peak broadening or strong tailing).*

The values obtained are not directly comparable to the characteristic values determined for the fused silica column for several reasons: The number of theoretical plates is depending on the flow rate, as expected from the van Deemter equation (see chapter 3.2.3); but a lower flow rate less than 10 ml/min was not feasible because peaks for the stronger retained compounds broadened substantially at low flow rates, to the point where evaluation was no longer possible. Plate number and retention volume are highly temperature dependent. Lower temperatures than 60°C also resulted in broad peaks or even difficulties desorbing substances completely from the trap. Nevertheless it is apparent and also expected from theory considering the geometry, that the number of theoretical plates is substantially smaller for Tenax filled tubes than for coated fused silica columns whereas the retention volume is about 2-3 orders of magnitude higher.

The selectivities of the Tenax tube operated isothermally at 100°C and the fused silica capillary are comparable. The resolution $R_S$ for E and P is 0.81 with the tube and 0.75 with the capillary, for T and O 0.87 and 0.82, respectively. Although the resolution with the differential thermodesorption set-up is slightly better, it is still not well separated. But unlike an oven for a chromatographic column, the trap has a very short response time to temperature changes

allowing temperature ramps to be used for improving resolution (see section 5.4.3).

As expected form literature the retention volume has been found to be independent from the flow rate for the relatively low flow rates as used in the measurements are conducted with MOSES II. But since the number of theoretical plates decreases with the flow rate, also the breakthrough volume changes. A decrease in flow rate from 20 to 10 ml/min was found to lead to a $V_B$ increase of 18% attributed to peak broadening. The mesh size and adsorbent tube geometry determine the breakthrough volume for higher concentrations and flow rates. Consideration of the pressure drop for each mesh size and bed packing dimensions allow selecting the practicable attainable flow rates. A pressure drop was found to be neglectable for flow rates less than 20 ml/min. In agreement with published data reporting linearly increasing back pressure with the adsorbent mass and with a square root dependency with the flow rate, but relevant only for flow rates exceeding 200 ml/min [133,135].

All further measurements where conducted at a flow rate of 20 ml/min.

### 5.4.2.2. Prediction of breakthrough volumes

The ability to predict retention, breakthrough, and safe sample volumes within a chemical class of compounds greatly facilitates the ability to select the appropriate sampling conditions to obtain quantitative and representative information on the constituents of a sample.

Data on these volumes have been published but the method of determination and therefore also the published values differ over a considerable range. Depending on measurement conditions and theoretical model applied for the calculation safe sample volumes differ over an order of magnitude (see chapter 3.2.8). The dependency of the trap properties on sample tube geometry, sorbent bed depth observed during the course of this study, and the experimental set-up of several different geometries (see chapter 4.4) suggest that figures acquired with one particular set-up are not necessarily transferable. Unlike the adsorption isotherm, the breakthrough volume $V_B$ is affected by geometric factors: the reduction of the inner diameter to half its original value leads to a 200 fold increase in linear velocity through the tube meaning an increase in $V_B$ and decrease in tube efficiency [135].

Table 16 shows breakthrough volumes for water, ethanol, and TOPE determined directly from the chromatogram after sample injection with the headspace sampler and for comparison published data acquired by calculation from

retention times (indirect method, see section 3.2.8.1, marked with *) or with continuous vapor assault and a second collection trap (direct method, safe sample volume). All data refer to 20°C trap temperature and have been extrapolated for substances where reasonable elution times were exceeded or peaks where broadened too much for evaluation (marked with -).

| Reference and method Compound | b.p. [°C] | measured $V_{BS}[l/g]$ | [60]* $V_{BS}[l/g]$ | [134]* $V_{BS}[l/g]$ | [29] $V_{BS}[l/g]$ | [132] $V_{BS}[l/g]$ |
|---|---|---|---|---|---|---|
| Water | 100 | 0.41 | 0.03 | | | |
| Ethanol | 78.4 | 5.3 | 0.5 | 0.9 | 0.9 | 1.9 |
| 1-Propanol | 97.4 | 32.0 | | 5.5 | 4.2 | 8.5 |
| Ethyl acetate | 71 | 178 | 10 | 17 | 18 | 35 |
| Octane | 125 | 827 | | 295 | 390 | 776 |
| Toluene | 110.8 | - | | 190 | 200 | |

*Table 16: Comparison of specific breakthrough volume data from literature and measurements with the differential thermodesorption set-up. Values obtained using the indirect method are marked with \*; Peaks broadened too much for evaluation are marked with '-'.*

It is crucial for the practical use of thermal desorption to ensure that the employed method of prediction of the chromatographic trap properties matches empirical measurement data obtained with the used set-up and therefore is applicable to a given application. Although published data on breakthrough volumes on various adsorbent materials is helpful to estimate operation parameters for a particular application, the empirical acquisition of test data and comparison with theoretical models is indispensable.

The breakthrough volume is reported to depend on the form and size of the trap, the sorbent (porosity, specific surface area, amount used, and inertness toward the analyte), on the flow rate and pressure drop of the stripping inert gas, the temperature, the concentration and chemical structure of the analytes, and the complexity of the mixture [133]. The dependency of the breakthrough volume of these parameters has been studied for TOPE and water as examples.

Most important for the operation of a thermal desorption unit is the operation temperature and its effect on breakthrough volumes.

Figure 48 shows the logarithms of specific breakthrough volumes in l/g and linear fit curves at different trap temperatures for TOPE, ethanol, and water. The values were directly measured with the Tenax trap used in this work
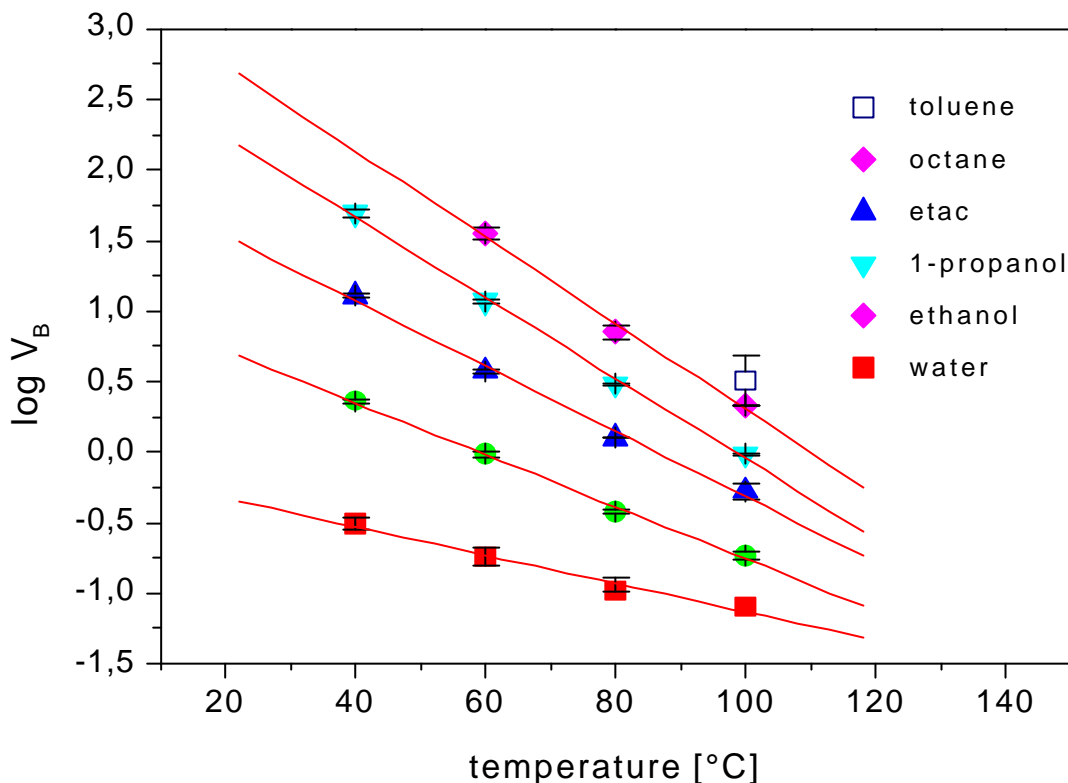


*Figure 48: Logarithms of specific breakthrough volumes and linear fit curves at different trap temperatures for TOPE, ethanol, and water.*

The isothermal measurements at different trap temperatures showed that the logarithmic specific breakthrough volume is linearly decreasing with the increasing temperature in °C for a given sample. This result is in agreement with several statements in literature, which also predict that the logarithm of $V_{BS}$ is linearly increasing with the boiling point, molecular weight, and number of carbon atoms within a class of chemicals of similar polarity, and decreasing with the vapor pressure [29,61,133]. The presence of an aromatic moiety in a molecule increases the affinity of Tenax for it and consequently the breakthrough volume. If the compound exhibits a high degree of basicity, the retention volume may be correspondingly higher than expected from its boiling point, hydroxylated compounds are eluted substantially faster than expected [63,131], which also could be confirmed.

Therefore, if the breakthrough volume of a substance on a given thermodesorption set-up can be determined at a given temperature, then the

breakthrough at other temperatures can be extrapolated. Moreover, if several compounds of one class have been characterized, the behavior of other compounds of this class at least can be predicted.

### 5.4.3. Optimization with TOPE standard samples

The differential thermodesorption unit was further optimized using the standard test mixtures containing different concentrations of Toluene, Octane, 1-Propanol and Ethyl acetate (TOPE), 500 ppm of each in PEG. Measurement results of a system having the differential thermodesorption unit interfaced to the electronic nose with analyte accumulated on the tube and then desorbed were compared to investigations of the same samples directly transferred to MOSES II. The operation of the trap was optimized to obtain a sufficient separation of compounds while not extending the cycle time over the time a sample needs for phase equilibration in the thermostatted headspace sampler.

Figure 49 shows measurement results for the TOPE mixture performed with QMB sensors. As stated before, the analyte concentration in the headspace depends on the partition coefficient, which results in different intensities of sensor response to compounds and the possible masking of mixture constituents. Although the deconvoluted analyte peaks [B] are not totally resolved, an evaluation with a time dependent feature extraction delivers additional information compared to the sum signals [A].
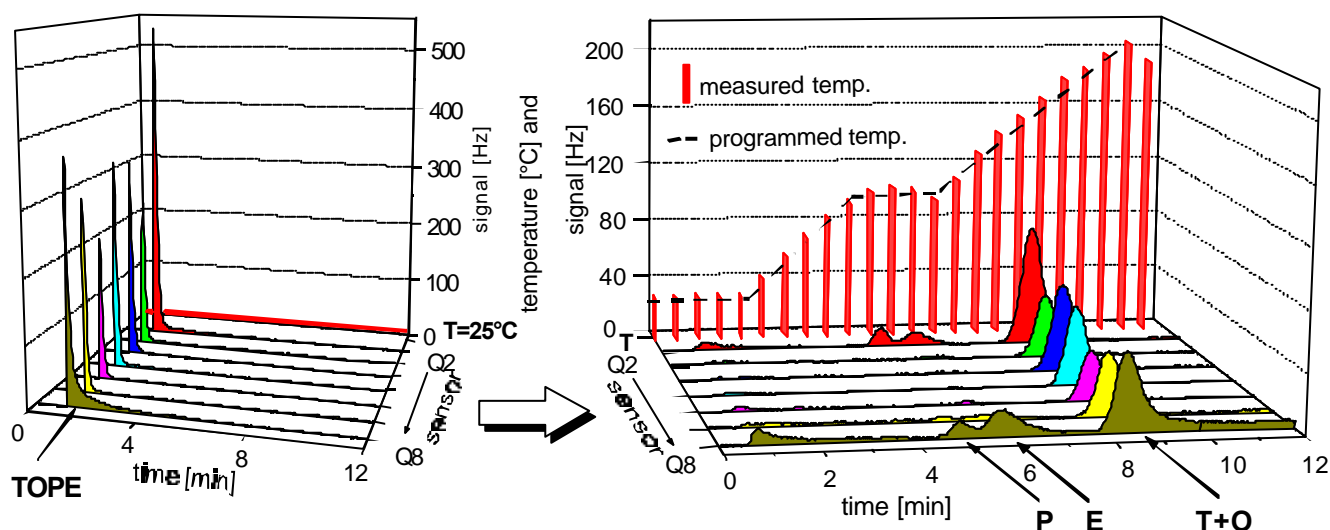


[A] without differential thermodesorption    [B] differential thermodesorption

*Figure 49: QMB sensor signals for 500 ppm TOPE; [A] without and [B] with differential thermodesorption. The thermodesorption trap was filled with 230 mg of Tenax.*

The sensor signals and temperature of the Tenax tube are displayed versus the measurement time. The measured tube temperature shows a slight deviation from the programmed temperature, which was optimized for the following measurements so that an isothermal ramp of two minutes at 100°C is assumed for the evaluation of desorption signals for the measurements. The time length of the ramp may be varied depending on the investigated mixture and is optimized with regard to the retention time of compounds contained in a mixture.

Figure 49 shows only three resolved peaks for the four substances in the TOPE mixture. The compounds were determined to elute from the desorption tube in the sequence 1-propanol, ethyl acetate, octane, and toluene but the retention times of the two non polar compounds octane and toluene were found to be very close (see also Figure 50), even when using an optimized heat ramp with a prolonged isothermal time period. Nevertheless, the toluene and octane content can be classified by the signal pattern of the sensor array.

The deconvolution of the single signal for TOPE in the isothermal measurement without the differential thermodesorption to the multiple signals displayed for differential thermodesorption mode also multiplies the information content possible to be used in a data evaluation.

This corresponds with data from literature where data on the specific retention volumes of various compounds are listed at elevated temperatures [134].

The specific retention volume data for each of the investigated analytes, expressed in liters of gas per gram of adsorbent resin at the various temperatures, is shown in Figure 50 for TOPE and water.
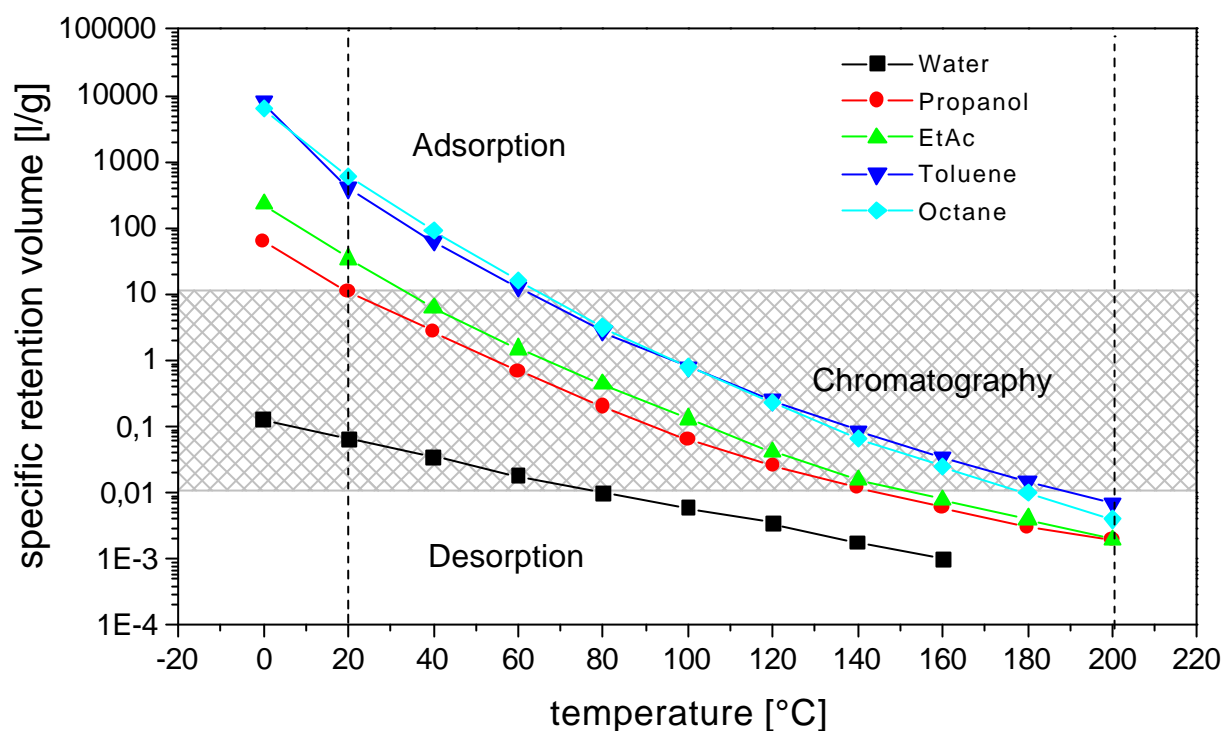
*Figure 50: Specific retention volumes on Tenax for TOPE and water at different temperatures [165]. The vertical lines at 20°C and 200°C represent the temperature range, within which heating ramps can be devised.*

The upper region of the figure indicates breakthrough volumes greater than 10 liters per gram of adsorbent resin, and is labeled 'Adsorption' in Figure 50. This region is generally considered to be the usable range for the trapping of analytes on the adsorbent resins. Breakthrough volumes of less than 10 liters/gram of resin, colored gray in Figure 50 and labeled 'Chromatography', would not be acceptable temperatures for the efficient external trapping of compounds on the resins for continuous vapor assault, although small concentrations are sufficiently retained (see section 3.2.8.2 and 134). This region of temperature and breakthrough volume, respectively, though can be used, as done in the following, to separate analytes by slow desorption utilizing the chromatographic effect.

The bottom region indicates breakthrough volumes of less than 10 ml/gram of resin. These are considered to be acceptable values for the efficient desorption or release of the analytes from the adsorbent resins. For differential thermodesorption this would mean for low concentrations complete desorption within about 20 seconds at the given temperature. Retention volumes greater than 10 ml/gram would either require excessive volumes of gas or to efficiently

desorb (or purge) the analyte of the adsorbent resin or extend the cycle time of a measurement. Using these data, one can predict the usefulness of the particular resin to both adsorb (trap) and desorb (purge) various organics and other analytes, to establish the time for complete elution, and therefore the necessary parameters of the differential thermodesorption set-up to successfully separate the investigated analyte mixtures.

The tabled data can be used to optimize the optimal temperature settings and gas volumes for gas sampling as well as for the desorption of the analytes into the electronic nose for subsequent analysis, and to predict retention times of target analytes for evaluation, which is maybe even more important.

Figure 50 shows that the breakthrough volumes of octane and toluene are very similar making separation by the thermodesorption unit alone difficult. But as shown in Figure 49, the signal patterns of the different sensors contain the information necessary to separate the content of these two analytes in the data evaluation as shown e.g. in Figure 52. With a substantially slower heating of the sample, the separation of the strongly retained compounds can be improved to some extent but substantially only for the price of exceeding the sample equilibration time of 20 minutes.

1-propanol and ethyl acetate are clearly separated by their lower retention time. The optimal temperatures determined for the differential thermodesorption of TOPE were determined to be room temperature for adsorption and a not lower than 200°C for complete and fast desorption with an isothermal ramp of 100°C for 2 min as shown in Figure 49. This is in line with the retention volume data and therefore also indicated in Figure 50. A lower maximum temperature results in accumulated analyte in the desorption tube which will be eluted during succeeding measurements. Water will not be efficiently trapped at room temperature and is usually directly eluted as first peak of the measurement. This effect and property of Tenax TA was used to eliminate water interfering with measurements [see section 5.4.3.5].

### 5.4.3.1.   Preconcentration

Using the trap for preconcentration improves the sensitivity of the sensor system. Figure 51 shows the regression plot for TOPE in different concentration (dots) and TOPE preconcentrated (diamonds) as independent test data set. Here, the TOPE concentration was 500ppm of each component in the matrix or a multiple of that, indicated with the prefix to tope (2,4,8, respectively), samples

preconcentrated on the trap are indicated with the accumulation factor (2 x 2 tope, etc.).

The collected sample desorbs completely and is classified according to the net concentration of compound detected by MOSES II in the principal component regression (PCR). Figure 51 shows a linear behavior of accumulation and subsequent desorption over a range of at least 1 order of magnitude of analyte concentration.
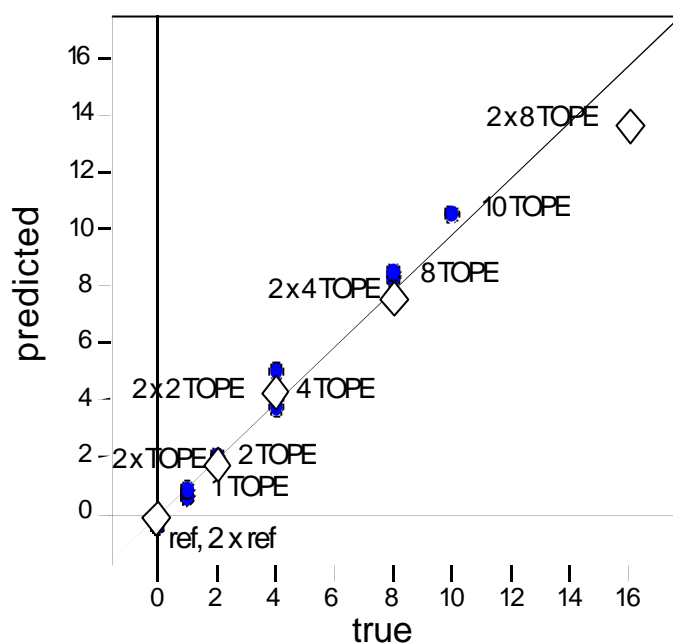


*Figure 51: PCR of different concentrations of TOPE compared to analyte concentrations accumulated on the tube and then desorbed.*

### 5.4.3.2. Chromatographic separation

Figure 52 shows the PCA scores plot for TOPE and mixtures with single components left out or in double or quadruple concentration, respectively. Samples are labeled according to components contained (TOE is TOPE without 1-Propanol) or labeled with a factor for the concentration of a single component (T2 is TOPE with double concentration of toluene or the T:O:P:E ratio 2:1:1:1). The PCA shows the signals of all 20 sensors at three selected retention times analogous to 60 input variables (features).

Although the retention times of octane and toluene are very similar and were not possible to evaluate separately for the classification, the discrimination is successful. The pattern of sensor signals is sufficient for classifying differences in

composition as in the measurement shown in Figure 52. A clear classification of variations in concentration of single components in TOPE samples is possible.
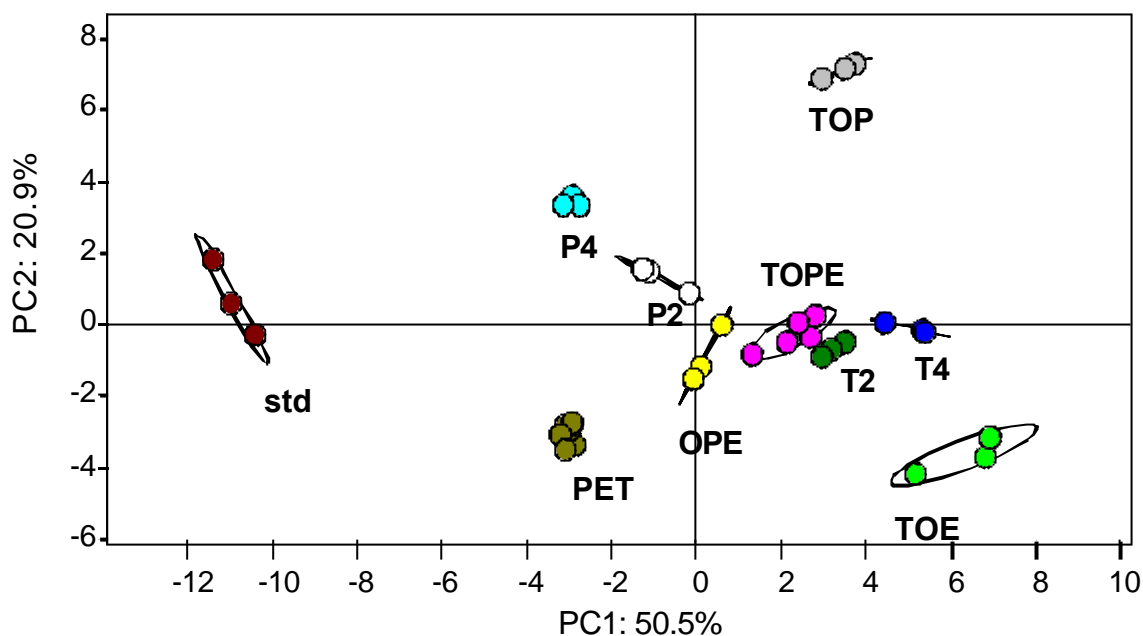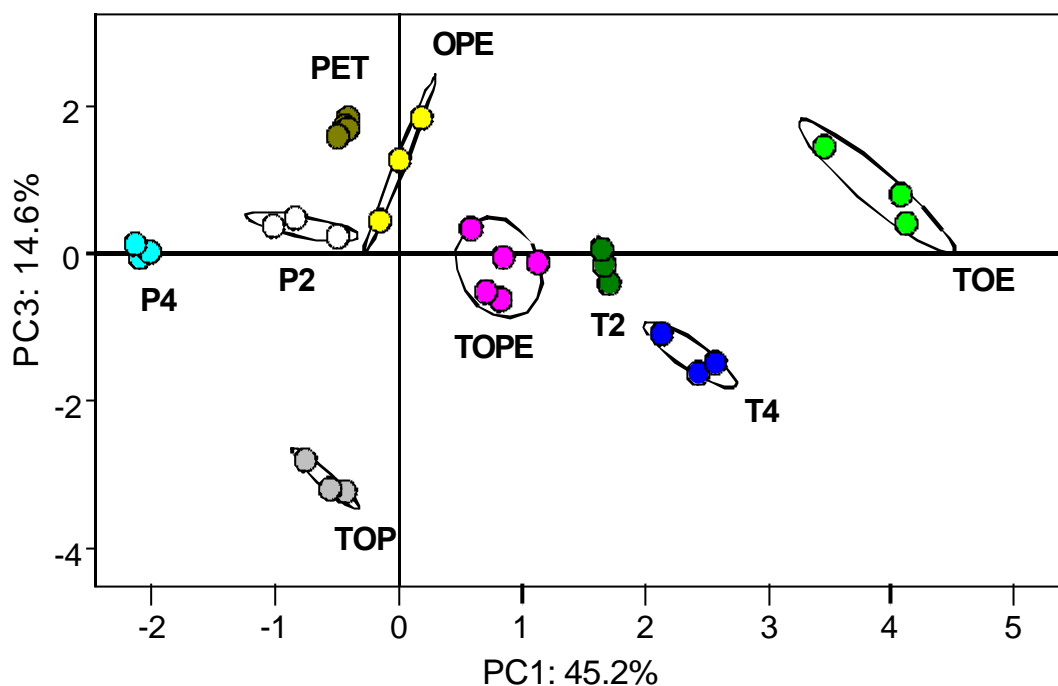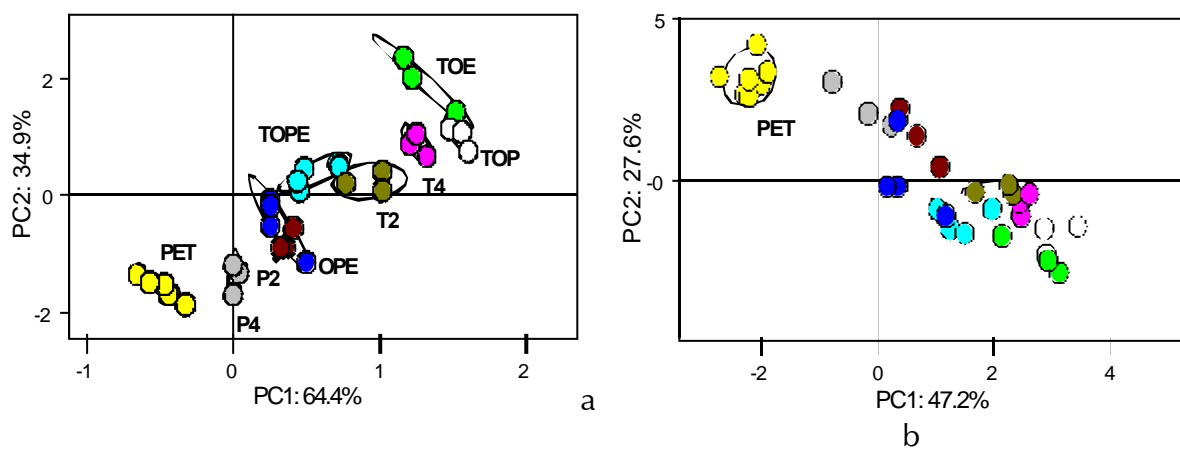


*Figure 52: PCA of TOPE with variation of the concentration of single components with differential thermodesorption (showing the information of all sensors, principle components 1 and 2). Samples are labeled according to components contained or with a factor indicating the multiplication of the concentration of the particular compound by this factor. For nomenclature see also text.*

Evaluating the sensor signals at chosen retention times and of sensors selected by their relevance from the loadings plot results in a classification performance as good as the classification using all sensors indiscriminately: In Figure 53 the signals of a subset of sensors, that is only four sensors (2 QMBs, 1 MOX and 1 AGS) chosen from the PCA loadings plot, are displayed (for determining sensors see section 3.4.2). Further information also is contained in the third principal component. The third principle component represents 14.6 % of the variance in the measurement data displayed. The classification of the samples is also performed successfully when PC1 versus PC3 are used for the representation of the data (Figure 53).

*Figure 53: PCA of TOPE with variation of concentration of single components with differential thermodesorption showing principal components 1 and 3 using only signals of 4 different sensors.*

The discrimination without the use of the differential thermodesorption set-up is also relatively good if sensors are carefully selected (Figure 54 a) but not at all successful using all sensors (Figure 54 b), thus showing the importance of evaluating the most relevant information contained in sensor signals and evaluating the optimal subset of sensors.



*Figure 54 a and b: PCA of TOPE with variation of concentration of single components without using the differential thermodesorption showing the information of selected sensors (a) and all sensors (b).*

5.4.3.3.    Consequences for data analysis

The evaluation of time resolved sensor signals for classification of samples has several consequences for the pattern recognition engine employed.

Firstly, for PCA, the selection of retention times, and therefore the selection of time resolved features building the PARC model, introduces a supervised step into an otherwise unsupervised process. In other words, the operator provides additional input for the selection of features. There are several possibilities of selecting and evaluating the retention times and therefore the features:

• Calibration to the pure target analytes contained in a mixture,

• Elimination of signals to obvious and identified interferents, e.g. water or ethanol, and

• Selection of features based on their position in the loadings plot.

The execution of the latter has been discussed in section 3.4, but remains an iterative process which has to be performed carefully if the initial model includes all possible combinations of features. An automated procedure, where the system is trained with a reference data set of known classification based on Mahalanobis distances (see section 3.4.1 and [137]) seems feasible, but would require a substantial extension of the MOSES II software package.

The second consequence is the integration of highly selective features in the data evaluation. In conventional e-nose operation one or more features are selected from the sensor responses of sensors with a certain degree of collinearity. Features deriving from the evaluation of sensor response at a given retention times ideally represent the concentration of only one analyte, in other words, are highly selective. The additional information and the time resolved variables generated are equivalent to the addition of independent sensors. The sensor response at a given retention time can be seen as additional sensor entering pattern recognition if - and this is very important - they are significantly independent from each other (evaluation of the loadings plot, see section 3.4.2).

The number of sensors in the ideal case described above increases to the number of sensors N multiplied with the number of significant retention times R.

The matrix of scores, and the information content of a measurement increases analogously. Figure 11 in section 3.4.1 schematically illustrated data analysis with PCA. For comparison, Figure 55 shows the consequences of chromatographic separation and time resolved feature extraction.
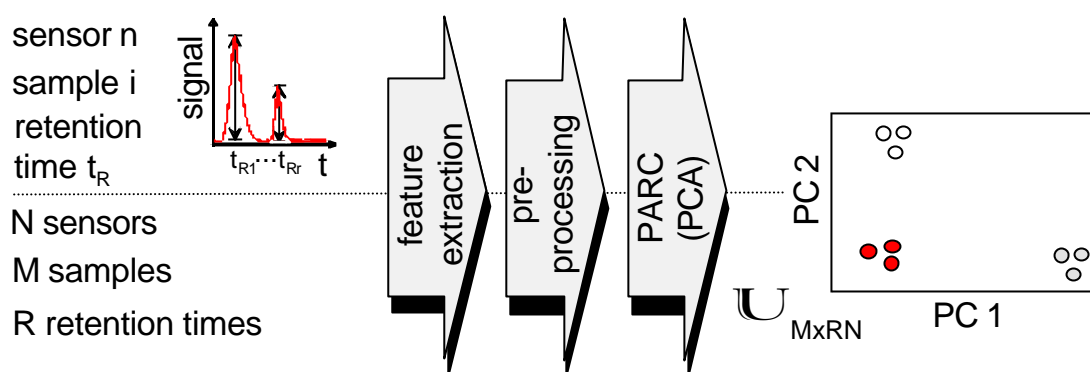
*Figure 55: Schematic data analysis with PCA of time resolved feature extraction, description see text.*

The third consequence is, that apart from representing more information, the visualization with scores plots derived from PCA changes. As the input variables are less correlated, the reduction of dimensionality leaves more information (systematic variation) in higher principal components. PCA scores plots display a smaller percentage of systematic variation in PC1 and PC2 although the overall classification capability of a measurement increases.

Figure 56 demonstrates the above described effect on the visualization of data with PCA scores plots. The four plots show the classification of the same three samples, TOE, TOP, and OPE, each in triplicate. For simplicity reasons only QMB sensors entered the feature extraction.

Figure 56 a and c depict the PCA performed with six different QMB sensors. The extracted feature was the area under the response curves representing a sum signal for each mixture. Figure 56 b and d show an evaluation performed with only two QMB sensors but with three 'SigAt-BaseAt' values extracted from each measurement, corresponding to the retention time of the mixture constituents. Thus, always six features where entered into the PARC.

Figure 56 a and b show PC1 versus PC2, c and d PC2 versus PC3, respectively.
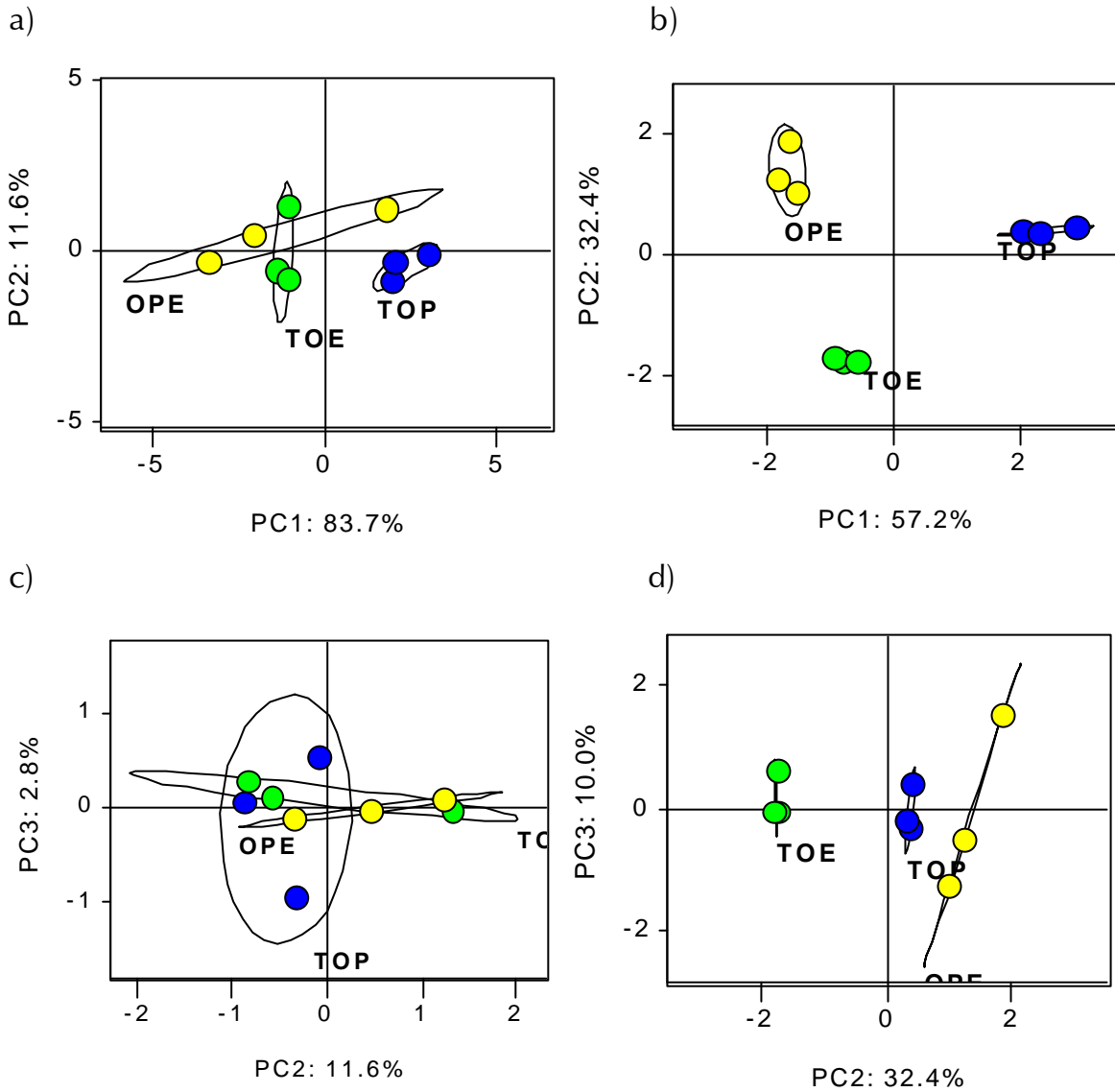
*Figure 56 a-d: PCA of three different three component mixtures evaluating six features, b and d time resolved features, a and c sum signals. Displayed are PC1 vs. PC2 (a,b) and PC2 vs. PC3 (c,d).*

As expected, the time resolved feature extraction leads to the better classification result although the numbers of features (sensors) did not increase. Also, the information content of the higher principle components significantly exceeds that of the sum signal evaluation. The scores plots show that the higher principle components represent a part of the systematic variance which enables enabling a classification also in PC2 and PC3 when largely independent features are used.

### 5.4.3.4. Quantitative evaluation

With the differential thermodesorption set-up an evaluation of quantitative information is also possible. Figure 57 exhibits different trajectories for the classification of TOPE samples containing varying concentrations of a single component (T,P) in an enlargement of Figure 53. Trajectories for the multiple concentrations are indicated parallel to the first principle component for the increase of concentration of 1-propanol and here in PC3 and PC1 for toluene. For PC1 and PC2 (as shown in Figure 52) the direction of possible trajectories can also be seen.
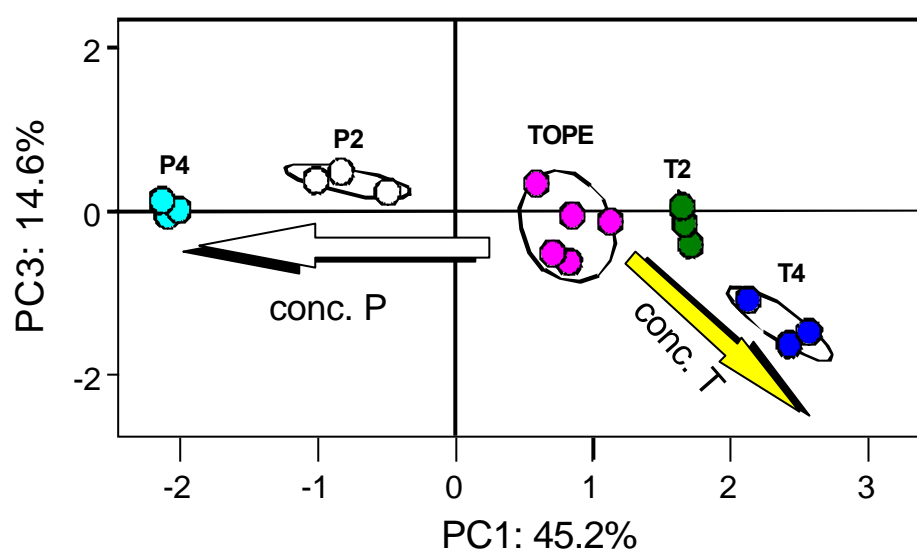


*Figure 57: PCA of TOPE with variation of concentration of 1-propanol and toluene evaluated differential using thermodesorption. The trajectories for samples with multiple concentrations of P and T, respectively, are shown in the direction of an increase in concentration.*

The quantitative information concerning the variation in the concentration of t one component (displayed as trajectories in Figure 57) is better shown in the PCR representation of the data, which indicate a good prediction of 1-propanol concentration (Figure 58 b) whereas without differential thermodesorption the prediction is not such successful (Figure 58 a). For the prediction of 1-propanol the root mean square error is 0,047 with, and 0,324 without differential thermodesorption if given in multiplication factors for the original concentration of 1-propanol in TOPE of 500 ppm. In other words, the concentration of 1-propanol in the mixtures can predicted within an error of 24 ppm with, and 162 ppm without time resolved signal evaluation.
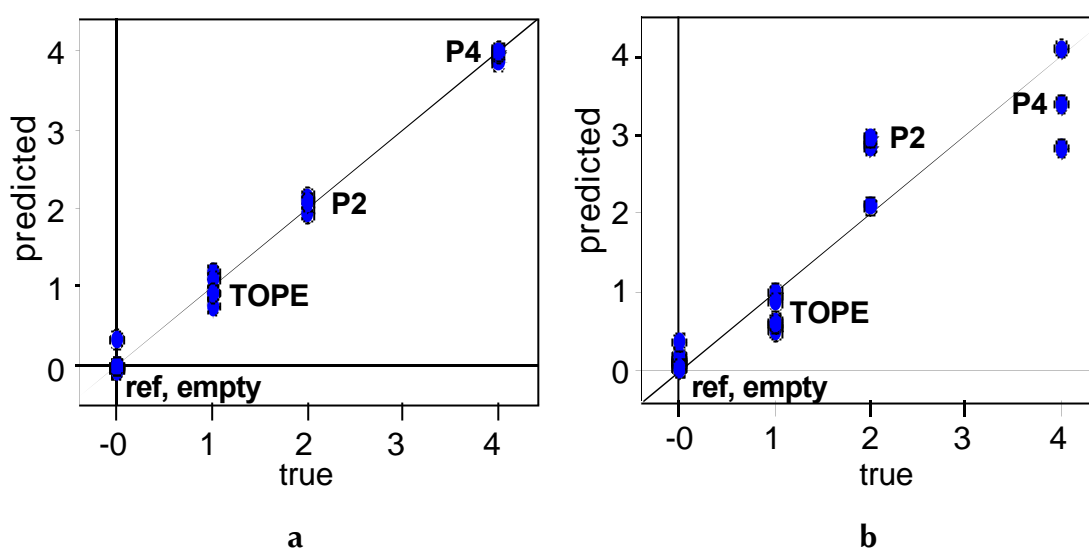
*Figure 58 a and b: PCR of different concentrations of 1-Propanol in TOPE without (a) and with (b) differential thermodesorption.*

Here, the differential thermodesorption set-up gives a noticeable improvement. Without differential thermodesorption it is apparent, that the prediction of concentration within the mixture is less successful even though no independent test data set is displayed. This is due to the fact that in the headspace extracted from the TOPE sample 1-propanol is present only with a fraction of the concentration of the other components (see Table 13, section 5.4.1). Without the differential thermodesorption the quantitative information on components present in small concentrations is superimposed and thereby masked by sensor responses to compounds present in comparatively high concentrations.

Interactions with other adsorbed molecules and displacement can take place with complex mixtures containing analytes with different chemical potentials present in different concentrations. This is decreasing the retention volume of compounds, and has previously been reported [59,133,136].

However, no appreciable effect has been measured with the thermodesorption set-up used. This is attributed to the fact that the capacity of the trap for adsorbed compounds considerably exceeds the applied analyte concentrations (see also section 3.2.8.3 and 4.7). This corresponds also to findings, that breakthrough volumes are independent from analyte concentration for analyte concentrations in the gas phase for up to 100 ppm. However, higher concentrations may lead to an exponential decrease of $V_B$. This is also supported by literature data [29,50,135] and was confirmed with measurements where water was added to the standard test mixture.

## 5.4.3.5. Reducing cross interference by water

The differential thermodesorption exhibits substantial benefits for the discrimination against a background of high concentrations of interfering compounds such as water.

In the separation of polar molecules on Tenax, the retention depends on the value of the dipole moment of the components. Polar compounds are less retained. Inorganic gases and high volatility compounds are not appreciably retained. The differential thermodesorption set-up shows large benefits if discrimination is most difficult as in the presence of high concentrations of interfering compounds.

Figure 59 shows the unsuccessful classification of TOPE and mixtures with single components left out (or in double or quadruple concentration, respectively) similar to the previous measurements with each TOPE component in a concentration of 500 ppm but now against a background of water in a high concentration. Water accounted 10% of the volume in the sample.
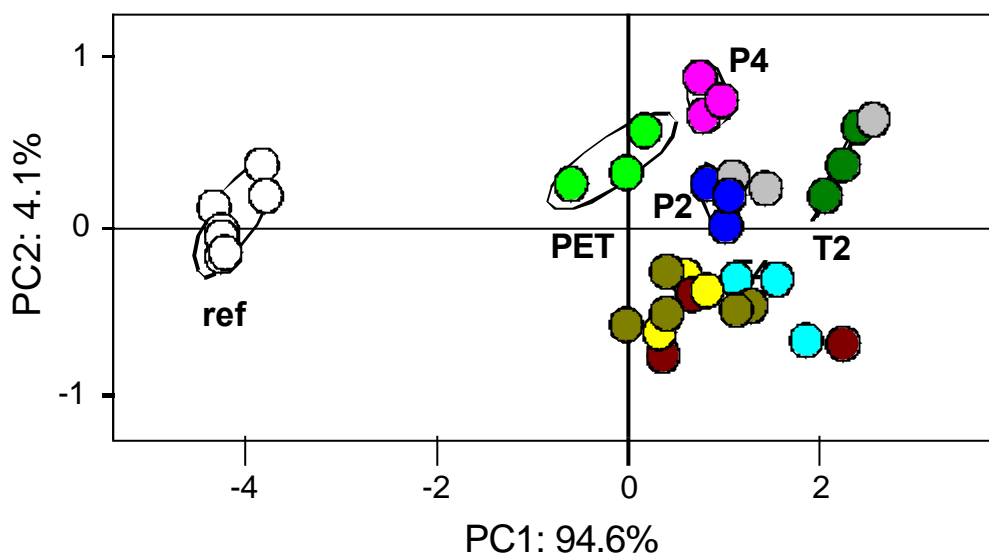


*Figure 59: PCA of TOPE with variation of concentration of single components against a background of water (10% of the sample volume).*

Figure 60 shows the PCA scores plot for the same mixtures with single components variation against a high humidity similar to the previous measurement.

The addition of water to the sample matrix simulates a measurement environment as found in many e-nose applications where a background of water, which is often not very well defined but usually orders of magnitude

larger in concentration than the target analytes, is interfering with the measurements. Examples for these applications are given in chapters 5.5 and 5.6.
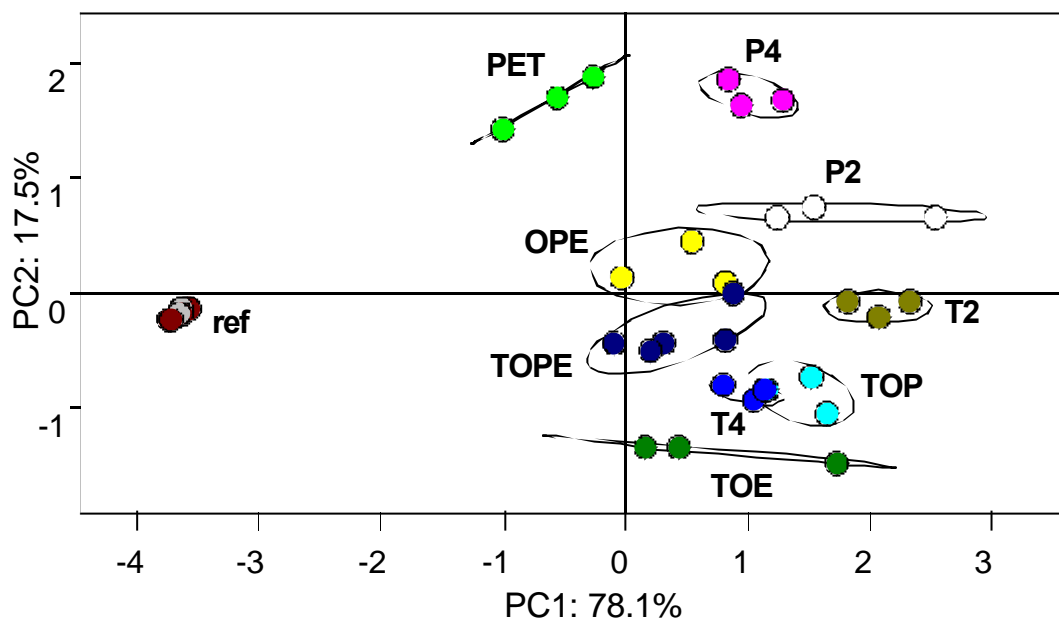


*Figure 60: PCA of TOPE with variation of concentration of single components against a background of water with differential thermodesorption.*

The classification is partly successful despite the high concentration of water interfering with the measurement. A careful selection of evaluated information i.e. sensors and signals at discrete retention times enables the classification of mixtures measured with water background as test data in the reference data set (Figure 52) as shown in Figure 61.
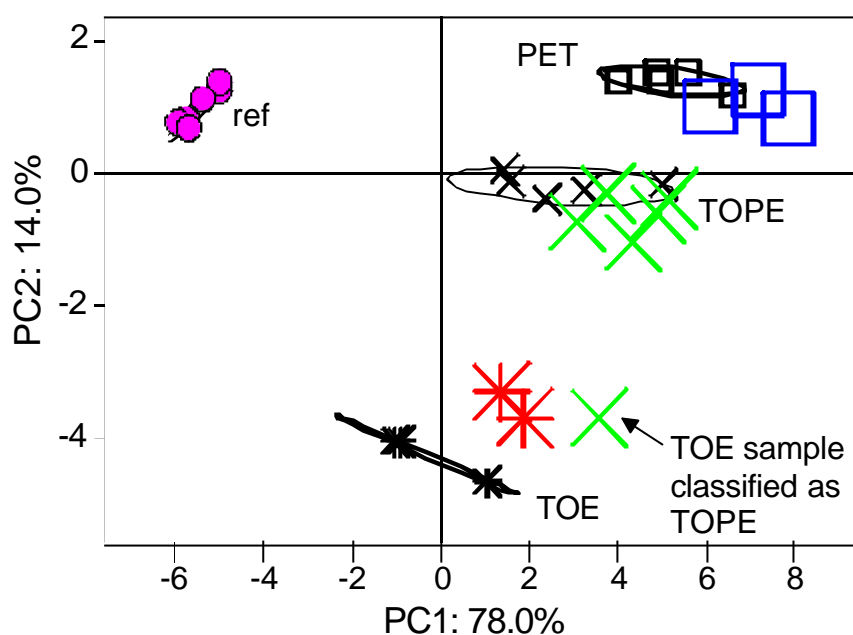
*Figure 61: TOPE with variation of concentration of single components against a background of water as test data (large symbols) classified in reference data generated without water interference.*

The classification is not completely successful. Using a classification algorithm included in the MOSES II software package for labeling unknown samples one TOE sample is classified as TOPE. The classification algorithm used was K nearest neighbour (KNN) classification [137] with K=3. For associating independent test data with a previously defined class, the KNN evaluates the Euclidean distances of test samples scores to a number of reference samples scores K. In other words the test samples are labeled according to their nearest neighbors in the scores plot.

The 1-propanol content has not been predicted accurately. The reason for this is, that with the chosen heating ramp the water is not completely eluted before the thermodesorption of the target compounds begins. Water then appears as offset in the signals of the TOPE mixtures (Figure 62). 1-propanol shows the retention time closest to water and is present in the smallest concentration in the headspace. For a correct classification the heating ramps and timing of the measurements need further improvement to completely eliminate the water influence on the data evaluated.
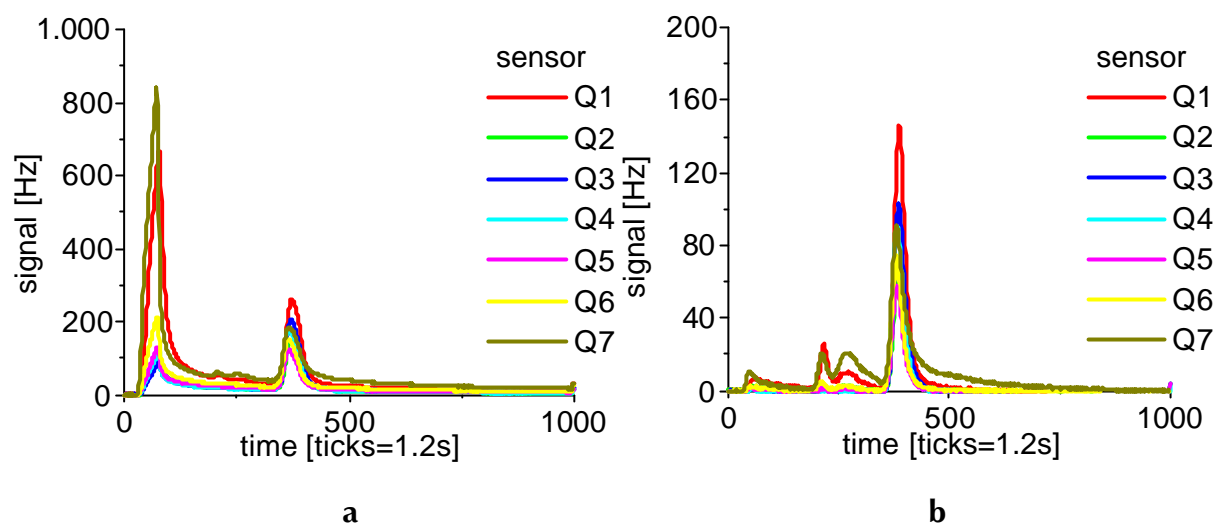
*Figure 62 a and b: QMB sensor signals for TOPE with water (a) and without water (b).*

It could not verified, that high ambient humidity has a neglectable effect on retention volumes as reported in literature [29, 135], at least not for very high concentrations. Nevertheless, by adapting the dry purge period at room temperature prior to heating of the trap according to the experiences with the test mixtures in following measurements water could completely be eluted prior to any other compound (see e.g. Figure 73 and Figure 81).

## 5.5. Investigation of beer

To test the results developed with model substances or mixtures of known chemical composition, the sample preconditioning techniques described previously were used and further modified in food applications. Goal of the investigation of beer was the discrimination of different commercial brands based on analytes other than ethanol or carbon dioxide content. The long term goal of investigations like the one conducted in this work, is the monitoring of the production process and/ or the ageing of the product with regard to flavor determining constituents. The discrimination of beer products with chemical sensors is challenging for several reasons. The humidity of the investigated headspace extract is high compared to the concentration of the target analytes; the discrimination should not be based on the differences in the alcohol content of the sample, which is thus also seen as interference of high concentrations; and carbon dioxide, although not directly detected by the sensors used, interferes with the desired reproducible sample uptake.

### 5.5.1. GC-MS

Beer was investigated with GC-MS in order to identify the analytes for the classification of different beer brands and to test the possibilities of preconditioning the samples with sample dryers and thermodesorption set-ups positioned between headspace sampler and GC-MS instrument. Table 17 shows the varied parameters of the conducted measurements using different dryer configurations.

| # | hss temperature settings | | | GC-MS inlet | dryer |
|---|---|---|---|---|---|
| | Oven [°C] | Loop [°C] | Tr.line [°C] | | |
| 1 | 50 | 60 | 70 | splitless | - |
| 2 | 50 | 60 | 70 | split 1:150 | - |
| 3 | 50 | 60 | 70 | split 1:150 | Nafion |
| 4 | 70 | 80 | 90 | splitless | Nafion |
| 5 | 50 | 60 | 70 | splitless | $NaSO_4$ |

*Table 17: Parameters of GC-MS beer measurements.*

Eight different beer brands have been investigated shown in Table 18, reference sample vials are marked bl (blank).

| # | beer brand | alcohol content [%] | abbreviation |
|---|---|---|---|
| 1 | Schwaben Bräu Meister Pils | 4.9 | M |
| 2 | Haigerlocher Weihnachtsbier | 4.9 | HW |
| 3 | Oettinger Original Export | 4.7 | O |
| 4 | Jever Pils | 4.9 | J |
| 5 | Fürstenberg Premium Pilsener | 4.8 | F |
| 6 | Rothaus Tannenzäpfle | 5.1 | T |
| 7 | Alpirsbacher Klosterbräu | 4.9 | A |
| 8 | Jever Light (*Becks) | 2.7 | JL |

*Table 18: Investigated samples and abbreviations (\*Lever Light was replaced by Becks in the e-nose investigation in conjunction with a chromatographic column).*

Figure 63 shows the chromatograms for one exemplary beer brand under the various conditions with the main peaks labeled. The large peak for ethanol at the retention time ($t_R$) of 5.84 minutes disappears with the introduction of the dryers to the set-up. Setting the headspace sampler to higher extraction temperatures does not increase the analyte signals.
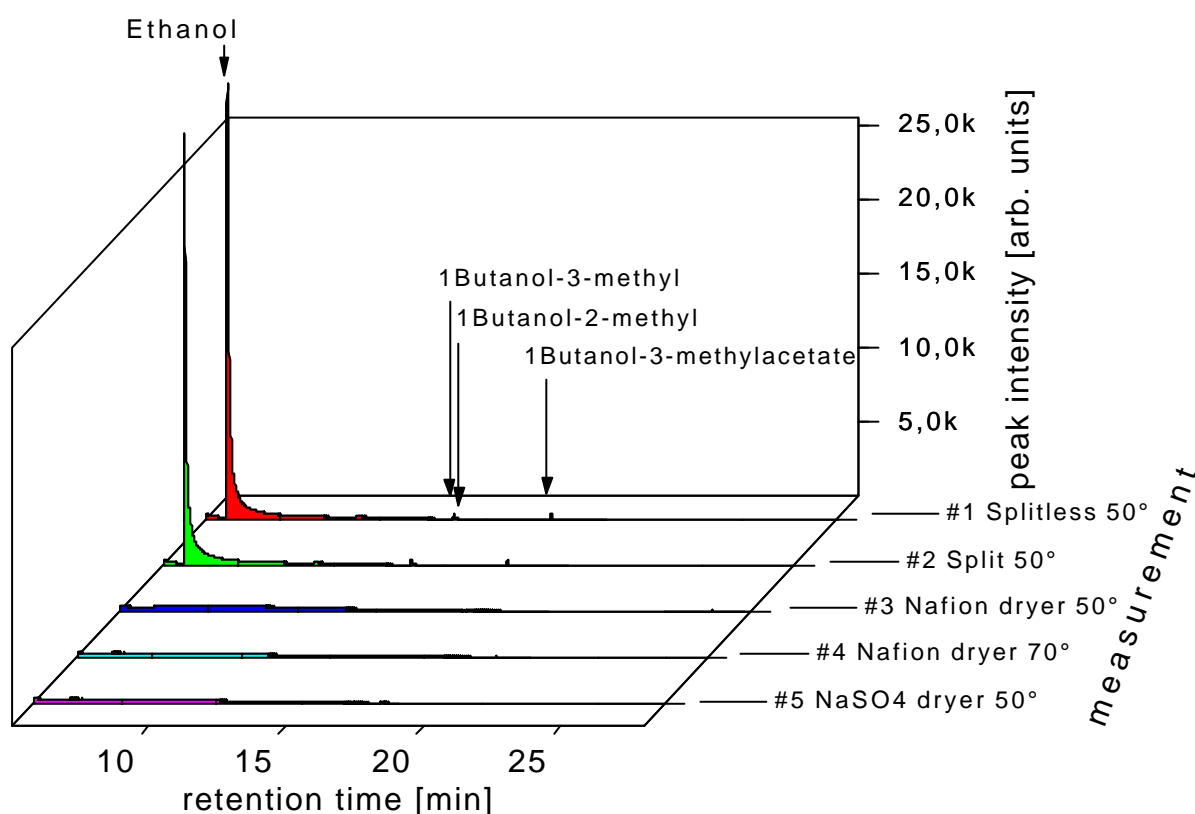


*Figure 63: chromatograms for one exemplary beer brand under the different measurement conditions.*

Figure 64 shows an enlarged section between $t_R$ of 12 to 18 minutes of the same chromatograms where the characteristic peaks for each beer brand for 1-butanol-3-and 2-methyl and to a smaller extent 1-butanol-3-methylacetate also are removed by both dryers.

Most of the analytes useful for the separation of beer, especially the 1-butanol derivatives, are relatively polar. Both dryer principles do not seem applicable to

the improvement of classification by the removal of the interfering compounds water and ethanol, because they are likely to at least partially adsorb also constituents necessary for a valid discrimination.
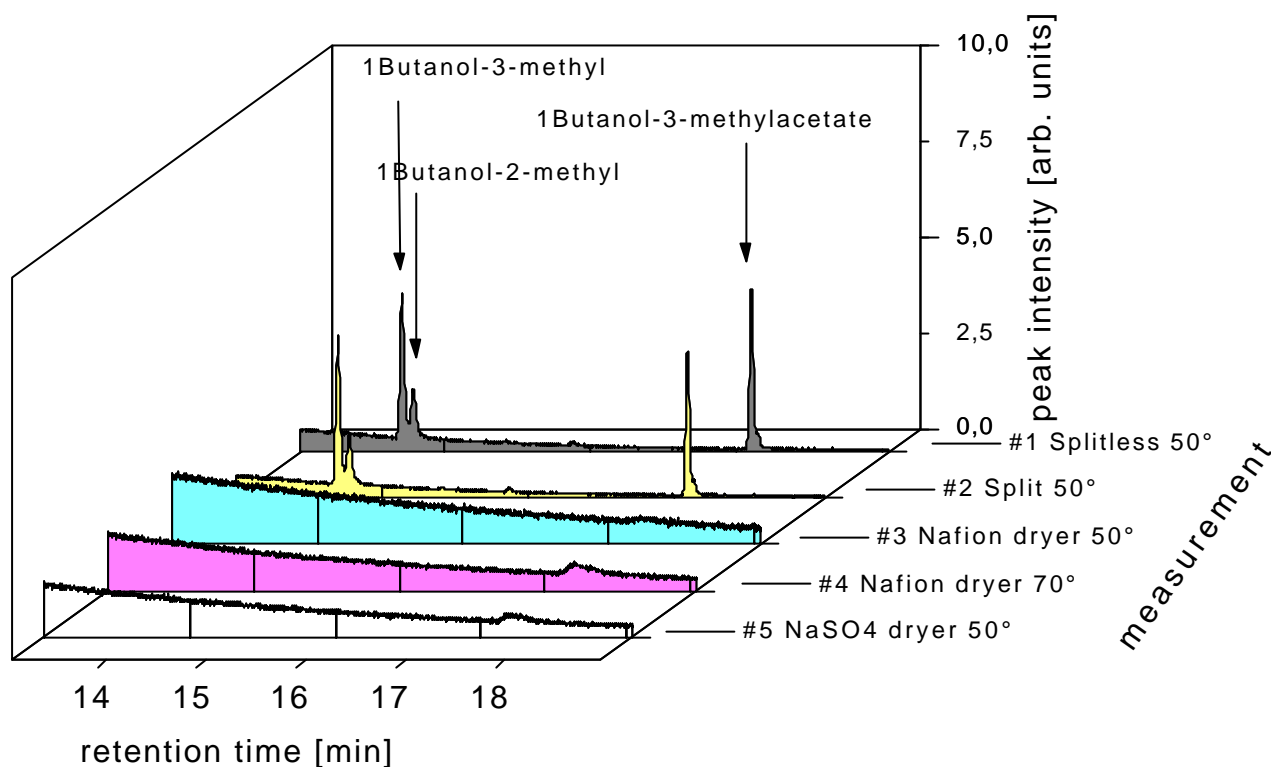


Figure 64: Enlarged section between $t_R$ 12 min to 18 min under the different measurement conditions.

Figure 64 also shows as an effect of the dryers, that the dryers will broaden the peaks or even entirely suppress the peaks for certain analytes. By releasing the removed water and ethanol in low concentration over the duration of the measurement the dryers increase the background noise, thus constricting the identification of characteristic analytes. The instrument looses sensitivity for the target analytes.

Figure 65 shows the chromatograms of four exemplary beer brands under measurement conditions without dryer and low extraction temperature. The characteristic peaks are enlarged in Figure 66.
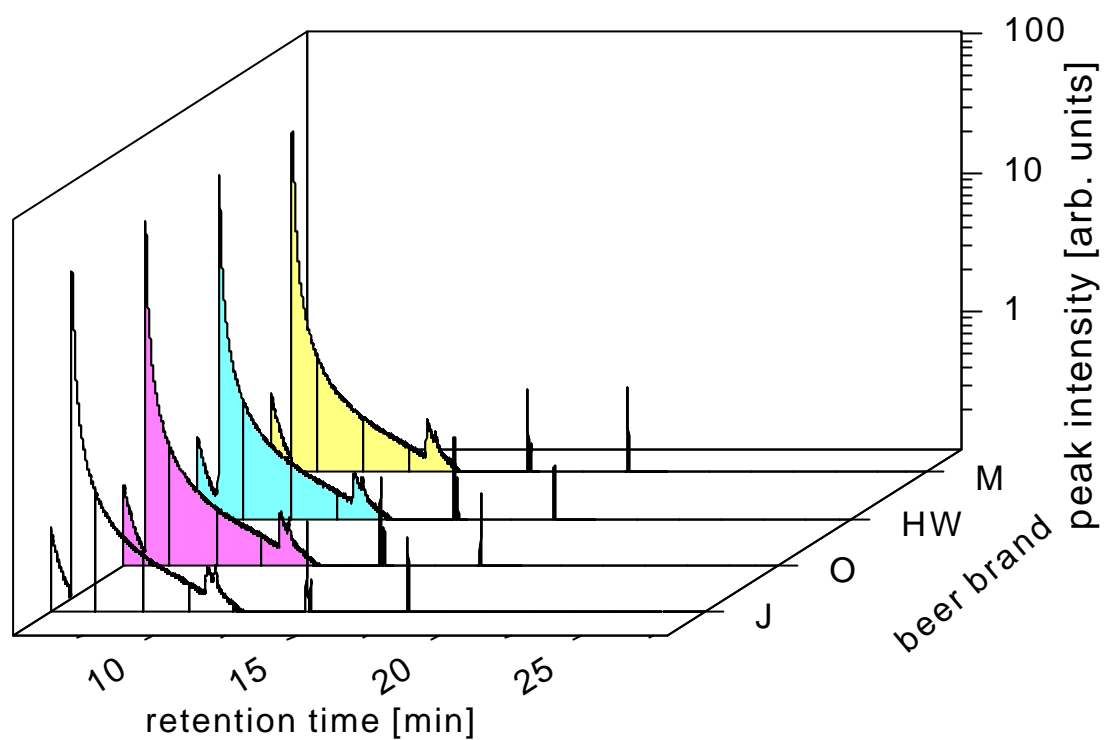
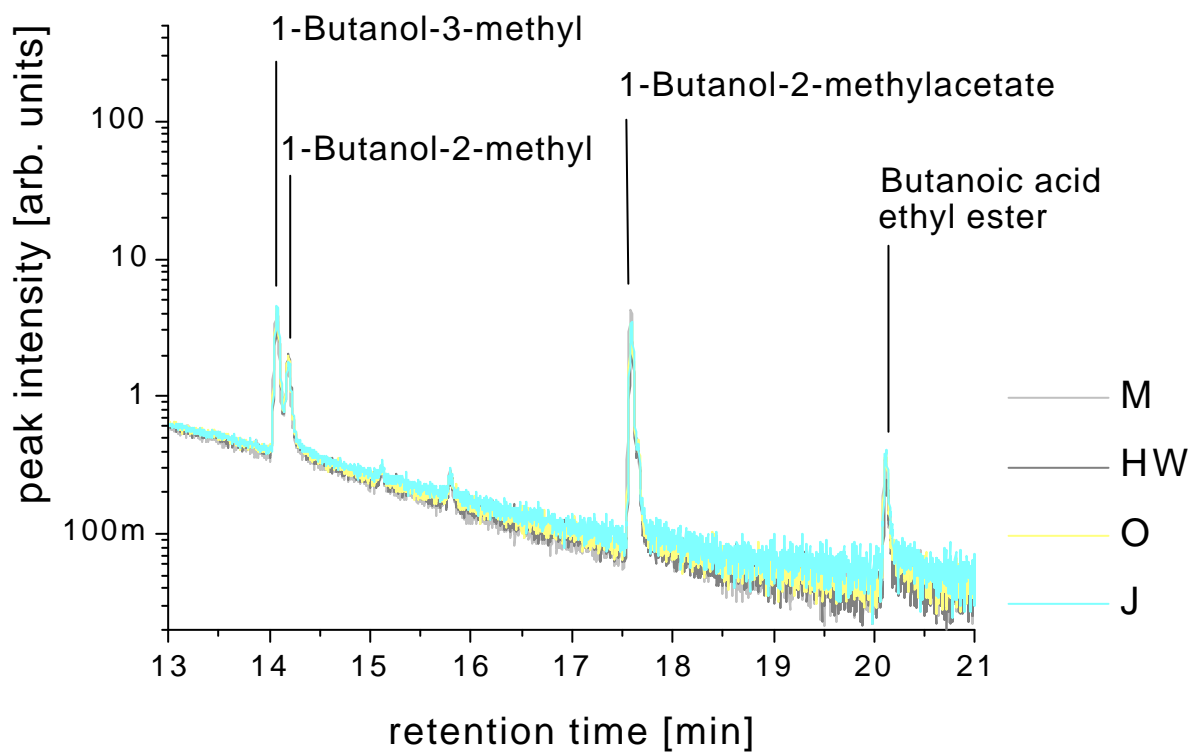Figure 65: Chromatograms for four exemplary beer brands.



Figure 66: Enlarged section for four exemplary beer brands.

Here, the enlarged peaks for four different beer brands show the similarity of the chromatograms. With GC-MS analysis conducted without optimization of the measurement parameters the beer brands are not separable.

The parameters of the MS scan can be set to optimize the sensitivity to higher molecular weight compounds by neglecting masses below 33 mass units and thus removing the background of e.g. water, nitrogen, oxygen, nitrous oxide, and carbon monoxide. However, this way the background is removed from the evaluation but not from the samples.

Constituents like water are still interfering with the measurement indirectly. The water content of a sample determines to a certain degree the content of other constituents in the headspace above this sample.

### 5.5.2. MOSES investigation with dryers

Three measurements were conducted, the parameters are shown in Table 19.

| # | hss temperature settings | | | dryer |
|---|---|---|---|---|
| | Oven [°C] | Loop [°C] | Tr.line [°C] | |
| 1 | 50 | 60 | 70 | - |
| 2 | 50 | 60 | 70 | Nafion |
| 3 | 50 | 60 | 70 | $NaSO_4$ |

*Table 19: Conducted measurements.*

All figures of the measurements are shown standardized and normalized. Figure 67 -Figure 69 show the results of the investigation.
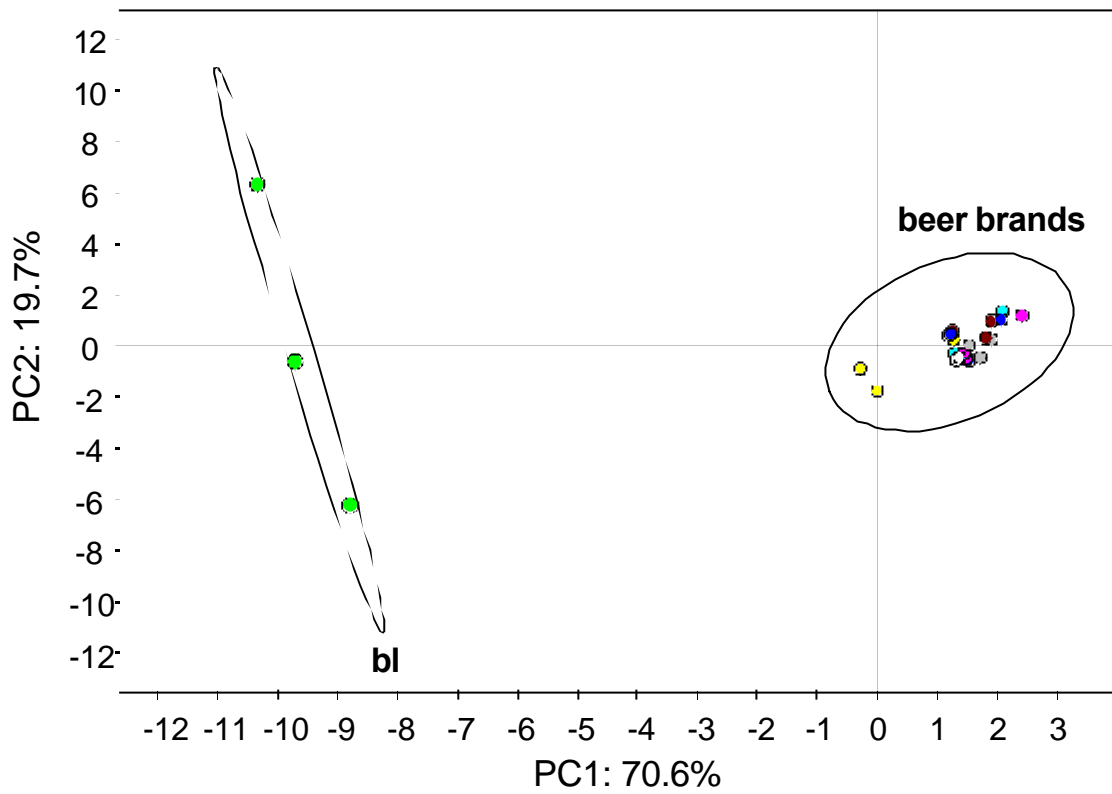
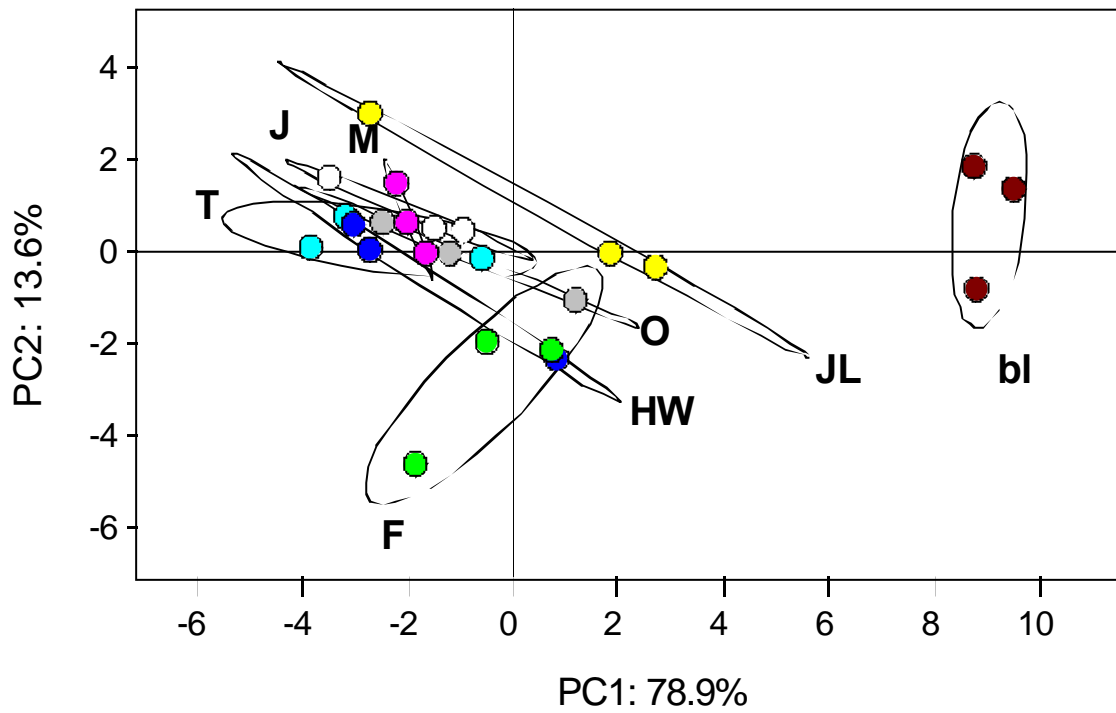*Figure 67: PCA of sensor signals for different beer brands without dryer.*



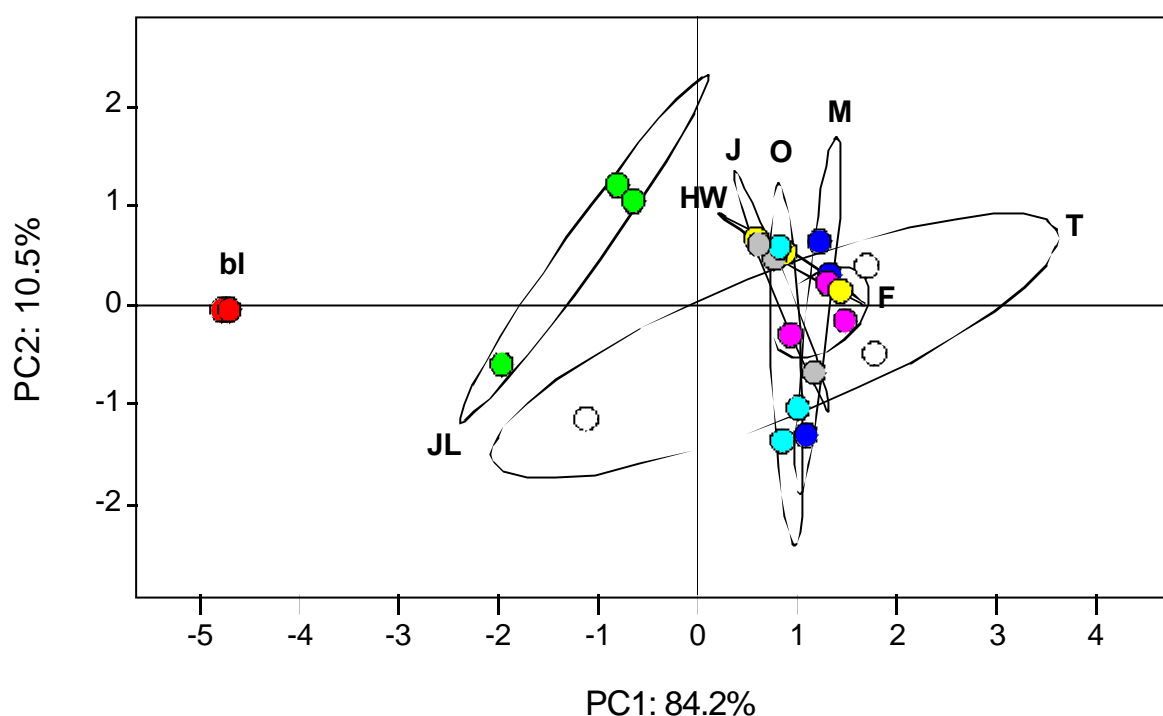*Figure 68: PCA of sensor signals for different beer brands with Nafion dryer.*

*Figure 69: PCA of sensor signals for different beer brands with NaSO$_4$ dryer.*

The figures show that without dryer the beers cannot even be distinguished by the alcohol content whereas both measurements with dryer result in a distinction of the JL samples with a clearly lower content in ethanol than the other samples (see Table 18). The other samples are not separable with any of the tested set-ups. Apparently the dryers remove too much of the characteristic compounds in the headspace of the beer samples together with water which was the target substance for removal because of its interference with the classification of samples. The water background has to be removed without removal of other species.

The second problem with the dryer set-up is the continuous contamination of the dryers by compounds absorbed in the dryer tubing resulting in these compounds eluting as background in following measurements (see Figure 64). For Nafion this is especially critical in applications where polar constituents in high concentrations are present as in the beer measurements.

## 5.5.3. MOSES investigation with a chromatographic column

In order to test the best achievable separation of the interfering sample headspace constituents ethanol, water, and carbon dioxide from the target analytes before the measurement with the e-nose, a commercial fused silica chromatographic column was interfaced to the existing setup of headspace

sampler and MOSES II. The carefully thermostatted capillary column (CP Sil 88) was used for sample separation prior to the chemical sensor detection (see section 5.4.1.) The beer measurements employing the CP Sil 88 column were performed by I. Heberle [124].

As an example, Figure 70 shows the result of the separation with a chromatographic for one beer sample.
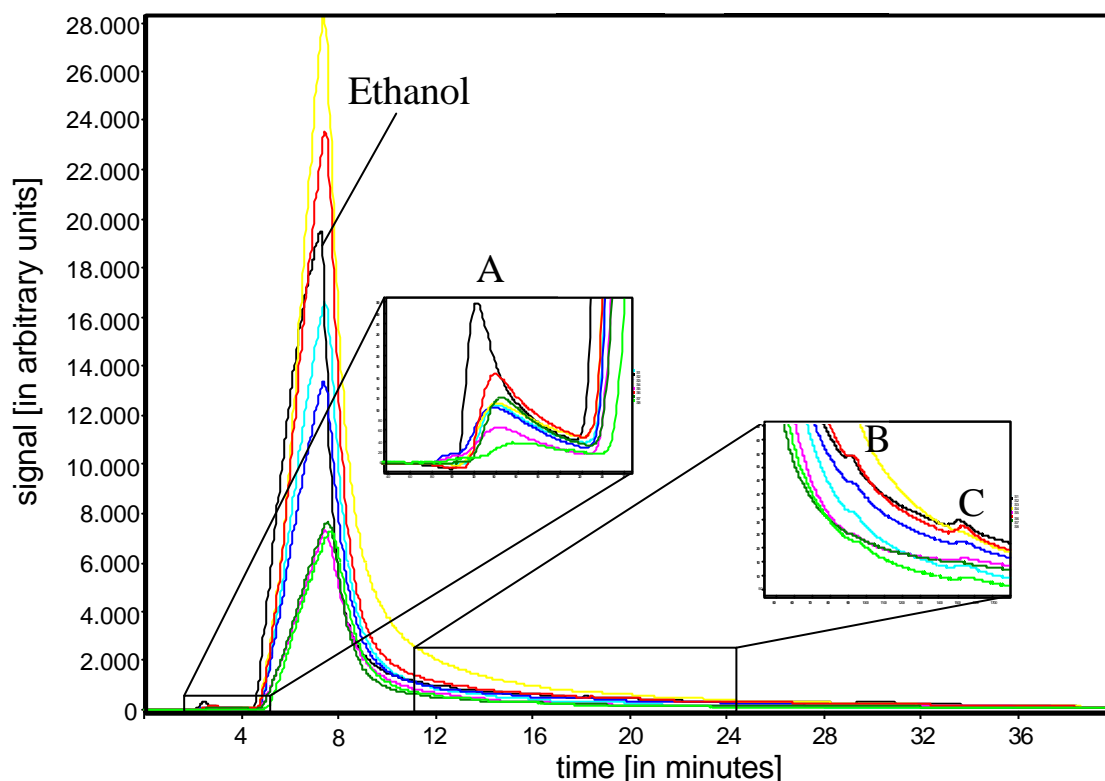


Figure 70: MOX sensor signals to beer sample 'A' after separation by a fused silica -chromatographic column (CP-Sil 88) [124].

The dominating peak has been identified as ethanol but an enlargement shows a small peak with a lower retention time (A) and two shoulders at higher retention times (B and C) with a two orders of magnitude lower intensity. Although the resolution for the latter two peaks could not be appreciably improved, they can be used for a classification with MOSES as their retention times and relative intensities are reproducible. For classification of the beer samples the ethanol peak was intentionally disregarded to focus on the aroma determining substances.

The QMB sensors show a separation of ethanol and water but it could be demonstrated that their signals to other constituents did not improve a distinction correlated to the characteristics of a specific beer brand.

135

A classification of the beer samples was possible only using the signals of the MOX sensors. Figure 71 shows the resulting PCA evaluation with all beer brands clearly distinguished.
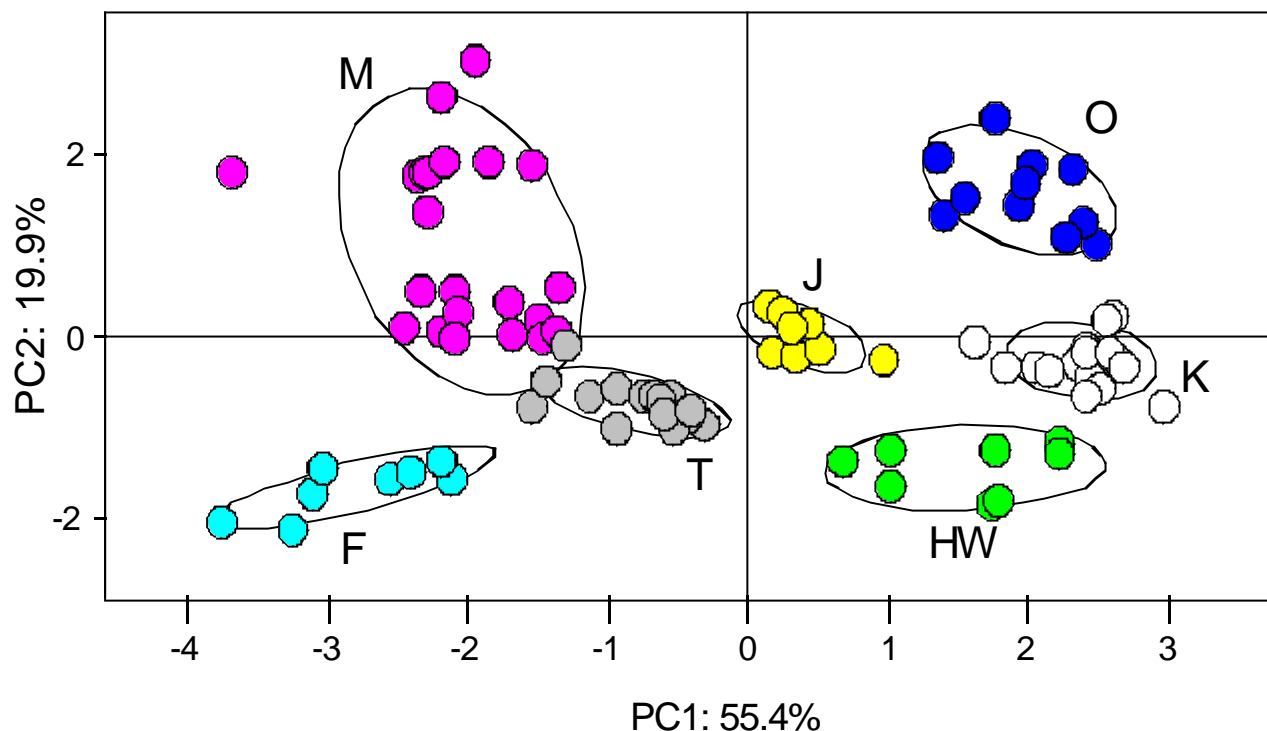


*Figure 71: PCA scores plot of eight different beer brands [124].*

A validation with an independent test data set proved that the probability for correct classification of unknown beer sample lies at about 80%.

A distinction of the different brands using the ethanol peak was not possible and not desired. It proved to be difficult to identify with GC-MS the aroma relevant peaks the separation was based on.

### 5.5.4. MOSES investigation with differential thermodesorption

The beer samples were investigated with differential thermodesorption. For this the heating cycle program was optimized by incorporating two isothermal periods in the heating ramp. The first isothermal operating period at room temperature was determined to be of optimal length with 10 minutes necessary to elute the water before starting to thermodesorb further constituents. This was followed by a ramp of slow heating in order to desorb the ethanol, a second isothermal term, and the fast heating to the maximum trap temperature of 210°C. Although the optimized heating cycle was suited to isolate the target analyte peaks from the most interfering compounds water and ethanol, the

resolution was not sufficient to classify the beer brands using the peaks of compounds eluted with higher retention times.

Changes in humidity affect the overall composition of the headspace above a sample. In a strategy comparable to the dryer experiments it was tried to minimize the cross sensitivity to humidity by changing the ratio of the headspace vapor constituents. Salting out experiments with the goal of changing the composition of the sample headspace in favor of the less polar substances and, most importantly, to reduce the humidity in the headspace were conducted with the addition of sodium- and magnesium-sulfate in various concentrations, also using the optimized thermodesorption technique. Although the concentration of the target analytes in the extracted headspace thus could be increased, the classification with MOSES II was still not successful.

Making optimal use of the combined properties of the differential thermodesorption, separation, and preconcentration (see chapters 5.4.3.2 and 5.4.3.1) was necessary to improve the distinction of the beer brands noticeably. With the above described heating cycle beer samples were conditioned. Classification was possible after enriching the target analytes for distinction on the trap. The loading of the trap with only three sample extracts prior to thermodesorption was sufficient to improve the distinction of samples. The first two of sample extracts were separated at room temperature to elute water and alcohol.

Thereby the analytes necessary for distinction were enriched threefold while part of the water and ethanol reaching the sensors were eliminated, that is disregarded in evaluation. This, on the other hand, increases also sampling time, cycle time, and therefore duration of the overall analysis, with the same factor used for cycles of enrichment.

Figure 72 shows the PCA of three different beer brands with clustering sufficient for the discrimination of those samples thermally desorbed. Also measured were ethanol and water in a concentration comparable to the beer sample (4,5%) and a standard.
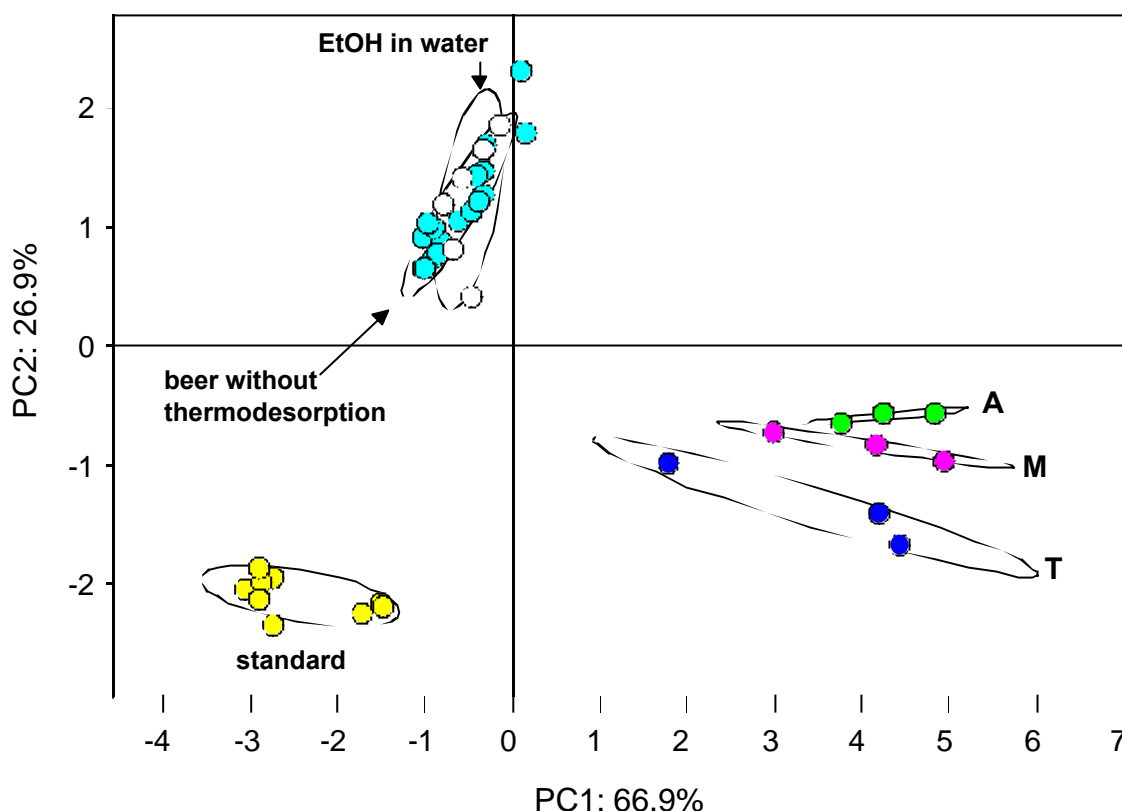
*Figure 72: PCA of three different beer brands (A,M,T) extracted by differential thermodesorption from the preconcentrator, the same beers measured passing the trap isothermally at room temperature, and a standard and ethanol in water samples as reference.*

For the evaluation of the sensor responses, features extracted from only 6 sensors were sufficient. An increase of the number evaluated sensors or extracted signals at retention times when the interfering components elute from the trap does not only not increase the performance of the classification but reduces it. The selection of a subset of variables for entering the pattern recognition and the consequences has been described before in sections 3.4.2, 5.3.2, and 5.4.3.3. Sensors and retention times contributing valuable information were selected by evaluating the loadings plot.

Table 20 shows the smallest number of evaluated peaks needed for an successful discrimination of the example brands A, M, and T. The feature extracted was signal minus baseline at their retention time in ticks (1 tick = 1.2 seconds, 'SigAt-BaseAt' feature).

| sensor type | sensors | SigAt | BaseAt |
|---|---|---|---|
| QMB | Q2 | 1162 | 1222 |
|  | Q7,8 | 1158 | 1215 |
| MOX | S3,S6 | 965 | 1600 |
|  | S3,S6 | 1205 | 1600 |
| AGS | S1 | 1250 | 1800 |

*Table 20: Peaks evaluated for the distinction of the beer brands with the retention times of peaks ('SigAt') and baselines or local minima subtracted ('BaseAt').*

The feature 'SigAt-BaseAt' allows the subtraction not only of the baseline but also of local minima from peaks, thus adding additional information, so that not only peaks but also the missing of responses at a specified retention time are evaluated.

The samples passing the thermodesorption trap without heating are, as stated before, distinguished only by their water and ethanol content. The rest of constituents are held back by the adsorption resin. Therefore, these samples cluster together with the ethanol/water samples and are undistinguishable by brand.

This observation is confirmed by a more detailed evaluation of the individual sensor signals. Figure 73 a shows the signals of the QMB sensor array to the beer sample M using the differential thermodesorption technique. Figure 73 b is an enlargement of the peaks evaluated and used in the PCA with the signal minus base feature at chosen retention times for chosen sensors (Q2,Q7, and Q8). Note that the shown peaks are the result of a triplicate enrichment on the adsorbent resin. For comparison to not thermally desorbed beer samples see Figure 75.
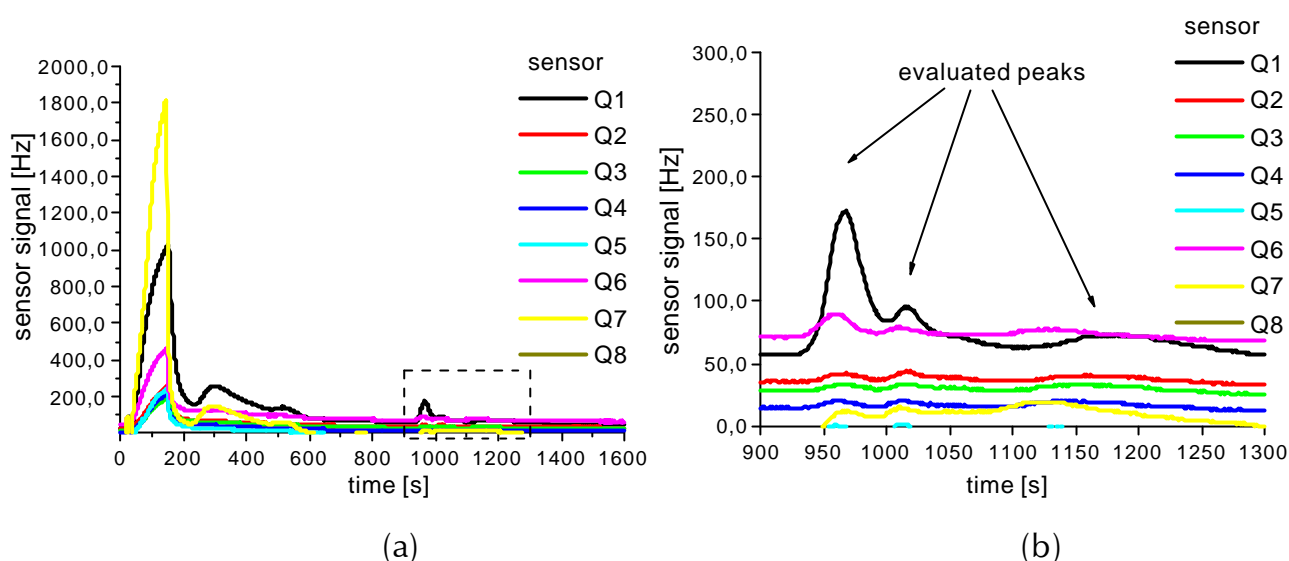
(a)            (b)

*Figure 73 a and b: Signals of the QMB sensors for beer sample M (a) with the evaluated signals shown in an enlargement of the dotted box (b).*

Figure 74 shows the signals of the other sensor types: Signals form the MOX sensors (a), and an enlargement of the evaluated AGS sensor peak (b).
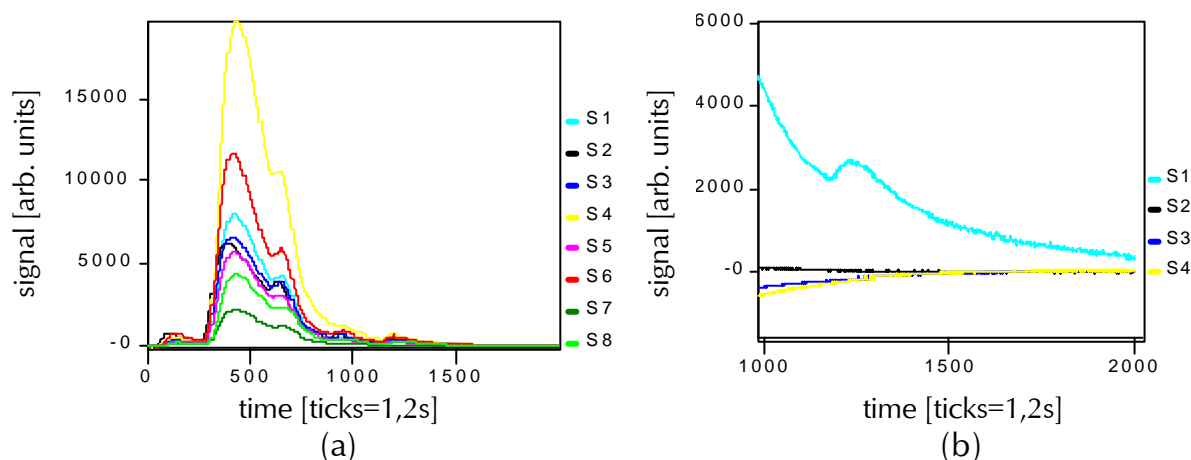


(a)            (b)

*Figure 74 a and b: Signals of the MOX sensors for beer sample M (a) with the evaluated signals for the AGS shown in an (b).*

Of the AGS only the CO sensor (S1) gives a response useful for the distinction of the beer brands. However, for this sensor also the response to ethanol, which without separation would cover any target analyte, is the largest.

Figure 75 shows examples of the signals of the QMB sensors to 4,5% ethanol in water as reference (a) and a beer sample eluted by the trap at room temperature without differential thermodesorption (b).
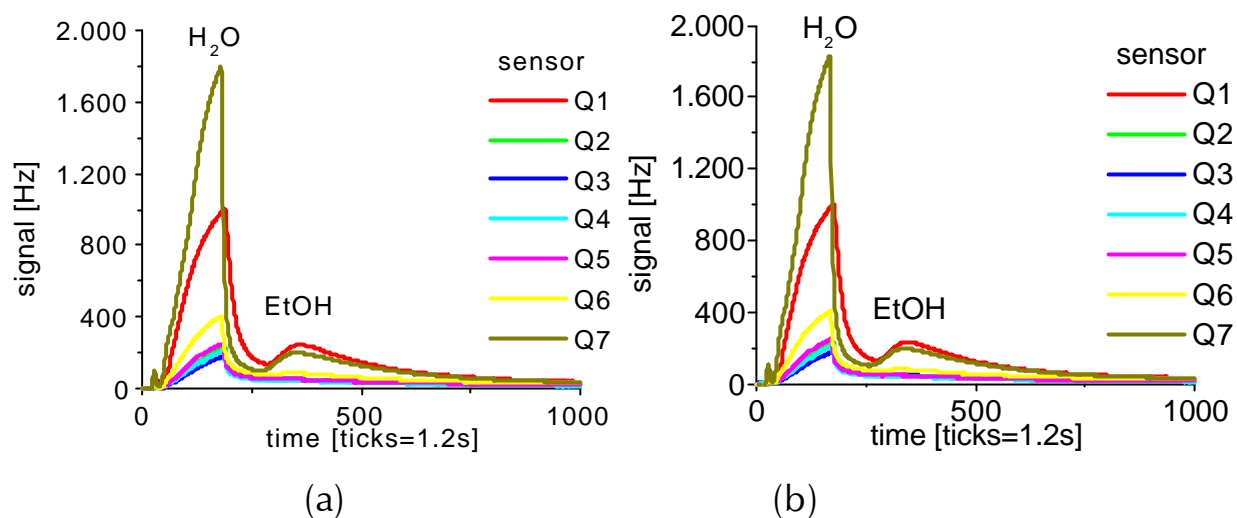
*Figure 75 a and b: Signals to a 4,5% ethanol in water reference sample (a) and a beer sample eluted by the trap without thermodesorption (b).*

The two sets of signals are indistinguishable with a feature extraction and PCA visualization. Here, the samples, when measured without thermodesorption, i.e. only separated isothermally by the trap, are classified by their ethanol content only (see also Figure 73).

## 5.6.  Investigation of mayonnaise

Another application for electronic noses, similar to the investigation of cheese described in section 5.3, is the discrimination of mayonnaise products. The target analytes for achieving a successful distinction, though, were found to be different ones (see following chapter). Therefore, also the sample uptake had to be optimized again. The long term goal of this investigations was the monitoring of the ageing of the products with regard to flavor determining constituents. In this work, the first step of any such investigation, the distinction of the products, was studied.

### 5.6.1.  GC-MS

Prior to the investigation with GC-MS and the electronic nose parameters for the sample uptake were tested. Thus, the yield of static headspace sampling can be influenced substantially. The most important sample uptake parameters which can be optimized are temperature, equilibration time, matrix constituents, and sample volume.

Weighed amounts of six different mayonnaise products, between five grams for the e-nose investigation and ten grams for GC-MS analysis, were filled into 20ml glass vials. Then, the samples were equilibrated for up to 60 minutes at different temperatures from 50°C to 90°C in the headspace sampler. An equilibration time of 20 min. proved sufficient for reaching repeatable headspace composition. Long equilibration times at low equilibration temperatures carry the risk of the headspace composition being influenced also by the storage time at room temperature within, respectively before the start of, the measurement cycle. Equilibration time of the mayonnaise samples as well as the weighed amount of the sample and therefore the headspace volume proved to be less important, whereas the equilibration temperature had a considerable influence on the headspace composition. A rise of the equilibration temperature results in an increase in concentration especially for the polar constituents in the sample headspace. Figure 76 shows the chromatograms of two measurements at 50°C and 90°C, respectively. The peaks for compounds with a high certainty of identification with the GC-MS databank (qualifier) are labeled (see section 4.6). The high concentration of 3-Methylisothiazol at 15,62 min. retention time is specific for the mayonnaise brand (*Lesieur*) investigated in this measurement.
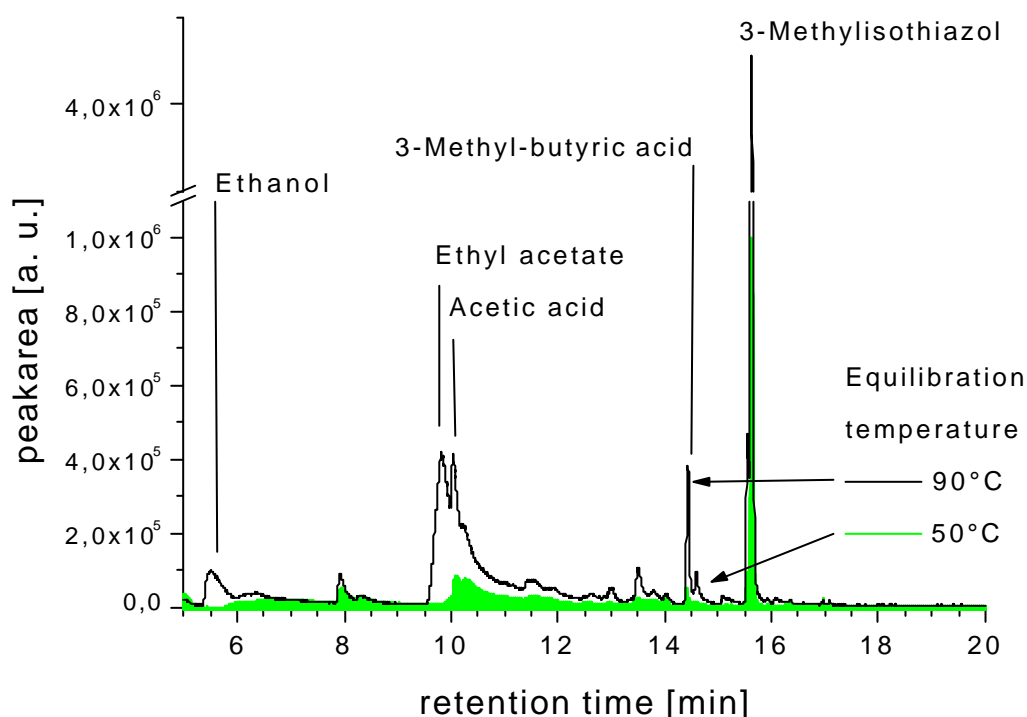


*Figure 76: Chromatograms of 'Lesieur' mayonnaise thermostatted at 50 and 90°C for 20 min.*

As the target compounds for this investigation were present in the headspace at sufficient concentration levels for the detection with chemical sensors at 50°C and ethanol was seen as interfering constituent not being a measure for the quality of the sample, the investigation was conducted with 50°C equilibration temperature.

Moreover, for the investigation with chemical sensor arrays, as many constituents as possible usually provide a better classification result than higher concentrations of only a few components. If classification is based on only a few components the concentration differences of those components dominate the results. Higher equilibration temperatures could improve the partitioning of constituents into the headspace but are undesirable, especially if as in this case there is the risk of irreversible reaction of the organic acids with the sensitive layers of the metal oxide sensors.

Figure 77 and Figure 78 show the chromatograms of the investigated mayonnaise brands. The small differences in the chromatograms are mainly due to the difference of compound concentrations, the overall constituents contained in the brands are mostly similar.
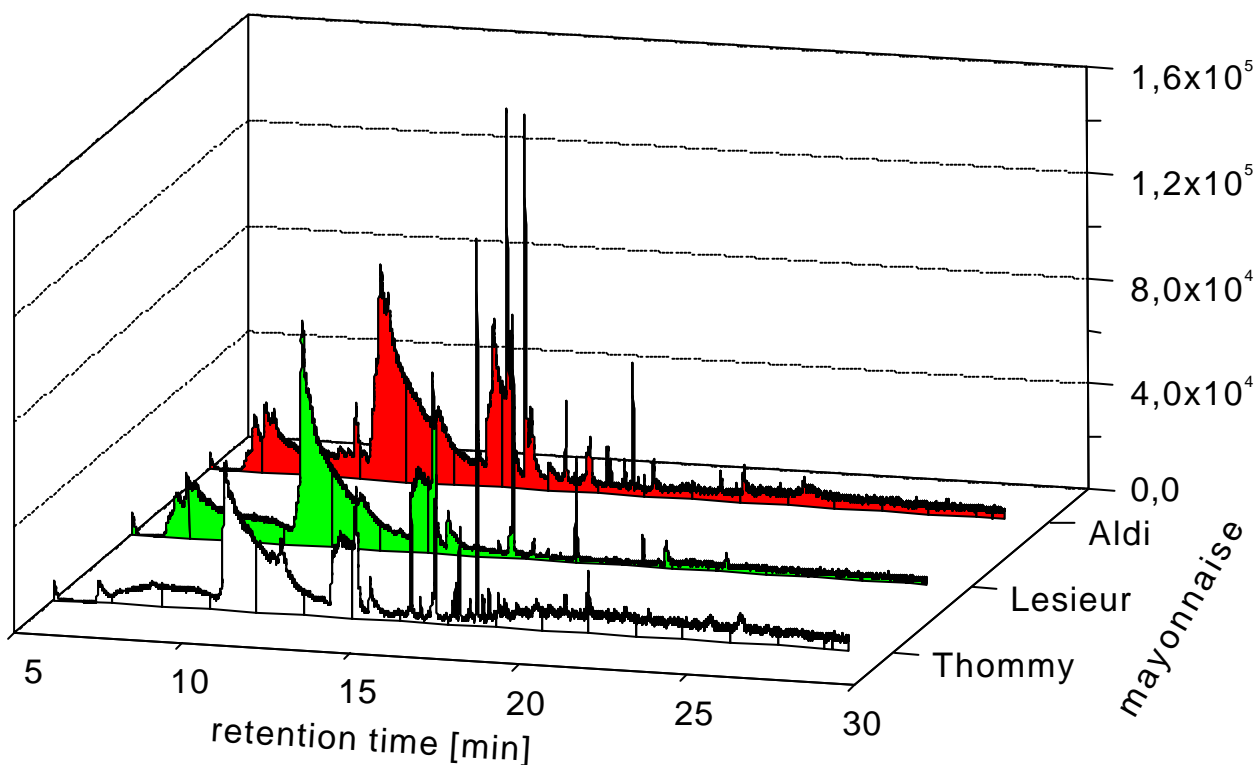


*Figure 77: Chromatogram of three investigated mayonnaise brands.*
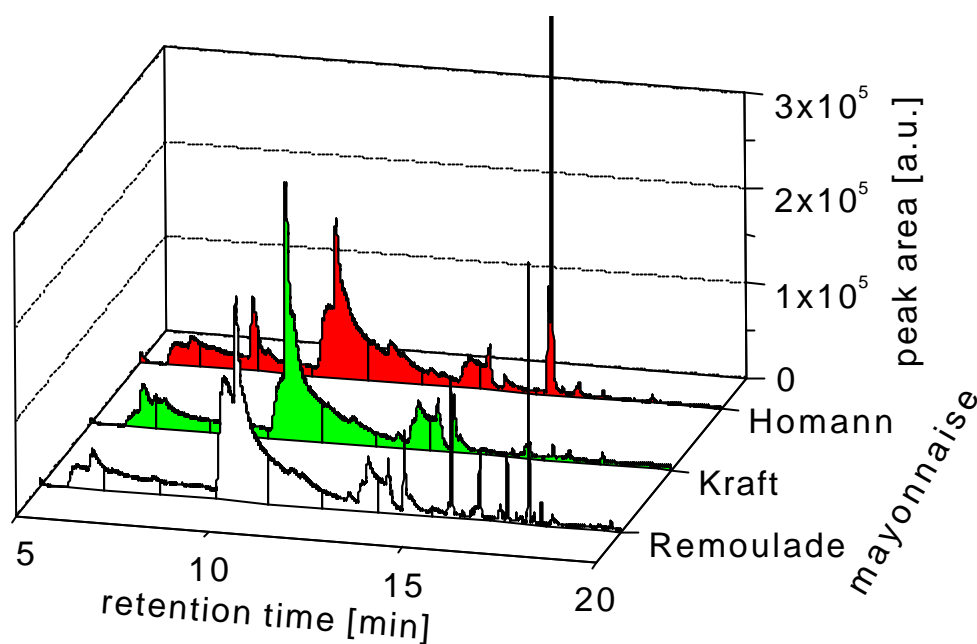
143

*Figure 78: Chromatogram of three investigated mayonnaise brands.*

Table 15 presents a list of the main constituents contained in the headspace over the mayonnaise samples. Only identified compounds, the peak area of which exceed two percent of the total peak area, are listed.

Components common to all brands, e.g. ethanol, ethyl acetate, acetic acid and butyric acid, are present in fairly high concentrations, also all mayonnaise samples contained benzaldehyde in small concentrations. 39 substances with a peak area of more than 1% of the total were identified [172]. The mayonnaise based *Remoulade* dressing, which was also investigated, produced a distinctly different chromatogram from the mayonnaise brands containing limonen, pinen, eucalyptol, and caren in substantial concentrations.

| Retention-time [min] | Substance brand: | Aldi | Homann | Kraft | Remoulade | Lesieur | Thomy |
|---|---|---|---|---|---|---|---|
| 5.92 | Ethanol | | 3.3 | 0.2 | 3.9 | 0.6 | 5.3 |
| 6.35 | Pentane | 3.3 | 3.5 | 7.3 | 5.3 | 3.7 | 1.4 |
| 6.67 | 1,2-dimethyl-cyclopropane | 2.5 | | | | | |
| 7.97 | Carbon disulfide | | 3.5 | | | | |
| 10.06 | Ethyl acetate | | 27.6 | 62.2 | 36.4 | 45.8 | |
| 10.32 | Acetic acid | 31 | 7.9 | 5.9 | 18.9 | 3 | 5.6 |
| 13.86 | Octane | 6.3 | | | | | |
| 13.99 | Arsenic acid (tris trimeth.sil.) | 4.2 | 2.1 | | 2.8 | 11.8 | |
| 14.41 | 3-Methyl-butyric acid | 5.2 | 1.1 | 2.7 | 2.7 | 2.3 | 1.9 |
| 15.55 | 4-Methylthiazol | | 2.2 | | | | 1.6 |
| 15.62 | Allylthiocyanate | 0.9 | 2.4 | | 0.25 | | 2.2 |
| 15.63 | 3-Methyl-isothiazol | | 20.3 | | 2.9 | | |
| 16.39 | alpha-Pinen | | | | | | 2.5 |
| 16.89 | 4-Methyl-bicyclo[3.1.0]hexane | | | | 2.1 | | |
| 16.96 | Benzaldehyde | 0.3 | 0.1 | 0.3 | 0.2 | 0.2 | 0.9 |
| 17.07 | beta-Pinen | | | | 0.4 | | 1.2 |
| 17.62 | Limonen | 1 | | | 4.3 | | |
| 17.95 | (+)-2-Caren | | | | | 5.56 | 0.44 |

*Table 21: Peak area percentage of the mayonnaise constituents identified in the headspace.*

### 5.6.2. MOSES investigation without differential thermodesorption

For the MOSES II measurements the same sample uptake parameters as in the GC-MS analysis were used, i.e. equilibration at 50°C for 20 min., loop and transfer line temperatures 100°C and 120°C, respectively. The MOX sensors were set to highest sensitivity and tested for cross sensitivity to humidity with pure water. The signal to water was a substantial part of the measurement signal. The overall goal of the investigation was the monitoring of the ageing of mayonnaise over several months. Therefore, a standard was measured together

with the sample to indicate possible sensor drift. ethyl acetate, contained in all mayonnaise samples and therefore close to the classification problem, was used as a standard in a concentration of 487 ppm weight in polyethylenglykol (PEG). The weighed concentration was established in test measurements to be a similar quantity also contained in the samples. PEG was chosen as matrix for containing almost no volatile material and therefore was not interfering with the sensor signals (see also TOPE measurements, chapter 5.4.3).
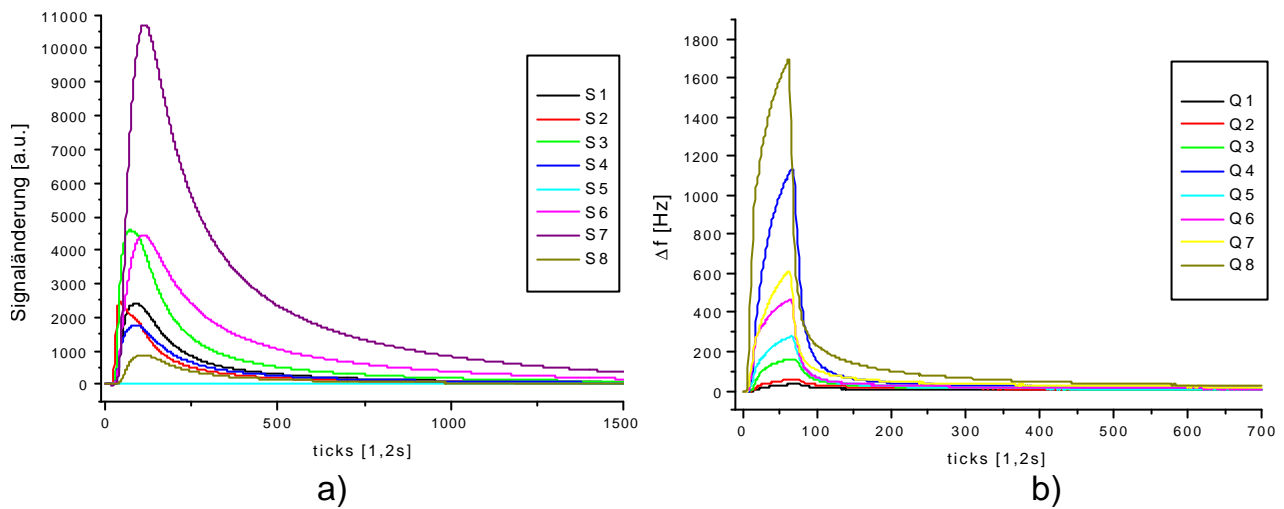


*Figure 79: a) Sensorsignals of MOX, b) sensorsignals of QMB sensors.*

For evaluation of the signals a PCA using the signal minus base feature was performed. Figure 80 shows the resulting scores plot for the six mayonnaise products and water, empty vials and the standard as references. Although the relatively large variation in the scores for water show that the sample uptake repeatability was not optimal the standard and empty vials were represented in reproducible small clusters. The mayonnaise products did not cluster with the exception of the *Lesieur* brand which could be classified.

In Figure 80, single measurements are labeled with their brand name. The MOX and QMB sensor signals for all different mayonnaise products are very similar resulting in the scattering of their scores in the PCA plot. Also the loadings plot of the same investigation showed a high redundancy of the QMB sensor responses to the samples.
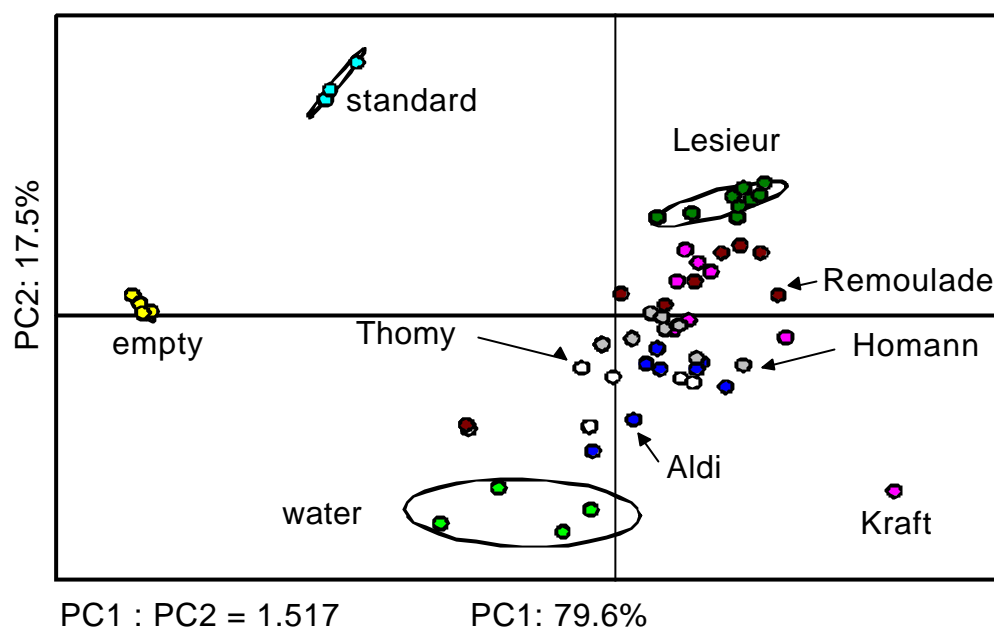
*Figure 80: PCA of sensor signals for mayonnaise products.*

The classification of the different mayonnaise brands is not possible without sample preconditioning. The samples show differences only in constituents being represented in relatively small concentrations in the headspace next to a relatively high humidity and high concentration in ethyl acetate and acetic acid (Table 21). The latter compounds forbid also the use of a dryer set-up for removing the humidity as they are enriched in the lining of the dryer, creating a background preventing a differentiation based on the target analytes.

The distinction of the *Lesieur* brand can be attributed to the content of ethyl acetate in the headspace above the samples (45.8% of the total GC-MS peak area). ethyl acetate was also used in the standard and the content appears to be represented at least partially by the second PC.

### 5.6.3. MOSES investigation using differential thermodesorption

For the investigation of mayonnaise using the differential thermodesorption set-up a heating protocol was established and programmed for the subsequent measurements. In this application, the trapping of higher molecular target analytes and sequential elution using a temperature ramp was preceded by an isothermal stage. The isothermal period was programmed in order to release polar compounds and especially water before the desorption of analytes useful for the identification of the sample. The signals were evaluated by extracting now several signal minus baseline values at different retention times.

147

Figure 81 shows the signals for MOX, QMB, and AGS sensors for a exemplary measurement.
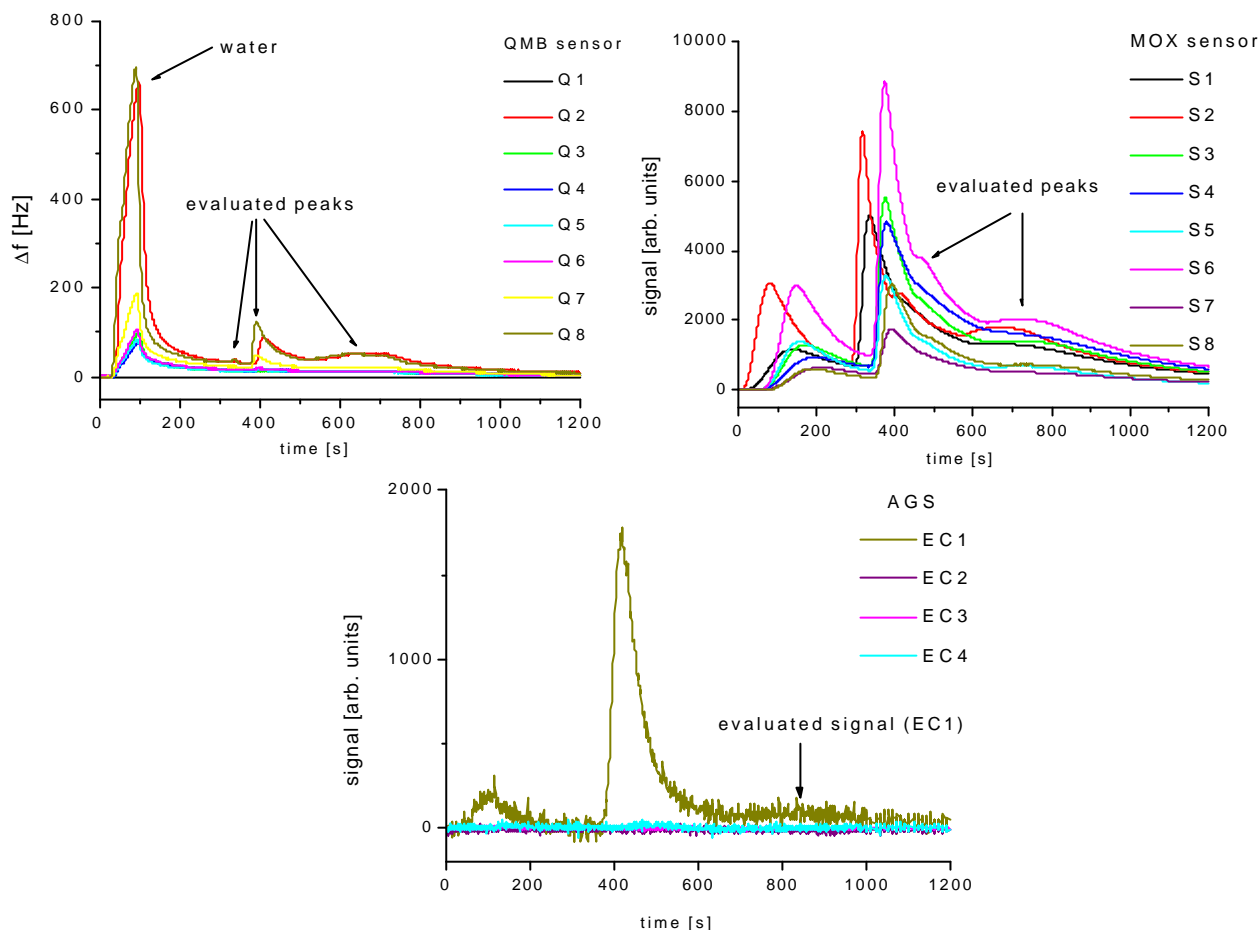


*Figure 81: Sensor signals for mayonnaise using differential thermodesorption.*

The sensor signals show several maxima or peaks for different analytes or mixtures of those which are evaluated independent from each other. The peaks representing mixtures or signals for single analytes are not deconvoluted much in these measurements. However, a classification using only a few retention times for each sensor principle and only up to three sensors of the same type is possible. Differences in the samples allowing for the distinction of brands lie in non polar constituents eluted to the end of the measurement at trap temperatures exceeding 120°C. The Tenax resin elutes polar compounds, especially water, without heating or at relatively low temperatures while non polar constituents are desorbed only at elevated temperatures. Although the peaks were not identified for their chemical composition, the peaks eluted early are very likely to derive from the polar constituents of the mayonnaise products,

e.g. ethyl acetate and acetic acid, partially overlapped by the large signal to water (QMB and MOX sensors). Figure 82 and Figure 83 show the standardized and normalized PCA evaluation of the mayonnaise samples and the ethyl acetate standard previously used with differential thermodesorption sample preconditioning.
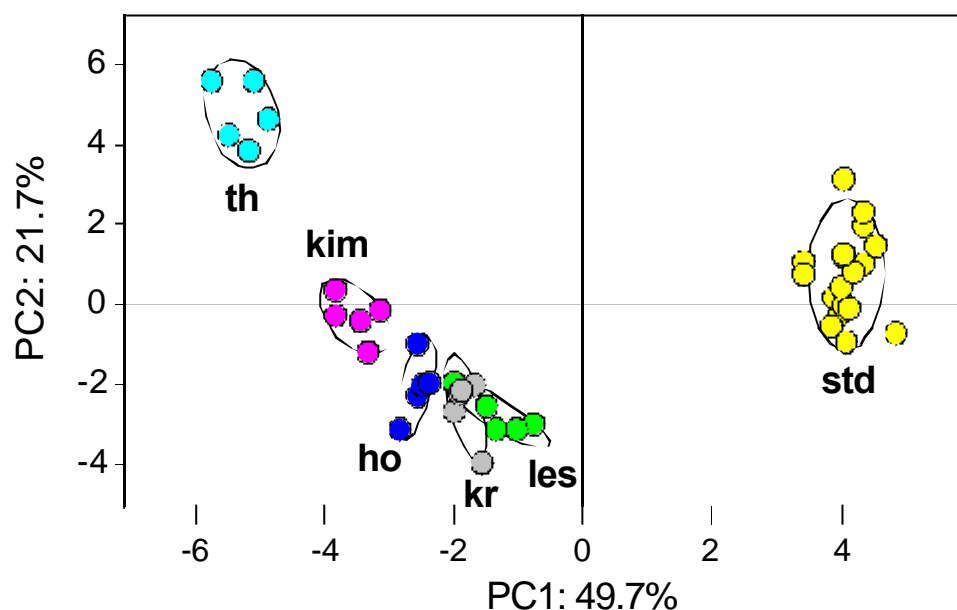


*Figure 82: PCA for mayonnaise using differential thermodesorption (principle component 1 and 2).*

Here, the normalization of the feature vectors was used to remove any influence of sampling variation. The samples contained the same amount of weighed mayonnaise,10g. However, the surface area of the mayonnaise in the vial depended on the manual method of filling the vial with a syringe and to a certain extent also was dependent on the viscosity of the sample.

The features selected for evaluation were chosen so that redundant and therefore highly correlated information was disregarded. The consequences for the data visualization and the information content of the higher PCs have been discussed in section 5.4.3.3. Figure 83 displays the scores plot for the same measurement for PC1 and PC3.
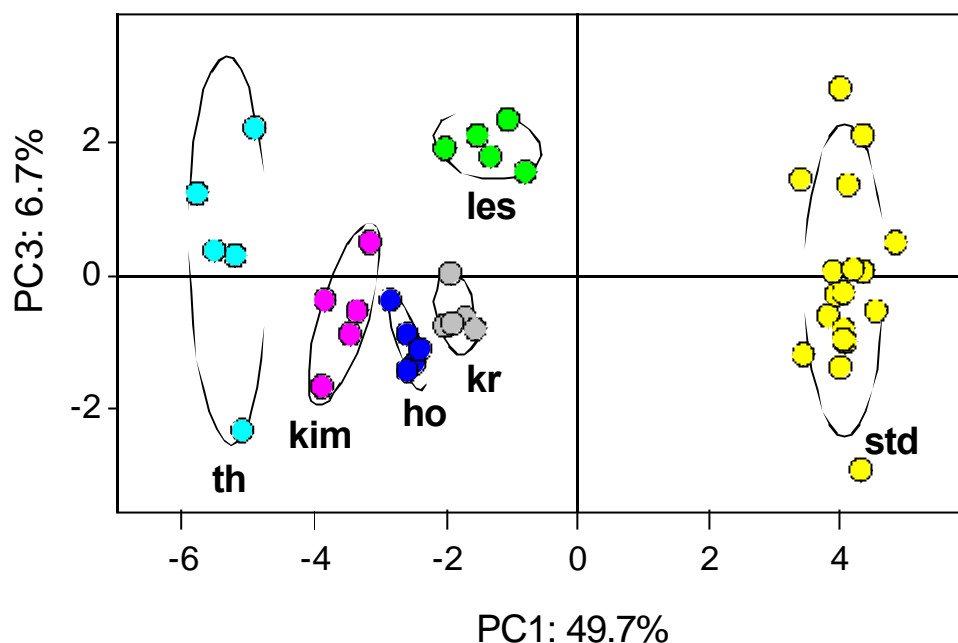
*Figure 83: PCA for mayonnaise using differential thermodesorption (principle component 1 and 3).*

The scores plots show, that the distinction for the two brands, which are not clustering distinctively in the plot of the first two principle components, is achieved when using also the third principle component for classification of the samples. Although the deconvoluted analyte peaks are not well resolved, the evaluation with a time dependent feature extraction delivers sufficient information for the identification of different commercial brands. Moreover, although the peaks were not identified for single constituents, the distinction using 36 chosen features for each sample is successful without extending the cycle time of the e-nose measurements. Compared to conventional operation with sample transfer directly from headspace autosampler to MOSES II the classification using time dependent signal evaluation after chromatographic separation with the programmed thermodesorption cycle does not extend the overall time of the investigation.

The differential thermodesorption sample uptake leads to improved selectivity when utilizing the chromatographic effect of the adsorbent tube, and especially for the application in food characterization reduces the influence of water vapor thus improving the detection limit for certain target analytes. The gained information content of the measurements is partially contained in the higher principal components of the pattern recognition visualization.

# 6. CONCLUSION AND SUMMARY

In summary three main tasks have been achieved in the course of this work: Firstly, the expansion of the sensor system to a further transduction principle; i.e. the integration of amperometric gas sensors with unique and complementary properties. Secondly, the set-up and integration of a sample conditioning and enrichment unit, i.e. the differential thermodesorption technique, which has been successfully tested, and the theoretical basis of which has been evaluated. Thirdly, the successful expansion of the modified electronic nose in new fields of applications, e.g. the detection of bacteria or the classification of foodstuff in a water matrix, making use of the developed sampling techniques.

## 6.1. The EC module

With the integration of an additional transducer type the selective detection of an additional class of target analytes in low concentrations has become possible. Amperometric gas sensors display no appreciable humidity dependence, exhibit complementary selectivity, and high sensitivity to certain permanent gases important e.g. for bacteria detection. Apart from the possibility of providing a reference signal for measurements in varying humidity, amperometric sensors make a further class of target analytes accessible to investigation with chemical sensor arrays. The long term stability of sensor responses, despite varying humidity backgrounds, is required in the great majority of applications electronic noses are subjected to.

## 6.2. Sampling

For future generations of e-noses the sampling will be more important than the sensor itself when searching for ways to improve the analytical performance. For sampling techniques, however, classical analytical chemistry holds a vast amount of data and provides enormous experience to draw from. The investigation of various sample classes with the e-nose has shown, that the development of sampling system and sample pretreatment are important means of increasing the utility and performance of sensor arrays.

## 6.2.1. Differential thermodesorption

In order to improve the sensitivity and selectivity of the e-nose, differential thermodesorption sample uptake has been developed and interfaced to the existing hardware. The modification to the system was characterized using a set of standard test mixtures and led to increased analytical performance in applications of practical relevance.

The differential thermodesorption sample uptake modification is a chemical enrichment system enhancing sensitivity and at the same time a chromatographic column improving selectivity.

The latter mode of operation multiplies the information content of the sensors by deconvolution of the signals and enables the elimination of sensor responses to interfering compounds from the signal evaluation.

The consequences and possibilities arising from the expansion of the variable set in the pattern recognition have been investigated for model samples and practical applications.

Chromatographic separation in conjunction with chemical sensors was investigated on a theoretical basis with model compounds and optimized for integration into e-nose analysis. The resulting differential thermodesorption led to several benefits to the analytical capability of the multi sensor system verified in application examples where the e-nose alone failed to provide a satisfactory analytical result. The programmable heating allows to target key analytes from a sample for chromatographic separation within the thermodesorption process.

Unlike in the conventional use of sensor arrays, single substances contained in chemically more complicated mixtures can now be separately detected. This enables a compound specific quantitative and qualitative evaluation for the classification of a sample.

Thus, compounds in relatively small concentrations or small analyte concentration differences are also recorded for evaluation. This opens up application fields vastly exceeding the fraction where target analytes at the same time are major constituents in a sample headspace.

Feature extraction of sensor responses with time resolution allows the identification of compounds by their retention time and the selection of sensor responses to sample constituents relevant for the classification problem of an application. The automated hyphenation of chromatographic separation with sensor array investigation expands the analytical capability of e-noses to

applications previously reserved to conventional chemical analysis. Nevertheless, the advantages of e-noses in cycle time, investigation cost, and ability to classify complex samples by organoleptic properties are retained.

The limitations of the new method have been established and a theoretical basis for the prediction of applicability has been shown.

The set-up and operating conditions of the sample preconditioning method must be optimized for each application and need to be tailored to the application.

Measurement results have shown, that for certain applications an even simpler sample conditioning set-up, e.g. dryers and catalytic filaments, is sufficient for successful classification.

The extraction and conditioning procedure determines the measurable sample characteristics. Sampling has to be performed application specific with control and numeric documentation of all sample uptake parameters. Changes in humidity affect the overall composition of the headspace above a sample. Different strategies give possible solutions to a cross sensitivity towards humidity or other interfering compounds but sample or extract alteration always affects the overall information.

The prior discussed methods of sample preconditioning greatly enhance the performance of the e-nose, yet for each application the optimal method for sample uptake and sample treatment has to be established and optimized.

## 6.3. Applications

Employing the novel sample conditioning techniques and the extended sensor array, the e-nose was successfully applied for the investigation of samples from different fields of application.

Metabolic products of aqueous bacterial growth could sensitively be detected. Different species of bacteria could be distinguished and their growth phase could be estimated based on chemical sensor responses.

Examples of various brands of foodstuff were classified. The key to successful analysis was the classification of samples based on target analytes not constituting the major compounds of a sample. The suppression of cross sensitivity allowed the classification of different cheese brands. Disregarding selected time resolved sensor responses to interferents, allowed the classification of beer brands despite interference by carbon dioxide, water, and alcohol. The same differential thermodesorption technique enabled the

classification of mayonnaise samples. None of the above mentioned tasks could be performed without sample preconditioning. However, a general or optimal method of sample uptake does not exist, devices and procedures have to be optimized for any specific application.

The modifications to the electronic nose described in this work, enable the successful application of sensor arrays to investigations previously constricted to sumptuary classical analysis.

# 7. OUTLOOK AND SUGGESTIONS FOR FURTHER WORK

The feasibility of a new technique and set-up could be proved with theoretical considerations, the characterization of the method with model samples, and the investigation of few application examples. Nevertheless, the conducted studies should be seen as the starting point for the classification and description of the large amount of samples where target analytes are minor constituents of a complex matrix.

Again, this work showed, that a general or optimal method of investigation does not exist. Therefore, the developed devices and procedures will have to be characterized and optimized for the numerous application for which e-noses investigations are of interest to.

The investigations described in this work will have to be continued in order to obtain all information of interest for the applications concerned. For example larger groups of microorganisms should be compared with one another to demonstrate the universality of the e-nose method for distinguishing bacterial species. Then, the research can be extended to the investigation of specific problems, where bacterial contamination has to be detected and identified, e.g. in food production, biotechnology, or medical applications. Dense cultures of cells were needed to acquire suitable data, implying that sensitivity rather than selectivity will be an obstacle to practical use of sensor array technology in bacterial diagnosis.

Likewise, the distinction of food samples is the starting point for the routine control of odor and off-odors caused by ageing, contamination, or packaging.

The system modification described constitutes the basis for further extension of the capability of the electronic nose. Extending the MOSES software package by an algorithm scanning all measurement with differential thermodesorption for local maxima, and selecting a finite number of retention times for extracting features, would add automated evaluation to the automated measurement system already realized.

# 8. REFERENCES

[1]     J. R. Stetter, S. Zaromb, W.R. Penrose, M.W. Findlay Jr. and T. Otagawa, Portable Device for Detecting and Identifying Hazardous Vapors 1984. Hazardous Materials Spills Conference (1984), pp. 183-190.

[2]     J.R. Stetter, M.W. Findlay, Jr., K.M. Schroeder, C. Yue, and W.R. Penrose, Quality Classification of Grain Using a Sensor Array and Pattern Recognition, Anal. Chim. Acta, 284 (1993) pp. 1-11.

[3]     U. Weimar and W. Göpel, Chemical Imaging II: Trends in practical multiparameter sensor systems, Sensors and Actuators B 52 (1998) pp. 143-161.

[4]     J. W. Gardner and P. Bartlett, A brief history of electronic noses, Sensors and Actuators B, 18-19 (1994) pp. 211-220.

[5]     G.H. Dodd, P.N. Bartlett, and J.W. Gardner, Odours–the stimulus for an electronic nose, in Sensors and Sensory Systems for an Electronic Nose, (J.W. Gardner and P.N. Bartlett, Eds.) Proc. NATO Advanced Research Workshop, Reykjavik, Iceland, August 5-8, 1991.

[6]     J.R. Stetter, Electrochemical Sensors, Sensor Arrays, and Computer Algorithms, in Fundamentals and Applications of Chemical Sensors, D. Schuetzle, R. Hammerle, and J. Butler, eds., ACS Symposium Series, No. 309 (1986) pp. 299-308.

[7]     Stetter, J.R., P.C. Jurs, and S.L. Rose, Detection of Hazardous Gases and Vapors: Pattern Recognition Analysis of Data from an Electrochemical Sensor Array, Anal. Chem. 58 (1986) pp. 860-866.

[8]     Stetter, J.R., S. Zaromb, and W.R. Penrose, 1984. Sensor Array for Toxic Gas Detection. U.S. Patent # 4,670,405 (1984).

[9 ]    Zaromb, S., R. Battin, W. R. Penrose, J.R. Stetter, V.C. Stamoudis, and J.O. Stull, "Extending the Capabilities of the Portable Chemical Parameter Spectrometer to the Identification of up to 100 Compounds," Proc. of the 2nd International Meeting on Chemical Sensors, J. L. Aucouturier et al., eds., Bordeaux, France, July 7-10, (1986) pp.739-742.

[10]   W.R. and S.E. Penrose, Designing Portable Computerized Instruments, TAB Books Inc., Blue Ridge Summit, PA 17214.

[11]   J.R. Stetter, S. Strathmann, C. McEntegart, M. DeCastro and W.R. Penrose, New sensor arrays and sampling systems for a modular electronic nose, Sensors and Actuators B 69(3) (2000) pp. 410-419

[12]   W. Göpel, K.D. Schierbaum, Chemical Sensors: Definitions and Typical Examples, In W. Göpel, J. Hesse, J.N. Zemel (Ed.), Sensors: Volume 2: Chemical and Biochemical Sensors Part I, VCH Verlag Chemie, Weinheim 1991, p. 1.

[13]   W. Göpel, Sensoren und Physikalische Chemie, Nachr. Chemie, Tech. Lab. 41, (1993), p. 332.

[14]   H.A. Schultens and D. Schild, Biophysical properties of olfactory receptor neurones, in Sensors and Sensory Systems for an Electronic Nose, (J.W. Gardner and P.N. Bartlett, Eds.) Proc. NATO Advanced Research Workshop, Reykjavik, Iceland, August 5-8, 1991.

[15]   U. Weimar and W. Göpel, Chemical Imaging I: Concepts and Vision for Electronic and Bioelectronic Noses, Sensors and Actuators B 52 (1998) pp.125-142.

[16]   J. Mitrovics, H. Ulmer, U. Weimar and W. Göpel, Modular Sensor System for gas sensing and odor monitoring: the MOSES concept. Acc. Chem Res. 31 (1998) pp. 307-315.

[17]   W. Göpel, New Materials and Transducers for Chemical Sensors, Sensors and Actuators B, 18-19 (1994) pp. 1-21.

[18]   S. Zaromb and J. R. Stetter, Theoretical Basis for Identification and Measurement of Air Contaminants Using an Array of Sensors Having Partly Overlapping Selectivities, Sensors and Actuators 6 (1984) pp. 225-243.

[19]   T.A. Dickinson, D.R. Dalt, J. White and J.S. Kauer, Analytical Chemistry (1997) 69, pp. 3413-3418.

[20]   B. Kolb an L.S. Ettre, Static Headspace - Gas Chromatography, (1997), Wiley - VCH, New York, pp. 2-6, 64-79.

[21]   H.J. Hübschmann, Handbuch der GC/MS, Grundlagen und Anwendung, Verlag Chemie, VCH, Weinheim, (1996).

[22]   H. Ulmer, Hybride modulare Sensorsysteme für die Gasanalytik und Olfaktometrie, Dissertation, (1999), University of Tübingen, pp. 54-57.

[23]   R. Bassette, S. Ozeris, and C.H. Whitnah, Gas chromatographic analysis of head space gas of dilute aqueous solutions, Anal. Chem, 34 (1962) pp. 1540-43.

[24]   B. MacGillivray, J. Pawliszyn, P. Fowlie, C. Sagra, Headspace solid-phase microextraction versus purge and trap for the determination of substituted benzene compounds in water, J. of Chrom. Sci. 32 (1994) pp. 317-22.

[25]   T.C. Voice, B. Kolb, J of Chrom. Sci., 32 (1994) p. 306.

[26]   B.V. Burger, Z. Munro, Quantitative trapping and thermal desorption of volatiles using fused silica open tubular capillary traps, J. of Chrom., 370 (1986) pp. 449-464.

[27]   M. Mehran, Purge and column trap techniques for the gas analysis of halogenated compounds, J. of Chrom. Sci. 24 (1985) pp. 546-548.

[28]   W.R. Betz, S.G. Maroldo, G.D. Wachob, and M.C. Firth, Characterization of Carbon Molecular Sieves and Activated Charcoal for Use in Airborne Contaminant Sampling., Am. Ind. Hyg. Assoc. 50 (4) (1989) pp. 181-187.

[29]   H.R. Brown, C.J. Purnell, Collection and analysis of trace organic vapor pollutants in ambient atmospheres, J. of Chrom. 178 (1979) pp. 97-80.

[30]   C. Bayer, Advances in trapping procedures for organic indoor pollutants, Journal of Chromatographic Science 32 (1994) pp. 312.

[31]   M.D. Askari, M.P. Maskarinec, S.M.Smith, P.M.Beam, C.C. Travis, Effektiveness of purge and trap for measurement of volatile organic compounds in aged soils, Anal. Chem. 65 (1993) pp. 2366.

[32]   P. Werkhoff, W. Breitschneider, Dynamic Headspace gas chromatography: concentration of volatile components after thermal desorption by intermediate cryofocussing in a cold trap, J. of Chrom. 405 (1987) pp. 87-98.

[33]   W.M. Coleman, III, Automated purge-and-trap-gas chromatography analysis of headspace volatiles from natural products, J. of Chrom. Sci. 30 (1992) pp. 159-163.

[34]  J. Namiesnik, T. Gorecki, M. Biziuk, Review : Isolation and Preconcentration of VOCs from water, Analytica Chimica Acta, 237 (1991) p. 1.

[35]  M. Frank, Vergleichende Messungen an Lebensmittelproben mit Verfahren der Analytischen Chemie und der Gassensorik, Diploma thesis, (1998), University of Tübingen.

[36]  R. Emele, Messung niedriger Gaskonzentrationen mit einem Sensorsystem, Diploma thesis, (1999), University of Tübingen, pp. 54-57.

[37]  K.D. Oliver, J.R. Adams, E. Hunter Daughtrey Jr.,W. A. McClenny, M.J. Yoong, M. Pardee, E.B. Almasi, and N. Kirshen, Technique for Monitoring Toxic VOCs in Air: Sorbent Preconcentration, Closed Cycle Cooler Cryofocussing, and GC/MS Analysis, Environ. Sci. Technol. 30 (1996) pp. 1939-1945.

[38]  D. Helmig and J.P. Greenberg, Automated in situ gas chromatographic-mass spectrometric analysis of ppt level volatile organic trace gases using multistage solid-adsorbent trapping, J. of Chrom. A 677 (1994) pp. 123-132.

[39]  T. Maeda, K. Funaki, Y. Yanaguchi, and K. Ichioka, On-site Monitoring System for Hazardous Air Pollutants Using an Adsorption-Thermal Desorption-Capillary GC System Equipped with a Photoionization Detector and an Electrolytic Conductivity Detector, J. High Resol. Chrom. 21 No. 8 (1998) pp. 471-474.

[40]  X.-L. Cao and C.N. Hewitt, Build-up of artifacts on adsorbents during storage and its effect on passive sampling and gas chromatography-flame ionization detection of low concentrations of volatile organic compounds in air, J. Of. Chrom. A 688 (1994) pp. 368-374.

[41]  H.A. Beck, Z. Bozoki, and R. Niessner, Screening Pentachlorphenol-Contaminated Wood by Thermodesorption Sampling and Photoacoustic Detection, Anal. Chem. 72 (2000) pp. 2171-2176.

[42]  H.P. Schlegelmilch, J.Horst and J. Schram, Die Thermodesorption als Probenvorbereitungsverfahren für die Untersuchung von Deponieabgasen, Laborpraxis 11/21 (1997) pp. 42-44.

[43]   A.C. Heiden, K. Kobel, and J. Wildt, Characterisation of biogenic Emissions by Online Thermal Desorption Gas Chromatography-Mass Spectrometrie, Laborpraxis 6 (1997), 21, pp. 26-32.

[44]   E. Baltussen, F. David, P. Sandra, H.-G- Janssen, and C.A. Cramers, Sorption Tubes Packed with Polydimethylsiloxane: A New and Promising Technique for the Preconcentration of Volatiles and Semi-Volatiles from Air and Gaseous Samples, J. High Resol. Chrom. 21 (1998) pp. 332-340.

[45]   K. Grob, and A. Habich, headspace Gas Analysis: the Role and the design of concentration traps specifically suitable for capillary gas chromatography, J. of Chrom. 321 (1985) pp. 45-58.

[46]   E. Baltussen, F. David, P. Sandra, H.-G- Janssen, and C.A. Cramers, Equilibrium Sorptive Enrichment on Poly(dimethylsiloxane) Particles for Trace Analysis of Volatile Compounds in Gaseous Sample, Anal. Chem. 71 (1999) pp. 5793-5199.

[47]   H.P. Tuan, H.-G- Janssen, and C.A. Cramers, Novel preconcentration method for on-line coupling to high speed narrow-bore capillary gas chromatography: sample enrichment by equilibrium (ab)sorption, J. of Chrom. A 791:1-2 (1997) pp. 177-185.

[48]   J.W. Grate, S.L. Rose-Pherson, D.L. Venezky, M. Klusty, and H. Wohltjen, Smart Sensor System for Trace Organophosphorous and Organosulfur Vapor Detection Employing a Temperature-Controlled Array of Surface Acoustic Wave Sensors, Automated Sample Preconcentration, and Pattern recognition, Anal. Chem. 65 (1993) pp. 1868-1881.

[49]   W.A. Groves and E.T. Zellers, Prototype instrument Employing a Microsensor Array for the Analysis of Organic Vapors in Exhaled Breath, Am. Ind. Hygiene Assoc. J. 57 (1996) pp. 1103-1108.

[50]   W.A. Groves, E.T. Zellers, and G.C. Frye, Analyzing organic vapors in exhaled breath using a surface acoustic wave sensor array with preconcentration: Selection and characterization of the preconcentrator adsorbent, Anal. Chim. Acta 371 (1998) pp. 131-143.

[51]   Q.-Y. Cai, J. Park, D. Heldsinger, M.-D. Hsieh, and E.T. Zellers, Vapor recognition with an integrated array of polymer-coated flexural plate wave sensors, Sensors & Actuators B 62 (2000) pp. 121-130.

[52] E.T. Zellers, M. Morishita, and Q.-Y. Cai, Evaluating porous-layer open-tubular capillaries in a microanalytical system, Sensors & Actuators B 67 (2000) pp. 244-253.

[53] B. Schäfer, P. Hennig, and W. Engewald, Methodological Aspects of Headspace SPME : Application of the Retention Index System. J. High Resol. Chromatogr. 20 (1997) pp. 217-221.

[54] R. T. Marsili, SPME-MS-MVA as an Electronic Nose for the Study of Off-Flavours in Milk, J. Agric. Food Chem. 47(2) (1999) pp. 648-654.

[55] Alpha-MOS press release of Jan 2000 at http://www.alpha-mos.com/preframe.htm (2000)

[56] E. Baltussen, H.-G- Janssen, P. Sandra, and C.A. Cramers, A New Method for Sorptive Enrichment of Gaseous Sample: Application in Air Analysis and Natural Gas Characterization, J. High Resol. Chromatogr. 20 (1997) pp. 385-393.

[57] G.A. Eiceman, H.H. Hill Jr., B. Davani, and J. Gardea Torresday, Gas Chromatography, Anal. Chem. 68 (1996) pp. 291R-306R.

[58] W. Münchmeyer, A. Walte, and G. Matz, Improving electronic noses using a trap and thermal desorption unit, Sensors & Actuators B 69 (2000) pp. 379-383.

[59] R.J.B. Petersen and H.A. Bakkeren, Sorbents in Sampling. Stability and Breakthrough Measurements, Analyst 119 (1994) pp. 71-74.

[60] K. Figge, W. Rabel, and A. Wieck, Adsorbtionsmittel zur Anreicherung von organischen Luftinhaltsstoffen, Fresenius Z. Anal. Chem. 327 (1987) pp. 261-278.

[61] K. Ventura, M. Dostal, and J. Churacek, Retention Characteristics of some Volatile Cmpounds on Tenax GR, J. of Chrom. 642 (1993) pp. 379-382.

[62] Tenax™ is a registered trademark of Enka BV N.L.

[63] K. Sakodinskii, L. Panina, and N. Klinskaya, A Study of Some Properties of Tenax, a Porous Polymer Sorbent, Chromatographia 7 (1974) pp. 339-344.

[64] Steffan and Pawlisyn, Analysis of flavor volatiles using headspace solid-phase microextraction, J. Agri. Food Chem. 44 (1996) pp. 2187-2193.

[65]    L. Vergnais, et al., Evaluation of solid-phase microextraction for analysis of volatile metabolites produced by staphylococci, J. Agri. Fod Chem. 46 (1998) pp. 228-234.

[66]    T. Eklöv and I. Lundström, Distributed Sensor System for Quantification of Individual Components in a Multiple Gas Mixture, Anal. Chem. 71 (1999) pp. 3544-3550.

[67]    K. Hartvigsen, P. Lund, L.F. Hansen, and G. Holmer, Dynamic Headspace Chromatography/ Mass Spectroscopy Characterization of Volatiles Produced in Fish Oil Enriched Mayonnaise during Storage, J. Agric. Food Chem. 48 (2000) pp. 4858-4867.

[68]    F. Jüttner, A cryotrap technique for the quantitation of Monoterpenes in humid and ozone-rich forest air, J. of Chrom. 442 (1998) pp. 157-163.

[69]    O. Hugon, M. Sauvan, P. Benech, C. Pijolat, and F. Lefebvre, Gas separation with a zeolite filter, application to the selectivity enhancement of chemical sensors, Sensors & Actuators B 67(3) (2000) pp. 235-245.

[70]    S. Strathmann, Filterkonzepte für $SnO_2$-Halbleitergassensoren, Diploma thesis (1997) University of Tübingen.

[71]    B. Kolb, Headspace sampling with capillary columns, J. of Chrom. A 842:1-2 (1999) pp. 163-205.

[72]    J. Namiesnik and W. Wardenicki, Water Vapour Removal from Gaseous Samples Used for Analytical Purposes. A Review, Int. J. of Env. Anal. Chem. (1998).

[73]    D. Kohl, L. Heinert, J. Bock, T. Hofmann, and P. Schieberle, Systematic studies on responses of metal-oxide sensor surfaces to straight chain alkanes, alcohols, aldehydes, ketones, acids and acids using the SOMMSA approach, Sensors & Actuators B 70 (2000) pp. 43-50.

[74]    T. Hofmann, P. Schieberle, C. Krummel, A. Freiling, J. Bock, L. Heinert, and D. Kohl, High resolution gas chromatography/selective odorant measurement by multisensor array (HRC/SOMSA): a useful approach to standardise multisensor arrays for use in detection of key food odorants, Sensors & Actuators B 41 (1997) pp. 81-87.

[75] B. Hivert, M. Hoummady, P. Mielle, G. Mauvais, J.M. Henrioud, and D. Hauden, A fast and reproducible methods for gas sensor screening to flavour compounds, Sensors & Actuators B 26-27 (1995) pp. 242-245.

[76] C.S. Creaser, J. W. Stygall, and D.J. Weston, Development in membrane inlet mass spectrometry, Anal. Comm. 35 (1998) pp. 9H-11H.

[77] C.S. Creaser, D.J. Weston, J.P. Wilkins, C.P. Yorke, J. Irwin, and B. Smith, Anal. Comm. 36 (1999) pp. 383-386.

[78] M.D. Luque de Castro and I. Papaefstathiou, Analytical pervaporation: a new separation technique, Trends in Anal. Chem. 17:1 (1999) pp. 41-49.

[79] C.S. Creaser, D.J. Weston, and B. Smith, In-Membrane Preconcentration/ Membrane Inlet Mass Spectrometry of Volatile and Semivolatile Organic Components, Anal. Chem 72 (2000) pp. 2730-2736.

[80] A. Segal, T. Gorecki, P. Mussche, J. Lips, and J. Pawliszyn, Development of membrane extraction with a sorbent interface-micro gas chromatography system for field analysis, J. of. Chrom. A 873:1 (2000) pp. 13-27.

[81] R.C. Johnson, R.G. Cooks, T.M. Allen, M.E. Cisper, and P.H. Hemberger, Membrane introduction Mass Spectrometry: Trends and applications, Mass Spectrometry Rev. 19/1 (2000) pp. 1-37.

[82] J.R. Stetter, S. Zaromb, and M. W. Findlay, Jr., Monitoring of Electrochemically Inactive Compounds by Amperometric Gas Sensors, Sensors & Actuators, 6, (1984), pp. 269-288.

[83] J. Unwin and P.T. Walsh, Monitoring Organic Vapors Using Pyrolysis-amperometry, Sensors and Actuators, 17 (1989) pp. 575-581.

[84] H. Komiya and S. Kimura, Freon and Halogenated Hydrocarbon Detection with Electrochemical Sensors, Sensors and Actuators B1 (1990) 68-72.

[85] J.R. Stetter, C-X. Shi, and G.J. Maclay, Modulated Photoionization Detection of Hydrazine Compounds in Mixtures without Prior Separation, Anal. Chem. 63, (1991), pp.1755-1759.

[86] G.J. Maclay and J.R. Stetter, Use of Time-Dependent Chemical Sensor Signals for Selective Identification, Transducers '87, Proc. of the 4th International Conference on Solid-State Sensors and Actuators, Pub. by Institute of EE of Japan, Tokyo, Japan, June 2-5, (1987), pp. 557-560.

[87]  E. L. Kalman, F. Winquist and Lundstrom, A New Pollen Detection Method Based on an Electronic Nose, Atmospheric Environment, Vol. 31 No. 11 (1997) pp. 1715-1719.

[88]  S. Strathmann, W.R. Penrose, J.R. Stetter and W. Göpel, Detection of TNT with chemical sensors, Proc. International Symposium on Olfaction and the Electronic Nose (ISOEN 99), Tuebingen, Germany, September 20-22 (1999) p. 362.

[89]  W. Hornik, A Novel Structure for Detecting Organic Vapors and Hydrocarbons Based on a Pd-MOS Sensor, Sensors and Actuators B1 (1990) pp. 35-39.

[90]  O.A. Sadik and J.M. Van Emon, Designing Immunosensors for Environmental Monitoring, Chemtec. 6 (1997) p. 27.

[91]  T. Otagawa, S. Zaromb, and J.R. Stetter, A Room-Temperature Electro-chemical Sensor and Instrument for Monitoring Methane, Journal of Sensors and Actuators, 8,(1985) pp. 65-88.

[92]  Stetter, J.R., G.J. Maclay, and S.V. Christesen, Time-dependent Sensor Signals for SelectiveDetection, Sensor and Actuators 20(3) (1989) pp. 277-287.

[93]  Stetter, J.R., M.W. Findlay, G.J. Maclay, J. Zhang, S. Vaihinger, and W. Göpel, Sensor Array and Catalytic Filament for Chem. Anal. of Vapors and Mixtures, Sensors and Actuators 21 B (1990) pp. 43-47.

[94]  S. Zaromb and J.R. Stetter, Portable System and Method Combining Chromatography and Array of Electrochemical Sensors, U.S. Patent #4,888,295; (ANL Case #S-64,127), (1989).

[95]  J. S. Brodbelt, R.G. Cooks, J. C. Tou, G.J. Kallos, In Vivo Mass Spectrometric Determination of Organic Compounds in Blood with a Membrane Probe, Analytical Chemistry 59 (3) (1987) pp. 454-458.

[96]  B.B Lakshmi and C.R. Martin, Enantioseparation Using Apoenzymes Immobilized in a Porous Polymeric Membrane, Nature (1997) 388, (6644) pp. 758-760.

[97]  D.K. Mandal, A.K. Guha and K.J. Sirkar, Isomer Separation by Hollow Fiber Contained Liquid Membrane Permeator, Membrane Science (1998) 144 (1-2) pp. 13-24.

[98]    M. R. Salemme, Sulfonated Polyxylene Oxide as a Permselective Membrane for Water Vapor Transport, U.S. Patent # 3735559. (1973).

[99]    E. Pellizarini and B. Demian, Sampling of Organic Compounds in the Presence of Reactive Inorganic Gases with Tenax GC, Anal. Chem. 56 (1984) pp. 793-798.

[100]   R. Kellner, J.-M. Mermet, M. Otto, and H.M. Widmer, Analytical chemistry, (1998), Wiley - VCH, New York.

[101]   T. Hirschfeld, Anal. Chem. 52 (1980) pp. 297A.

[102]   S.M. Abeel, A. K. Vickers, D. Decker, Trends in Purge and Trap, J. of Chrom. Sci. 32 (1994) pp. 328-37.

[103]   A. Kindlund, H. Sundgren, I. Lundström, Quartz crystal gas monitor with a gas concentrating stage, Sensors and Actuators 6 (1984) pp. 1-17.

[104]   T. Hoffmann, P. Schieberle, C. Krummel, A. Freiling, J. Bock, L. Heinert, and D. Kohl, High resolution gas chromatography / selective odorant measurement by multisensor array (HRGC/SOMSA): a useful approach to standardise multisensor arrays for use in the detection of key food odorants, Sensors and Actuators41 B (1997) pp. 81-87.

[105]   Compendium of Analytical Nomenclature, IUPAC Definitive Rules 1977, Oxford: Pergamon 1978; Pure Appl. Chem. 37, 499 (1974); 51, 1 (1979); 57, 105 (1985).

[106]   S.C. Chang, J. R. Stetter, C.S. Cha, Amperometric gas sensors (1993), Talanta, Vol 40, No. 4. pp. 461-477.

[107 ]  Z. Zao, W.J. Buttner, J.R. Stetter, Electroanalysis, The Properties and Applications of Amperometric Gas Sensors, Electroanalysis 4 (1992) pp. 253-266.

[108]   J.W. Gardner, P.N. Bartlett, Electronic Noses Principles and Applications, (1999), Oxford University Press, ISBN 0-19-855955-0, p. 102.

[109]   B.S. Hobbs, A.D.S. Tantrum, R. Chan-Henry, Liquid Electrolyte Fuel Cells, In Techniques and Mechanisms in Gas Sensing, (1991) Adam Hilger, Bristol, pp. 161-188.

[110]   L.C. Clark, R. Wolf, D. Granger and Z. Taylar, J. Appl. Physiol. 6 (1953) p. 189.

[111] S. Vaihinger, Mehrkomponentenanalyse durch zeitabhängige Signale chemischer Gassensoren, PhD thesis, (1992), University of Tuebingen.

[112] G.J. Maclay, W.J. Buttner, J.R.Stetter, Microfabricated Gas Sensors, IEE Transactions on electron devices Vol 35, No. 6 (1988) pp. 793-799.

[113] M.E. Tess and J.A. Cox, Humidity Independent Solid-State Amperometric Sensor for Carbon Monoxide Based on an Electrolyte Prepared by Sol-Gel Chemistry, Anal. Chem. 70 (1998) pp. 187-190.

[114] J.R. Stetter, Instrumentation to monitor chemical exposure in the synfuel industry, Ann. Am. Conf. Ind. Hyg. Vol. 11 (1984), pp. 225-268.

[115] A.W.E. Hodgson, P. Jacquinot, and P.C. Hauser, Electrochemical Sensor for the Detection of $SO_2$ in the Low-ppb Range, Anal. Chem. 71 (1999) pp. 2831-2837.

[116] K.F. Blurton and J.R. Stetter, J. Chromatogr. 155, (1978), pp. 34-45.

[117] J.R. Stetter, J.M. Sedlak and K.F. Blurton, J. Chromatogr. Sci. 15 (1977) pp. 125-28.

[118] J.R. Stetter, S. Chang, Electrochemical $NO_2$ Gas Sensors: Model and Mechanism for the Electroreduction of $NO_2$, Eletroanalysis 2 (1990) pp.359-365.

[119] W.J. Becker, W. Breuer and J. Deprez, U.S. Patent 4,049,503 (1977).

[120] J. Janata, Principles of Chemical Sensors, Plenum Press (1989) Chapter 4, pp. 81-237.

[121] J.R. Stetter, and S. Zaromb, Sensors & Actuators 6 (1984) pp. 225.

[122] J.R.Stetter, Electrochemical gas sensors for identification of solid and liquid compounds, (1987), Proceedings of Transducers '87.

[123] G. Olafsdottir, E. Martinsdottir, and E.H. Jonsson, Rapid Gas Sensor Measurements To Determine Spoilage of Capelin (Mallotus villosus), J. Agric. Food Che. 45 (1997) pp. 2654-2659.

[124] I. Heberle, Modellstudien zur Verknüpfung chromatographischer Methoden mit optimierten Sensorarrays, Diploma thesis, (1999), University of Tübingen.

[125] G. Guichon, C.L. Guillemin, Quantitative Gas Chromatography, Elsevier, Amsterdam 1988.

[126] J.N. Miller, The Method of Standard Additions, Spectroscopy Europe 1992, 4/6, pp. 26-27.

[127] V.R. Meyer, Richtigkeit bei der Peakflächenbestimmung, GIT Fachz. Lab.,(1994), pp. 4-5.

[128] M. Otto, Analytische Chemie, (1995), Verlag Chemie (VCH), Weinheim.

[129] Agilent Technologies, Katalog für Zubehör und Verbrauchsmaterialien Chemische Analysentechnik, 2000/2001, Publ. Nr. 5968-8361 GE (2000).

[130] Sigma-Aldrich.Co, U.S.A, Produkte für Chromatographie und Probenvorbereitung, Katalog 2000, Publ. Nr. T9000001-003g (2000).

[131] K.J. Krost, E.D. Pellizarini, S.G. Walburn, and S.A. Hubbard, Collection and Analysis of Hazardous Organic Emissions, Anal. Chem. 54 (1982), pp 810-817.

[132] J.F. Pankow, Gas Phase Retention Volume Behavior of Organic Compounds on the Sorbent Poly(oxy-m-terphenyl-2',5'-ylene), Anal. Chem. 60 (1988), pp 950-958.

[133] A. J. Nunez, L. F. Gonzalez, and J. Janak, Pre-concentration of headspace volatiles for trace organic analysis by gas chromatography, J. of Chrom. 300 (1984) pp. 127-162.

[134] J.J. Manura, Scientific Instrument Services, 1027 Old York Rd., Ringoes, NJ, http://www.sisweb.com/index/referenc/resin10.htm.

[135] M. Harper, Evaluation of Solid Sorbent Sampling Methods by Breakthrough Volume Studies., Ann. Occup. Hyg. Vol. 37, No. 1 (1993) pp. 65-88.

[136] P. Comes, N. Gonzalez-Flesca, T. Menard, and J. Grimalt, Langmuir-Derived Equations for the Prediction of Solid Adsorbent Breakthrough Volumes of Volatile Organic Compounds in Atmospheric Emission Effluents., Anal. Chem. 65 (1993) pp. 1048-1053.

[137] T. Hermle, Bewertung und Optimierung rechnerbasierter Auswertemethoden für chemische Gassensoren, Diploma thesis, (1998), University of Tübingen.

[138] F. Dieterle, Multivariate Analysen zur Mehrkomponentenbestimmung, Diploma thesis, (1999), University of Tübingen.

[139] K.R. Beebe, R.J. Pell, M.B. Seasholtz, Chemometrics, A Practical Guide, (1998) Wiliey-Interscience, New York.

[140] Lennartz electronic GmbH / Motech GmbH, Germany, MOSES II User's Manual (1998).

[141] P.C. Jurs, G.A. Bakken, and H.E. McCelland, Computational Methods for the Analysis of Chemical Sensor Array Data from Volatile Analytes, Chem. Rev. 100 (2000) pp. 2649-2678.

[142] M. Holmberg, F. Winquist, I. Lundström, J. W. Gardner, and E. L. Hines, Sensors and Actuators B 26-27 (1995) pp. 246-249.

[143] H. Baltes, W. Göpel and J. Hesse (Series Eds.), Sensors Update: Sensor Technology - Applications - Markets, VCH, Weinheim (Germany) Vol. 2 (1996), ISBN 3-527-29432-5.

[144] M. Frank, personal communication.

[145] J.W. Grate, Acoustic Wave Microsensor Arrays for Vapor Sensing, Chem. Rev. 100 (2000) pp. 2627-2648.

[146] Lennartz electronic GmbH, Germany, http://www.lennartz-electronic.de.

[147] J. Mitrovics, H. Ulmer, U. Weimar, and W. Göpel, Modular Sensor Systems for Gas Sensing and Odor Monitoring: The MOSES Concept, (1997), ACS Symposium Series: "Chemical Sensors and Interfacial Design", 31 (1998) pp. 307-315.

[148] J. Mitrovics, U. Weimar, H. Ulmer, G. Noetzel and W. Göpel, Hybrid Modular Sensor Systems: A New Generation of Electronic Noses, Conf.Proc. Sensor 97, Vol. 1, Nürnberg (D) (5/1997) pp. 95-100; Conf. Proc. ISIE, Guimaraes (P), IEEE Catalog, ISBN 0-7083-3936-3 (7/1997), pp. 116-121.

[149] J. Mitrovics, H. Ulmer, G. Noetzel, U. Weimar and W. Göpel, Design of a Hybrid Modular Sensor System for Gas and Odor Analysis, Conf.Proc. Transducers 97, Chicago (USA), IEEE Catalog, ISBN 0-7803-3829-4/97 (6/1997) pp. 1355-1358.

[150] S. Strathmann, W.R. Penrose, J.R. Stetter, and W. Göpel, Approaches to a More Versatile Electronic Nose, Proc. International Symposium on Olfaction and the Electronic Nose (ISOEN 99), Tuebingen, Germany, September 20-22 (1999) p. 15.

[151] J. Mitrovics, H. Ulmer, G. Noetzel, U. Weimar and W. Göpel, Transducers and Algorithms for Odor Recognition with Hybrid Modular Sensor Systems, Conf. Proc. EUROSENSORS XI, Warschau (P), ISBN 83-908335-0-6 (9/1997) pp. 567-570

[152] Motech GmbH, Germany, (http://www.motech.de)

[153] TSI Inc., St Paul, MN, USA, (http://www.tsi.com).

[154] TSI Inc., St Paul, MN, USA, Application Note HS 497-1 (1998) and data sheet XX-MNL M-series, (1996).

[155] N. Barsan, J.R. Stetter, M. Findlay, Jr. And W. Göpel, High-Performance Gas Sensing of CO: Comparative Tests for Semiconducting (SnO2-Based) and Amperometric Gas Sensors, Anal. Chem. 71:13 (1999) pp. 2512-2517.

[156] TSI Inc., St Paul, MN, USA, APP Note HS 395-03, Electrochemical sensor operation and performance notes (1996).

[157] W. Schmid, Umsatzmessungen an Zinndioxidsensoren mit Massenspektromerie, Diploma thesis, (2000), University of Tübingen.

[158] Endress + Hauser Meßtechnik GmbH + Co., Germany, Werksunterlagen zu elektrochemischen Zellen der Baureihe CO5.1 und ND2.1, (1996).

[159] A. Krauss, G. Noetzel, personal communication

[160] A. Krauss, PhD thesis in preparation, (2000), University of Tübingen.

[161] G. Matz, T. Hunte, S. Döhren, Gas-sensor Array mit integrierter Anreicherungseinheit, Techn. Univ. Harburg, Airsense Produktbeschreibung PEN, Airsense Analysentechnik GmbH.

[162] Perkin Elmer Corporation, Norwalk, CT, USA, ATD 400 Automated Thermal desorber user's manual, (1998).

[163] W.W. Wendlandt, Thermal Analysis. Third Ed. J.Wiley & Sons, New-York (1986).

[164] W.F. Hemminge, H.K. Cammenga, Methoden der thermischen Analyse, Springer Verlag Berlin, (1989).

[165] Data from Scientific Instrument Services, Ringoes, NJ, USA. (http://www.sisweb.com/index/referenc/resins).

[166] J.W. Gardner, M. Craven, C. Dow, and E. Hines, The prediction of bacteria type and culture growth phase by an electronic nose with a multi-layer perceptron network. Meas. Sci. Technol. 9 (1998) pp. 120-127.

[167] T.D. Gibson, O. Prosser, J.N. Hulbert, R.W. Marshall, P. Corcoran, P. Lowery, E.A. Ruck-Keene, and S. Heron, Detection and simultaneous identification of microorganisms from headspace samples using an electronic nose. Sensors and Actuators B44 (1997) pp. 413-422.

[168] M. Holmberg, F. Gustafsson, E.G. Hornsten, F. Winquist, L.E. Nilsson, L. Ljung, and I. Lundstrom, Bacteria classification based on feature extraction from sensor data. Biotechnology Techniques 12 (1998) pp. 319-324.

[169] K. Pope, Technology Improves on the Nose as Science Tries to Imitate Smell, Wall Street Journal, pp. B1-2, 1 March 1995.

[170] C.M. McEntegart, W.R. Penrose, S. Strathmann, and J.R. Stetter, Detection and discrimination of coliform bacteria with gas sensor arrays, Sensors and Actuators B 70 (2000) pp. 170-176.

[171] E.J. Staples, An Electronic NOSE Containing 500 Orthogonal Sensors With Pattern Recognition Based Upon VaporPrints™, Proc. International Symposium on Olfaction and the Electronic Nose (ISOEN 99), Tuebingen, Germany, September 20-22,(1999), p. 42.

[172] S. Strathmann, S. Hahn, and U. Weimar, Food Investigation by an Electronic Nose with Differential Thermodesorption and GC-MS, submitted to ISOEN 8 (2001), Washington D.C., U.S.A., S. Hahn, Untersuchung von verschiedenen Mayonnaise Marken mit GC/MS und einer Elektronischen Nase (MOSES II), Project report, 8.2000, p. 9.

# 9. PUBLICATIONS

Parts of this work have been previously published or presented.

**Full papers**

- M. Schweizer-Berberich, S. Strathmann, U. Weimar, R. Sharma, A. Seube, A. Peyre-Lavigne, and W. Göpel, Strategies to avoid cross-sensitivities of $SnO_2$-based CO sensors, Sensors and Actuators B 58 (1999) pp. 318-324.

- C.M. McEntegart, W.R. Penrose, S. Strathmann, and J.R. Stetter, Detection and discrimination of coliform bacteria with gas sensor arrays, Sensors and Actuators B 70 (2000) pp. 170-176.

- J.R. Stetter, S. Strathmann, C. McEntegart, M. DeCastro and W.R. Penrose, New sensor arrays and sampling systems for a modular electronic nose, Sensors and Actuators B 69(3) (2000) pp. 410-419.

**Posters and Presentations**

- M. Schweizer-Berberich, S. Strathmann, A. Seube, R. Sharma, A. Peyre-Lavigne, and W. Göpel, Filters for tin dioxide CO gas sensors to pass the UL2034 standard ,Poster at the 7th IMCS July 27-30, 1998, Beijing

- S. Strathmann, M.Schweizer-Berberich, U. Weimar, W. Göpel, R.Sharma, A.Seube, A.Peyre-Lavigne, Strategies to avoid cross-sensitivities of $SnO_2$-based CO sensors, Poster at the XIIth Eurosensors September 1998, Southampton

- S. Strathmann, W.R. Penrose, J.R. Stetter and W. Göpel, Detection of TNT with chemical sensors, Proc. International Symposium on Olfaction and the Electronic Nose (ISOEN 99), Tübingen, Germany, September 20-22 (1999) p. 362.

- S. Strathmann, W.R. Penrose, J.R. Stetter, and W. Göpel, Approaches to a More Versatile Electronic Nose, Proc. International Symposium on Olfaction and the Electronic Nose (ISOEN 99), Tübingen, Germany, September 20-22 (1999) p. 15.

- C.M. McEntegart, W.R. Penrose, S. Strathmann, and J.R. Stetter, Discrimination of Coliform Bacteria Using Headspace Vapors, Proc. International Symposium on Olfaction and the Electronic Nose (ISOEN 99), Tübingen, Germany, September 20-22 (1999) p. 380.

- S. Strathmann, A. Krauß, and U. Weimar, Differential thermodesorption sample uptake for Electronic Noses, Proc. International Symposium on Olfaction and the Electronic Nose (ISOEN 2000), ISOEN 99), Brighton, UK, July 20-24 (2000) p. 131.

**Patent**

- S. Strathmann, U. Weimar, A. Krauß, and M. Wandel, Differentielle Thermodesorption für Gassensorsysteme. Probenvorbereitungssystem für gasförmige Analyte für die Verwendung mit chemischen Gassensoren bzw. Gassensorsystemen. Patent application, Deutsches Patent u. Markenamt, AZ #100 32 409.2, July 7 (2000).

# 10. ACKNOWLEDGEMENTS

First of all, I would like to thank Prof. Dr. Drs. hc. Wolfgang Göpel for providing the great opportunity to pursue a Ph.D. at the Institute of Physical and Theoretical Chemistry at the University of Tübingen. He sparked the professional, ambitious, enthusiastic, and positive atmosphere in the group and will always be remembered for his contagious passion for science.

I wish to thank Prof. Dr. Christiane Ziegler for her readiness to take over as my promoter after the tragic accidental death of Prof. Göpel. She was a great help to keep this work focussed and it was a pleasure to work with her.

Special thanks go to my co-examiner Prof. Dr. Joseph R. Stetter. He provided extremely valuable suggestions and corrections and he inspired me with his enthusiasm about the achievements. His friendly and competent support throughout my work was so stimulating and of such high quality that I greatly enjoyed the time I spent in Chicago.

I would like to thank Prof. Dr. Günter Gauglitz for his readiness to co-examine the doctoral exam, the support of our group and the pleasurable working atmosphere in the Institute.

I owe special thanks to Dr. Udo Weimar. He supported me and motivated me throughout the whole project, offered me guidance, advice and friendship. I appreciate very much his continuing support as well as the technical and personal experience I could gain by being part of his group.

This work could not have been completed without the help and support of many people. To them I would like to express my deepest gratitude. In particular I would like to thank Michael Frank for his expert technical help, humor, and readiness to assist whenever needed; Andreas Krauss, who always was willing to share his technological experience and served as a living dictionary; Dr. Gerd Noetzel for insights way beyond circuitry; and Michael Wandel for technical help in the automation of the set-up.

I sincerely appreciate the support with my project work of Ute Harbusch releasing most valuable time for the accomplishment of this thesis.

## LISTE DER AKADEMISCHEN LEHRER

Meine akademischen Lehrer waren:

K. Albert, E. Bayer, M. Brendle, D. Christen, H. Eckstein, G. Gauglitz, J. Gelinek, W. Göpel, G. Häfelinger, H.P. Hagenmaier, M. Hanack, D. Hoffmann, V. Hoffmann, G. Jung, S. Kemmler-Sack, W. Koch, D. Krug, N. Kuhn, E. Lindner, I.-P. Lorenz, U. Nagel, W. Nakel, H. Oberhammer, D. Oelkrug, H. Pauschmann, G. Pausewang, B. Rieger, A. Rieker, W. Rundel, V. Schurig, F.F. Seelig, H.-U. Siehl, H. Stegmann, J. Strähle, H. Suhr, W. Voelter, M .Wolff, K.-P. Zeller, C. Ziegler.

# Lebenslauf

**Stefan Strathmann**

Geboren: 04.03.1968, Winchester, Massachusetts, U.S.A.

Nationalitäten: Bundesrepublik Deutschland / United States of America

**Schulbildung**

| | |
|---|---|
| Aug. 1974 - Juni 1978 | Winkelwiese Grundschule in Tübingen |
| Aug. 1978 - Juni 1987 | Kepler Gymnasium in Tübingen |
| Juni 1987 | Abitur |

**Wehrdienst**

| | |
|---|---|
| Okt. 1987 - Okt. 1988 | 5. Raketenartillerie Batallion 250 in Großengstingen |

**Studium**

| | |
|---|---|
| Okt. 1988 – Mai 1997 | Studium der Chemie an der Eberhard-Karls-Universität Tübingen |
| Nov.1996 | Diplomhauptprüfungen |
| Dec. 1996 - Juni 1997 | Diplomarbeit unter Anleitung von Prof. W. Göpel Titel: "*Filterkonzepte für SnO$_2$-Halbleitergassensoren*" |

**Promotion**

| | |
|---|---|
| Sept. 1997 - | Wissenschaftlicher Mitarbeiter in Institut für Physikalische und Theoretische Chemie und Anfertigung der Dissertation unter Anleitung von Prof. W. Göpel und Prof. C. Ziegler mit dem Titel: "*Sample Conditioning for Multi-Sensor Systems, Probenaufbereitung für Multisensorsysteme*" |
| Feb. 1999 - Mai 1999 | Forschungsaufenthalt am Illinois Institute of Technology, Chicago, IL, U.S.A. im Rahmen der Dissertation |

# CURRICULUM VITAE

**Stefan Strathmann**

| | |
|---|---|
| March 04th 1968 | born in Winchester, Massachusetts, U.S.A. |
| Nationalities: | Bundesrepublik Deutschland / United States of America |

| | |
|---|---|
| Sept. 1997 - present | Work at a Ph.D. thesis at the Institute for Physical and Theoretical Chemistry at the University of Tübingen directed by Prof. W. Göpel and Prof. C. Ziegler, Titel: *"Sample Conditioning for Multi-Sensor Systems, Probenaufbereitung für Multisensorsysteme"* |
| Feb. 1999 - May 1999 | Research at the Illinois Institute of Technology, Chicago, IL, U.S.A. within the Ph.D. thesis |
| June 1996 | Diploma in Chemistry at the University of Tübingen |
| Dec. 1996 - June 1997 | Diploma thesis directed by Prof. W. Göpel, Titel: *"Filterkonzepte für $SnO_2$-Halbleitergassensoren"* |
| Okt. 1988 – May 1997 | Student of Chemistry at the University of Tübingen |
| Okt. 1987 - Okt. 1988 | Military service in Großengstingen |
| June 1987 | Abitur |
| Aug. 1978 - June 1987 | Kepler Gymnasium Tübingen |
| Aug. 1974 - June 1978 | Winkelwiese Grundschule Tübingen |